Importance of Chirality to Flavor Compounds

ACS SYMPOSIUM SERIES **1212**

Importance of Chirality to Flavor Compounds

Karl-Heinz Engel, Editor
*Technische Universitaet Muenchen,
Freising, Germany*

Gary Takeoka, Editor
*U.S. Department of Agriculture, Agricultural Research Service,
Albany, California*

American Chemical Society, Washington, DC

Distributed in print by Oxford University Press

The paper used in this publication meets the minimum requirements of American National Standard for Information Sciences—Permanence of Paper for Printed Library Materials, ANSI Z39.48n1984.

Foreword

The ACS Symposium Series was first published in 1974 to provide a mechanism for publishing symposia quickly in book form. The purpose of the series is to publish timely, comprehensive books developed from the ACS sponsored symposia based on current scientific research. Occasionally, books are developed from symposia sponsored by other organizations when the topic is of keen interest to the chemistry audience.

Before agreeing to publish a book, the proposed table of contents is reviewed for appropriate and comprehensive coverage and for interest to the audience. Some papers may be excluded to better focus the book; others may be added to provide comprehensiveness. When appropriate, overview or introductory chapters are added. Drafts of chapters are peer-reviewed prior to final acceptance or rejection, and manuscripts are prepared in camera-ready format.

As a rule, only original research papers and original review papers are included in the volumes. Verbatim reproductions of previous published papers are not accepted.

ACS Books Department

Preface

Chiral molecules are ubiquitous in nature. Thus, it is not surprising to come across this phenomenon in the world of flavor substances. This book has been developed from a Symposium held at the 248th National Meeting of the American Chemical Society held August 10-14, 2014 in San Francisco, CA. The motivation was to bring together renowned scientists from various disciplines in order to highlight the importance of chirality to flavor compounds from different angles.

The book provides an overview on the analytical procedures currently applied to analyze chiral flavor substances at trace levels. It demonstrates several examples for the application of these techniques to determine naturally occurring enantiomeric compositions of chiral key flavor compounds in various natural systems. In addition to the analytical aspects, the contributions focus on the sensory properties of enantiomers and enlarge our knowledge on the correlation between configurations and odor properties and intensities of chiral flavor compounds.

The practical importance of the topic is reflected by a discussion of merits and limitations of chiral analysis for the authenticity control of food flavorings. In addition, examples for the use of enzymes and microorganisms to obtain enantiopure flavor substances and thus to meet legal requirements for "natural" labeling are presented.

Finally, the book covers aspects recently getting more and more in the focus of flavor science: What are the physiological mechanisms underlying the perception of sensory properties and does chirality matter in that respect?

The book will be of interest to flavor researches involved in analysis, biotechnology, sensory sciences as well as regulatory affairs. The editors hope that it will be a further stimulus for an extremely exciting aspect of flavor science.

Acknowledgments

Prof. Dr. Karl-Heinz Engel
Technische Universitaet Muenchen
Chair of General Food Technology
Maximus-von Imhof-Forum 2
D-85354 Freising, Germany

Dr. Gary Takeoka
United States Department of Agriculture
Agricultural Research Service
800 Buchanan Street
Albany, California 94710

Editors' Biographies

Karl-Heinz Engel

Karl-Heinz Engel is Professor of General Food Technology at the TUM School of Life Sciences Weihenstephan of the Technische Universität München, Germany. His areas of research are (i) analysis of chiral aroma compounds, (ii) metabolite profiling of crops, and (iii) analysis of phytosterols/-stanols and their fatty acid esters. He published more than 280 scientific articles and contributed to various American Chemical Society Series books as author as well as co-editor. He is also involved in the safety assessment of flavorings, enzymes and novel foods performed by the European Food Safety Authority (EFSA) in Parma, Italy.

Gary Takeoka

Gary Takeoka is a research chemist in the Healthy Processed Foods Research Unit, Western Regional Research Center, U.S. Department of Agriculture in Albany, CA. He received his B.S. and M.S. in Food Science and Technology and Ph.D. in Agricultural and Environmental Chemistry, all degrees from the University of California, Davis. His areas of research are (i) analysis of volatiles and non-volatiles from agricultural crops and medicinal plants, and (ii) determining the effects of processing conditions on the composition of food components. He has published more than 100 scientific articles and has served as chairperson, vice-chairperson and secretary of the Flavor Subdivision of the ACS Division of Agricultural and Food Chemistry.

Chapter 1

Authenticity Control of Food Flavorings - Merits and Limitations of Chiral Analysis

Uwe Schäfer,[1] Johannes Kiefl,[1] Wenqi Zhu,[2] Michael Kempf,[1] Marcus Eggers,[1] Michael Backes,[1] Torsten Geissler,[1] Rüdiger Wittlake,[1] Katharina V. Reichelt,[1] Jakob P. Ley,[1] and Gerhard Krammer*,[1]

[1]Symrise AG, Mühlenfeldstrasse 1, 37603 Holzminden
[2]Department of Food Science and Human Nutrition, University of Illinois at Urbana−Champaign, 1302 West Pennsylvania Avenue, Urbana, Illinois 61801, United States
*E-mail: gerhard.krammer@symrise.com.

Chirality plays an important role in nature. In bio-recognition and transformation processes chirality acts as a basic selector for enzymes, microorganisms, plants and human beings. In 1848, Louis Pasteur was the first to report on the two stereoisomers of ammonium tartrate, and the famous British physicist Lord Kelvin concluded in 1883: "I call any geometrical figure or any groups of points chiral and say it has chirality if its image in a plane mirror, ideally realized cannot be brought to coincide with itself." Nowadays the principles of chirality are important for the investigation of natural products and xenobiotics as well. Multiple fields of research like pharma, plant physiology, feed, food and flavor chemistry are using enantioselective methods. Since chiral flavoring substances are sometimes characterized by different aroma and/or taste profiles as well as flavor intensities, enantiospecific evaluation of aroma compounds is key.

Regulatory Situation for Chiral Flavoring Substances in the European Union

The understanding of chirality has meanwhile been incorporated into legal frameworks such as the flavor legislation in the European Union (*1*).

In this context, there are two main aspects, which need to be considered: The registration on the European positive list, also known as Union List, and the use of selected flavoring substances for authenticity control. There are three guiding principles for registered flavoring substances, which need to be considered in order to maintain the natural status. The occurrence of the corresponding natural flavoring substance has to be reported free of doubt. The source material has to be of vegetable, animal or microbiological origin and the manufacturing process has to follow approved natural production processes according to the sequence and a given set of conditions. The European flavor association EFFA published in 2010 a guidance document, which also includes an interpretation for optical isomers: "Mixtures of optical isomers shall be allowed in any ratio provided that all the isomers are identified in nature" (*2*). Resulting from these regulatory criteria, various chirospecific analytical methods such as enantiospecific gas chromatography (enantioGC), enantiospecific high performance liquid chromatography (enantioHPLC) as well as enantiospecific capillary zone electrophoresis (enantioCE) are combined with results from isotope ratio mass spectrometry (IRMS) and quantitative deuterium nuclear magnetic resonance (Deuterium NMR) for the purpose of authenticity control of natural flavoring substances (*3*).

Development of Chirospecific Methods for the Analysis of Flavor Mixtures

In the early 1990s the development of chiral stationary phases and their use in multidimensional gas chromatography led to the decoding of the enantiomeric distributions of chiral natural compounds such as γ-decalactone [(*R*)-(+) 89.4% : (*S*)-(-) 10.6%] and γ-octalactone [(*R*)-(+) 50.2% : (*S*)-(-) 49.8%] in genuine raspberry fruits. Direct chirospecific analysis via gas chromatography-mass spectrometry (GC-MS) in the so-called single ion monitoring mode (SIM) of a flavor extract of water-phases obtained from genuine raspberry and strawberry fruits revealed almost racemic mixtures of several 4- and 5-alkanolides at trace level (*4*).

Multidimensional gas chromatography has been used for more than 30 years to resolve chiral compounds in complex mixtures in certain essential oils and flavor extracts. The need for enhanced separation capabilities to accurately determine enantiomeric excess is shown for α-ionone in carrot extracts (Figure 1). α-Ionone is a norisoprenoid flavor compound whose (*R*)-isomer can be formed by enantioselective enzyme-catalyzed cleavage of carotenoids (*5*), whereas only traces of maximum 4% of the (*S*)-isomer have been detected in certain raspberry cultivars up to now (*6*). The thermally induced degradation of α-carotene in carrots was therefore studied to elucidate the generation of (*S*)-α-ionone.

Fresh carrots (1 kg) were sliced, stressed in an oven at 100°C for three hours, cooked and extracted using a Likens-Nickerson apparatus for four hours. The SDE extract containing less than 0.1 % α-ionone was analyzed with one-dimensional GC-MS; however, severe coelution occurred within the target elution window. Comprehensive two-dimensional separation (enantioGC×GC) comprising a *tert*-butyldimethylsilyl β-cyclodextrin column (25 m × 0.25 mm ID, Macherey & Nagel) in the first and a VF-5 column (2 m × 0.15 mm ID, Varian) in the second dimension showed about hundred compounds of the extract eluting together with α-ionone solely within 10 minutes (t_R = 40-50 min). Figure 1 demonstrates that enantioGC×GC facilitated the separation of the α-ionone enantiomers by avoiding further coelution and thus revealing that only (*R*)-α-ionone was present in the carrot extract.
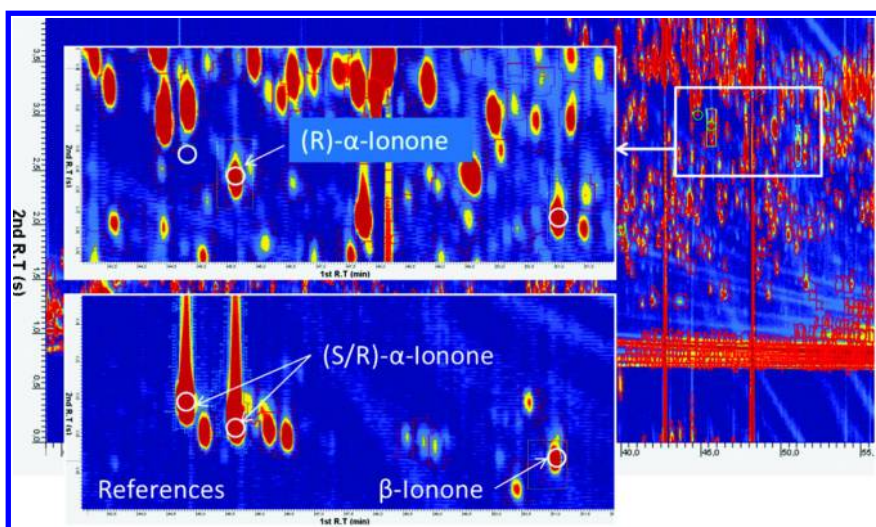
Figure 1. Separation of α-ionone enantiomers in carrot extract by enantioGC×GC.

The results indicate that the formation of the (*S*)-enantiomer is facilitated by other processes than oxidative stress and cooking. This confirms the role of high (*R*)-α-ionone excess as decisive parameter in authenticity control. Thus, comprehensive two-dimensional gas chromatography shows significant advantages for the analysis of complex mixtures and complements one-dimensional GC in substantiating enantiomeric data.

Enantiomeric Distribution of 2-Methylbutyric Acid

There are several examples for a wide enantiomeric distribution of 2-methylbutyric acid in nature. Strawberries with >99 % (*S*)-2-methylbutyric acid and *Veratrum album* with >95% (*R*)-2-methylbutyric acid are the most extreme representatives but there are also more moderate examples like Roman chamomile

[68% (*S*) : 32 % (*R*)] (*7*) and rhubarb stalks [36% (*S*) : 64 % (*R*)] (*8*). For quite some time only (*S*)-2-methylbutyric acid was believed to be "natural" due to its biosynthetic origin from enantiomerically pure L-isoleucine. Nevertheless, the before mentioned examples clearly demonstrate that there has to be another pathway leading to the formation of (*R*)-2-methylbutyric acid. So far this pathway has not been elucidated by e.g., isotope labeling experiments, but it was found that ethyl tiglate administered to apple fruits is converted to considerable amounts of (*R*)-2-methylbutyl derivatives (*9*). In mammals the *R*-pathway leading to the interconversion of L-isoleucine to alloleucine is well known (*10*). This proceeds via a transaminase reaction forming the α-keto acid which is subject to keto-enol tautomerism and gives rise to the (*R*)-enantiomer. Reamination leads then to the formation of alloleucine. Another proposed reaction mechanism occurs via (*R*)-methylmalonyl-CoA which is formed by propionyl-CoA-carboxylase. So far, this would be the only proposed pathway leading to enantiomeric excess of (*R*)-2-methylbutyric acid similar to the one found in *Veratrum album*.

Formation of Esters of 2-Methylbutyric Acid

The ethyl ester of 2-methylbutyric acid (EMB) is another important flavor compound whose (*S*)-configuration has been found with high enantiomeric purity in nature (*11–14*). For this reason it is assumed that artificial EMB is racemic (*15*) although the precursor 2-methylbutyric acid from natural sources could have any enantiomer ratio as discussed in the previous paragraph. Moreover, systematic investigation of the esterification indicates that EMB can even be of high (*S*)-enantiomeric excess if artificial processes are used.

Sulfuric acid is a common catalyst in industrial scale applications to convert acids to esters. 2-Methylbutyric acid [(*R*)/(*S*)=0.9/99.1] was esterified with ethanol from natural sources and sulfuric acid to give EMB with a yield of 84.3 % (2 h, 80 °C). The (*R*)/(*S*) ratio of EMB was 1.7/98.3 and, hence, in compliance with authentic reference material [(*R*)/(*S*)=2.2/97.8].

A biomimetic approach was developed next to form the ester by using ascorbic acid as catalyst (63 h, 60°C). The reaction yielded more than 10 % of natural EMB with an enantiomer ratio of (*R*)/(*S*)=1.5/98.5.

In conclusion, the enantiomer ratio of EMB is not a sufficient marker to distinguish natural from artificially produced EMB. The corresponding enantiomer ratios do not differ significantly from the authentic material. For this reason, a multilevel analytical approach e.g., by further analyzing by-products has to be applied to confirm the authenticity of EMB.

Chiral Analysis of Flavonoids

Some chiral flavonoids, e.g., flavanons as homoeriodictyol or hesperetin, or the flavonoid-like phyllodulcin have been newly introduced as flavoring substances or in the form of flavoring preparations or tastants during the last decade (*16–18*).

As well documented in the literature, flavanons are generated stereospecifically as (*2S*)-enantiomers from their corresponding chalcones with the enantiospecific chalcone isomerases *in vivo* (*19*) (Figure 2). Therefore, it could be assumed that determination of the enantiopurity will give a hint for authenticity. Generally, they occur as glycosides but have to be hydrolyzed to yield the aglycons as the most active flavoring compounds. During ripening, extraction and/or work up, the (*2S*)-flavanons can easily racemise via base/acid catalyzed abiotic mechanisms (Figure 2).
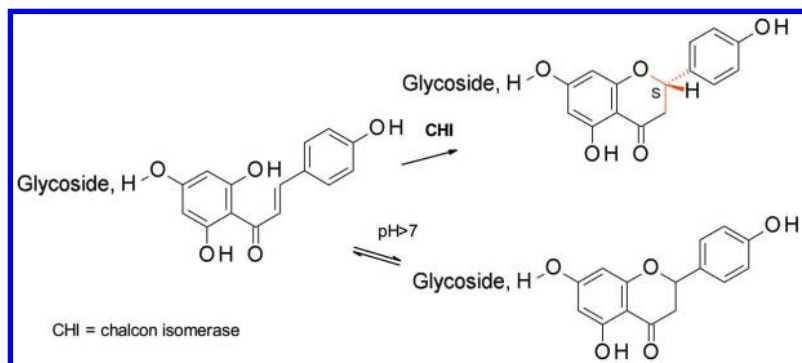
Figure 2. Mechanism of biotic generation of (2S)-flavanons and abiotic racemisation.

In fact, most commercially available flavanons, especially the aglycons are more or less racemic as shown for naringenin and hesperetin (*16*). But even native flavanons can occur or be exudated in a partially racemic form, as proven for homoeriodictyol from *Eriodictyon californicum*: even careful isolation from leaves, more specific from the leaf waxes led to a 4:6 (*R*)/(*S*) mixture (*16*). In contrast, we were able to isolate nearly pure (*2S*)-hesperitin via a similar mild extraction with methanol from a sample of fermented honeybush, *Cyclopia intermedia* (Figure 3).
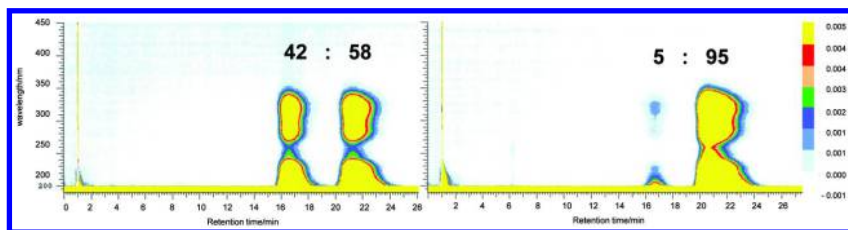
Figure 3. Chiral analysis of commercial hesperetin (Sigma, left) and (2S)-hesperetin isolated from fermented honeybush (right). Analytical conditions: ChromTec CHIRAL-AGP, 5 μm, 100x4.0 mm, 10 mM Na$_2$HPO$_4$, pH 7 / 2-propanol (99:1 / v:v) isocratic, 0.9 mL/min, room temperature, detection via DAD.

In contrast to the commonly occurring hesperetin, phyllodulcin (Figure 4) has only been detected in special variations of *Hydrangea ssp.* so far (e.g., Amacha (*20*),) and can be used as a potential marker for extracts and flavoring preparations originating from amacha. In nature, it occurs in the form of its glycosides mainly as the (3*R*)-(+) enantiomer but is mostly accompanied by its (3*S*)-(-) antipode in a ratio up to 5(+):1(-) (*21*). According to sensory studies, only (3*R*)-(+)-phyllodulcin expresses a strong sweetness (*22*).
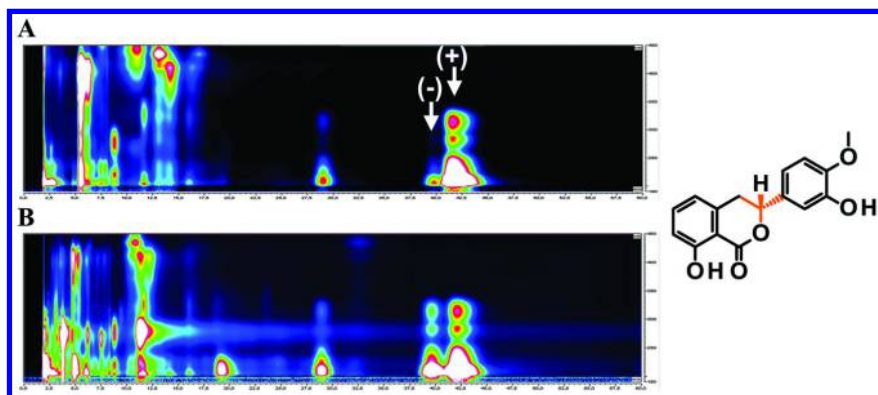
Figure 4. Chiral analysis of commercial (3R)-(+)-phyllodulcin (Sigma, A) and phyllodulcin in an extract treated with ion exchanger (B). Conditions see Table 1.

Table 1. Chiral Analysis of Phyllodulcin from Various Sources. Analytical Conditions: ChromTec CHIRAL-AGP, 5 μm, 100x4.0 mm, 10 mM Na₂HPO₄, pH 7 / 2-propanol (99:1 / v:v) isocratic, 0.9 mL/min, Room Temperature, Detection via DAD.

Test sample	Conc. [mass-%]	Conc. [area-%]	
	Phyllodulcin	(3S)-(–)	(3R)-(+)
Commercial standard	> 98	7.3	92.7
Isolated via prep. HPLC	> 98	4.9	95.1
Extracted with EtOH/H₂O	6.59	4.7	95.3
Extracted purified via ion exchange	4.03	26.6	73.4

In order to elucidate the potential of chiral analysis to authenticate extracts from *Hydrangea dulcis,* we analyzed the ratio of both enantiomers of the aglycone after different treatments during extraction (Table 1).

Due to the uncertainty whether racemization of chiral flavonoids has already occurred or might take place during the test, in most biological tests data about enantiospecific activity on biological targets is not or only insufficiently documented.

Reliable and Nonreliable Chiral Markers

Among the chiral flavoring substances only a few are recognized to have reliable enantiomeric distributions. Many flavoring substances are subject to variation arising from biogeneration, processing and storage. Well characterized, for example, is the degradation of linalool and linalyl acetate in bergamot essential oil and tea, respectively (*23*).

However, variations in enantiomer ratios of chiral flavoring substances can also arise from biosynthetic transformation of different raw materials. As an example rose oxide is usually obtained from geranium oils with *cis*-(-) (2*S*, 4*R*) being the most abundant isomeric form. Hereby, the enantiomeric ratio of (-)- and (+)-rose oxide is shifted during extraction of fresh and dried leaves by 80-75 % to 65-60 % (-)-*cis*- and *trans*-rose oxide, respectively (*24*, *25*). We could confirm these findings (Table 2) with the exception of 98.4 % *cis*-(-)-rose oxide in a self-prepared extract from *Pelargonium graveolens* leaves (*25*).

Table 2. Enantiomer Ratios of Citronellol and Rose Oxide Obtained from Dried and Fresh Leaves of *Pelargonium graveolens*

		citronellol		cis-rose oxide		trans-rose oxide	
P. graveolens	*Extraction*	*3S (%)*	*3R (%)*	*2S,4R (%)*	*2R,4S (%)*	*2R,4R (%)*	*2S,4S (%)*
dried leaves	Soxhlet (TBME)[1]	60.4	39.6	63.6	36.4	66.6	33.4
dried leaves	solvent extraction[2]	60.4	39.6	64.8	35.2	68.7	31.3
fresh leaves	Soxhlet (TBME)[1]	75.7	24.3	74.9	25.1	79.8	20.2
fresh leaves	solvent extraction[2]	75.7	24.3	76.1	23.9	78.4	21.6

[1] 20g sample with Soxhlet apparatus.   [2] 20g sample with Speed extractor, 1 min, 40°C, 100 bar, average values of dichloromethane, ethyl acetate and heptane extracts.

The enantiomer shift of rose oxide during processing of *Pelargonium graveolens* leaves is correlated with the enantiomeric ratio of the precursor compound citronellol (*26*, *27*). With plant material other than Pelargonium spec., inverted enantiomer ratios of rose oxide can be obtained when converting citronellol by biomimetic synthesis. For example, *Melissa officinalis* essential oil with > 84% (+)-citronellol (*28*) mixed with a chlorophyll containing plant extract and and ambient air forms citronellyl hydroperoxides via a biomimetic oxidation upon exposure to daylight. These hydroperoxides easily degrade to the corresponding citronellyl diols. Rose oxide is then obtained by cyclization of the diols catalyzed by citric acid while keeping the chirality at position C4. Furthermore, own experiments have shown that the *cis* diastereomer is predominantly formed (80 % *cis* : 20 % *trans*) due to stereochemical hindrance

during cyclization. This biomimetic approach leads to rose oxide qualities, which differ in their stereoisomeric compositions. This needs to be considered in authenticity evaluation.

Conclusions

Enantiomeric distributions of chiral flavor compounds show broad variation in nature. Physical treatment, enzymes and fermentation also generate enantiomeric shifts. In addition, food processing and storage affect the enantio-distribution. Therefore, for final interpretations and conclusions all data need to be based on multiple methods and authentic reference samples.

References

1. Regulation (EC) No 1334/2008 of the European Parliament and of the Council on flavourings and certain food ingredients with flavouring properties for use in and on foods. *Off. J. Eur. Union* **2008**, L 354/34.

2. *EFFA Guidance Document for the Production of Natural Flavouring Ingredients V2.0 (11/03/13) 5.2. Geometric and optical isomers*; http://www.effa.eu/en/publications/guidance-documents.

3. Schreier, P.; Bernreuther, A.; Huffer, M. *Analysis of Chiral Organic Molecules*; Walter de Gruyter: Berlin, 1995.

4. Krammer, G. E.; Weckerle, B.; Brennecke, S.; Weber, B.; Kindel, G.; Ley, J.; Hilmer, J.-M.; Reinders, G.; Stöckigt, D.; Hammerschmidt, F.-J.; Ott, F.; Gatfield, I.; Schmidt, C. O.; Bertram, H.-J. Product-Oriented flavour research: Learnings from the past, visions for the future. *Mol. Nutr. Food Res.* **2006**, *50*, 345–350.

5. Baldermann, S.; Kato, M.; Fujita, A.; Fleischmann, P.; Winterhalter, P.; Watanabe, N. Biodegradation of Carotenoids - An Important Route to Scent Formation. In *Carotenoid Cleavage Products*; Winterhalter, P., Ebeler, S., Eds.; ACS Symposium Series 1134; American Chemical Society: Washington, DC, 2013; pp 65−72.

6. Malowicki, S. M. M.; Martin, R.; Qian, M. C. Volatile composition in raspberry cultivars grown in the Pacific Northwest determined by stir bar sorptive extraction-gas chromatography-mass spectrometry. *J. Agric. Food Chem.* **2008**, *56*, 4128–4133.

7. Karl, V.; Guster, J.; Dietrich, A.; Maas, B.; Mosandl, A. Stereoisomeric flavour compounds LXVIII. 2-, 3-, and 4-alkyl-branched acids, part 2. chirospecific analysis and sensory evaluation. *Chirality* **1994**, *6*, 427–434.

8. Dregus, M.; Schmarr, H. G.; Takahisa, E.; Engel, K. H. Enantioselective analysis of methyl-branched alcohols and acids in rhubarb (*Rheum rhabarbarum* L.) stalks. *J. Agric. Food Chem.* **2003**, *51*, 7086–7091.

9. Hauck, T.; Weckerle, B.; Schwab, W. Metabolism of ethyl tiglate in apple fruits leads to the formation of small amounts of *(R)*-ethyl 2-methylbutanoate. *Enantiomer* **2000**, *5*, 505–512.

10. Mamer, O. A. Initial catabolic steps of isoleucine, the R-pathway and the origin of alloisoleucine. *J. Chromatogr., B* **2001**, *758*, 49–55.

11. Rettinger, K.; Karl, V.; Schmarr, H.-G.; Dettmar, F.; Hener, U.; Mosandl, A. Chirospecific analysis of 2-alkyl-branched alcohols, acids, and esters: chirality evaluation of 2-methylbutanoates from apples and pineapples. *Phytochem. Anal.* **1991**, *2*, 184–188.

12. Matich, A.; Rowan, D. Pathway analysis of branched-chain ester biosynthesis in apple using deuterium labeling and enantioselective gas chromatography-mass spectrometry. *J. Agric. Food Chem.* **2007**, *55*, 2727–2735.

13. Werkhoff, P.; Güntert, M.; Krammer, G.; Sommer, H.; Kaulen, J. Vacuum headspace method in aroma research: flavor chemistry of yellow passion fruit. *J. Agric. Food Chem.* **1998**, *46*, 1076–1093.

14. de la Peña Moreno, F.; Blanch, G. P.; Flores, G.; Ruiz del Castill, M. L. Development of a method based on on-line reversed phase liquid chromatography and gas chromatography coupled by means of an adsorption–desorption interface for the analysis of selected chiral volatile compounds in methyl jasmonate treated strawberries. *J. Chromatogr., A* **2010**, *1217*, 1083–1088.

15. Krueger, D. A. Detection of adulterated fruit flavors. In *Fruit Flavors: Biogenesis, Characterization, and Authentication*; Rouseff, R. L., Leahy, M. M., Eds.; ACS Symposium Series 596; American Chemical Society: Washington, DC, 1995 pp 70−78.

16. Ley, J. P.; Krammer, G.; Reinders, G.; Gatfield, I. L.; Bertram, H.-J. Evaluation of bitter masking flavanones from Herba Santa (*Eriodictyon californicum* (H. & A.) Torr., Hydrophyllaceae). *J. Agric. Food Chem.* **2005**, *53*, 6061–6066.

17. Ley, J. P.; Kindel, G.; Paetz, S.; Riess, T.; Haug, M.; Schmidtmann, R.; Krammer, G. *Use of Hesperetin for enhancing the sweet taste*; Patent WO 2007, 014, 879.

18. Reichelt, K. V.; Ley, J. P.; Hoffmann-Lücke, P.; Blings, M.; Paetz, S.; Riess, T. *Sweetener-reduced products, flavoring mixtures for same, and method of producing such products*; 2011 EP 2, 298, 084-B1.

19. Jez, J. M.; Noel, J. P. Reaction mechanism of chalcone isomerase. *J. Biol. Chem.* **2002**, *277*, 1361–1369.

20. Kinghorn, A. D.; Soejarto, D. D.; Katz, N. L.; Kamath, S. K. Studies to identify, isolate, develop and test naturally occurring noncarinogenic sweeteners that may be used as dietary sucrose substitutes. *Gov. Rep. Announce. Index (U.S.)* **1985**, *85* (11), 47; Report, NIDR/CR-85/01; Order Number PB85-158079/GAR .

21. Yoshikawa, M.; Murakami, T.; Ueda, T.; Shimoda, H.; Yamahara, J.; Matsuda, H. Development of bioactive functions in *Hydrangea dulcis* folium. VII. Absolute stereostructures of 3*S*-phyllodulcin, 3*R*- and 3*S*-phyllodulcin glycosides, and 3*R*- and 3*S*-thunberginol H glycosides from the leaves of *Hydrangea macrophylla* Seringe var. thunbergii Makino. *Heterocycles* **1999**, *50*, 411–418.

22. Kinghorn, A. D.; Compadre, C. M. Less common high-potency sweeteners. *Food Sci. Technol. (N.Y.)* **2001**, *112*, 209–233.

23. Orth, A. M.; Engel, K. H. Assessment of dietary exposure to flavourings via consumption of flavoured teas. Part 1: occurrence and contents on monoterpenes in Earl Grey teas marketed in the European Union. *Food Addit. Contam., Part A* **2013**, *30*, 1701–1714.

24. Kreis, P.; Mosandl, A. Chiral compounds of essential oils. Part XIII. Simultaneous chirality evaluation of geranium oil constituents. *Flavour Fragrance J.* **1993**, *8*, 161–168.

25. Wüst, M.; Rexroth, A.; Beck, T.; Mosandl, A. Structure elucidation of *cis*- and *trans*-rose oxide ketone and its enantioselective analysis in geranium oils. *Flavour Fragrance J.* **1997**, *12*, 381–386.

26. Wüst, M.; Beck, T.; Mosandl, A. Conversion of citronellyl diphosphate and citronellyl β-D-glucoside into rose oxide by *Pelargonium graveolens*. *J. Agric. Food Chem.* **1999**, *47*, 1668–1672.

27. Wüst, M.; Rexroth, A.; Beck, T.; Mosandl, A. Mechanistic aspects of the biogenesis of rose oxide in *Pelargonium graveolens* L'Héritier. *Chirality* **1998**, *10*, 229–237.

28. Kreis, P.; Mosandl, A. Chiral compounds of essential oils. Part XVI. Enantioselective multidimensional gas chromatography in authenticity control of balm oil (*Melissa officinalis* L.). *Flavour Fragrance J.* **1994**, *9*, 249–256.

Chapter 2

Cyclodextrin Derivatives as Stationary Phases for the GC Separation of Enantiomers in the Flavor and Fragrance Field

Cecilia Cagliero, Barbara Sgorbini, Chiara Cordero, Erica Liberto, Patrizia Rubiolo, and Carlo Bicchi*

Dipartimento di Scienza e Tecnologia del Farmaco, University of Torino, Via Pietro Giuria 9, 10125 Torino, Italy
***E-mail: carlo.bicchi@unito.it.**

This chapter will examine the chiral recognition of volatile odorants in the flavor and fragrance field, by enantioselective gas chromatography (Es-GC) with cyclodextrin derivatives as chiral stationary phases. The first part covers enantiomers and odor, the need for chiral recognition, and the evolution of chiral stationary phases for Es-GC. This is followed by a more detailed discussion of cyclodextrins and the theoretical aspects of enantiomer separation, and applications of these techniques to Es-GC. The last part deals with the strategies of routine chiral recognition using cyclodextrin derivatives as chiral stationary phases; this is illustrated through some examples concerning complex samples. The section describes (i) the potential of multidimensional techniques in routine analysis, (ii) automatic identification and recognition of enantiomers, (iii) the role of mass spectrometry in Es-GC-MS, (iv) fast Es-GC in chiral recognition, and (v) the use of total analysis systems in chiral recognition.

1. Introduction

Metabolic processes in plants or animals are almost always stereospecific, and the resulting metabolites are very often characterized by an excess of one if the enantiomers. Enantiomer recognition and the determination of enantiomeric excess (ee) and/or ratio (er) of a chiral compound, are therefore important steps to

characterize a matrix and its biological activity, in particular in the fields of flavor and fragrance. Enantiomeric recognition is important (i) to correlate chemical composition to organoleptic properties; (ii) to define the biosynthetic pathway of a metabolite, (iii) to characterize a matrix; (iv) to determine the geographic origin of a "natural" sample; and (v) to implement quality control and to detect frauds or adulteration of "natural" samples (*1*).

2. Chiral Recognition and Enantioselective Gas Chromatography (Es-GC)

Gas chromatography (GC), in particular when combined with mass spectrometry (MS), is currently the preferred technique to study the composition of the volatile fraction of natural products. However, enantiomer separation with GC requires chiral stationary phases (CSPs) able to interact in different ways with each enantiomer of the investigated chiral compound(s). Several chiral selectors operating on different principles have been proposed for Es-GC, and three selectors, distinguishable for their selector-selectand interaction mode, have been successfully applied to routine separation of enantiomers (*2*):

- chiral amino acids via hydrogen bonding;
- chiral metal coordination compounds via complexation;
- cyclodextrin derivatives via inclusion (inter alia).

Cyclodextrin derivatives (CDs) are the most popular chiral stationary phases in the flavor and fragrance field today, because of their wide range of applicability and high enantioselectivity. These characteristics make it possible to separate the enantiomers of a large number of chiral molecules with different structures and organic functions, without the need for preliminary derivatization to the corresponding diastereoisomers. The variety of CSPs now available means that most enantiomer pairs can be separated.

3. Chiral Stationary Phases Based on (inter alia) Inclusion: Cyclodextrin Derivatives as Chiral Selectors for Es-GC

Cyclodextrins, also known as cycloamyloses, cycloglucanes or cyclomaltooligoses, are a homologous series of non-reducing cyclic oligosaccharides made up of six to twelve (β)-D-glucopyranose units linked by α-1,4-glycosidic bonds. They are obtained via enzymatic degradation of starch by cyclodextrin glycosyltransferase, from either *Klebsiella pneumonia* or *Bacillus macerans*. The best known and most widely available CDs are those with six (α-CD), seven (β-CD) or eight (γ-CD) sugar units (Figure 1).

The first chiral separation via GC using CD as stationary phase was described by Koscielski and Sybilska (*3*); in 1983 they separated the enantiomers of α- and β-pinene, Δ-3-carene, and hydrogenated derivatives, on columns packed with a mixture of native α-cyclodextrin in formamide. Despite their high separation factor α, these columns had a limited lifetime and low efficiency. CDs were

next applied to capillary gas chromatography, almost contemporarily in 1987 by Juvancz's (*4*, *5*) and in 1988 by Schurig's groups (*6*). Two different approaches were adopted to provide columns with high efficiency and enantioselectivity: (a) the use of CD derivatives that are liquid at room temperature, e.g., per-*n*-pentylated cyclodextrins (*7*, *8*) and (b) the use of solid or semi-solid persubstituted β- or γ-cyclodextrins diluted in moderately polar polysiloxanes (e.g., OV-1701) in order to combine the high enantioselectivity of the modified CDs with the very good gas chromatographic properties of polysiloxanes (*6*, *9–12*). Dilution in polysiloxane is almost the only approach now adopted for routine use.
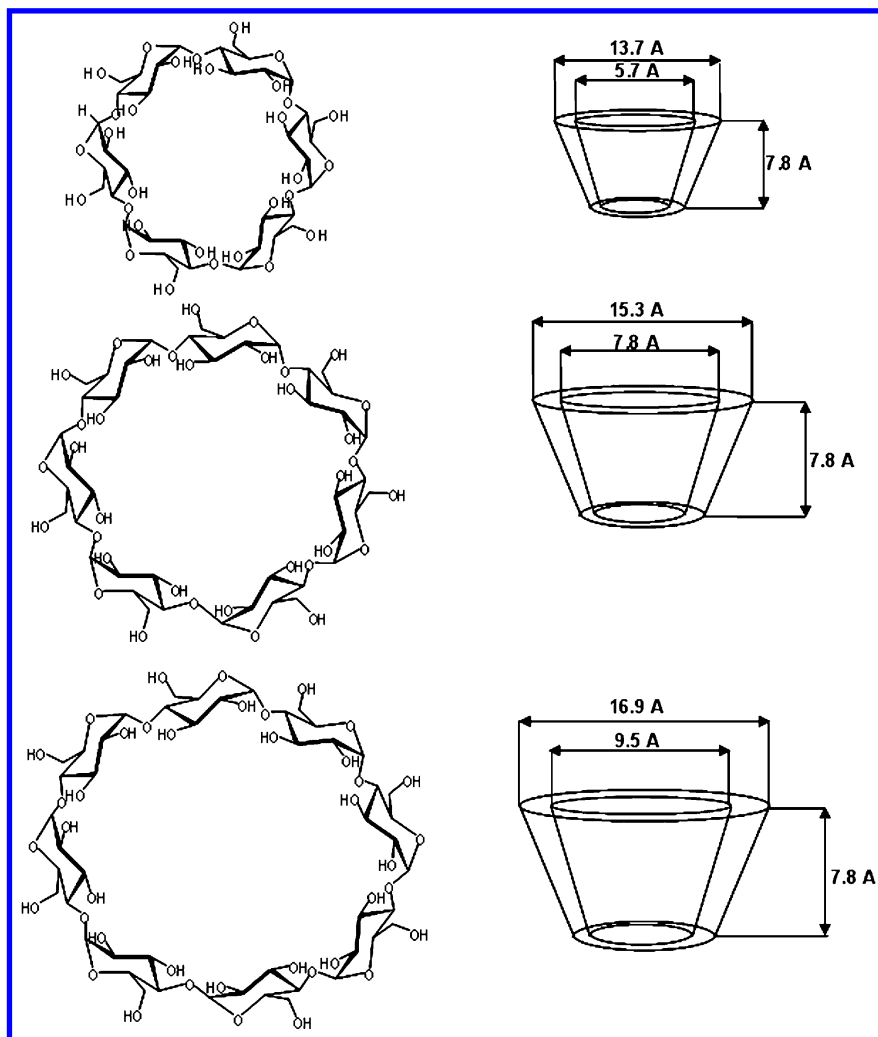

Figure 1. Structures of α-, β- and γ-cyclodextrins.

3.1. Chemistry of Cyclodextrin Derivatives as Chiral Selectors for Es-GC

The presence of three hydroxyl groups that can be regio-selectively alkylated and acylated offers an enormous number of possible α-, β-, γ-cyclodextrin derivatives. Several derivatives have been described, mainly based on β-CDs, but a universally applicable derivative has not yet been found. A fundamental improvement was the introduction of bulky substituents (e.g., the *tert*-butyldimethylsilyl (TBDMS) or *tert*-hexyldimethylsilyl-(THDMS) groups) at the primary C6-hydroxyl groups, first proposed by Blum and Aichholz (*13*), but mainly developed by Mosandl's group (*14*). The bulky substituent affects the CD conformation, and inhibits the entrance to the cavity at the smaller rim, thus orienting the analyte/CD interaction towards the wider rim, where the substituents at the C2- and C3-secondary hydroxyl groups drive the enantioselective interaction.

Several approaches to improve enantioselectivity and chromatographic results have been attempted: (a) synthesis of "fully asymmetrically substituted derivatives" (*15*), i.e., with different substituents at the C2- and C3-secondary hydroxyl groups, and a bulky substituent (e.g., *tert*-butyldimethylsilyl-, TBDMS) at the C6-primary hydroxyl groups, to obtain synergic enantioselectivity, (b) mixing two CDs or condensing two CD units, although in this case the resulting enantioselectivity was not as satisfactory as expected (*16*, *17*); (c) mixing two structurally different chiral selectors, e.g., amino acid derivatives and cyclodextrin derivatives (*18–20*), to extend the range of enantioselectivity, and (d) cyclodextrin selector(s) chemically and permanently linked to a polysiloxane backbone (Chirasil-Dex) (*21–23*).

3.2. Mechanism of Chiral Recognition of Cyclodextrin-Based CSP in ES-GC

Chiral recognition with modified cyclodextrins is a multimodal process and may, among others, involve inclusion, hydrogen-bonding, dispersion forces, dipole–dipole interactions, electrostatic interactions, and hydrophobic interactions (*24*, *25*). The separation of enantiomers is due to the differences in the low-energy interaction between the diastereomeric CD selector–selectand (enantiomer) association equilibria; the high efficiency of capillary GC columns also plays a fundamental role in achieving separation (*26*). Important contributions to the understanding of the mechanisms of chiral recognition with CD derivatives were made by Schurig and coworkers, who developed a thermodynamic model to describe enantiomer separation (*26*, *27*), and by Lipkowitz et al. (*28*, *29*), who studied some aspects of the enantiomer separation with molecular modelling.

The thermodynamic results have a concrete impact on routine Es-GC, because the separation of enantiomers by ES-GC with CD derivatives as CSP is based on fast kinetics and is thermodynamically driven, implying that optimal enantiomer separation requires the lowest possible operation temperature.

4. Measurement of the Enantiomeric Distribution

Enantiomeric distribution is usually expressed in terms of *enantiomeric excess* (*ee*), *enantiomeric composition* (*ec*) or *enantiomeric ratio* (*er*) (*30*).

Enantiomeric excess, also known as enantiomeric purity, expresses the increased abundance of one enantiomer compared to the other, and is defined as

$$ee = \frac{E_1 - E_2}{E_1 + E_2} \tag{1}$$

where E_1 and E_2 are the areas of the enantiomers, E_1 being the major enantiomer; *ee* ranges from 0 for racemic mixtures to 1 for pure E_1. In routine practice, *ee* is often expressed as a percentage.

Enantiomeric composition (*ec*) is defined as the molar fraction of the major enantiomer in a mixture:

$$ec = x_{E_1} = \frac{E_1}{E_1 + E_2} \tag{2}$$

In this case, ec is also generally expressed as a percentage.

Finally, the *enantiomeric ratio*, *er*, is defined as

$$er = \frac{E_1}{E_2} \tag{3}$$

where E_1 is the major enantiomer; *er* can range from *er* = 1, for a racemic mixture, to *er* = ∞, for pure E_1. The terms er and ee are correlated as follows

$$ee = \frac{(er - 1)}{(er + 1)} \tag{4}$$

and

$$er = \frac{(1 + ee)}{(1 - ee)} \tag{5}$$

In routine analysis, correct measurement of the above parameters requires that the peaks of the two enantiomers are baseline-separated, i.e., their resolution must be $R_S \geq 1.5$.

5. Enantioselective GC Analysis with Cyclodextrins in the Flavor and Fragrance Field

Cyclodextrin derivatives are the most widely used chiral selectors in Es-GC in the flavour and fragrance field. Their main advantages are:

- They can separate underivatized enantiomers, therefore natural product samples can be analyzed directly without further manipulation;
- they can separate almost all classes of volatile chiral compounds, owing to the wide range of selectivity covered by the large number of available CD derivatives;

19

In Importance of Chirality to Flavor Compounds; Engel, et al.;
ACS Symposium Series; American Chemical Society: Washington, DC, 2015.

- the CD-based CSP columns have good chromatographic performance (efficiency and inertness) and operate at a wide range of temperatures, owing to their dilution in moderately polar polysiloxanes.

However, CDs also have some disadvantages:

- The absence of a "universal" cyclodextrin derivative separating most chiral compounds; a laboratory must therefore have a number of columns coated with different CD-based CSPs;
- the difficulty of identifying enantiomers and measuring ee and/or er in complex samples with mono-dimensional Es-GC, because of the increased possibility of peak overlapping, exacerbated by the double number of peaks when chiral analyte(s) are separated;
- the long analysis time, due to the need for long columns and low temperature program rates, because of the cyclodextrin mechanism of separation.

Partly in view of these disadvantages, the next three sections will examine the optimization of strategies for the chiral recognition of volatile markers by Es-GC and Es-GC-MS, with CD as chiral selectors, in complex mixtures in the flavor and fragrance field; the observations are mainly based on the authors' everyday experience.

6. Analysis of Enantiomers in Complex Samples

Two complementary but distinct approaches are available for the qualitative (and, as a consequence, in some cases quantitative) recognition of enantiomers in complex samples: i) the first is to adopt a second dimension in separation (by conventional heart-cut GC-GC or comprehensive 2D GC), (ii) the second approach is to use a second dimension in detection, by coupling GC with mass spectrometry (*31*). The latter method applies a strategy that is the converse of the conventional one, i.e., the enantiomer(s) are located in the chromatogram by their MS spectra and identified by GC data (i.e., Kovats retention indices (*Is*) (*32*) or linear retention indices (*I^Ts*) (*33*). This is because MS is not a chiral probe, making the mass spectra of two enantiomers indistinguishable. Conversely, chromatographic data (and in particular linear retention indices) are reliable and effective parameters for enantiomer identification, being characteristic for each analyte (enantiomer); similar considerations can be made with locked retention times (*34*) (see below).

Based on these considerations, a MS library specific for the identification of enantiomers in the flavor and fragrance field has been developed at an interlaboratory level, using I^Ts values "interactively" in parallel to MS spectra (*31*). It is based on the interactive I^T/mass spectrum system (*35*) developed by Costa et al. (*36*) for the flavor and fragrance field: I^Ts are calculated automatically and incorporated as an active part of the matching criteria, together with mass spectra. The correct identification of an analyte is assured by the

range (determined preliminarily) within which its I^T must fall (Retention Index Allowance (RIA). Four cyclodextrin derivatives diluted at 30% in PS-086 were used to separate a large number of racemates usually analyzed in the flavor and fragrance field; these are:

(i) 6[I-VII]-O-methyl-3[I-VII]-O-pentyl-2[I-VII]-O-methyl-β-cyclodextrin (*37, 38*),
(ii) 6[I-VII]-O-TBDMS-3[I-VII]-O-methyl-2[I-VII]-O-methyl-β-cyclodextrin (*39*),
(iii) 6[I-VII]-O-TBDMS-3[I-VII]-O-ethyl-2[I-VII]-O-ethyl-β-cyclodextrin (*40*),
(iv) 6[I-VII]-O-TBDMS-3[I-VII]-O-acetyl-2[I-VII]-O-acetyl-β-cyclodextrin (*39*).

The library consists of 134 racemates whose I^T values were determined on four columns coated with these four CD chiral selectors. Table 1 reports the list of racemates included in the first version of the library.

The same approach can be adopted with another software package, AMDIS, (Automatic Mass Spectral Deconvolution), developed by the National Institute of Standards and Technology (USA) (*41*).

Retention time locking (RTL) is an approach that provides reliable identification of an analyte from its GC retention data in programmed temperature analysis, based on the adjustment of the inlet pressure necessary to achieve the desired match in retention time(s) of an analyte(s) with similarly configured GC systems (*34*).

7. Fast Es-GC Analysis with Cyclodextrins as Chiral Stationary Phases

As already mentioned, Es-GC separation of enantiomers with CDs as chiral selectors is based on fast kinetics, and is entirely governed by thermodynamics; as a consequence, it closely depends on temperature. Long analysis times are therefore to be expected, since long columns and low temperature program rates have to be applied.

Routine application requires the development of fast Es-GC methods, in order to run the large number of control analyses required. Routine fast-GC can in general be obtained by acting on column length, inner diameter, and/or flow-rate, and has resulted in the adoption of narrow bore (NB) columns (d_c: 100 μm) (*42*). NB columns not only increase analysis speed and analyte detectability, because of peak sharpening (*43*), but also reduce the enantiomer elution temperature, because of their shorter length. Together, this results in a gain of enantioselectivity that compensates (in full or in part) for the loss of efficiency (N) due to column shortening. Fast enantiomer separations (even in a few seconds) were already achieved in the early 1990s, with short columns for low-complexity samples and/or those containing a limited number of enantiomers to be simultaneously analyzed (*44–46*). With medium-to-high complexity samples, as in the flavor and fragrance field, a highly efficient separation system combined with single- or multiple-ion monitoring-MS detection (SIM-MS or MIM-MS) is necessary to measure ee and/or er correctly. This paragraph discusses the two complementary

methods developed and adopted in the authors' laboratory to speed up routine Es-GC analyses (*47*, *48*). They are illustrated through the analysis of rosemary and bergamot essential oils.

Table 1. List of Compounds Included in the Library (*31*)

Hydrocarbons	*Heterocycles*	*Lactones*
α-Phellandrene	Ambroxide	Aerangis lactone
α-Pinene	Menthofuran	3-Methyl-γ-decalactone
β-Citronellene	Rose oxide	δ-Decalactone
β-Phellandrene	*Alcohols*	δ-Dodecalactone
β-Pinene	α-Bisabolol	δ-Heptalactone
Camphene	1-Octen-3-ol	δ-Hexalactone
Caryophyllene	1-Phenylethanol	δ-Nonalactone
Limonene	1-Phenyl-1-propanol	δ-Octalactone
Sabinene	1-Phenyl-2-pentanol	δ-Undecalactone
Acids	2-Butanol	ε-Decalactone
Citronellic acid	2-Heptanol	ε-Dodecalactone
2-Methylbutyric acid	2-Hexanol	γ-Decalactone
2-Phenylpropionic acid	2-Methylbutanol	γ-Dodecalactone
Chrysanthemic acid	2-Octanol	γ-Heptalactone
Esters	2-Pentanol	γ-Hexalactone
α-Terpinyl acetate	2-Phenyl-1-propanol	γ-Nonalactone
Bornyl acetate	3-Hexanol	γ-Octalactone
Bornyl isovalerate	3-Octanol	γ-Pentadecalactone
Butyl butyrolactate	4-Methyl-1-phenylpentanol	γ-Pentalactone
cis-3-Hexenyl 2-methylbutyrate	6-Methyl-5-hepten-2-ol	γ-Tetradecalactone
cis-Carvyl acetate	α-Terpineol	γ-Undecalactone
Dihydrocarvyl acetate	Borneol	Massoia decalactone
Dimethyl methylsuccinate	*cis*- Myrtanol	Massoia dodecalactone
Ethyl 2-methylbutyrate	Citronellol	Whiskey lactone
Ethyl 2-phenylbutyrate	Fenchyl alcohol	*Ketones*
Ethyl 3-hydroxybutyrate	Geosmin	1,8-Epoxy p-menthan-3-one

Table 1. (Continued). List of Compounds Included in the Library (*31*)

Hydrocarbons	*Heterocycles*	*Lactones*
Ethyl 3-hydroxyhexanoate	Isoborneol	3,6-Dimethylocta 2-en-6-one
Ethyl 3-methyl-3-phenylglycidate	Isomenthol	3-Methylcyclohexanone
Isobornyl acetate	Isopinocampheol	3-Oxocineole
Isobornyl isobutyrate	Isopulegol	α-Damascone
Lavandulyl acetate	Lavandulol	α-Ionone
Linalyl acetate	Linalool	β-Irone
Linalyl cinnamate	Linalool oxide	Camphor
Menthyl acetate	Menthol	Camphorquinone
Methyl 3-hydroxyhexanoate	Neoisomenthol	Carvone
Methyl dihydrofarnesoate	Neomenthol	Fenchone
Neomenthyl acetate	Nerolidol	Isomenthone
Nopyl acetate	Octan-1,3-diol	Menthone
Propylene glycolbutyrate	Patchouli alcohol	Methylcyclopentenolone
Aldehydes	Perillyl alcohol	Nootkatone
Citronellal	Terpinen-4-ol	Piperitone
Cyclamen aldehyde	Tetrahydrolinalool	Pulegone
Hydroxycitronellal	*trans*-Myrtanol	Verbenone
Myrtenal	Viridiflorol	
Perillyl aldehyde		

The first approach consists of searching for the best trade-off between speed of analysis and loss of resolution of chiral compounds (*48*). This may be at the expense of the separation of the other sample components, provided that baseline separation of the enantiomers of the chiral compound(s) investigated is maintained, in order to determine *ee* or *er* correctly. MS therefore plays a crucial role, because it can assign the separated enantiomers by operating in extract-ion, SIM- or MIM-MS modes. Analysis time is reduced by exploiting the increased resolution obtained with columns coated with the latest-generation CD derivatives (6[I-VII]-*O*-TBDMS-2[I-VII]-*O*-ethyl-3[I-VII]-*O*-methyl-β-CD in PS086) simultaneously applied to the chiral recognition of several chiral compounds ("the one column for one problem" approach) (*49*), by acting on column dimension, flow rate and temperature program.

Rosemary essential oil is characterized by various chemotypes that contain several chiral components (*50*); in this case, the sample investigated contained, among others, camphor, linalool, borneol, terpinen-4-ol, and α-terpineol.

Figure 2 shows the part of the Es-GC–MS profile of the rosemary essential oil where chiral markers elute, together with the identification of peaks of chiral components.
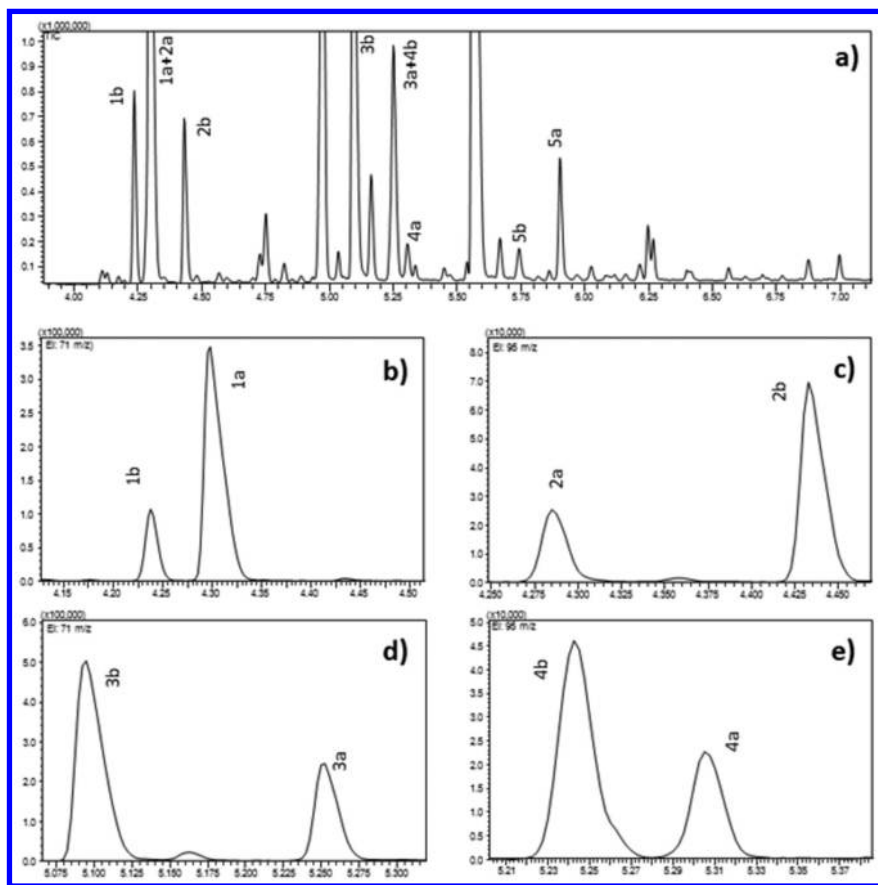

Figure 2. (a) Es-GC–MS profile of a rosemary essential oil. Column: 30% 6I-VII-O-TBDMS-2I-VII-O-ethyl-3I-VII-O-methyl-β-CD in PS086 (10m ×0.10mm d_c, 0.10 μm d_f); flow rate: 1 mL/min; temperature program: 50°C-10°C/min-220°C); extract-ion profiles of (b) linalool (71 m/z), (c) camphor (95 m/z), (d) terpinen-4-ol (71 m/z), (e) borneol (95 m/z). Peaks: 1: camphor 2: linalool, 3: borneol, 4: terpinen-4-ol, 5: α-terpineol; a: (R) enantiomer, b: (S) enantiomer.

The results of the analysis on a NB column (l: 10m, d_c: 0.10mm, d_f: 0.10 μm) at 10°C/min show that the analysis time is reduced to 7 minutes, but that (R)-camphor (1a) and (R)-linalool (2a) and (R)-borneol (3a) and (S)-terpinen-4-ol (4b) coelute; however, the selected extract-ion profiles are base-line separated, thus affording a correct *er* or *ee* determination.

The second approach (*47*) is based on the opposite strategy, i.e., the analysis time is shortened by seeking to maximize separation efficiency of the chromatographic system, by optimizing analysis conditions. Routine analyses of large numbers of different samples in a given field (e.g., aromas from different matrices) are in general carried out under the same standardized GC conditions, partly because of the possibility of automatically identifying peaks from chromatographic data (relative retention times, linear retention indices, retention time locking, etc.). Usually, satisfactory separations are obtained under non-specific routine-conditions, thanks to much-higher-than-required efficiency of the chromatographic system, to the detriment of analysis times. Optimization of analysis conditions for a specific sample, with a dedicated method for each matrix, can successfully speed up routine GC analyses considerably. This approach is based on the theoretical and practical studies done by Blumberg and co-workers on fast-GC (*51*, *52*), which resulted in the well-known GC method-translation (*53*). This method requires the optimal temperature program to be defined for a given sample; from this the flow-rate producing the highest efficiency (i.e., the plate number) of a given column (efficiency-optimized flow, EOF), or flow-rate, column dimensions, and carrier gas corresponding to the shortest analysis time for a given required plate number (speed-optimized flow, SOF) are determined (*51*, *53*).

The optimization of Es-GC analysis conditions of bergamot essential oil with a conventional column (30% 6[I-VII]-*O*-TBDMS-2[I-VII]-*O*-ethyl-3[I-VII]-*O*-methyl-β-CD in PS086, l: 25 m, d_c: 0.25 mm, d_f: 0.25 μm) involved three main steps: (a) choice of initial conditions to be optimized, (b) determination of optimal multi-rate temperature program for a pre-determined fixed column pressure, and (c) determination of optimal pressure (i.e., flow-rate) for the normalized optimal multi-rate temperature program.

Bergamot essential oil is characterized by seven main chiral markers: α-pinene (1), β-pinene (2), sabinene (3), limonene (4), linalool (5), linalyl acetate (6), and α-terpineol (7) (*54*). Under the initial analysis conditions, i.e., with the conventional column and using routine reference conditions (flow rate: 1 mL/min, temperature program: 50°C-220°C at 2°C/min), bergamot essential oil presented two non-separated critical clusters: (*R*)-β-pinene (2a), (*R*)-sabinene (3a), and β-myrcene, and (*R*)-α-terpineol (7a) and neral. Figure 3 reports the Es-GC patterns of the bergamot essential oil analyzed (a) under routine conditions and (b) under optimized multi-rate temperature program with the conventional column and (c) under optimized conditions after method translation with a NB column (l: 10 m, d_c: 0.10 mm, d_f: 0.10 μm). The optimized temperature program with the conventional column (50°C//2.33°C/min //102°C//10.4°C/min//220°C) provided the separation of (*R*)-α-terpineol (7a) from neral but not that of (*R*)-β-pinene (2a) from β-myrcene. The next step was to optimize the flow rate by determining the initial EOF (initial flow that maximizes column efficiency and peak resolution) and calculating the initial SOF (initial flow that minimizes analysis time at fixed efficiency) (*55*). SOF can be calculated from EOF with the equation SOF = √2 EOF (*55*), i.e., the initial EOF was here 1 mL/min, so that the initial SOF was 1.4 mL/min, and the corresponding heating rates were 2.76 and 12.55°C/min. Under these conditions, the analysis time was about 23 min.
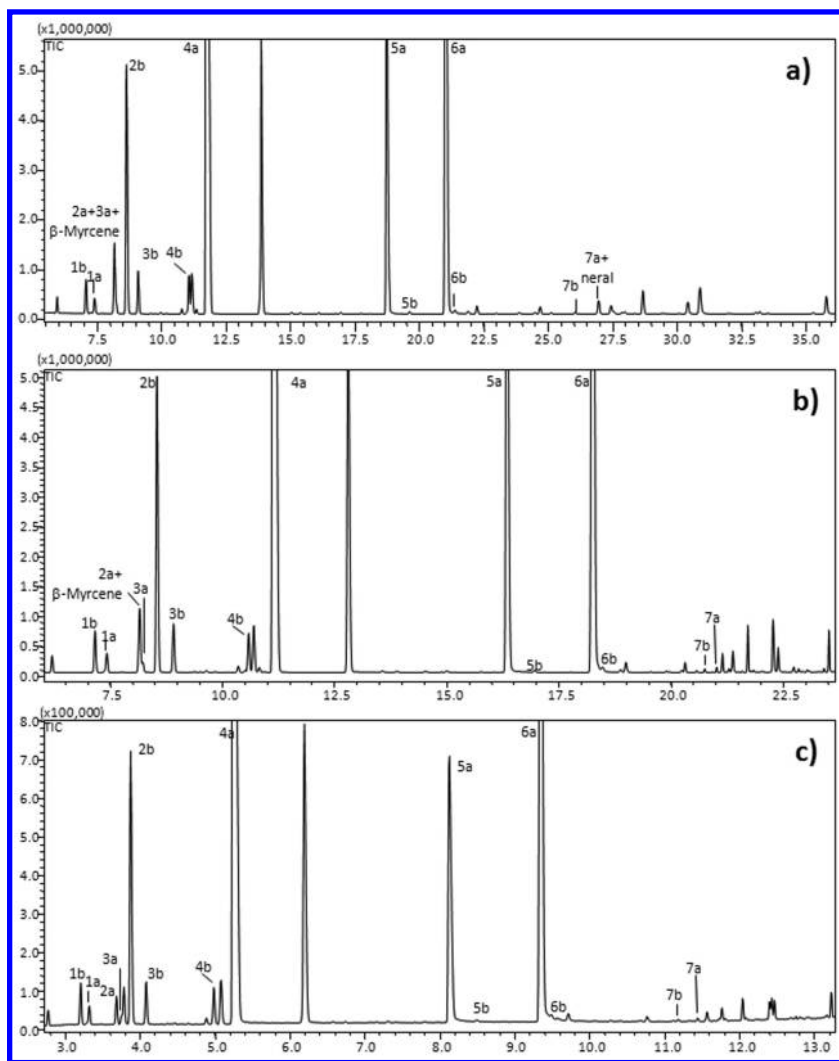
Figure 3. Es-GC–MS profile of a bergamot essential oil. Column: 30% 6[l-VII]-O-TBDMS-2[l-VII]-O-ethyl-3[l-VII]-O-methyl-β-CD in PS086 (25m×0.25mm d_c, 0.25 μm d_f); a) reference conditions (flow: 1 mL/min, temp. prog.: 50°C-2°C/min-220°C), b) optimized cond. conventional d_c column (flow: 1 mL/min, temp. prog.: 50°C-2.33°C/min-102-10.4°/min-220°C), c) optimized cond. 10m NB column (flow: 0.4 mL/min, temp. prog.: 50°C-4.74°C/min-102-21.12°C/min-220°C). Peaks: 1: α-pinene 2: β-pinene, 3: sabinene, 4: limonene, 5: linalool, 6: linalyl acetate, 7: α-terpineol; a: (R) enantiomer, b: (S) enantiomer.

The optimized EOF method with a conventional ((l: 25 m, d_c: 0.25 mm, d_f: 0.10 μm) column was then translated to the corresponding NB column (l: 10 m, d_c: 0.10 mm, d_f: 0.10 μm). The flow rate was reduced in proportion to the column

d_c, i.e., from 1.0 mL/min to 0.40 mL/min, thus assuring EOF operation of the NB column. Under these conditions, analysis time was reduced to nearly one third (i.e., the retention time of the last investigated peak was reduced from about 35 min to 13 min), with an improvement of peak resolution and separation of (R)-β pinene (2a) from β-myrcene.

8. Bornyl Acetate, a Common Chiral Compound Whose Enantiomers Are Difficult To Separate

The last example aims to emphasize the role of the diluting phase in chiral recognition with CDs as chiral selector. It concerns the "intriguing" story of the chiral recognition of camphor, borneol, isoborneol, iso-bornyl acetate, and bornyl acetate (Figure 4). While the first four are currently separated at least by one of the four CSPs used to build up the above-described automatic database, bornyl acetate is one of the few compounds that were not separated at all by one of them (see section 6). This made it necessary to explore other CSPs available in the library of columns of the authors' laboratory.
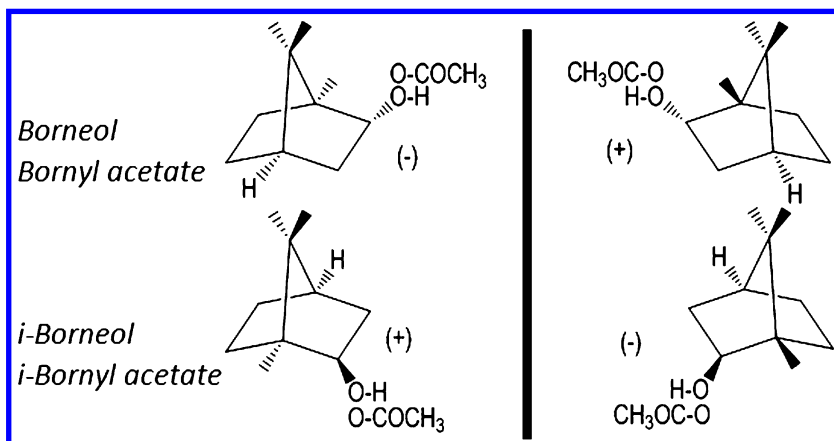

Figure 4. Absolute configurations of borneol, i-borneol, bornyl acetate and i-bornyl acetate.

Several attempts were made, and separation was achieved only with a conventional 50% 6[I-VIII]-O-THDMS-3[I-VIII]-O-acetyl-2[I-VIII]-O-acetyl-γ-CDX but diluted in OV-1701 (Figure 5c) column (l: 40 m, d_c: 0.20 mm, d_f: 0.20 μm) in 93 minutes; Figure 5b shows that the application of the same CD however diluted in PS-086 was not successful at all. The adoption of the strategy of optimization with a narrower and shorter column (column: l: 20 m, d_c: 0.15 mm, d_f: 0.15 μm) enabled the analysis time to be reduced to 35 minutes, while keeping the base-line separation of all five chiral compounds (Figure 5d). This example is a clear demonstration that the true enantioselective system is the combination stationary phase /diluting phase, although the chiral discrimination is of course due to the CD chiral selector.
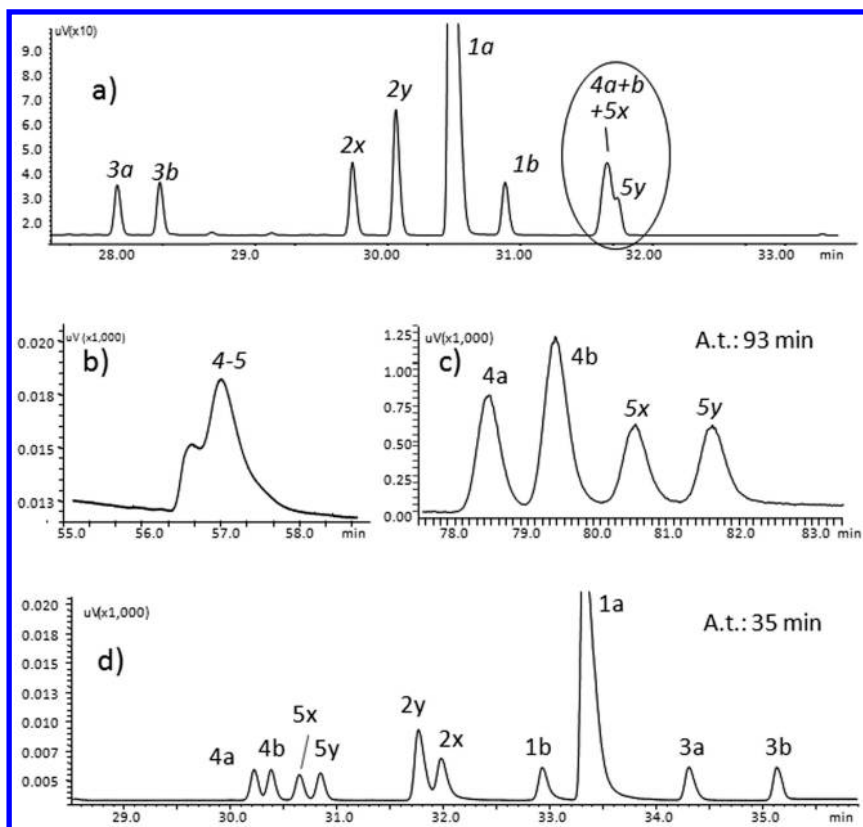
Figure 5. Separation of the enantiomers of 1: borneol, 2: i-borneol, 3: camphor, 4: bornyl acetate, 5: i-bornyl acetate; a: (-); b: (+); x and y: configuration not attributed; A.t.: analysis time. a) Column: 30% 6^{I-VII}-O-TBDMS-3^{I-VII}-O-ethyl-2^{I-VII}-O-ethyl-β-CDX in PS086; l: 25m, d_c: 0.25 mm, d_f: 0.25 μm, Anal. cond.: temp. prog.: 50°C/2°C/min/200°C , carrier: H$_2$; flow rate: 1.0 mL/min; b) Column: 50%6^{I-VIII}-O-THDMS-3^{I-VIII}-O-acetyl-2^{I-VIII}-O-acetyl-γ-CDX in PS086; l: 25m, d_c: 0.25 mm, d_f: 0.25 μm; Anal. cond.: temp. prog.: 80°C/2°C/min/200°C; carrier: H$_2$; flow rate: 1.0 mL/min; c) Column: 50% 6^{I-VIII}-O-THDMS-3^{I-VIII}-O-acetyl-2^{I-VIII}-O-acetyl-γ-CDX in OV-1701; l: 40m, d_c: 0.20 mm, d_f: 0.20 μm; Anal. cond.: temp. prog.: 70°C/0.4°C/min/200°C, carrier: H$_2$; flow rate: 0.8 mL/min; d) Column: 50% 6^{I-VIII}-O-THDMS-3^{I-VIII}-O-acetyl-2^{I-VIII}-O-acetyl-γ-CDX in OV-1701; l: 20m, d_c: 0.15 mm, d_f: 0.15 μm, Anal. cond.: temp. progr.: 70°C/1°C/min/200°C; carrier: H$_2$; flow rate: 0.6 mL/min.

9. Total Analysis Systems and Analysis of Complex Samples

The sections above show that Es-GC can be very effective as a technique for chiral recognition in the flavor and fragrance field, and that it can be adapted to modern strategies of analysis based on fully-automatic systems, also known as "Total Analysis Systems" (TAS). TAS are systems in which the three main steps of the analytical process (sample preparation, analysis, and data processing) are integrated on-line into a single step (*56, 57*).

Adoption of these systems has been made possible by the parallel improvements achieved not only in Es-GC but also in sample preparation and mass spectrometry as detector. In particular, the volatile nature of most odorants in the flavour and fragrance field makes headspace sampling, when applicable, the technique of choice for these analyses (*58–60*). HS techniques have the advantages of being solvent-free, fast, simple, reliable, and, above all, easy to automate and to combine on-line to GC-MS systems. These techniques include both conventional (static (S-HS) or dynamic (D-HS) modes, and High Concentration Capacity Headspace (HCC-HS) techniques (*58, 60*); the latter act as a "bridge" between S-HS and D-HS, in which volatiles are statically or dynamically accumulated on polymers, such as polydimethylsiloxane (PDMS), operating in sorption and/or adsorption modes or, less frequently, they are accumulated on solvents (HS-SPME, HSSE, HS-STE, HS-LPME, etc.) (*61*). A successful example of this strategy is the authentication of fruit juices and flavoured foods through the γ-lactone fraction by fast Es-GC-MS analysis combined on-line with HS-SPME which involves all the concepts mentioned above (*62*).

10. Conclusions

Cyclodextrin derivatives are nowadays the most effective chiral stationary phases available for Es-GC in the flavor and fragrance field, because of their (i) high stability and separation repeatability, (ii) acceptable analysis times, (iii) high inertness with several classes of compounds of different polarities, and (iv) extended range of operative temperatures (20-250°C). However, much work remains to be done, mainly to further increase our understanding of their mechanisms of enantiomer recognition (*63*), and to design a new generation of CD derivatives with a more universal enantioselectivity, so as to extend, for instance, their use to highly polar chiral compounds.

References

1. Koppenhoefer, B.; Behnisch, R.; Epperlein, U.; Holzschuh, H.; Bernreuther, A.; Piras, P.; Roussel, C. Enantiomeric odor differences and gas chromatographic properties of flavors and fragrances. *Perfum. Flavor.* **1994**, *19*, 1–14.
2. Schurig, V. Separation of enantiomers by gas chromatography. *J. Chromatogr., A* **2001**, *906*, 275–299.

3. Koscielski, T.; Sybilska, D.; Jurczak, J. Separation of α-and β-pinene into enantiomers in gas-liquid chromatography systems via α-cyclodextrin inclusion complexes. *J. Chromatogr.* **1983**, *280*, 131–134.

4. Alexander, G.; Juvancz, Z.; Szejtli, J. Cyclodextrins and their derivatives as stationary phases in GC capillary columns. *HRC & CC, J. High Resolut. Chromatogr. Chromatogr. Commun.* **1988**, *11*, 110–113.

5. Juvancz, Z.; Alexander, G.; Szejtli, J. Permethylated β-Cyclodextrin as stationary phase in capillary gas chromatography. *J. High Resolut. Chromatogr.* **1987**, *10*, 105–107.

6. Schurig, V.; Nowotny, H. P. Separation of enantiomers on diluted permethylated β-cyclodextrin by high-resolution gas chromatography. *J. Chromatogr.* **1988**, *441*, 155–163.

7. König, W. A.; Lutz, S.; Mischnick-Lübbecke, P.; Brassat, B.; Wenz, G. Cyclodextrins as chiral stationary phases in capillary gas chromatography. Part 1. Pentylated α-cyclodextrin. *J. Chromatogr., A* **1988**, *447*, 193–197.

8. König, W. A.; Lutz, S.; Wenz, G. Modified cyclodextrins – novel highly enantioselective stationary phases for gas chromatography. *Angew. Chem., Int. Ed. Engl.* **1988**, *27*, 979–980.

9. Bicchi, C.; Artuffo, G.; D'Amato, A.; Manzin, V.; Galli, A.; Galli, M. Cyclodextrin derivatives in the GC separation of racemic mixtures of volatile compounds. Part VI: The influence of the diluting phase on the enantioselectivity of 2,6-di-*O*-methyl-3-*O*-pentyl-β-cyclodextrin. *J. High Res. Chromatogr.* **1993**, *16*, 209–214.

10. Bicchi, C.; D'Amato, A.; Manzin, V.; Galli, A.; Galli, M. Cyclodextrin derivatives in GC separation of racemic mixtures of volatiles. Part IX. The influence of the different polysiloxanes as diluting phase for 2,3-di-*O*-acetyl-6-*O*-*t*-butyldimethylsilyl-β-cyclodextrin on the separation of some racemates. *J. Microcolumn Sep.* **1995**, *7*, 327–336.

11. Schurig, V.; Bürkle, W. Extending the Scope of Enantiomer Resolution by Complexation Gas Chromatography. *J. Am. Chem. Soc.* **1982**, *104*, 7573–7580.

12. Schurig, V.; Jung, M.; Schmalzing, D.; Schleimer, M.; Duvekot, J.; Buyten, J. C.; Peene, J. A.; Mussche, P. CGC enantiomer separation on diluted cyclodextrin derivatives coated on fused-silica columns. *J. High Resolut. Chromatogr.* **1990**, *13*, 470–474.

13. Blum, W.; Aichholz, R. Gas chromatographic enantiomer separation on *tert*-butyldimethylsilylated β-cyclodextrin diluted in PS-086 - a simple method to prepare enantioselective glass-capillary columns. *J. High Resolut. Chromatogr.* **1990**, *13*, 515–518.

14. Dietrich, A.; Maas, B.; Karl, V.; Kreis, P.; Lehmann, D.; Weber, B.; Mosandl, A. Stereoisomeric flavor compounds. Part 55. Stereodifferentiation of some chiral volatiles on heptakis(2,3-di-*O*-acetyl-6-*O*-*tert*butyldimethylsilyl)-β-cyclodextrin. *J. High Resolut. Chromatogr.* **1992**, *15*, 176–179.

15. Bicchi, C.; Cagliero, C.; Liberto, E.; Sgorbini, B.; Martina, K.; Cravotto, G.; Rubiolo, P. New asymmetrical per-substituted cyclodextrins (2-*O*-methyl-3-*O*-ethyl- and 2-*O*-ethyl-3-*O*-methyl-6-*O*-*t*-butyldimethylsilyl-β-derivatives)

as chiral selectors for enantioselective gas chromatography in the flavour and fragrance field. *J. Chromatogr., A* **2010**, *1217*, 1106–1113.

16. Bayer, M.; Mosandl, A. Improved gas chromatographic stereodifferentiation of chiral main constituents from different essential oils using a mixture of chiral stationary phases. *Flavour Frag. J.* **2004**, *19*, 515–517.

17. Nie, M. Y.; Zhou, L. M.; Wang, Q. H.; Zhu, D. Q. Gas chromatographic enantiomer separation on single and mixed cyclodextrin derivative chiral stationary phases. *Chromatographia* **2000**, *51*, 736–740.

18. Levkin, P. A.; Levkina, A.; Schurig, V. Combining the enantioselectivities of L-valine diamide and permethylated β-cyclodextrin in one gas chromatographic chiral stationary phase. *Anal. Chem.* **2006**, *78*, 5143–5148.

19. Stephany, O.; Dron, F.; Tisse, S.; Martinez, A.; Nuzillard, J.-M.; Peulon-Agasse, V.; Cardinaël, P.; Bouillon, J.-P. (L)- or (D)-Valine *tert*-butylamide grafted on permethylated β-cyclodextrin derivatives as new mixed binary chiral selectors: Versatile tools for capillary gas chromatographic enantioseparation. *J. Chromatogr., A* **2009**, *1216*, 4051–4062.

20. Stephany, O.; Tisse, S.; Coadou, G.; Bouillon, J. P.; Peulon-Agasse, V.; Cardinael, P. Influence of amino acid moiety accessibility on the chiral recognition of cyclodextrin-amino acid mixed selectors in enantioselective gas chromatography. *J. Chromatogr., A* **2012**, *1270*, 254–261.

21. Armstrong, D. W.; Tang, Y. B.; Ward, T.; Nichols, M. Derivatized cyclodextrins immobilized on fused-silica capillaries for enantiomeric separations via capillary electrophoresis, gas chromatography, or supercritical fluid chromatography. *Anal. Chem.* **1993**, *65*, 1114–1117.

22. Dönnecke, J.; Paul, C.; König, W. A.; Svensson, L. A.; Gyllenhaal, O.; Vessman, J. Immobilization of heptakis (6-*O-tert*-butyldimethylsilyl-2,3-di-*O*-methyl)-β-cyclodextrin for capillary gas chromatography and supercritical fluid chromatography and micro-liquid chromatography. *J. Microcolumn Sep.* **1996**, *8*, 495–505.

23. Schurig, V.; Juvancz, Z.; Nicholson, G. J.; Schmalzing, D. Separation of enantiomers on immobilized polysiloxane-anchored permethylated-β-cyclodextrin (Chirasil-Dex) by supercritical fluid chromatography. *J. High Resolut. Chromatogr.* **1991**, *14*, 58–62.

24. Berthod, A.; Li, W. Y.; Armstrong, D. W. Multiple enantioselective retention mechanisms on derivatized cyclodextrin gas chromatographic chiral stationary phases. *Anal. Chem.* **1992**, *64*, 873–879.

25. Schurig, V.; Nowotny, H. P. Gas chromatographic separation of enantiomers on optically active metal-complex-free stationary phases. Part 2. Gas chromatographic separation of enantiomers on cyclodextrin derivatives. *Angew. Chem. Int. Ed. Engl.* **1990**, *29*, 939–957.

26. Jung, M.; Schmalzing, D.; Schurig, V. Theoretical approach to the gas chromatographic separation of enantiomers on dissolved cyclodextrin derivatives. *J. Chromatogr.* **1991**, *552*, 43–57.

27. Schurig, V. Enantiomer separation by gas chromatography on chiral stationary phases. *J. Chromatogr., A* **1994**, *666*, 111–129.

28. Lipkowitz, K. B.; Coner, R.; Peterson, M. A. Locating regions of maximum chiral discrimination: A Computational Study of Enantioselection on a Popular Chiral Stationary Phase Used in Chromatography. *J. Am. Chem. Soc.* **1997**, *119*, 11269–11276.

29. Lipkowitz, K. B.; Coner, R.; Peterson, M. A.; Morreale, A.; Shackelford, J. The Principle of Maximum Chiral Discrimination: Chiral Recognition in Permethyl-β-Cyclodextrin. *J. Org. Chem.* **1998**, *63*, 732–745.

30. Schurig, V. Terms for the quantitation of a mixture of stereoisomers. *Enantiomer* **1996**, *1*, 139–143.

31. Liberto, E.; Cagliero, C.; Sgorbini, B.; Bicchi, C.; Sciarrone, D.; Zellner, B. D.; Mondello, L.; Rubiolo, P. Enantiomer identification in the flavour and fragrance fields by "interactive" combination of linear retention indices from enantioselective gas chromatography and mass spectrometry. *J. Chromatogr., A* **2008**, *1195*, 117–126.

32. Kovats, E. Gas chromarographische charakteriserung organischer verbindungen. Retention indices aliphatischer halogenide, alkohole, aldehyde und ketone. *Helv. Chim. Acta* **1958**, *41*, 1915–1932.

33. Van den Dool, H.; Kratz, P. D. A generalization of the retention index system including linear temperature programmed gas-liquid partition chromatography. *J. Chromatogr.* **1963**, *11*, 463–471.

34. Blumberg, L. M.; Klee, M. S. Method translation and retention time locking in partition GC. *Anal. Chem.* **1998**, *70*, 3828–3839.

35. *FFNSC 2.0 Flavors and Fragrances of Natural and Synthetic Compounds - Mass Spectral Database*; Chromaleont: Messina, Italy, 2007.

36. Costa, R.; De Fina, M. R.; Valentino, M. R.; Dugo, P.; Mondello, L. Reliable identification of terpenoids and related compounds by using linear retention indices interactively with mass spectrometry search. *Nat. Prod. Commun.* **2007**, *2*, 413–418.

37. Bicchi, C.; Artuffo, G.; D'Amato, A.; Manzin, V.; Galli, A.; Galli, M. Cyclodextrin derivatives in the GC separation of racemic mixtures of volatile compounds. Part 5. Heptakis 2,6-dimethyl-3-pentyl-β-cyclodextrin. *J. High Resolut. Chromatogr.* **1992**, *15*, 710–714.

38. König, W. A.; Gehrcke, B.; Icheln, D.; Evers, P.; Dönnecke, J.; Wang, W. C. New selectively substituted cyclodextrins as stationary phases for the analysis of chiral constituents of essential oils. *J. High Resolut. Chromatogr.* **1992**, *15*, 367–372.

39. Maas, B.; Dietrich, A.; Bartschat, D.; Mosandl, A. *tert*-Butyldimethylsilylated cyclodextrins: versatile chiral stationary phases in capillary gas chromatography. *J. Chromatogr. Sci.* **1995**, *33*, 223–228.

40. Bicchi, C.; D'Amato, A.; Manzin, V.; Galli, A.; Galli, M. Cyclodextrin derivatives in the gas chromatographic separation of racemic mixtures of volatile compounds. Part 10. 2,3-di-*O*-ethyl-6-*O*-tert-butyldimethylsilyl-β- and γ-cyclodextrins. *J. Chromatogr., A* **1996**, *742*, 161–173.

41. *AMDIS (2012) Version 2.71*; http://chemdata.nist.gov/dokuwiki/doku.php?id=chemdata:amdis (accessed July 2015).

42. Rubiolo, P.; Liberto, E.; Sgorbini, B.; Russo, R.; Veuthey, J. L.; Bicchi, C. Fast-GC-conventional quadrupole mass spectrometry in essential oil analysis. *J. Sep. Sci.* **2008**, *31*, 1074–1084.

43. Hardt, I.; König, W. A. Diluted versus undiluted cyclodextrin derivates in capillary gas chromatography and the effect of linear carrier gas velocity, column temperature, and length on enantiomer separation. *J. Microcolumn Sep.* **1993**, *5*, 35–40.

44. Bicchi, C.; Artuffo, G.; D'Amato, A.; Galli, A.; Galli, M. Cyclodextrin derivatives in GC separation of racemic mixtures of volatiles. Part 3. *Chirality* **1992**, *4*, 125–131.

45. Grosenick, H.; Schurig, V.; Costante, J.; Collet, A. Gas chromatographic enantiomer separation of bromochlorofluoromethane. *Tetrahedron: Asymmetry* **1995**, *6*, 87–88.

46. Lindstrom, M. Improved enantiomer separation using very short capillary columns coated with permethylated β-cyclodextrin. *J. High Resolut. Chromatogr.* **1991**, *14*, 765–767.

47. Bicchi, C.; Blumberg, L.; Cagliero, C.; Cordero, C.; Rubiolo, P.; Liberto, E. Development of fast enantioselective gas-chromatographic analysis using gas-chromatographic method-translation software in routine essential oil analysis (lavender essential oil). *J. Chromatogr., A* **2010**, *1217*, 1530–1536.

48. Bicchi, C.; Liberto, E.; Cagliero, C.; Cordero, C.; Sgorbini, B.; Rubiolo, P. Conventional and narrow bore short capillary columns with cyclodextrin derivatives as chiral selectors to speed-up enantioselective gas chromatography and enantioselective gas chromatography-mass spectrometry analyses. *J. Chromatogr., A* **2008**, *1212*, 114–123.

49. Bicchi, C.; D'Amato, A.; Manzin, V. Derivatized cyclodextrins in enantiomer GC separation of volatiles. In *Flavours and Fragrances;* Swift, K. A. D., Ed.; The Royal Society of Chemistry: Cambridge, 1997; pp 57−69.

50. Kreis, P.; Dietrich, A.; Mosandl, A. Chiral compounds of essential oils. Part 18. On the authenticity assessment of the essential oil of *Rosmarinus officinalis* L. *Pharmazie* **1994**, *49*, 761–765.

51. Blumberg, L. M.; Klee, M. S. Optimal heating rate in gas chromatography. *J. Microcolumn Sep.* **2000**, *12*, 508–514.

52. Klee, M. S.; Blumberg, L. M. Theoretical and practical aspects of fast gas chromatography and method translation. *J. Chromatogr. Sci.* **2002**, *40*, 234–247.

53. *GC Method Translation Software*; www.chem.agilent.com (accessed July 2015).

54. Mondello, L.; Sciarrone, D.; Costa, R.; Dugo, G. The chiral compounds of citrus oils. In *Citrus oils, Composition, Advanced Analytical Techniques, Contaminants and Biological Activity*; Dugo, G., Mondello, L., Eds.; CRC Press: Boca Raton, FL, 2011; pp 349−404.

55. Blumberg, L. M. Theory of fast capillary gas chromatography - Part 3: Column performance vs. gas flow rate. *J. High Resolut. Chromatogr.* **1999**, *22*, 403–413.

56. Cagliero, C.; Sgorbini, B.; Cordero, C.; Liberto, E.; Bicchi, C.; Rubiolo, P. Analytical strategies for multipurpose studies of a plant volatile fraction.

In *Handbook of Chemical and Biological Plant Analytical Methods*; Hostettmann, K., Stuppner, H., Marston, A., Chen, S., Eds.; Wiley: Chichester, U.K., 2014; pp 1−20.

57. Manz, A.; Graber, N.; Widmer, H. M. Miniaturized total chemical analysis systems: a novel concept for chemical sensing. *Sens. Actuators, B* **1990**, *1*, 244–248.

58. Bicchi, C.; Cordero, C.; Liberto, E.; Sgorbini, B.; Rubiolo, P. Headspace sampling in flavor and fragrance field. In *Comprehensive Sampling and Sample Preparation*; Pawliszyn, J., Ed.; Elsevier, Academic Press: Oxford, U.K., 2012; pp 1−25.

59. Rubiolo, P.; Sgorbini, B.; Liberto, E.; Cordero, C.; Bicchi, C. Analysis of the plant volatile fraction. In *The Chemistry and Biology of Volatiles*; Herrmann, A., Ed.; Wiley: Chichester, U.K., 2010; pp 50−93.

60. Sgorbini, B.; Bicchi, C.; Cagliero, C.; Cordero, C.; Liberto, E.; Rubiolo, P. Headspace sampling and gas chromatography: a successful combination to study the composition of a plant volatile fraction. In *Handbook of Chemical and Biological Plant Analytical Methods*; Hostettmann, K., Stuppner, H., Marston, A., Chen, S., Eds.; Wiley: Chichester, U.K., 2014; pp 1−31.

61. Baltussen, E.; Cramers, C. A.; Sandra, P. J. F. Sorptive sample preparation - a review. *Anal. Bioanal. Chem.* **2002**, *373*, 3–22.

62. Cagliero, C.; Bicchi, C.; Cordero, C.; Rubiolo, P.; Sgorbini, B.; Liberto, E. Fast headspace-enantioselective GC-mass spectrometric-multivariate statistical method for routine authentication of flavoured fruit foods. *Food Chem.* **2012**, *132*, 1071–1079.

63. Bicchi, C.; Blumberg, L. M.; Rubiolo, P.; Cagliero, C. General retention parameters of chiral analytes in cyclodextrin gas chromatographic columns. *J Chromatogr., A* **2014**, *1340*, 121–127.

Chapter 3

Vibrational CD (VCD) Spectroscopy as a Powerful Tool for Chiral Analysis of Flavor Compounds

Yoshihiro Yaguchi,[1] Atsufumi Nakahashi,[2] Nobuaki Miura,[2] Tohru Taniguchi,[2] Daisuke Sugimoto,[1] Makoto Emura,[1] Kyoko Zaizen,[1] Yumi Kusano,[1] and Kenji Monde*,[2]

[1]Corporate Research & Development Division, Takasago International Corporation, 4-11, Nishi-yawata 1-Chome, Hiratsuka City, Kanagawa 254-0073, Japan [2]Faculty of Advanced Life Science, Frontier Research Center for the Post-Genome Science and Technology, Hokkaido University, Kita 21, Nishi 11, Sapporo 001-0021, Japan *E-mail: kmonde@sci.hokudai.ac.jp.

Several flavor compounds have chiral centers in their structures, and it has been shown that there are differences in odor characteristics and odor thresholds between enantiomers. Vibrational CD (VCD) is a recently developed technique for the determination of the absolute stereochemistry of organic compounds assisted by *ab initio* quantum theoretical calculations. In this study, the VCD technique was at first applied to patchoulol, a rigid and fused tricyclic sesquiterpene alcohol. The absolute stereochemistry proposed from the observed and calculated VCD data was in agreement with the configuration reported for patchoulol. Moreover, this method was extended to odor-active flavorous furanones having a unique keto-enol tautomeric structure that is prone to racemization. The absolute stereochemistry of flavorous 2- or 5-substituted furanones such as 2,5-dimethyl-4-hydroxy-3(2*H*)-furanone (DMHF, furaneol), 2,5-dimethyl-4-methoxy-3(2*H*)-furanone (DMMF, mesifuran), 4-acetoxy-2,5-dimethyl-3(2*H*)-furanone (ADMF, furaneol acetate), 4,5-dimethyl-3-hydroxy-2(5*H*)-furanone

(sotolon), and 5-ethyl-3-hydroxy-4-methyl-2(5*H*)-furanone (maple furanone) was investigated. The examples show that the VCD technique is a very powerful tool for the determination of the absolute stereochemistry of flavor compounds.

Introduction

Patchouli (*Pogostemon cablin*.) is a herbal plant originating from India and is mainly produced in Southeastern Asia such as the Malay Peninsula, Sumatra, and Java. In this area, patchouli has been used as a medicine, repellant, and incense from ancient time. The essential oil of patchouli possesses a complex woody odor with an earthy-camphoraceous nuance evoking oriental images. Therefore, patchouli essential oil has been recognized as a very important flavor and fragrance ingredient. Patchouli essential oil contains many types of sesquiterpenes, among which patchoulol ((−)-(1*R*,3*R*,6*S*,7*S*,8*S*)-2,2,6,8-tetramethyltricyclo[5.3.1.0^{3,8}]undecan-3-ol, **1**) is a main component (*1–3*) (Figure 1). It also has a woody and earthy-camphor odor representative of the essential oil.

2-Substituted-3(2*H*)-furanones and 5-substituted-2(5*H*)-furanones, such as 2,5-dimethyl-4-hydroxy-3(2*H*)-furanone (DMHF, Furaneol, trademark of Firmenich S.A., Switzerland, **2**), 2,5-dimethyl-4-methoxy-3(2*H*)-furanone (DMMF, mesifuran, **3**), 4-acetoxy-2,5-dimethyl-3(2*H*)-furanone (ADMF, furaneol acetate, **4**), 2(or 5)-ethyl-4-hydroxy-5(or 2)-methyl-3(2*H*)-furanone (EHMF, homofuraneol, **5a** or **5b**), 4,5-dimethyl-3-hydroxy-2(5*H*)-furanone (sotolon, **6**) and 5-ethyl-3-hydroxy-4-methyl-2(5*H*)-furanone (maple furanone, **7**) are important naturally occurring flavor compounds having burnt sugary and caramel sweet odor and contributing to the sensory properties of many natural products and thermally processed foods (*4–7*) (Figure 1).
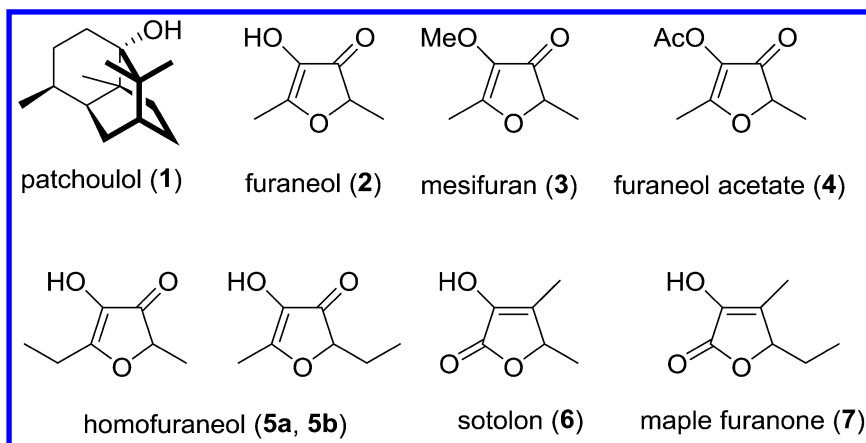

Figure 1. Patchoulol, and Naturally Occurring 2-substituted-3(2H)-furanones and 5-substituted-2(5H)-furanones.

They possess extremely low odor-thresholds, such as 60 ppb for **2**, 20 ppb for **5**, 1 ppt for **6**, and 0.01 ppt for **7**, respectively (*8*, *9*). Furanone **7** shows one of the lowest odor thresholds reported for organic compounds.

Naturally occurring aroma compounds often exhibit enantiomeric excesses, and the respective enantiomers possess different organoleptic characteristics and intensities (*10*, *11*). However, 2-substituted-3(2*H*)-furanones such as **2**, **3**, **4**, **5a**, and **5b** were isolated as optically inactive compounds, due to their unique keto-enol tautomeric structures causing racemization (Figure 2). Moreover, regioisomerization between **5a** and **5b** occurs during this tautomeric isomerization.
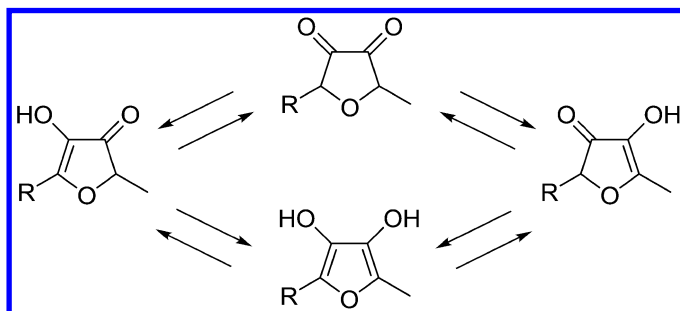

*Figure 2. Keto–enol Tautomerization of 2-Substituted-3(2H)-furanones [R = Me (**2**) or Et (**5a, 5b**)].*

Despite their organoleptic properties and their importance for flavor and fragrance industries as raw materials, the relationship between the sign of optical rotation and the absolute stereochemistry of these furanones, except for **6**, had not been unveiled. Although these compounds possess rather simple structures, the determination of the absolute configuration by conventional methods has been extremely difficult due to their unique keto-enol tautomeric structures. The high chemical reactivity of the enol and carbonyl groups hampers X-ray crystallographic studies and derivatizations required for application of the standard Mosher method.

CO_2 supercritical fluid chromatographic (SFC) chiral separation is known as an effective preparative-scale optical resolution method in the pharmaceutical field for chemicals that have an aromatic group (*12*). Lately, we reported the SFC optical resolution for flavor materials (*13*). This method has the advantage of minimizing thermal procedures, such as organic solvent evaporation, a potential factor of racemization.

Meanwhile, the recently developed combination of vibrational circular dichroism (VCD) spectroscopy with density functional theory (DFT) calculation has been applied as a reliable technique for stereochemical analyses in the field of life sciences as well as material sciences (*14–22*). VCD measures the differential absorption of left versus right circularly polarized infrared radiation by molecular vibrational transition. The recent commercially available VCD equipment prompted determination studies of small organic chiral

molecules' absolute configurations (*22–24*) as well as stereochemical analysis of biologically significant macromolecules, such as proteins (*14*) and carbohydrates (*19*). Advantages of the VCD technique for determination of the absolute stereochemistry are as follows; (i) no need of UV chromophores for UV-CD, because VCD uses infrared absorption; (ii) no need of recrystallization like in X-ray studies; (iii) no need of derivatization for Mosher's method; and (iv) high reliability of *ab initio* theoretical calculations. A disadvantage of VCD is its low sensitivity.

In this report, the result of a VCD application to patchoulol **1,** a compound for which the absolute stereochemistry was known, is shown as a "proof of principle"-study. Secondly, investigations of the absolute configurations of 2-substituted-3(2*H*)-furanones (*25–27*) having a unique keto-enol tautomeric structure and 5-substituted-2(5*H*)-furanones (*28*) using the VCD method coupled with chiral SFC optical resolution as well as organoleptic properties of the enantiomers (*25–28*) are presented.

Materials and Methods

Materials

Patchoulol **1** was purified from natural patchouli oil obtained from Takasago International Corp. using HPLC. Furaneol **2** was purchased from Firmenich S.A. (Geneva, Switzerland). Mesifuran **3**, furaneol acetate **4**, and sotolon **6** were obtained from Takasago International Corp. (Tokyo, Japan).

General Procedures

Optical rotations were measured using a JASCO P-1020 polarimeter or a Perkin-Elmer 343 spectrometer at 589 nm (sodium D-line) at 20 °C in a 10 mm cell. The chiral GC analyses were performed on a GC2010 system (Shimadzu Corp.) using a CP-Chirasil-DEX CB capillary column (Varian, Inc., Palo Alto, CA) and/or a Supelco β-DEX 325 column (Sigma-Aldrich Corp., St. Louis, MO).

Isolation of Patchoulol 1

Patchouli oil was washed with 5 % aqueous sodium hydroxide, followed by fractionation using mid-pressure LC with silica gel as a stationary phase. Flow conditions were 60 mL/min with hexane and ethyl acetate as mobile phase at a gradient rate from 1 % to 13 % of ethyl acetate content. The obtained fraction containing **1** was separated using preparative reverse phase HPLC. Flow conditions were 1 mL/min with water and acetonitrile as a mobile phase at a gradient rate from 60 % to 95 % of acetonitrile content. Finally, 200 mg of **1** with 99 % purity was isolated.

Preparative Chiral SFC

Optical resolution and isolation of chiral flavor furanones were performed on an SFC System (Jasco Corp., Tokyo, Japan) equipped with a CHIRALPAK IA column (250 mm × 20 mm, 5 μm) on 20–25 mL/min CO_2 flow and 0.08–0.5 mL/min 2-propanol flow as an entrainer. The back pressure was kept at 15 MPa. The UV signal was recorded at 220 or 280 nm. The column oven temperature was kept at 25 °C.

Derivatization of Furaneol 2 to Its Methyl Ether, Mesifuran 3

To a 1 mL methanol solution of 5 mg of (−)-**2** an excess of trimethylsilyldiazomethane was added in hexane at 0 °C, and the mixture was warmed to room temperature. Stirring at room temperature for an additional 1 h afforded the optically active (−)-**3**. In a similar manner, (+)-**2** gave (+)-**3**.

VCD Spectroscopy

VCD and IR spectra were measured on a Chiral*IR* or Chiral*IR*-2X spectrometer (Bomem/BioTools, Jupiter, FL). All spectra were recorded for 1–3 h at a resolution of 8 cm^{-1} under ambient temperature. Samples were dissolved in CCl_4 and then placed in a 72 or 100 μm CaF_2 cell. The concentrations were as follows: **1**, 0.30 M; (+)-**3**, 0.17M; (−)-**3**, 0.085 M; (+)-**4**, 0.080 M; (−)-**4**, 0.080 M; (+)-**6**, 0.15 M; (−)-**6**, 0.15 M; (+)-**7**, 0.15 M; (−)-**7**, 0.15 M. The IR and VCD spectra were corrected by a solvent spectrum obtained under the same experimental conditions and presented in molar absorptivity ε (L/mol•cm).

Density Functional Theory Calculation

Preliminary conformational searches of each molecule were conducted based on the molecular mechanics with MMFF94S force fields using a SPARTAN'10 software (*29*) (for patchoulol, **1**) or a CONFLEX program (*30, 31*) (for furanones (*R*)-**3**, (*R*)-**4**, (*R*)-**6**, (*R*)-**7**). For obtained conformers with lower energies, the geometry optimizations and harmonic frequency analysis were carried out using the density functional theory calculations at the B3LYP/6-311G(d,p) (for **1**) or B3PW91/6-31G(d,p) (for furanones) level. Using the frequency and intensity sets, the IR and VCD spectra were obtained for each conformer by convolution with the Lorentzian function. These spectra were averaged with the Boltzmann-weighted population. The frequencies were scaled with the equation of 0.9894ν − 0.0000104ν^2 (*32*) or with a factor of 0.97. The Boltzmann-weighted populations were evaluated with the DFT energy corrected with the thermal free energy with respect to the vibration motion. DFT calculations were conducted with the Gaussian09 (revision C01) (*33*) or Gaussian03 (revision C02) program code (*34*).

Sensory Evaluations

The sensory evaluations were performed by expert panels of flavorists. The study was approved by the Institutional Review Board of Takasago International Corp.

Results and Discussion

Confirmation of the Absolute Stereochemistry of Patchoulol 1

Preparation of Patchoulol 1

Patchoulol **1** was isolated and purified from patchouli oil (Takasago International Corp.) by means of the above-described protocol. Analysis of isolated **1** was performed by GC/MS, NMR, and polarimetry. The specific rotation value of isolated **1** was $[\alpha]_D^{20}$ −121 (*c* 0.363, CHCl$_3$), which is identical to reported values (*35*, *36*).
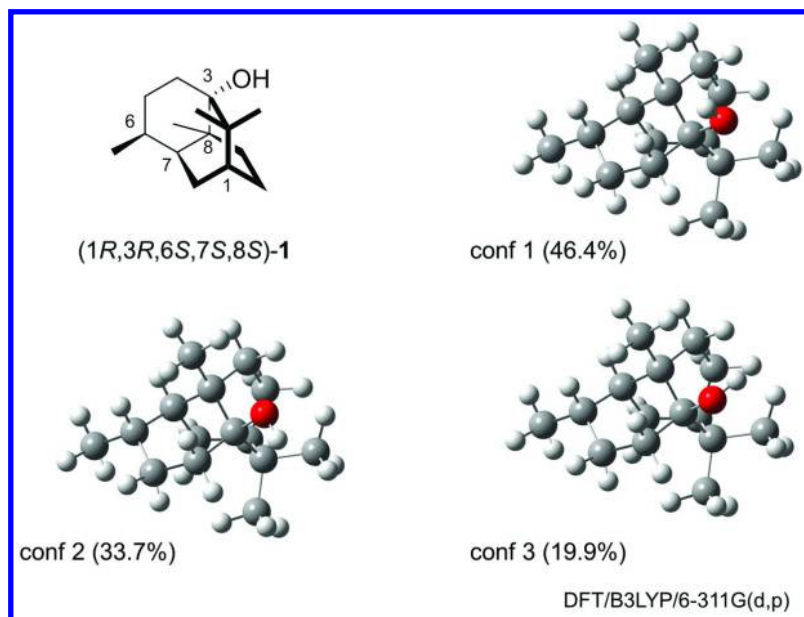
Figure 3. Three Stable Conformers of (1R,3R,6S,7S,8S)-1. The Six-Membered Ring C3-C8 Takes a Chair Conformation.

IR and VCD Theoretical Calculation for Patchoulol 1

Theoretical calculations of the VCD spectrum of **1** were performed using density functional theory (DFT) at the B3LYP/6-311G(d,p) level. The initial geometries were generated for a (1*R*,3*R*,6*S*,7*S*,8*S*)-enantiomer, whose relative

configuration was determined by NMR, with a MMFF search. The DFT conformational analysis found only three low-lying conformers that differ in the orientation of the hydroxyl group (Figure 3), due to its rigid and fused ring structure. Finally, the IR and VCD spectra of each conformer were obtained by simulating with Lorentzian lineshapes of 6 cm^{-1} width, and were averaged with the Boltzmann-weighted population shown in Figure 4.
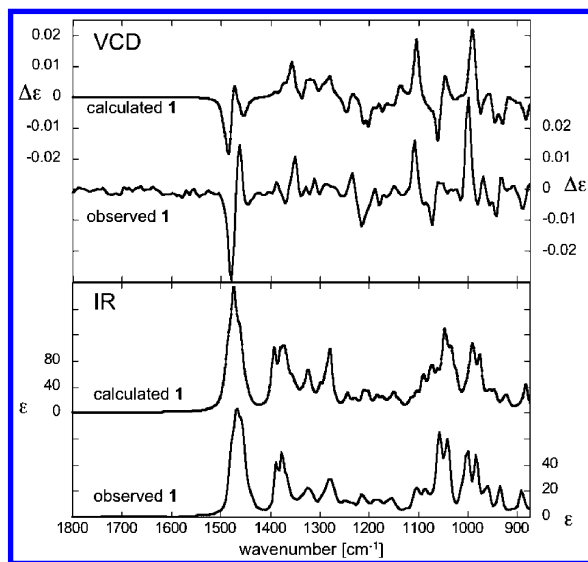

*Figure 4. Comparison of IR (Lower Frame) and VCD (Upper Frame) Observed Spectra (CCl₄, c = 0.30 M, l = 100 μm) for Isolated (−)-**1** with Calculated Spectra for (1R,3R,6S,7S,8S)-**1**.*

Absolute Stereochemistry of Patchoulol 1

The observed IR and VCD spectra of patchoulol **1** isolated from natural patchouli oil and the calculated IR and VCD spectra of (1*R*,3*R*,6*S*,7*S*,8*S*)-**1** are shown in Figure 4. Observed VCD spectra of (−)-**1** showed a strong negative Cotton effect around 1460 cm^{-1}, which was attributed to a vibrational transition involving various C–H bending motions. The calculated IR spectrum of (1*R*,3*R*,6*S*,7*S*,8*S*)-**1** was in good agreement with that observed for (−)-**1.** The calculated VCD signals of (1*R*,3*R*,6*S*,7*S*,8*S*)-**1** agreed well with those observed for isolated (−)-**1** in their fingerprint regions (from 1500 to 900 cm^{-1}). We therefore confirmed the absolute configurations of (−)-**1** to be (1*R*,3*R*,6*S*,7*S*,8*S*) (Figure 3), and thus demonstrated the reliability of the VCD method with DFT theoretical calculation.
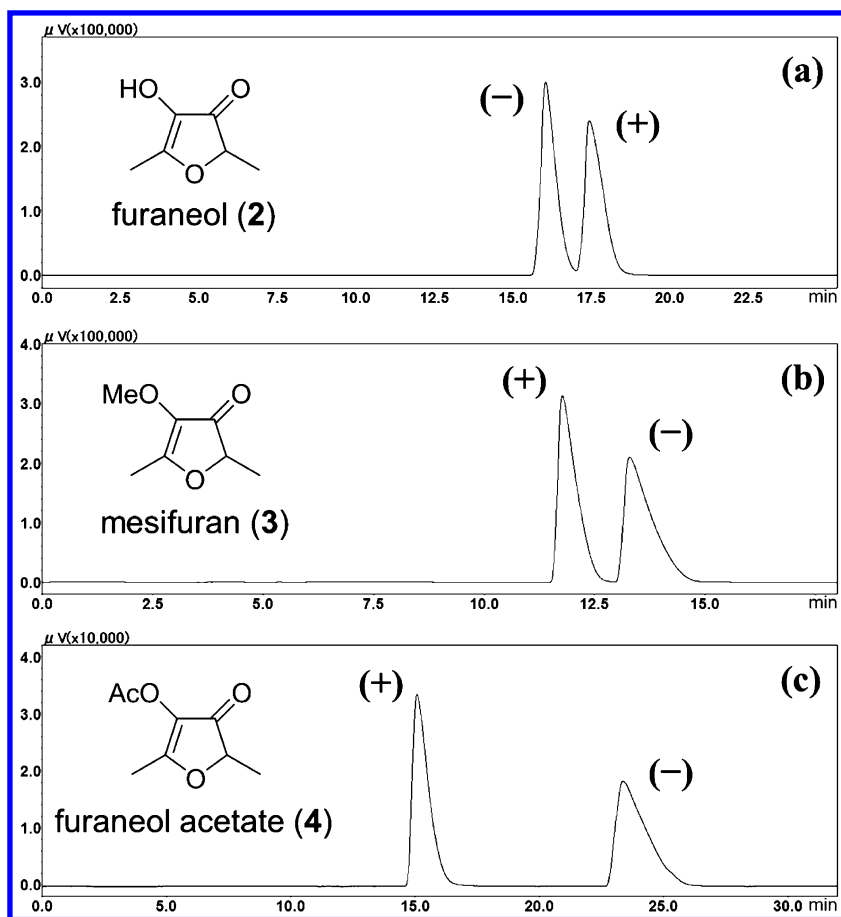
Figure 5. Optical Resolution of 2 (a), 3 (b), and 4 (c) by Enantioselective CO_2 SFC.

Determination of Absolute Stereochemistry of Furaneol 2, Mesifuran 3, and Furaneol Acetate 4

Preparative Supercritical Fluid Chromatographic Optical Resolution for Furanones 2, 3, and 4

CO_2 supercritical fluid chromatography (SFC) is known to enable fine resolution even at a high flow rate due to the low viscosity and high diffusivity of supercritical CO_2. Moreover, SFC uses less organic solvent than HPLC. Therefore, using SFC is expected to reduce the risk of racemization of isolated optically active furanones in both the separation and the solvent removing steps.

After several trials with chiral stationary columns, efficient optical separations of **2**, **3**, and **4** were achieved by Chiralpak IA using 2-propanol as entrainer with excellent separation factors (**2**, α = 1.12; **3**, α = 1.22; **4**, α = 1.80) as shown in Figure 5. The afforded enantiomers had specific optical rotation values shown in Table 1. No racemization was observed during the collection of fractions, the evaporation of solvents and the optical rotation measurements.

Table 1. Specific Optical Rotations and Enantiomeric Excesses of Isolated Furanones

compound	$[\alpha]_D^{20}$	condition	ee (%)
(+)-**2**	+172	c 0.472, CCl$_4$	80
(−)-**2**	−153	c 0.526, CCl$_4$	82
(+)-**3**	+148	c 0.324, CCl$_4$	94
(−)-**3**	−188	c 0.262, CCl$_4$	91
(+)-**4**	+113	c 0.784, CHCl$_3$	99
(−)-**4**	−128	c 0.664, CHCl$_3$	99
(+)-**6**	+13.4	c 0.30, CHCl$_3$	88
(−)-**6**	−21.4	c 0.30, CHCl$_3$	96
(+)-**7**	+36.8	c 0.30, CHCl$_3$	99
(−)-**7**	−35.5	c 0.30, CHCl3	98

IR and VCD Theoretical Calculation for Furanones 3 and 4

Conformational Analysis of (R)-mesifuran [(R)-3]

The IR and VCD spectra of (*R*)-**3** are shown in Figure 6; the theoretical calculations were based on the DFT/B3PW91/6-31G(d,p) level. Because (*R*)-**3** has only one rotatable bond, there were a small number of starting geometries for conformational analysis differing in the directions in the methoxy group. As seen in Figure 7a, the geometry optimizations gave a single stable conformer for **3**. After harmonic vibrational analysis, simulated absorption and VCD spectra were obtained by using convolution with Lorentzian functions with 8 cm^{-1} full width at half-height.

Conformational Analysis of (R)-Furaneol acetate [(R)-4]

CONFLEX search with MMFF94F force fields was performed. Geometry optimizations and harmonic vibrational analyses were carried out with the density functional theory calculation at the B3PW91/6-31G(d,p) level of theory for the four obtained conformers in the CONFLEX search. Geometry optimizations and harmonic vibrational analyses were carried out at the same level of theory. Two low-lying conformations (Figure 7b, c) were used to calculate the IR and VCD spectra. The energy difference between these two conformers was 0.06 kcal/mol. This suggests that these two conformers have almost equal contributions for the IR and VCD spectra. The spectra of these conformers were calculated in the same manner as for (*R*)-**3**. Finally, the spectra were averaged with the Boltzmann-weighted population.
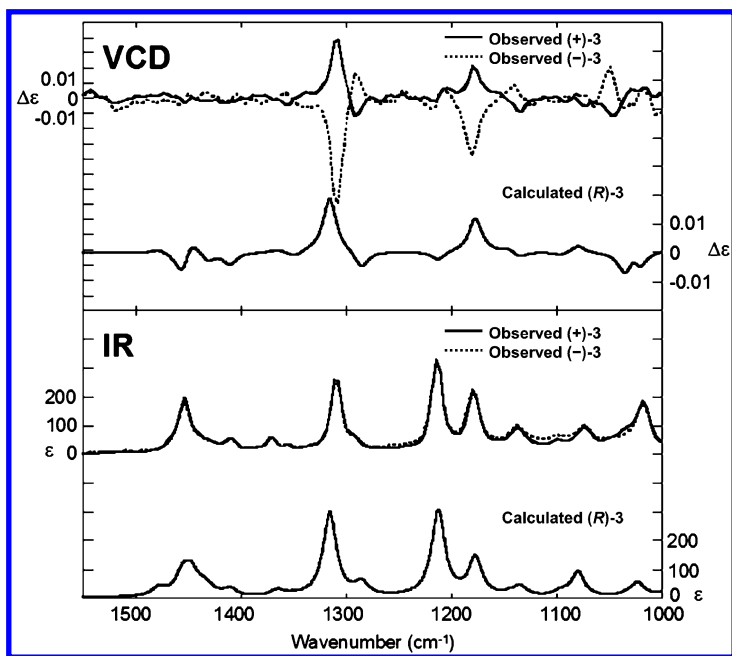

*Figure 6. Comparison of IR (Lower Frame) and VCD (Upper Frame) Observed Spectra (CCl₄, c = 0.17 M, l = 100 μm) for (+)-3 with Calculated Spectra for (R)-**3**.*

44

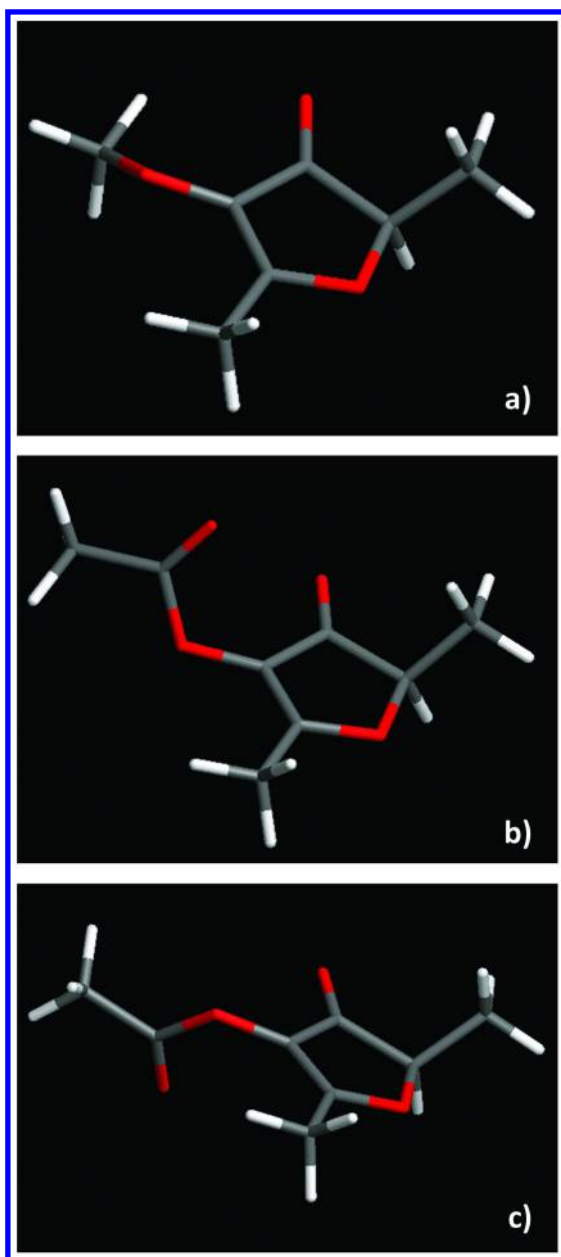*Figure 7. The Most Stable Conformer of (R)-3 (a) and Two Stable Conformers of (R)-4 (b, c).*

Absolute Configuration of Furanones 3 and 4

VCD and IR spectra were measured for furanones **2**, **3**, and **4** by the above-described protocols. Unfortunately, **2** decomposed during measurement because of its low stability in CDCl$_3$ and CCl$_4$. On the other hand, enantiomers of mesifuran (**3**) showed entirely opposite VCD signals. The enantiomer (+)-**3** showed a strong positive Cotton effect at around 1300 cm^{-1} attributable to C−H bending at the chiral center. As shown in Figure 6, the observed VCD spectrum of (+)-**3** was essentially identical to the calculated spectrum of (*R*)-**3**, whereas both IR spectra were almost superimposable. Therefore, (+)-**3** was shown to have the (*R*)-configuration. Similar to **3**, the observed IR spectra of **4** were almost superimposable to the calculated IR spectra. The observed VCD spectrum of (+)-**4** closely matched with the calculated spectrum of (*R*)-**4** (Figure 8). As a result, the absolute configurations of **4** were confirmed as (*R*)-(+)-**4** and (*S*)-(−)-**4**, respectively.
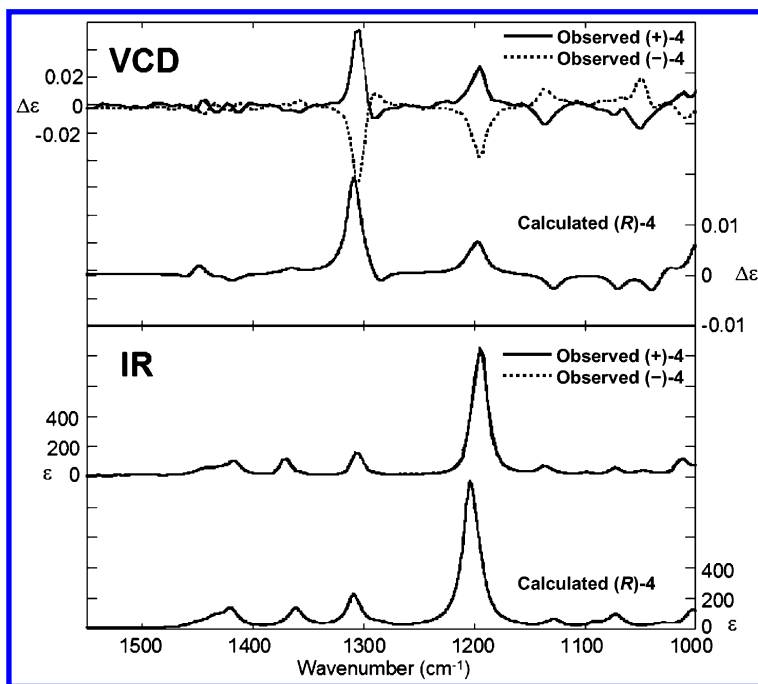

Figure 8. Comparison of IR (Lower Frame) and VCD (Upper Frame) Observed Spectra (CCl$_4$, c = 0.080 M, l = 100 μm) for (+)-4 with Calculated Spectra for (R)-4.

Absolute Stereochemistry of Furaneol 2 Using Chemical Relay Reaction

To determine the absolute configuration of **2** causing immediate racemization in CCl4, CDCl3, and CD2Cl2 (*26*), derivatization from **2** to **3** by mild methylation reactions was attempted (Figure 9). Careful treatments of (+)-**2** and (−)-**2** with trimethylsilyldiazomethane successfully afforded the corresponding optically active methyl ether **3**. The enantiomer from (+)-**2** was identified as (*R*)-(+)-**3** by chiral MDGC-MS analysis, and *vice versa*. Therefore, the relationship of the absolute configuration and optical rotation of **2** was confirmed as (*R*)-(+)-**2** and (*S*)-(−)-**2**.
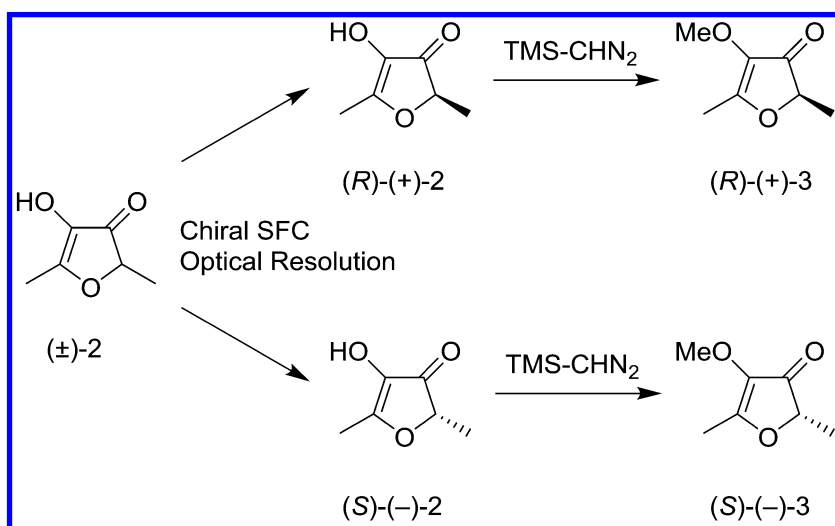

*Figure 9. Derivatization of Furaneol (**2**) into Mesifuran (**3**).*

Confirmation of Absolute Stereochemistry of Sotolon 6 and Determination of Absolute Stereochemistry of Maple Furanone 7

Preparative Supercritical Fluid Chromatographic Optical Resolution for Sotolon 6 and Maple Furanone 7

Optically active **6** and **7** were obtained by the use of CHIRALPAK IA columns using 2-propanol as an entrainer (Figure 10). The obtained enantiomers exhibited the specific rotations shown in Table 1. The enantiomeric ratios were determined by chiral GC.
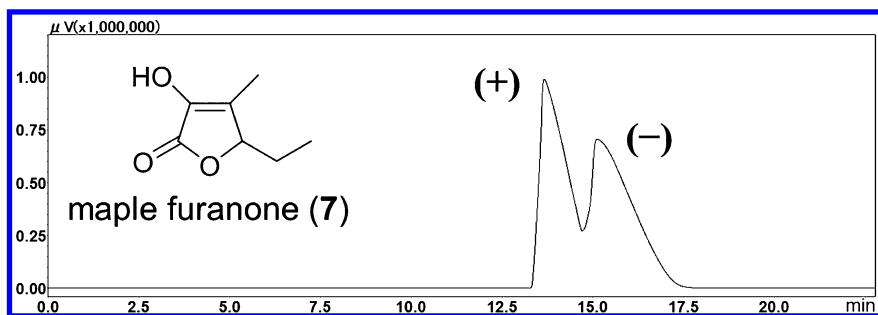
Figure 10. Optical Resolution of 7 by Enantioselective CO₂ SFC.

IR and VCD Theoretical Calculation for Furanones 6 and 7

Theoretical calculations of the VCD spectra of **6** and **7** were performed using DFT at the B3PW91/6-31G(d,p) level. The initial geometries were generated with the CONFLEX search. The DFT conformational analysis revealed one and three low-lying conformers for **6** and **7**, respectively (Figure 11). The observed IR and VCD spectra of sotolon (**6**) and the calculated IR and VCD spectra of (*R*)-**6** are shown in Figure 12.
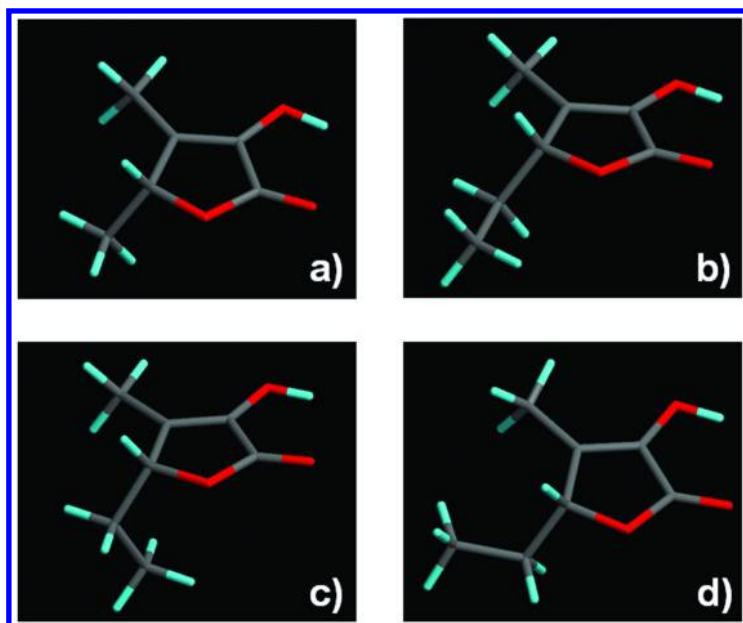

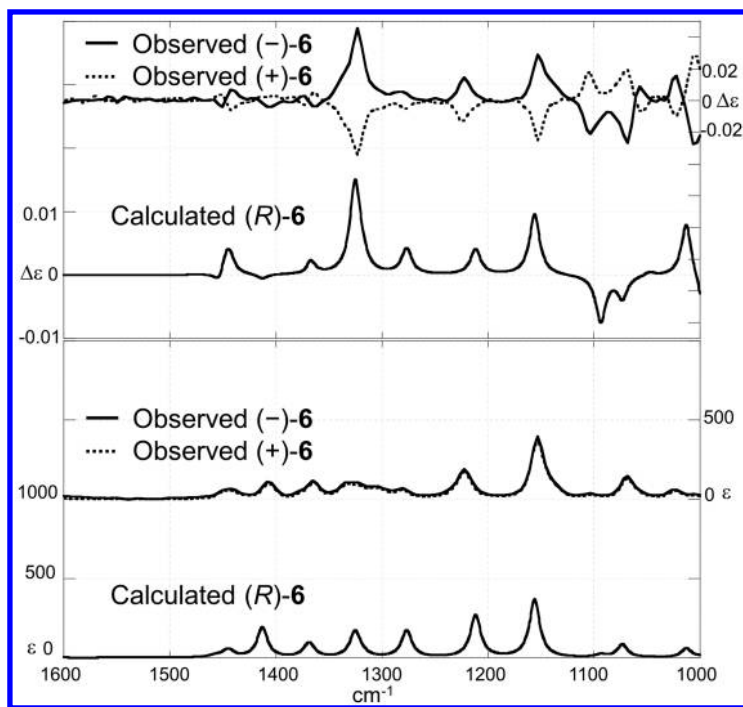*Figure 11. The Most Stable Conformer of (R)-6 (a) and Three Stable Conformers of (R)-7 (b, c, d).*

*Figure 12. Comparison of IR (Lower Frame) and VCD (Upper Frame) Observed Spectra (CCl₄, c = 0.15 M, l = 72 μm) for **6** with Calculated Spectra for (R)-**6**.*

Absolute Stereochemistry of Sotolon 6

As shown in Figure 12, observed VCD spectra of (+)-**6** and (−)-**6** are mirror images. The levorotatory enantiomer (−)-**6** showed an obvious positive Cotton effect around 1335 cm⁻¹, which can be attributed to a C–H bending at the stereogenic center. Interestingly, the corresponding VCD bands were observed in the previously measured VCD spectra of **3** and **4**, which implied the possibility of a convenient assignment of the absolute stereochemistry of these types of furanones using the distinctive VCD signal as a reliable marker. The calculated IR spectrum of (R)-**6** showed a good agreement with the observed IR spectra of both (+)-**6** and (−)-**6**, which suggests the high reliability of the calculation performed in this study. The calculated VCD signals of (R)-**6** agreed well with those observed for (−)-**6** in their fingerprint regions (from 1500 to 1000 cm⁻¹). We therefore concluded the absolute configurations of **6** to be (R)-(−)-**6** and (S)-(+)-**6**, which is consistent with the results previously assigned by the synthetic works (*37*, *38*)

Most of the observed characteristic IR absorptions of **7** are similar to those of **6** (Figure 13). On the contrary, the observed VCD spectrum of **7** is different from that of **6** especially around 1254 cm^{-1}, exquisitely reflecting their structural differences. Since the calculated VCD spectrum of (*R*)-**7** showed an excellent agreement with the observed VCD spectrum of (+)-**7**, configurations of **7** were successfully determined as (*R*)-(+)-**7** and (*S*)-(−)-**7**.
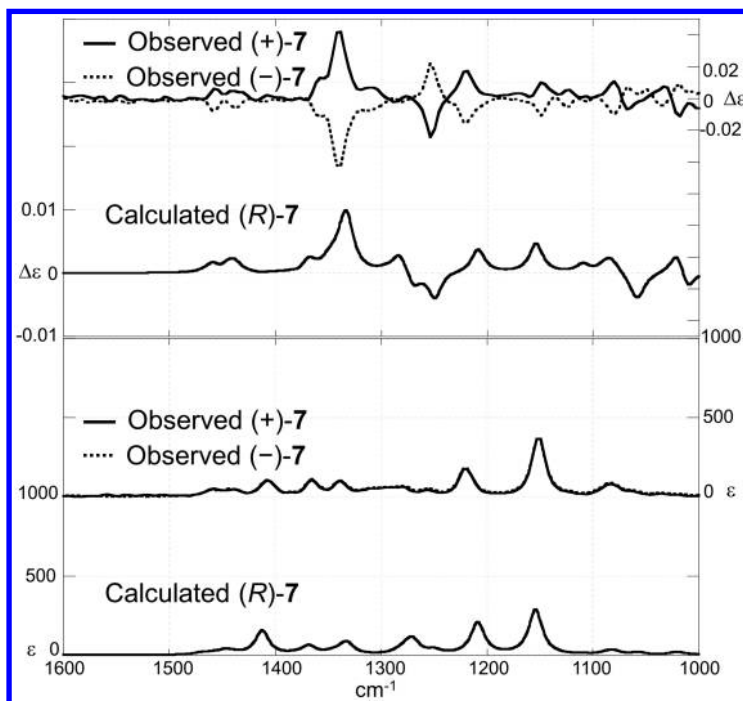

Figure 13. Comparison of IR (Lower Frame) and VCD (Upper Frame) Observed Spectra (CCl$_4$, c = 0.15 M, l = 72 μm) for (+)-7 with Calculated Spectra for (R)-7.

Opposite Signs of the Specific Rotation for 6 and 7

It should be noted that the signs of the specific rotation of **7** [(*R*)-(+)-**7** and (*S*)-(−)-**7**] are opposite to those of **6** [(*R*)-(−)-**6** and (*S*)-(+)-**6**]. This might be a rare case in which slight differences of the substituent are responsible for a sign inversion of the [α]$_D$ regardless of their identical absolute configurations. However, this inversion is also supported by our results of chiral GC analyses, in which (*R*)-(−)-**6** and (*R*)-(+)-**7**, namely, (*R*)-forms of both compounds, eluted earlier than their corresponding antipodes. Furthermore, Mosandl *et al.* also reported that (*R*)-(−)-**6** and (+)-**7** eluted earlier on their chiral GC analyses performed under

conditions similar to our study, although the absolute configuration of **7** had not been determined (*39*, *40*). These experimental results ensure the stereochemical assignment in this study, and this unexpected and interesting finding illustrates the risk of the absolute configuration determination that relies only on the sign of optical rotation measured with a single wavelength (*41*).

Odor Evaluation of Enantiopure Furanones

For both enantiomers of **2**, **3**, **4**, and **7** odor evaluations were carried out. As expected, significant organoleptic differences between these enantiomers were perceived as shown in Table 2. Contrary to the data reported for **2** (*42*), our result show that the (*R*)-(+)-isomer exhibits intense odor, whereas the considerable difference of odor intensity between the enantiomers of **3** is in agreement with the earlier results. On the other hand, the (*R*)-(+)-isomer of **4** was revealed to possess a stronger odor than (*S*)-(−)-**4**. It is of interest that the (2*R*)-configurations of **2**, **3**, and **4** might play an important role for the intense sweet note that is characteristic for 2-substituted-3(2*H*)-furanones. (*R*)-(+)-**7** possessed a significantly intense maple syrup-like odor at 100 ppt solution in H_2O, while (*S*)-(−)-**7** was less intense (Table 2). This result is consistent with the results of previous work (*40*).

Table 2. Odor Description of Isolated Optically Active Furanones

compound	*odor description*
(*R*)-(+)-**2**	obviously strong, sugary, jammy, sweet
(*S*)-(−)-**2**	extremely weak
(*R*)-(+)-**3**	burnt, intense caramel
(*S*)-(−)-**3**	lactone, coumarin-like, no caramel odor
(*R*)-(+)-**4**	burnt, intense caramel
(*S*)-(−)-**4**	weak caramel odor
(*R*)-(+)-**7**	maple syrup-like odor
(*S*)-(−)-**7**	less intense than (*R*)-(+)-**7**

Conclusion

In conclusion, we confirmed the previously reported absolute stereochemistry of patchoulol (**1**) as (1*R*,3*R*,6*S*,7*S*,8*S*) by means of the VCD technique. The application of this technique was extended to odor-active furanones that are prone to racemize due to keto-enol tautomerism. After successful efficient optical resolutions by SFC, we unveiled for the first time the absolute stereochemistries

of (*R*)-(+)-**2**, (*S*)-(−)-**2**, (*R*)-(+)-**3**, (*S*)-(−)-**3**, (*R*)-(+)-**4**, (*S*)-(−)-**4**, (*R*)-(+)-**7**, and (*S*)-(−)-**7** by using a state of the art VCD technique and chemical relay reaction. Surprisingly, our result showed (*R*)-(−)-**6**, (*R*)-(+)-**7**, (*S*)-(+)-**6**, and (*S*)-(−)-**7** configurations (Figure 14). It must be emphasized that these furanones exhibit opposite optical rotation signs despite their same absolute configurations. This finding warns that even simple and rigid molecules with the same absolute configuration may have opposite optical rotation. We also investigated the structure-activity relationships between absolute configurations and odor characteristics. Our result shows that the (2*R*)-isomers of 2-substituted-3(2*H*)-furanones are the principal contributors representing the characteristic burnt sugar like odor. Finally, we believe that the VCD method should also be useful for the chiroptical characterization of other aroma-active compounds.
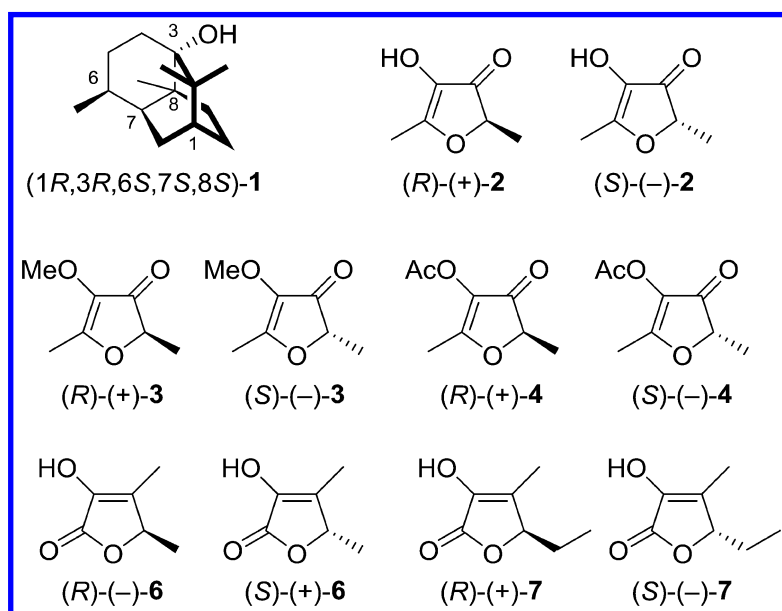

Figure 14. Absolute Configurations of Patchoulol and Furanones.

Acknowledgments

References

1. Teisseire, P.; Maupetit, P.; Corbier, B. Contribution to the knowledge of Patchouli oil. *Recherches* **1974**, *19*, 8–35.
2. Teisseire, P.; Maupetit, P.; Corbier, B.; Rouillier, P. Norpatchoulenol, chemical study, structure and absolute configuration. *Recherches* **1974**, *19*, 36–61.
3. Mookherjee, B. D.; Light, K. K.; Hill, I. D. A study on the odor-structure relationship of patchouli compound. In *Essential Oils*; Mookherjee, B. D., Mussinan, C. J., Eds.; Allured Publishing Corp.; Wheaton, IL, 1981; pp 247–272.
4. Zabetakis, I.; Gramshaw, J. W.; Robinson, D. S. 2,5-Dimethyl-4-hydroxy-2*H*-furan-3-one and its derivatives: analysis, synthesis, and biosynthesis—a review. *Food Chem.* **1999**, *65*, 139–151.
5. Slaughter, J. C. The naturally occurring furanones: formation and function from pheromone to food. *Biol. Rev.* **1999**, *74*, 259–276.
6. Raab, T. Untersuchungen zur Erdbeerfruchtreifung Biosynthese von 4-Hydroxy-2,5-dimethyl-3(2*H*)-furanon und Enzymaktivitäten während des Reifungsprozesses. Ph.D. Thesis, University of Würzburg, Würzburg, Germany, 2003.
7. Hauck, T. Zuckerphosphate als Vorläufer von 4-Hydroxy-3(2*H*)-furanonen. Ph.D. Thesis, University of Würzburg, Würzburg, Germany, 2004.
8. Kobayashi, A. In *Flavor Chemistry Trends and Developments*; Teranishi, R., Buttery, R. G., Shahidi, F., Eds.; ACS Symposium Series 388; American Chemical Society: Washington, DC, 1989; pp 49–59.
9. Buttery, R. G. In *Flavor Chemistry: Thirty Years of Progress*; Teranishi, R., Wick, E. L., Hornstein, I., Eds.; Kluwer Academic/Plenum Publishers: New York, 1999; pp 353–365.
10. Werkhoff, P.; Brennecke, S.; Bretschneider, W.; Güntert, M; Hopp, R.; Surburg, H. Chirospecific analysis in essential oil, fragrance and flavor reserch. *Z. Lebensm.−Unters. Forsch.* **1993**, *196*, 307–328.
11. Bentley, R. The nose as a stereochemist. Enantiomers and odor. *Chem. Rev.* **2006**, *106*, 4099–4112.
12. Terfloth, G. Enantioseparations in super- and subcritical fluid chromatography. *J. Chromatogr. A* **2001**, *906*, 301–307..
13. Sugimoto, D.; Yaguchi, Y.; Kasuga, H.; Okajima, S.; Emura, M. In *Recent Highlights in Flavor Chemistry and Biology*; Hofmann, T., Meyerhof, W., Schieberle, P., Eds.; Deutsche Forschungsanstalt für Lebensmittelchemie: Garching, Germany, 2008; pp 340–344.
14. Keiderling, T. A. In *Circular Dichroism: Principles and Applications*; Berova, N., Nakanishi, K., Woody, R. W., Eds.; Wiley-VCH: New York, 2000; pp 621–666.
15. Freedman, T. B.; Cao, X.; Dukor, R. K.; Nafie, L. Absolute configuration determination of chiral molecules in the solution state using vibrational circular dichroism. *Chirality* **2003**, *15*, 743–758.
16. Polavarapu, P. L.; He, J. Chiral Analysis Using mid-IR Vibrational CD Spectrospcopy. *Anal. Chem.* **2004**, *76*, 61A–67A.

17. Taniguchi, T.; Miura, N.; Nishimura, S.-I.; Monde, K. Vibrational circular dichroism: chiroptical analysis of biomolecules. *Mol. Nutr. Food Res.* **2004**, *48*, 246–254.

18. Nafie, L. A.; Dukor, R. K. In *Chiral Analysis*; Busch, K. W., Busch, M. A., Eds.; Elsevier: Amsterdam, The Netherlands, 2006; pp 505–544.

19. Taniguchi, T.; Monde, K. Chiroptical analysis of glycoconjugates by vibrational circular dichroism (VCD). *Trends Glycosci. Glycotechnol.* **2007**, *19*, 149–166.

20. Kellenbach, E. R.; Dukor, R. K.; Nafie, L. A. Absolute configuration determination of chiral molecules without crystallisation by vibrational circular dichroism (VCD). *Spectrosc. Eur.* **2007**, *19*, 15–17.

21. Polavarapu, P. L. Renaissance in chiroptical spectroscopic methods for molecular structure determination. *Chem. Rec.* **2007**, *7*, 125–136.

22. Stephens, P. J.; Devlin, F. J.; Pan, J.-J. The determination of the absolute configurations of chiral molecules using vibrational circular dichroism (VCD) spectroscopy. *Chirality* **2008**, *20*, 643–663.

23. He, J.; Wang, F.; Polavarapu, P. L. Absolute configurations of chiral herbicides determined from vibrational circular dichroism. *Chirality* **2005**, *17*, S1–S8.

24. Nafie, L. A. Vibrational circular dichroism; a new tool for the solution-state determination of the structure and absolute configuration of chiral natural product molecule. *Nat. Prod. Commun.* **2008**, *3*, 451–466.

25. Yaguchi, Y.; Nakahashi, A.; Miura, N.; Sugimoto, D.; Monde, K; Emura, M. Stereochemical Study of Chiral Tautomeric Flavorous Furanones by Vibrational Circular Dichroism. *Org. Lett.* **2008**, *10*, 4883–4885.

26. Emura, M.; Yaguchi, Y.; Nakahashi, A.; Sugimoto, D.; Miura, N.; Monde, K. Stereochemical Studies of Odorous 2-Substituted-3(2*H*)-Furanones by Vibrational Circular Dichroism. *J. Agric. Food Chem.* **2009**, *57*, 9909–9915.

27. Monde, K.; Nakahashi, A.; Miura, N.; Yaguchi, Y.; Sugimoto, D.; Emura, M. Stereochemical study of a novel tautomeric furanone, homofuraneol. *Chirality* **2009**, *21*, E110–E115.

28. Nakahashi, A.; Yaguchi, Y.; Miura, N.; Emura, M.; Monde, K. A Vibrational Circular dichroism approach to the determination of the absolute configurations of flavorous 5-substituted-2(5H)-furanones. *J. Nat. Prod.* **2011**, *74*, 707–711.

29. *SPARTAN'10*; Wavefunction, Inc.: Irvine, CA; www.wavefun.com/products/ spartan.html (accessed November 2015).

30. Goto, H.; Osawa, E. Corner Flapping: A Simple and Fast Algorithm for Exhaustive Generation of Ring Conformations. *J. Am. Chem. Soc.* **1989**, *111*, 8950–8951.

31. Goto, H.; Osawa, E. An efficient algorithm for searching low-energy conformers of cyclic and acyclic molecules. *J. Chem. Soc., Perkin Trans. 2* **1993**, 187–198.

32. Kudoh, S.; Takayanagi, M.; Nakata, M. Infrared spectra of Dewar 4-picoline in low-temperature argon matrices and vibrational analysis by DFT calculation. *Chem. Phys. Lett.* **2000**, *322*, 363–370.

33. Frisch, M. J.; Trucks, G. W.; Schlegel, H. B.; Scuseria, G. E.; Robb, M. A.; Cheeseman, J. R.; Scalmani, G.; Barone, V.; Mennucci, B.; Petersson, G. A.; Nakatsuji, H.; Caricato, M.; Li, X.; Hratchian, H. P.; Izmaylov, A. F.; Bloino, J.; Zheng, G.; Sonnenberg, J. L.; Hada, M. Ehara, M.; Toyota, K.; Fukuda, R.; Hasegawa, J.; Ishida, M.; Nakajima, T.; Honda, Y.; Kitao, O.; Nakai, H.; Vreven, T.; Montgomery, J. A., Jr.; Peralta, J. E.; Ogliaro, F.; Bearpark, M.; Heyd, J. J.; Brothers, E.; Kudin, K. N.; Staroverov, V. N.; Keith, T.; Kobayashi, R.; Normand, J.; Raghavachari, K.; Rendell, A.; Burant, J. C.; Ivengar, S. S.; Tomasi, J.; Cossi, M.; Rega, N.; Millam, J. M.; Klene, M.; Knox, J. E.; Cross, J. B.; Bakken, V.; Adamo, C.; Jaramillo, J.; Gomperts, R.; Stratmann, R. E.; Yazyev, O.; Austin, A. J.; Cammi, R.; Pomelli, C.; Ochterski, J. W.; Martin, R. L.; Morokuma, K.; Zakrzewski, V. G.; Voth, G. A.; Salvador, P.; Dannenberg, J. J.; Dapprich, S.; Daniels, A. D.; Farkas, O.; Foresman, J. B.; Ortiz, J. V.; Cioslowski, J.; Fox, D. J. *Gaussian 09*, revision C.01; Gaussian, Inc.: Wallingford CT, 2010.

34. Frisch, M. J.; Trucks, G. W.; Schlegel, H. B.; Scuseria, G. E.; Robb, M. A.; Cheeseman, J. R.; Montgomery, J. A., Jr.; Vreven, T.; Kudin, K. N.; Burant, J. C.; Millam, J. M.; Iyengar, S. S.; Tomasi, J.; Barone, V.; Mennucci, B.; Cossi, M.; Scalmani, G.; Rega, N.; Petersson, G. A.; Nakatsuji, H.; Hada, M.; Ehara, M.; Toyota, K.; Fukuda, R.; Hasegawa, J.; Ishida, M.; Nakajima, T.; Honda, Y.; Kitao, O.; Nakai, H.; Klene, M.; Li, X.; Knox, J. E.; Hratchian, H. P.; Cross, J. B.; Bakken, V.; Adamo, C.; Jaramillo, J.; Gomperts, R.; Stratmann, R. E.; Yazyev, O.; Austin, A. J.; Cammi, R.; Pomelli, C.; Ochterski, J. W.; Ayala, P. Y.; Morokuma, K.; Voth, G. A.; Salvador, P.; Dannenberg, J. J.; Zakrzewski, V. G.; Dapprich, S.; Daniels, A. D.; Strain, M. C.; Farkas, O.; Malick, D. K.; Rabuck, A. D.; Raghavachari, K.; Foresman, J. B.; Ortiz, J. V.; Cui, Q.; Baboul, A. G.; Clifford, S.; Cioslowski, J.; Stefanov, B. B.; Liu, G.; Liashenko, A.; Piskorz, P.; Komaromi, I.; Martin, R. L.; Fox, D. J.; Keith, T.; Al-Laham, M. A.; Peng, C. Y.; Nanayakkara, A.; Challacombe, M.; Gill, P. M. W.; Johnson, B.; Chen, W.; Wong, M. W.; Gonzalez, C.; Pople, J. A. *Gaussian 03*, revision C.02; Gaussian, Inc.: Wallingford, CT, 2004.

35. Srikrishna, A.; Satyanarayana, G. An enantiospecific total synthesis of (−)-patchouli alcohol. *Tetrahedron: Asymmetry* **2005**, *16*, 3992–3997.

36. Nishiya, K.; Tsujiyama, T.; Kimura, T.; Takeya, K.; Itokawa, H.; Iitaka, Y. Sesquiterpenoids from *Valeriana fauriei. Phytochemistry* **1995**, *39*, 713–714.

37. Okada, K.; Kobayashi, A.; Mori, K. Synthesis of both the enantiomers of 3-hydroxy-4, 5-dimethyl-2(5H)-furanone (sotolon), the key compound for sugary flavor. *Agric. Biol. Chem.* **1983**, *47*, 1071–1074.

38. Guichard, E.; Etievant, P.; Henry, R.; Mosandl, A. Enantiomeric ratios of pantolactone, sorerone, 4-carboethoxy-4-hydroxy-butyrolactone and of sotolon, a flavor impact compound of flor-sherry and botrytized wines. *Z. Lebensum.-Unters. Forsch.* **1992**, *195*, 540–544.

39. Bruche, G.; Mosandl, A.; Kinkel, J. N. Stereoisomeric flavor compounds part LXV: Preparative resolution of the enantiomers of chiral dihydrofuranones by recycling chromatography. *J. High Resolut. Chromatogr.* **1993**, *16*, 254–257.

40. Podebrad, F.; Heil, M.; Reichert, S.; Mosandl, A.; Sewell, A. C.; Bohles, H. 4,5-Dimethyl-3-hydroxy-2[5*H*]-furanone (sotolone) — The odour of maple syrup urine disease. *J. Inherited Metab. Dis.* **1999**, *22*, 107–114.

41. Stephens, P. J.; Mccann, D. M.; Cheeseman, J. R.; Frisch, M. J. Determination of absolute configurations of chiral molecules using ab initio time-dependent Density Functional Theory calculations of optical rotation: How reliable are absolute configurations obtained for molecules with small rotations? *Chirality* **2005**, *17*, S52–S64.

42. Bruche, G.; Dietrich, A.; Mosandl, A. Stereoisomeric flavor compounds LXXI: determination of the origin of aroma–active dihydrofuranones. *Z. Lebensm.-Unters. Forsch.* **1995**, *201*, 249–252.

Chapter 4

Multi-Enzymatic Cascade Procedures for the Synthesis of Chiral Odorous Molecules

Elisabetta Brenna,*,[1],[2] Michele Crotti,[1] Francesco G. Gatti,[1] Fabio Parmeggiani,[1] Andrea Pugliese,[1] and Sara Santangelo[1]

**[1]Dipartimento di Chimica, Materiali e Ingegneria Chimica "G. Natta", Politecnico di Milano, Via Mancinelli 7, I-20131 Milano, Italy
[2]Istituto di Chimica del Riconoscimento Molecolare – CNR, Via M. Bianco 9, I-20131 Milano, Italy
*E-mail: mariaelisabetta.brenna@polimi.it.**

Nowadays, several isolated enzymes have been made available to be employed as catalysts for stereoselective organic reactions. The high chemo- and stereoselectivity of enzyme-mediated reactions can be exploited to develop effective and sustainable manufacturing processes in particular for those chiral compounds for which the influence of absolute configuration on odor properties could justify the commercialization in enantiopure form. The development of multi-enzyme systems to be used for multistep reactions in one-pot cascade synthesis has the potential to reduce costs by avoiding work-up and purification of synthetic intermediates. The application of biocatalyzed procedures to the preparation of the single isomers of chiral odorous molecules, such as γ- and δ-lactones, Muguesia® and nootkatone, will be described.

Introduction

The phenomenon of enantioselectivity in odor perception has been investigated intensively in the last years (*1*), and it has been attributed to the fact that human olfactory receptors are chiral and thus can interact differently with the enantiomers of a chiral odorous molecule (*2*). For several flavors and fragrances the most potent stereoisomer or the one showing the most desired odor profile has been determined (*3*).

Many flavorings are of natural origin, and they can be obtained by extraction procedures. Several are chiral, and they are biogenerated by natural systems as enantioenriched compounds. In this case, the challenge is to develop enantioselective synthetic methods that can be competitive with or even better than extractive techniques, and that are in agreement with the conditions for "natural" labeling requested by current legislations.

As for chiral fragrance chemicals employed in fine and functional perfumery, their use as enantiopure compounds offers two advantages. The first one is the improvement of the odor performance of perfumed products, if in their formulation racemic chiral fragrances can be substituted by the single stereoisomers showing the finest odor quality and the highest potency. The other one is related to a reduction of the environmental load of final products for the following reasons: (i) The use of the most potent stereoisomer allows the same odor sensation to be elicited by using a lower amount of material; (ii) in some cases a specific stereoisomer may have a better safety profile than the others. An example is represented by rose oxide: Of the four possible stereoisomers, (4R)-cis-rose oxide is the one showing not only the lowest odor threshold and the superior olfactory quality, but also the highest biodegradability (*4*).

Obviously, optically active fragrance chemicals are more expensive than the corresponding racemates. An improvement of stereoselective synthetic technology is necessary to promote the commercialization of single enantiomers of odorous molecules. The manufacturing routes have to be competitive in terms of costs with the synthesis of the corresponding racemic products, and to satisfy the criteria of sustainability now required for chemical processes.

Among the available stereoselective synthetic methods, those involving enzymes have already been employed successfully for the industrial production of commodities and fine-chemicals, especially pharmaceuticals (*5*). The applications of enzymes and microorganisms in synthetic procedures have been growing tremendously in the last decade (*6–11*). Biocatalysis can offer effective catalysts for several chemical reactions, in order to face specific problems in synthetic chemistry, especially those connected with the preparation of chiral compounds.

As for the synthesis of flavorings, according to current European legislation, flavoring substances obtained by enzymatic or microbiological processes, with no chemical steps, from material of vegetable, animal, or microbiological origin can be labeled as natural (*12*). Thus, biocatalyzed processes represent an attractive alternative to extraction for the preparation of natural flavorings (*13*, *14*), especially since they are carried out under mild conditions and they usually provide very high chemo-, regio- and stereoselectivity.

In the field of fragrance chemistry, where there are no restrictions either regarding the source of the starting material or the nature of the synthetic steps, the high selectivity of enzyme-mediated reactions can be exploited to develop effective and sustainable manufacturing processes for the single stereoisomers of those chiral compounds for which the influence of absolute configuration on odor properties could justify the commercialization in enantiopure form.

Recently, multi-enzyme systems have been investigated for applications in one-pot cascade procedures (*15–18*), in which a consecutive series of chemical reactions occur in the same reaction vessel. Cascades with two or more bio- as

well as chemo-catalysts can be performed in simultaneous or sequential mode: In simultaneous cascades all the catalysts and reactants are present from the outset; in the sequential approach the next catalyst is added only after the completion of the previous step. Work-up and purification of synthetic intermediates is avoided, with the advantage of reducing reaction time, costs and waste. In the optimization of cascade procedures, problems may arise from the compatibility of the reaction conditions of the steps that are to be combined. Biocatalytic cascades are generally easier to realize as most enzymes reach their performance optimum at similar temperature and pH values in aqueous buffers, and this peculiarity of biocatalysis is a significant advantage over traditional chemical catalysis. Indeed, applications of enzymatic techniques to the preparation of optically enriched chiral odorous molecules appear very promising. The most recent examples reported in the literature are described in this chapter.

γ and δ-Lactones

Lactones are widely spread in many different kinds of fruits and represent an important class of flavoring substances, extensively employed in beverages and dairy products. The enzymatic one-pot cascade enantioselective syntheses reported so far for these compounds are based on the following procedures: (i) alcohol dehydrogenase (ADH)-mediated reduction of keto esters, followed by spontaneous or induced lactonization; (ii) ene-reductase (ER)-catalyzed reduction of unsaturated keto esters, combined with ADH reduction of the carbonyl group and final cyclization; (iii) ER-catalyzed reduction of unsaturated ketones, followed by Baeyer-Villiger oxidation promoted by monooxygenases; (iv) ADH-mediated oxidation of diols, followed by spontaneous lactonization.

Procedures Starting From Keto Esters

The ADH-mediated reduction of keto esters **1a-f** (Figure 1) was investigated in order to prepare the corresponding hydroxy esters and lactones (*19*).
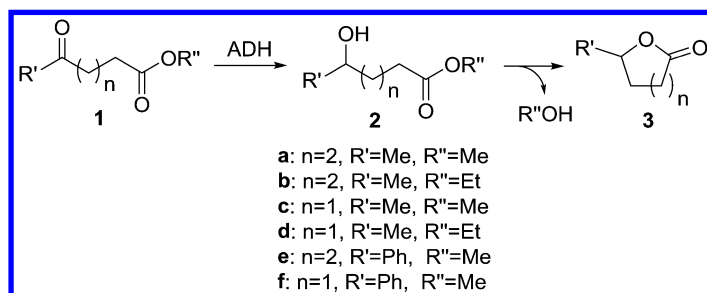

a: n=2, R'=Me, R"=Me
b: n=2, R'=Me, R"=Et
c: n=1, R'=Me, R"=Me
d: n=1, R'=Me, R"=Et
e: n=2, R'=Ph, R"=Me
f: n=1, R'=Ph, R"=Me

Figure 1. From Keto Esters to Lactones.

ADHs from *Rhodococcus ruber* (ADH-A) and *Lactobacillus brevis* (LBADH) converted small keto esters **1a-d** with opposite enantioselectivities, to afford the enantiomers of the corresponding reduced compounds with ee (enantiomeric excess) >99%. With bulky substrates **1e-f** the ADH from *Ralstonia* sp. (RasADH) was successfully employed to achieve the synthesis of the (*R*)-enantiomer of the corresponding hydroxy ester. Two different approaches were then followed to isolate the corresponding lactones: a cascade reaction with spontaneous cyclization of the hydroxy ester intermediate, or a one-pot two-step sequential protocol with the addition of HCl.
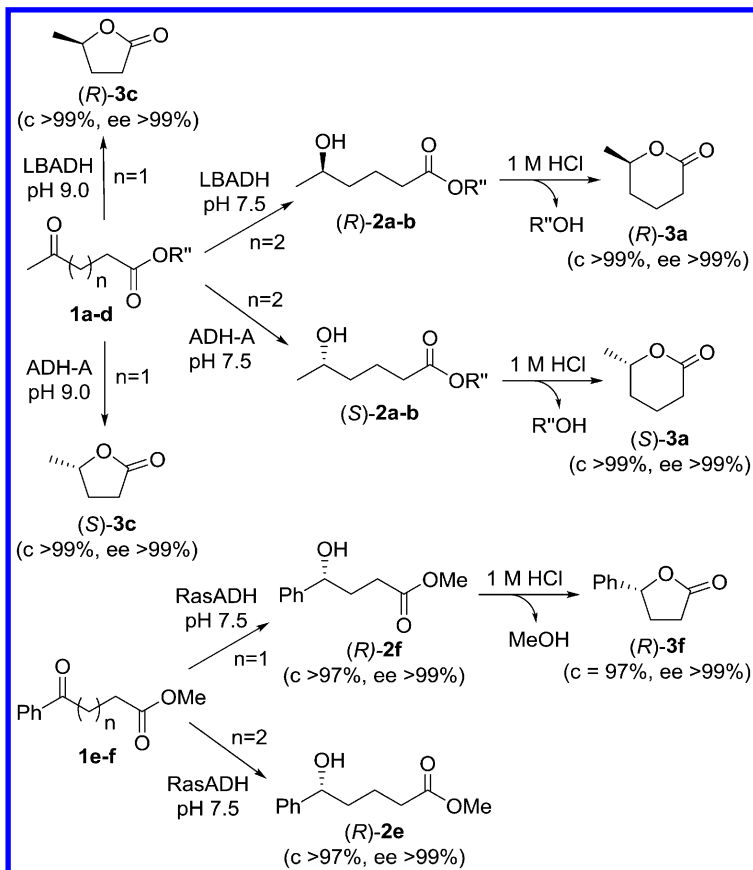

Figure 2. Chiral γ- and δ-Lactones Obtained by ADH Reduction of Keto Esters.

The effect of pH was investigated in the reaction of compound **1a**, in order to establish whether this parameter could shift the equilibrium in favor of one of the two possible products, the hydroxy ester and the lactone. At neutral pH the hydroxy ester **2a** was the only product; at higher pH detectable amounts of lactone **3a** were obtained with both ADHs, **2a** still being the main product. When the reaction was carried out at pH 5.0, the formation of lactone **3a** was inhibited and the enzymatic activity reduced. The addition of 1 M HCl to the reaction

mixture of hydroxy ester **2a** and lactone **3a**, obtained after the ADH-catalyzed bioreduction, promoted the complete conversion into lactone **3a** without loss of enantiomeric purity (ee >99%). A one-pot, two-step tandem protocol to the synthesis of δ-caprolactone **3a** was then optimized: After reduction, mediated either by LBADH or by ADH-A, HCl solution was added to the reaction medium, affording quantitatively lactones (*R*)- and (*S*)-**3a** (ee >99% in both cases) after 24 h (Figure 2).

The resulting intramolecular cyclization was spontaneous for 5-membered lactones: The two enantiomers of lactone **3c** were obtained as the main product in a one-pot cascade reaction at 30°C and pH 9.0, recycling the cofactor simply by addition of 2-propanol, starting from either γ-keto esters **1c** or **1d**.

For the reduction of bulky substrates **1e-f** only an (*R*)-selective ADH could be found (RasADH). The reduction of **1e** at pH 7.5 gave hydroxy ester **2e** (c (conversion) >97% and ee >99%) which could not be converted efficiently into the corresponding lactone. On the contrary, γ-keto ester **1f** was reduced and then cyclized by addition of HCl to afford (*R*)-**3f** (c = 97%, ee = 99%).

These findings were also applied by the same authors to obtain a brominated lactone, which was employed in sequential Pd-catalyzed transformations for the synthesis of functionalized chiral lactones useful in biological applications.

Procedures Starting From Unsaturated Keto Esters

Enantio- and diastereomerically pure γ-butyrolactones (3*R*,5*S*)-*syn*-**4** and (3*R*,5*R*)-*anti*-**4** were prepared by using a one-pot two-enzyme sequential reaction starting from ethyl 2-methyl-4-oxopent-2-enoate (**5**) as a common precursor (*20*). The reduction of the C=C double bond catalyzed by the ene-reductase from *Saccharomyces carlsbergensis* (Old Yellow Enzyme 1; OYE1) consistently afforded the (*R*)-enantiomer of the corresponding reduced keto ester **6** with ee >99%, starting from either (*E*)- or (*Z*)-**5** (Figure 3). When performing the reaction on a preparative scale, a cofactor regeneration system was employed based on the reduction of NADP$^+$ by means of a glucose dehydrogenase (GDH) at the expense of the oxidation of glucose as a sacrificial substrate.
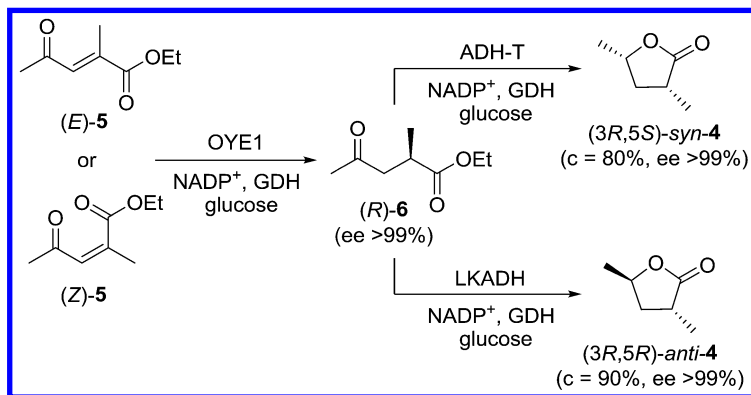

Figure 3. One-Pot Sequential Procedure to syn- and anti-4.

Enantiopure ketone (*R*)-**6** was then subjected to the reduction of the carbonyl group by means of an ADH. The use of ADH from *Thermoanaerobacter* sp. (ADH-T) afforded, after spontaneous lactonization, γ-butyrolactone (3*R*,5*S*)-*syn*-**4** (ee >99%), whereas ADH from *Lactobacillus kefir* (LKADH) gave the stereoisomer (3*R*,5*R*)-*anti*-**4** (ee >99%).

A one-pot procedure was optimized by sequential addition of the two enzymes without isolation of the intermediate ketone. GDH/glucose was used as the recycling system for the cofactor (NADPH for both enzymatic steps). The γ-butyrolactones *syn*- and *anti*-**4** were synthesized in high enantiopurities (ee >99%), and excellent yields (80% and 90%, respectively).

In a further development of this work, besides derivatives (*E*)-and (*Z*)-**5**, other ethyl 4-oxopent-2-enoate derivatives **7a-c** (Figure 4) were reduced in two subsequent steps (first by an ER, then by an ADH) to afford chiral γ-lactones as single stereoisomers in a one-pot two-enzyme sequential procedure (*21*).
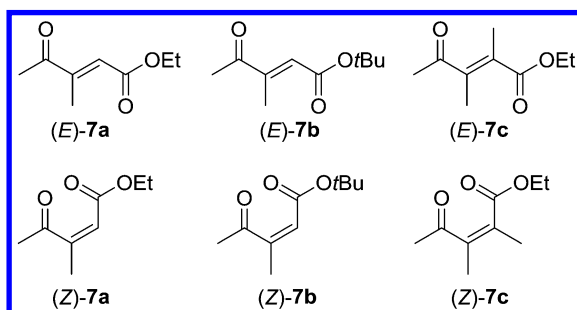

Figure 4. Unsaturated Esters Subjected to ER/ADH Sequential Reduction.

The starting (*E*)- and (*Z*)-keto esters **7a-c** were prepared in diastereomerically pure form by Wittig-type reactions. The ene-reductase from *Bacillus subtilis* (YqjM) was employed to reduce the C=C double bond of compounds **7a-c**, affording the corresponding reduced products in high yields and enantiomeric purities. In particular, derivatives (*E*)-**7a-b** afforded, respectively, (*S*)-**8a-b**, while (*Z*)-**7a-b** were converted into (*R*)-**8a-b**; compound (*E*)-**7c** was reduced entirely with complete enantioselectivity to (2*R*,3*S*)-**8c**, whereas the (*Z*)-diastereoisomer was not accepted as substrate at all.

After the C=C double bond reduction, the ADH was added to the reaction medium to promote the reduction of the carbonyl group. Commercial ADHs were screened to achieve the reduction of the carbonyl group with opposite enantioselectivity: evo-030 (ADH 030, evocatal, Monheim, Germany) and LKADH were selected for this purpose. Combining the stereoselectivity of the two subsequent reductions, each creating a stereogenic center, lactones **9** and **10** could be obtained after spontaneous cyclization (Figures 5 and 6). In both enzymatic steps, the cofactor NADPH was recycled with the glucose/GDH system. The hydroxy *t*-butyl esters **11** did not undergo cyclization.

The 4,5-dimethyl substituted γ-lactone **9** can be found in the sun-cured leaves of *Nicotiana tabacum* to which it conveys a typical and pleasant fruity character (*22*). Both the odor profile and threshold of each stereoisomer depend on the absolute configuration (*23*).

In a publication that appeared nearly simultaneously to that of Pietruszka *et al.* (*21*), an alternative sequential procedure for the synthesis of the four stereoisomers of lactone **9** was described (*24*), based on the ER/ADH sequential reductions, followed by final lactonization promoted by trifluoroacetic acid.
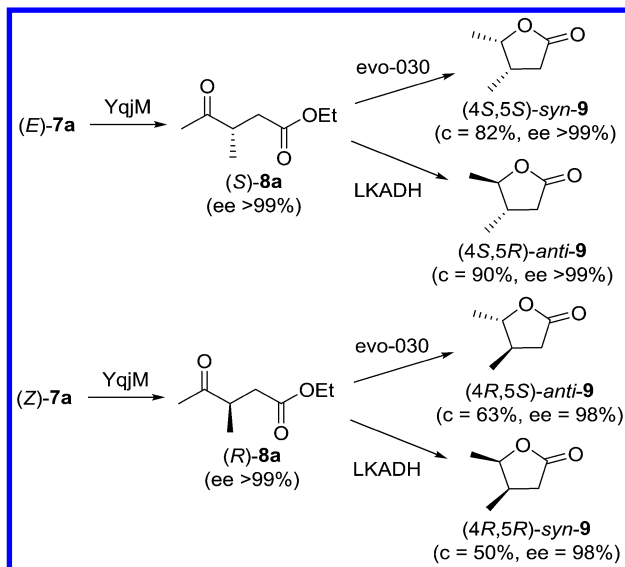

Figure 5. Products of ADH-mediated Reduction of (S)- and (R)-8a.

Ethyl keto ester (*E*)-**7a** and the corresponding methyl keto ester (*E*)-**12** (Figure 7) were prepared by Wittig olefination of diacetyl (2,3-butanedione) with the suitable triphenylphosphonium ylide, and purified by chromatography. The corresponding (*Z*)-isomers were either isolated as side products of the Wittig reaction (in low yield), or prepared by photoisomerization of the corresponding (*E*)-isomers (in very good yield, but modest diastereomeric excess, *Z/E* = 74:26).

For the ER mediated step, OYE1 and OYE2-3 from *Saccharomyces cerevisiae* were employed. The regeneration of the NADPH cofactor was carried out using a GDH (from *Bacillus megaterium*), with glucose as the sacrificial cosubstrate. The reduction of the (*E*)-stereoisomer of the unsaturated keto ester **7a** and **12** by these three ERs afforded the (*S*)-enantiomer of the corresponding reduced compound in a quantitative yield and with high ee values (96-99%). (Z)-**7a** and (Z)-**12** were converted quantitatively by OYE1-3 into the (*R*)-enantiomer with modest ee values in the range 52-80%. For this reason, a different approach was devised to obtain (*R*)-**8a**.
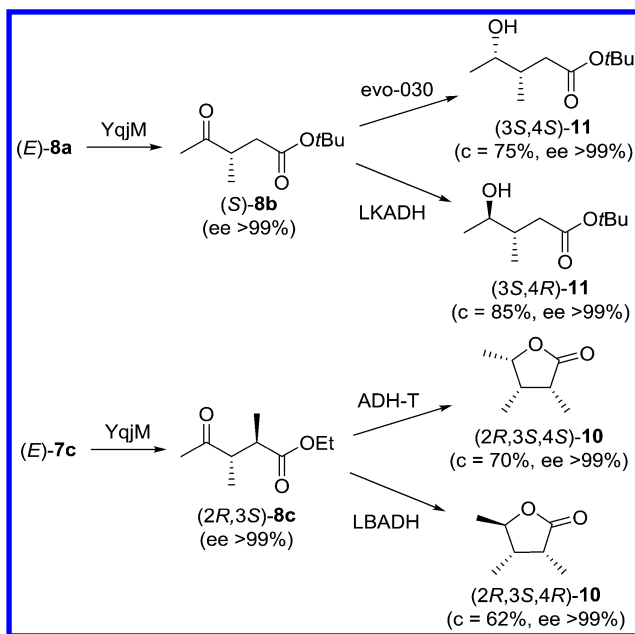
*Figure 6. Products of ADH-mediated Reduction of (S)-**8b** and (2R,3S)-**8c**.*
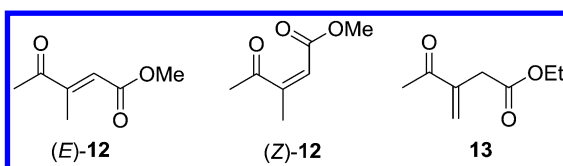

*Figure 7. Substrates for the Preparation of the Stereoisomers of Lactone **9**.*

The reduction of **13** (easily synthesized from acetylacetone) gave (*R*)-**8a** in a quantitative yield and with excellent ees, as a consequence of a different orientation adopted by the substrate in the active site of the enzymes with respect to the binding mode of compound (*E*)-**7a**. The biotransformations of (*E*)-**7a** and **13** with OYE2 were scaled up to afford (*S*)-**8a** (ee = 98%) and (*R*)-**8a** (ee = 99%), respectively, on a multi-mg scale. As for the ADH catalyzed step, the reduction of the carbonyl group of each enantiomer of **8a** was investigated using again the glucose/GDH system for cofactor regeneration. Among all screened enzymes, ADH from *Rhodococcus erythropolis* (READH), LKADH and ketoreductase (KRED, recombinant in *E. coli*) gave the best results in terms of conversion and stereoselectivity (de >94%). In addition, READH exhibited a pro-(*S*) stereoselectivity (Prelog ADH), while the other two enzymes were pro-(*R*) (anti-Prelog ADH). Finally, the three-step sequential procedure was carried out for both substrates (*E*)-**7a** and **13** with OYE2 as the ER, and READH

or KRED as ADHs, including the TFA-catalyzed lactonization, affording all four stereoisomers of *N. tabacum* lactone on a preparative scale, with an excellent diastereoselectivity (de >94%) and without any loss of optical purity (ee >98%).

Procedures Starting From Unsaturated Ketones

The odor properties of (*S*)- and (*R*)-lactones **14** and **15** were described by Yamamoto *et al.* (*25*) in 2002: (*S*)-**14** and **15** have lower threshold values (30 and 50 ppb, respectively) than the corresponding (*R*)-enantiomers (100 and 500 ppb, respectively), although they possess very similar odor characteristics (fruity, sweet and creamy for lactone **14**, fruity, sweet and apricot for **15**).

A multienzymatic two-step sequential procedure for the (*R*)-enantiomers of these lactones was optimized by Li *et al.* (*26*) in 2013, consisting of the enantioselective reduction of the carbon-carbon double bond of 2-alkylidenecyclopentanones **16** and **17**, followed by Baeyer-Villiger (BV) oxidation (Figure 8).
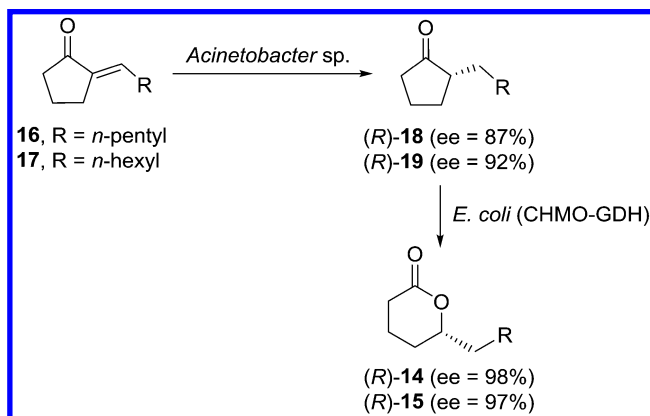

Figure 8. From Unsaturated Ketones to Lactones.

The first step was performed by using the resting cells of the microorganism *Acinetobacter* sp. RS1, which contains an ene-reductase capable of reducing the exo alkene bond of the starting ketones to afford (*R*)-**18** in 87% ee and (*R*)-**19** in 92% ee, both with complete conversion.

Recombinant *E. coli* strains, expressing cyclohexanone monooxygenase (CHMO) or cyclopentanone monooxygenase (CPMO), were engineered to catalyze the BV oxidation of **18** and **19** to **14** and **15**. Coexpression of CHMO and GDH from *Bacillus subtilis* within the same *E. coli* strain was then achieved, in order to obtain a more efficient whole-cell catalyst for the BV oxidations through intracellular cofactor recycling. *Acinetobacter* sp. RS1 and *E. coli* (CHMO-GDH) were combined to perform the reduction-oxidation in one pot. Preliminary experiments showed that *E. coli* (CHMO-GDH) had also some unexpected oxidation activity on substrates **16** and **17**; thus, the one-pot reactions were carried out in a sequential manner. The reduction of ketone **16** (40 mg)

with the resting cells of *Acinetobacter* sp. RS1 in the presence of glucose for 3 h, followed by the oxidation with resting cells of *E. coli* (CHMO-GDH) for 1.5 h, afforded (*R*)-**14** with 98% ee and 56% isolation yield. The same procedure was applied to substrate **17** (40 mg) to afford (*R*)-**15** with 98% ee and 56% isolation yield. The fact that the ee values of the final products were higher than those of the intermediate ketones was attributed by the authors to an enantioselective degradation of the lactones in the reaction medium.

Procedures Starting From Diols

Another enzymatic approach to the synthesis of lactones is based on the oxidation of 1,4-, 1,5-, and 1,6-diols by means of horse liver alcohol dehydrogenase (HLADH) (*27, 28*). In a first approach (*27*)), the oxidized nicotinamide cofactor NAD+ was regenerated by using a laccase from *Myceliophthora thermophila* (*Mt*laccase) and acetosyringone as a redox mediator (laccase-mediator system; LMS). Molecular oxygen acted as the terminal electron acceptor producing water as the sole by-product (Figure 9).

1,4-Diols **20-21** and 1,5-diols **22-23** were converted efficiently by the HLADH/LMS system (Figure 10), whereas ε-caprolactone formation (from 1,6-hexanediol **24**) reached only 26% conversion even after prolonged reaction times. The enantiomeric purity of the lactone product obtained from diol **21** was very low (ee = 17%) and decreased with increasing conversion. On the contrary, the oxidative lactonization of 3-methyl-1,5-pentanediol (**23**) proceeded with high conversion and stereoselectivity, affording the (*S*)-enantiomer of the corresponding lactone, which is a key building block in the total synthesis of (*R*,*Z*)-5-muscenone (*29*).
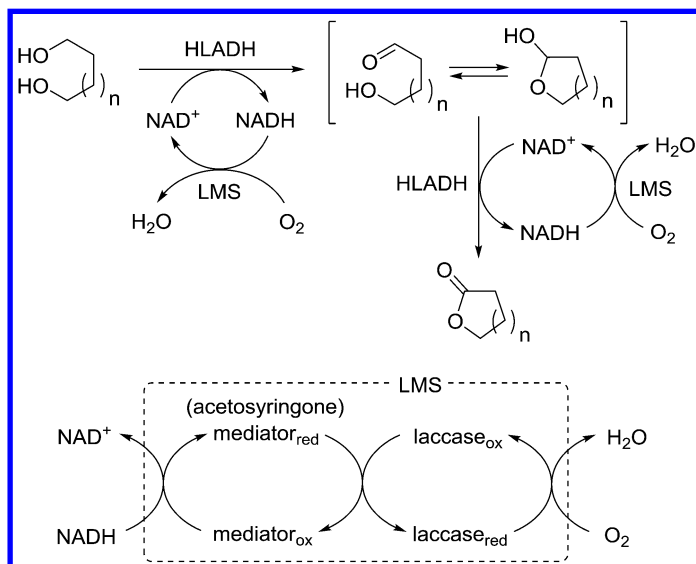

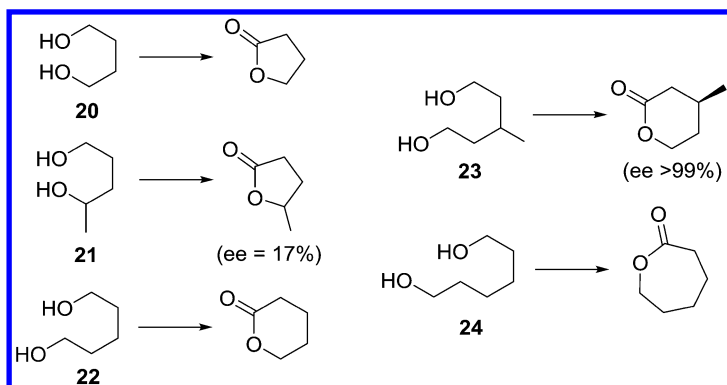*Figure 9. From 1,4-, 1,5- and 1,6-Diols to Lactones.*

Figure 10. Lactones Obtained by Oxidation of Diols.

Spontaneous hydrolysis of the lactone products in the reaction medium was found to be a limiting factor toward preparative application of the system. A biphasic system (water / diisopropyl ether) was thus investigated for the *in situ* extraction of the less hydrophilic lactone products into an organic phase, in order to prevent or reduce the occurrence of lactone hydrolysis. Preliminary results were satisfactory for all the diols in terms of conversions, and for diol **23** the enantioselectivity was maintained.
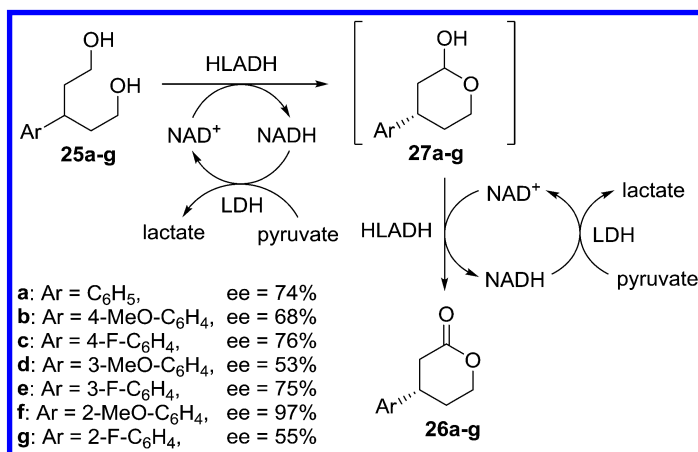

a: Ar = C$_6$H$_5$,   ee = 74%
b: Ar = 4-MeO-C$_6$H$_4$,   ee = 68%
c: Ar = 4-F-C$_6$H$_4$,   ee = 76%
d: Ar = 3-MeO-C$_6$H$_4$,   ee = 53%
e: Ar = 3-F-C$_6$H$_4$,   ee = 75%
f: Ar = 2-MeO-C$_6$H$_4$,   ee = 97%
g: Ar = 2-F-C$_6$H$_4$,   ee = 55%

Figure 11. δ-Lactones Obtained by Oxidation of 1,5-Diols.

In a second procedure (*28*), developed for the conversion of 3-aryl-1,5-diols **25** into the corresponding (*S*)-δ-valerolactones **26** by means of HLADH-mediated oxidation (Figure 11), NAD$^+$ was regenerated by the concomitant reduction of pyruvate to lactate catalyzed by L-lactate dehydrogenase (LDH). The formation of lactones **26** occurred by oxidation of the starting prochiral diols **25** to afford unstable cyclic hemiacetals **27**, which were then converted into the final lactones through a second oxidation step. The use of tetrahydrofuran (THF) as a cosolvent

showed beneficial effects on the enantioselectivity of the process. Lactones **26** could be obtained with satisfactory conversion values and modest to good enantiomeric purities.

Muguesia®

Muguesia (**28**) is a commercial fragrance available as a mixture of two racemic diastereoisomers (Figure 12). It is described as floral, muguet, rose and minty, and its usage is suggested when aldehydic muguet ingredients are not stable. The four stereoisomers of Muguesia® were prepared in 2005 according to a procedure based on the use of lipase-mediated kinetic resolution, and subjected to odor evaluation (*30*). The odor properties of Muguesia® were found to be highly dependent upon the configuration of the carbon atom in position 3: The (3*R*)-stereoisomers **28c-d** were described as weak and completely devoid of odor in the dry down note; the (3*S*)-stereoisomers **28a-b** were found to be the odor vectors of the commercial odorant, with floral and lily of the valley notes.

An efficient biocatalyzed procedure for the stereoselective synthesis of the most odorous (3*S*)-stereoisomers of Muguesia® was recently published (*31*) (Figure 13). It consists of a two-enzyme cascade reaction which combines the reduction of the activated carbon-carbon double bond of (*E*)-3-methyl-4-phenylbut-3-en-2-one (**29**), mediated by an ER, with the reduction of the carbonyl group promoted by an ADH, with the creation of two stereogenic centers in 1,2 relative position under high stereochemical control. All the enzymes were added to the reaction mixture from the beginning and no isolation of the intermediate saturated ketone (*S*)-**30** was carried out. This was possible by employing ADHs showing high preference for the reduction of the carbonyl group of the saturated intermediate ketone **30**, with no concomitant formation of the allylic alcohol **31**.
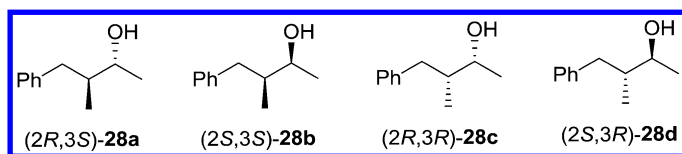

Figure 12. Stereoisomers of Muguesia®.

The OYE-mediated reduction of substrate **29** had been already investigated (*32*), and it had been established that OYE3 gave the best results affording the reduced product (*S*)-**30** showing ee >98% in quantitative yields. The regeneration of the NADPH cofactor was performed using the glucose/GDH system (GDH from *Bacillus megaterium*).

As for the ADHs to be used in the cascade procedures, a panel of commercial ADHs was screened, in order to select those showing the highest chemoselectivity towards the reduction of the saturated ketone, to avoid the formation of the allylic

alcohol **31** which cannot be further transformed by OYEs. The ADHs from *Rhodococcus erythropolis* (READH) and from *Parvibaculum lavamentivorans* (PLADH) were selected because of their chemoselectivity and their high conversion and stereoselectivity towards the two desired diastereoisomers.
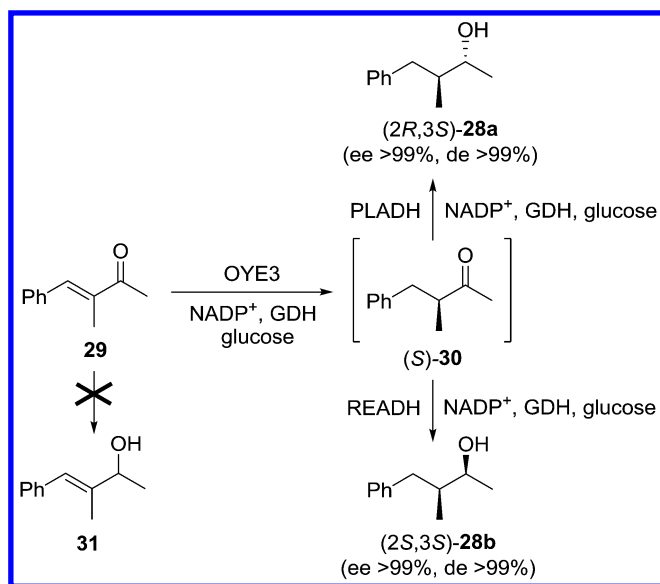

Figure 13. Cascade Synthesis of the "Best" Stereoisomers of Muguesia®.

The reaction conditions were optimized, in order to develop a preparative synthesis of the two stereoisomers **28a** and **28b**. The OYE3-PLADH- and OYE3-READH-mediated cascades were performed by using a 5 g L^{-1} substrate loading, and, after 48 h reaction time, the conversion to the corresponding alcohol was nearly complete with productivity values of 4.8 and 4.4 g L^{-1} d^{-1}, respectively. Only in the reaction with PLADH traces of the allylic alcohol were detected.

Nootkatone

(+)-Nootkatone (**32**) is a sesquiterpenoid found in grapefruit, pummelo and Nootka cypress tree. It is characterised by powerful citrusy, woody, sweet juicy notes, and a grapefruit-like aroma. It is used in the formulation of grapefruit and other citrus-flavored beverages, and in the creation of dry and citrusy men's perfumes (*33*). (+)-**32** has a low odor threshold (1 μg L^{-1} water) (*34*), whereas the non-natural (−)-enantiomer shows a weak woody and spicy flavor, and its odor threshold in aqueous phase is three orders of magnitude higher (*34*). The extraction from natural sources suffers from low yields, while chemical synthetic procedures involve oxidation with heavy metal salts, affording a final product that cannot be labelled as natural. Thus, the development of biotechnological approaches to (+)-nootkatone has become a relevant topic in flavor research (*35*).

Recently, a one-pot two-enzyme cascade route in aqueous solution for the synthesis of (+)-nootkatone has been described (*36*). In the first step, a cytochrome P450 monooxygenase promoted the selective allylic hydroxylation of (+)-valencene (**33**) to the intermediate alcohols *cis*- (**34a**) and *trans*- (**34b**) nootkatol (Figure 14), upon formation of water as byproduct. In the second step, the alcohols were further oxidized to (+)-**32** by a non-selective ADH. The same ADH converted simultaneously a suitable cosubstrate to ensure effective regeneration of the cofactor NADH.

Two previously developed P450 BM3 (CYP102A1) mutants, F87A/A328I (BM3-AI) and F87V/A328V (BM3-VV) (*37*), and ADH-21 from c-LEcta (c-LEcta GmbH, Leipzig, Germany) were employed for the optimisation of the cascade reaction. ADH-21 acted as a dual-functional enzyme, performing the oxidation of intermediates **34**, and that of the cosubstrate 2-butanol to make NADH available for the P450-catalyzed reaction.
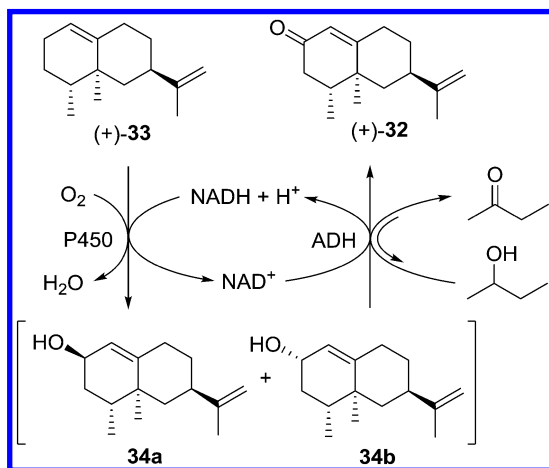

Figure 14. Cascade Synthesis of (+)-Nootkatone.

To increase the solubility of valencene, cyclodextrins were added instead of a cosolvent. The P450-ADH cascade with 2-butanol as cosubstrate was also scaled up, to obtain (+)-nootkatone concentrations of up to 360 mg L^{-1} and a space-time yield of 18 mg L^{-1} h^{-1}.

Conclusions

Efficient multi-enzymatic systems in one-pot reactions offer great advantages in terms of selectivity, yields, operating time and waste reduction. A careful optimization of reaction parameters is required in order to make most enzymes reach their catalytic optimum.

The use of these cascade procedures is of particular interest for the production of odorous molecules to be employed as fragrances in fine and functional perfumery. According to a recent survey (*38*), 5% of global fragrance volume

comes from nature (essential oils, exctracts and concretes), about 80% is based on fossil sources, and 15% on renewable resources. Thus, most fragrance ingredients are obtained through traditional chemical processes, and to make these procedures greener represents a great opportunity for enhancing sustainability in the fragrance industry. Another important aspect, which is now to be considered in every field of industrial production, is related to the reduction of material consumption for a more sustainable use of resources. For the fragrance industry this would mean to elicit stronger odor sensations from lower fragrance volumes or concentrations. The use of the most potent stereoisomers of chiral odorous molecules can contribute to achieve this aim. For the production of these enantiomerically enriched high-impact fragrance materials, biocatalyzed cascade procedures offer valuable tools for the development of cost-effective, and highly selective synthetic procedures, in the respect of the rules of Green Chemistry (*39*).

References

1. Brenna, E.; Fuganti, C.; Gatti, F. G.; Serra, S. Biocatalytic Methods for the Synthesis of Enantioenriched Odor Active Compounds. *Chem. Rev.* **2011**, *111*, 4036–4072.
2. Kraft, P.; Mannschreck, A. The enantioselectivity of odor sensation: some examples for undergraduate chemistry courses. *J. Chem. Educ.* **2010**, *87*, 598–603.
3. Brenna, E.; Fuganti, C.; Serra, S. Enantioselective perception of chiral odorants. *Tetrahedron: Asymmetry* **2003**, *14*, 1–42.
4. Matsuda, H.; Yamamoto, T. *Perfume composition containing (4R)-cis-4-methyl-2-substituted-tetrahydro-2H-pyran derivative and method for improving fragrance by using it*. EP0770670 A2, October 11, 1996.
5. Meyer, H.-P.; Eichhorn, E.; Hanlon, S.; Lütz, S.; Schürmann, M.; Wohlgemuth, R.; Coppolecchia, R. The use of enzymes in organic synthesis and the life sciences: perspectives from the Swiss Industrial Biocatalysis Consortium (SIBC). *Catal. Sci. Technol.* **2013**, *3*, 29–40.
6. Torrelo, G.; Hanefeld, U.; Hollmann, F. Biocatalysis. *Catal. Lett.* **2015**, *145*, 309–345.
7. Toogood, H. S.; Scrutton, N. S. New developments in "ene"-reductase catalysed biological hydrogenations. *Curr. Opin. Chem. Biol.* **2014**, *19*, 107–115.
8. *Synthetic Methods for Biologically Active Molecules: Exploring the Potential of Bioreductions*; Brenna, E., Ed.; Wiley-WCH Verlag GmbH & Co. KGaA: Weinheim, Germany, 2014.
9. Toogood, H. S.; Scrutton, N. S. Enzyme engineering toolbox - A catalyst for change. *Catal. Sci. Technol.* **2013**, *3*, 2182–2194.
10. Hollmann, F.; Arends, I. W. C. E.; Holtmann, D. Enzymatic reductions for the chemist. *Green Chem.* **2011**, *13*, 2285–2313.
11. Hollmann, F.; Arends, I. W. C. E.; Buehler, K.; Schallmey, A.; Bühler, B. Enzyme-mediated oxidations for the chemist. *Green Chem.* **2011**, *13*, 226–265.

12. Regulation (EC) No 1334/2008 of the European Parlament and of the Council of 16 December 2008 on flavorings and certain food ingredients with flavoring properties for use in and on foods and amending Council Regulation (EEC) No 1601/91, Regulations (EC) No 2232/96 and (EC) No 110/2008 and Directive 2000/13/EC. *Off. J. Eur. Union* **2008**, *L354/34* (31), 12.

13. Akacha, N. B.; Gargouri, M. Microbial and enzymatic technologies used for the production of natural aroma compounds: Synthesis, recovery modeling, and bioprocesses. *Food Bioprod. Process.* **2015**, *94*, 675–706.

14. Gounaris, Y. Biotechnology for the production of essential oils, flavours and volatile isolates. A review. *Flavour Fragrance J.* **2010**, *25*, 367–386.

15. Muschiol, J.; Peters, C.; Oberleitner, N.; Mihovilovic, M. D.; Bornscheuer, U. T.; Rudroff, F. Cascade catalysis – strategies and challenges en route to preparative synthetic biology. *Chem. Commun.* **2015**, *51*, 5798–5811.

16. Monti, D.; Ferrandi, E. *Synthetic Methods for Biologically Active Molecules: Exploring the Potential of Bioreductions*; Brenna, E., Ed.; Wiley-WCH Verlag GmbH & Co. KGaA: Weinheim, Germany, 2014; Chapter 11, pp 285−306.

17. Ricca, E.; Brucher, B.; Schrittwieser, J. H. Multi-enzymatic cascade reactions: overview and perspectives. *Adv. Synth. Catal.* **2011**, *353*, 2239–2262.

18. García-Junceda, E.; Lavandera, I.; Rother, D.; Schrittwieser, J. H. (Chemo)enzymatic cascades – Nature's synthetic strategy transferred to the laboratory. *J. Mol. Catal. B: Enzym.* **2015**, *114*, 1–6.

19. Díaz-Rodríguez, A.; Borzęcka, W.; Lavandera, I.; Gotor, V. Stereodivergent Preparation of Valuable γ- or δ-Hydroxy Esters and Lactones through One-Pot Cascade or Tandem Themoenzymatic Protocols. *ACS Catal.* **2014**, *4*, 386–393.

20. Korpak, M.; Pietruszka, J. Chemoenzymatic one-pot synthesis of γ-butyrolactones. *Adv. Synth. Catal.* **2011**, *353*, 1420–1424.

21. Classen, T; Korpak, M.; Schölzel, M.; Pietruszka, J. Stereoselective Enzyme Cascades: An Efficient Synthesis of Chiral γ-Butyrolactones. *ACS Catal.* **2014**, *4*, 1321–1331.

22. Kimland, B.; Aasen, J.; Almqvist, S.-O.; Arpino, P.; Enzell, C. R. Volatile acids of sun-cured greek *Nicotiana tabacum*. *Phytochemistry* **1973**, *12*, 835–847.

23. Mosandl, A.; Günther, C. Stereoisomeric Flavor Compounds. 20. Structure and Properties of Gamma-Lactone Enantiomers. *J. Agric. Food Chem.* **1989**, *37*, 413–418.

24. Brenna, E.; Gatti, F. G.; Monti, D.; Parmeggiani, F.; Sacchetti, A.; Valoti, J. Substrate-engineering approach to the stereoselective chemo-multienzymatic cascade synthesis of *Nicotiana tabacum* lactone. *J. Mol. Catal. B: Enzym.* **2015**, *114*, 77–85.

25. Yamamoto, T.; Ogura, M.; Amano, A.; Adachi, K.; Hagiwara, T.; Kanisawa, T. Synthesis and odor of optically active 2-*n*-hexyl- and

2-*n*-heptylcyclopentanone and the corresponding δ-lactones. *Tetrahedron Lett.* **2002**, *43*, 9081–9084.

26. Liu, J.; Li, Z. Cascade biotransformations via enantioselective reduction, oxidation, and hydrolysis: preparation of (*R*)-δ-lactones from 2-alkylidenecyclopentanones. *ACS Catal.* **2013**, *3*, 908–911.

27. Kara, S.; Spickermann, D.; Schrittwieser, J. H.; Weckbecker, A.; Leggewie, C.; Arends, I. W. C. E.; Hollmann, F. Access to Lactone Building Blocks via Horse Liver Alcohol Dehydrogenase-Catalyzed Oxidative Lactonization. *ACS Catal.* **2013**, *3*, 2436–2439.

28. Díaz-Rodríguez, A.; Iglesias-Fernández, J.; Rovira, C.; Gotor-Fernández, V. Enantioselective Preparation of δ-valerolactones with horse liver alcohol dehydrogenase. *ChemCatChem* **2014**, *6*, 977–980.

29. Lehr, K.; Fürstner, A. An efficient route to the musk odorant (*R*,*Z*)-5-muscenone via base-metal-catalysis. *Tetrahedron* **2012**, *68*, 7695–7700.

30. Abate, A.; Brenna, E.; Fuganti, C.; Gatti, F. G.; Giovenzana, T.; Malpezzi, L.; Serra, S. Chirality and Fragrance Chemistry: Stereoisomers of the Commercial Chiral Odorants Muguesia and Pamplefleur. *J. Org. Chem.* **2005**, *70*, 1281–1290.

31. Brenna, E.; Crotti, M.; Gatti, F. G.; Monti, D.; Parmeggiani, F.; Pugliese, A.; Santangelo, S. Multi-enzyme cascade synthesis of the most odorous stereoisomers ofthe commercial odorant Muguesia®. *J. Mol. Catal. B: Enzym.* **2015**, *114*, 37–41.

32. Brenna, E.; Cosi, S. L.; Ferrandi, E. E.; Gatti, F. G.; Monti, D.; Parmeggiani, F.; Sacchetti, A. Substrate scope and synthetic applications of the enantioselective reduction of α-alkyl-β-arylenones mediated by Old Yellow Enzymes. *Org. Biomol. Chem.* **2013**, *11*, 2988–2996.

33. Zviely, M. Molecule of the Month: Nootkatone. *Perfum. Flavor.* **2009**, *34*, 20–22.

34. Haring, H. G.; Rijkens, F.; Boelens, H.; van der Gen, A. Olfactory Studies on Enantiomeric Eremophilane Sesquiterpenoids. *J. Agric. Food Chem.* **1972**, *20*, 1018–1021.

35. Fraatz, M. A.; Berger, R. G.; Zorn, H. Nootkatone – a biotechnological challenge. *Appl. Microbiol. Biotechnol.* **2009**, *83*, 35–41.

36. Schulz, S.; Girhard, M.; Gaßmeyer, S. K.; Jäger, V. D.; Schwarze, D.; Vogel, A.; Urlacher, V. B. Selective enzymatic synthesis of the grapefruit flavor (+)-nootkatone. *ChemCatChem* **2015**, *7*, 601–604.

37. Seifert, A.; Vomund, S.; Grohmann, K.; Kriening, S.; Urlacher, V. B.; Laschat, S.; Pleiss, J. Rational design of a minimal and highly enriched CYP102A1 mutant library with improv J. Rational design of a minimal and highly enriched CYP102A1 mutant library with improved regio-, stereo- and chemoselectivity. *ChemBioChem* **2009**, *10*, 853–861.

38. Kulke, T. Fragrance and Sustainability. *Perfum. Flavor.* **2015**, *40*, 16–23.

39. Anastas, P. T.; Warner, J. C. *Green Chemistry: Theory and Practice*; Oxford University Press: New York, 1998; p 30.

Enantioselectivities of Uridine Diphosphate-Glucose:Monoterpenol Glucosyltransferases from Grapevine (*Vitis vinifera* L.)

Friedericke Bönisch,[1] Johanna Frotscher,[2] Sarah Stanitzek,[3] Ernst Rühl,[3] Oliver Bitz,[3] Wilfried Schwab,[1] and Matthias Wüst[*,2]

[1]Biotechnology of Natural Products, Technische Universität München, Liesel-Beckmann-Strasse 1, 85354 Freising, Germany
[2]Geisenheim University, Department of Grapebreeding, Von-Lade-Strasse 1, 65366 Geisenheim, Germany
[3]Bioanalytics, Institute of Nutritional and Food Sciences, University of Bonn, Endenicher Allee 11-13, D-53115 Bonn, Germany
[*]E-mail: matthias.wuest@uni-bonn.de.

Aroma-active substances, like monoterpene alcohols, often occur as non-aromatic, glycosidically bound forms and accumulate during grape ripening. Although these compounds are a precious source of aroma, little is known about the enzymes catalyzing this glycosylation. Recently, heterologous expression and biochemical assays of candidate genes extracted from the *V. vinifera* (*Vv*) genome database has led to the identification of several UDP-glucose:monoterpenol β-D-glucosyltransferases (UDP-Glc GTs). Here, kinetic resolution of racemic monoterpenols is demonstrated for several of these GTs. Thus, the enantioselective "aroma-hiding" biochemistry of these enzymes is shown for the first time in grapevine.

Terpenoids represent one of the major classes of natural products and are used in many applications, from health care and pharmaceutical uses to color, flavor and fragrance compounds in food and cosmetics. Biosynthesis in grapevine occurs through either the mevalonic acid or the 1-deoxy-D-xylulose 5-phosphate pathway (*1*–*3*). In plants, terpenoids are further conjugated with sugars which are linked to the active groups OH and/or COOH. In grapes (*Vitis vinifera*) and wines, where the importance of monoterpenes to varietal flavor is widely recognized, a major fraction of these compounds is present as non-volatile, aroma-inactive terpene glycosides (Figure 1) (*4*, *5*).
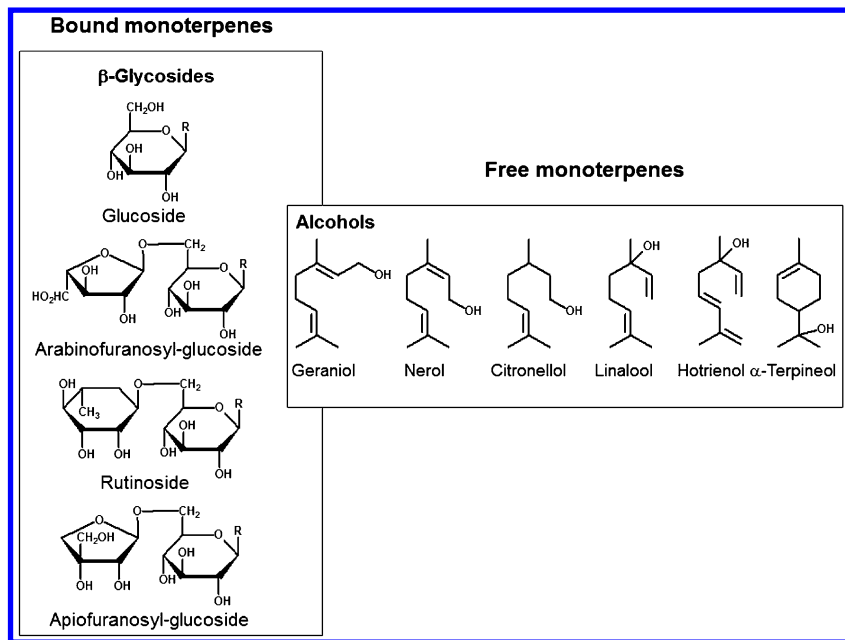

Figure 1. Structures of selected free monoterpenols and their glycosylated conjugates found in grapes and wines.

Although this water-soluble fraction is a precious source of aroma, little is known about the genes and their encoded enzymes catalyzing the glycosylation of terpenols in grapes (*6*). A functional analysis of *Arabidopsis thaliana* glycosyltransferase (GT) genes has yielded 27 sequences whose encoded proteins glucosylate a diversity of terpenes (*7*). In a previous project, we identified 67 homologous, putative GT sequences in the *Vitis vinifera* genome database and performed spatial and temporal expression analysis of nine selected potential VvGT genes in different grapes varieties (*8*). Comparison with the levels of terpene glycosides in different tissues and heterologous expression followed by biochemical characterization yielded the first three monoterpenyl GTs from *V. vinifera* (*9*). Here, we demonstrate that these GTs are able to discriminate between the enantiomers of the chiral monoterpenols linalool and citronellol.

Experimental

Plant Material and Chemicals

V. vinifera grapevines of different cultivars (Gewürztraminer, Muscat, White Riesling) were grown in the Geisenheim University vineyard at Geisenheim, Germany, during vintages 2011 and 2012. Grape berries were collected as previously described between 4 and 18 weeks after bloom (*8*, *9*). Citronellyl ß-D-glucoside was synthesized according to the Koenigs-Knorr-procedure (*10*). Linaloyl ß-D-glucoside was synthesized from linalool, as less reactive tertiary alcohol, according to a modified Koenigs-Knorr-procedure, using another catalyst (*11*). Spectral data of the synthesized compounds were in all cases in good agreement with previously published data.

Transcription Analysis, Heterologous Protein Expression, and Assays

RNA was extracted from different grape tissues and transcription analysis of seven putative GT genes was performed by GeXP profiling (*12*). Furthermore, DNA was extracted and comparative sequencing was performed as previously described (*9*). Recombinant protein was expressed as GST fusion proteins in *E. coli* BL21 (DE3) pLysS. After a purification step by GST bind resin (*8*), activity assays were conducted. A reaction mixture containing buffer solution, UDP-Glucose, racemic substrate and enzyme was applied, and activity measurements were carried out via GC/MS and LC-MS/MS measurements. To determine the enantioselectivities of the GTs the enantiomeric ratios of glucosidically bound citronellol and linalool were determined by enantioselective GC-MS. Following the incubation, residual citronellol and linalool were completely removed by extraction with dichloromethane. Citronellyl ß-D-glucoside which remained in the aqueous phase was hydrolyzed by HCl (2 mL, 0.1 M, pH 1) for one hour at 100 °C to release citronellol (*13*). In case of linalyl ß-D-glucoside, an enzymatic hydrolysis (AR 2000, citric acid buffer pH 4, 24 h) was applied due to the instability of linalool in acid solutions (*14*). Hydrolysis of a synthetic 1:1 mixture of (*R*)- and (*S*)-linalyl ß-D-glucoside revealed that AR 2000 does not discriminate between the two diastereomeric glucosides. After hydrolysis, citronellol and linalool were analyzed by SPME-GC/MS as previously described (*9*).

GC-MS and LC-MS/MS Analysis

A Varian Saturn 3900 GC/Varian Saturn 2100T-MS ion-trap was used for the analysis of free monoterpenes. EI (electron impact ionization)-MS spectra were recorded from *m/z* 40 to 300 (ionization energy 70 eV). The column was a DiAcß (heptakis-(2,3-di-*O*-acetyl-6-*O-tert*-butyldimethylsilyl)-ß-cyclodextrin), 26 m x 0.32 mm i.d. with a 0.1 µm film. For HPLC-MS/MS analysis of monoterpenyl-ß-D-glucosides, an HP 1050 HPLC system coupled to an API 2000 (Applied Biosystems, AB Sciex, Framingham, USA) triple-quadrupole-MS was used. The RP-column was eluted with a linear gradient of water/acetonitrile containing 0.2% ammonia. The column temperature was maintained at 40

°C. The mass spectrometer was operated in ESI-MRM negative ion mode. Nitrogen was used as curtain (setting 20), nebulizing and collision gas (setting 1; collision energy was -20 eV). Monoterpenyl ß-D-glucosides were identified by the following characteristic MRM transitions: LinGlc: *m/z* 315→161(Glu), 315→113(Glu); CitrGlc: *m/z* 317→101(Glu), 317→161(Glu).

Results and Discussion

Previous research has shown that monoterpenol ß-glucosides in *Vitis vinifera* are formed by the action of glycosyltransferases (GTs) that catalyze the transfer of glucose from uridine diphosphate glucose (UDP-Glc) to the acceptor molecule (Figure 2) (*8*, *9*). These GTs recognize small-molecule scaffolds and belong to the so-called class 1 family that are characterized by a conserved plant secondary product GT motif (PSPG motif) (*7*). Beside the glucosylation of a rather broad monoterpenol spectrum, these GTs show also considerable activities toward aliphatic alcohols and benzoic compounds and thus add to the chemical diversity of the grapevine metabolome. Because numerous monoterpenols in *V. vinifera* are chiral (e.g., citronellol, linalool, hotrienol and alpha-terpineol; Figure 1) the enantioselectivity of these GTs is of interest. The relationship between the absolute configuration and the odor quality of chiral aroma compounds is well known and an enantiodiscriminating effect of GTs might thus modulate the aroma quality of the final wine (*15*). To determine the enantioselectivities of GTs that were shown to catalyze the glucosylation of chiral monoterpenols, racemic mixtures of citronellol and linalool were incubated with three different GTs, namely VvGT7, VvGT14a, and VvGT15a. The identities of the generated ß-glucosides were confirmed by the synthesis of reference compounds and analysis by LC-MS/MS. Because the diastereomeric glucosides of the respective monoterpenol enantiomers could not be separated by LC, the generated glucosides were hydrolyzed and the enantiomeric ratios of the liberated aglycons were determined by enantioselective GC/MS using a modified cyclodextrin as chiral selector.

Figure 3A/B shows the results of the enantioselective analysis of citronellol, liberated by acid-catalyzed hydrolysis from its glucoside, that was generated from racemic citronellol and VvGT7 (linalool was not glucosylated by VvGT7). VvGT7 clearly preferred (*R*)- over (*S*)-citronellol even in long term assays. However, VvGT14a and VvGT15a preferentially glucosylated (*S*)-citronellol in short-term assays and enantioselectivity was not observed in long-term studies. This kinetic effect is characteristic for studies on the kinetic resolution of racemates. In this context it is noteworthy that free and glycosylated citronellol in grape berries is usually (*S*)-configured with an enantiomeric excess greater than 90% (*16*). Thus, it is obvious that VvGT7 is probably not involved in the production of (*S*)-citronellyl-ß-*D*-glucoside. VvGT14a also glucosylated linalool and preferred (*R*)-linalool even in long term assays (Figure 3D). In grape berries free linalool is usually present as *S*-configured enantiomer with enantiomeric purities up to 99.8 % in Muscat varieties (*17*, *18*). However, in the glycosidically bound fraction of linalool in Morio Muscat and Muscat Ottonel

the (*R*)-enantiomer is enriched (up to 12.7%) (*17*). This previously observed enantiodiscrimination can be explained by the preference of VvGT14a for the (*R*)-enantiomer as described above.
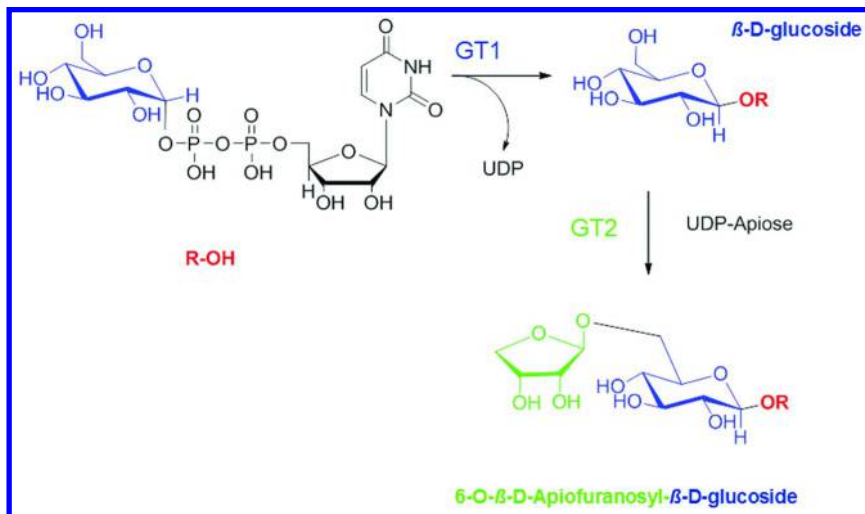

Figure 2. Sequential biosynthesis of glycosides by glycosyltransferases. GT1 is a glucosyltransferase while GT2 is a postulated apiosyltransferase which has not yet been characterized in V. vinifera.
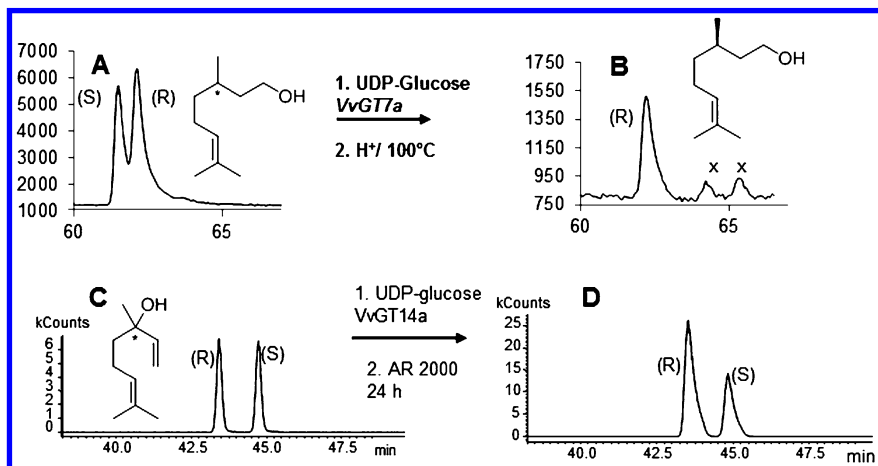

Figure 3. Separation of racemic mixtures of citronellol (A) and linalool (C) by enantioselective GC. When racemic citronellol is incubated with VvGT7 and the generated glucoside is hydrolyzed only (R)-citronellol is detected (B). The analogous reaction sequence using VvGT14a and racemic linalool yields (R)-enriched linalool (D). x are impurities.

Conclusions

UDP-glucose:monoterpenol-GTs from *V. vinifera* are able to discriminate between the enantiomers of linalool and citronellol. Thus, the enantiomeric ratios of free and glycosylated chiral monoterpenols might differ considerably. The potential aroma of the bound fraction of volatiles is therefore not only modulated by the substrate specificities of the involved GTs but also by their enantioselectivities.

References

1. Luan, F.; Wüst, M. Differential incorporation of 1-deoxy-D-xylulose into (3*S*)-linalool and geraniol in grape berry exocarp and mesocarp. *Phytochemistry* **2002**, *60*, 451–459.

2. May, B.; Lange, B. M.; Wüst, M. Biosynthesis of sesquiterpenes in grape berry exocarp of *Vitis vinifera* L.: Evidence for a transport of farnesyl diphosphate precursors from plastids to the cytosol. *Phytochemistry* **2013**, *95*, 135–144.

3. Hampel, D.; Mosandl, A.; Wüst, M. Induction of de Novo Volatile Terpene Biosynthesis via Cytosolic and Plastidial Pathways by Methyl Jasmonate in Foliage of *Vitis vinifera* L. *J. Agric. Food Chem.* **2005**, *53*, 2652–2657.

4. Günata, Y. Z.; Bayonove, C. L.; Tapiero, C.; Cordonnier, R. E. Hydrolysis of Grape Monoterpenyl-β-*D*-Glucosides by Various β-glucosidases. *J. Agric. Food Chem.* **1990**, *38*, 1232–1236.

5. Maicas, S.; Mateo, J. J. Hydrolysis of terpenyl glycosides in grape juice and other fruit juices: a review. *Appl. Microbiol. Biotechnol.* **2005**, *67*, 322–335.

6. Hjelmeland, A. K.; Ebeler, S. E. Glycosidically bound volatile aroma compounds in grapes and wine: A review. *Am. J. Enol. Vitic.* **2015**, *66*, 1–11.

7. Caputi, L.; Lim, E.-K.; Bowles, D. J. Discovery of new biocatalysts for the glycosylation of terpenoid scaffolds. *Chem.−Eur. J.* **2008**, *14*, 6656–6662.

8. Bönisch, F.; Frotscher, J.; Stanitzek, S.; Rühl, E.; Wüst, M.; Bitz, O.; Schwab, W. A UDP-glucose: monoterpenol glucosyltransferase adds to the chemical diversity of the grapevine metabolome. *Plant Physiol.* **2014**, *165*, 561–581.

9. Bönisch, F.; Frotscher, J.; Stanitzek, S.; Rühl, E.; Wüst, M.; Bitz, O.; Schwab, W. Activity-based profiling of a physiologic aglycone library reveals sugar acceptor promiscuity of family 1 UDP-glucosyltransferases from grape. *Plant Physiol.* **2014**, *166*, 23–39.

10. Wüst, M.; Beck, T.; Mosandl, A. Conversion of Citronellyl Diphosphate and Citronellyl β-D-glucoside into Rose Oxide by *Pelargonium graveolens*. *J. Agric. Food Chem.* **1999**, *47*, 1668–1672.

11. Hattori, S.; Kawaharada, C.; Tazaki, H.; Fujimori, T.; Kimura, K.; Ohnishi, M.; Nabeta, K. Formation mechanism of 2, 6-dimethyl-2, 6-octadienes from thermal decomposition of linalyl β-*D*-glucopyranoside. *Biosci., Biotechnol., Biochem.* **2004**, *68*, 2656–2659.

12. Drew, J. E.; Mayer, C.-D.; Farquharson, A. J.; Young, P.; Barrera, L. N. Custom design of a GeXP multiplexed assay used to assess expression profiles of inflammatory gene targets in normal colon, polyp, and tumor tissue. *J. Mol. Diagn.* **2011**, *13*, 233–242.

13. Skouroumounis, G. K.; Sefton, M. A. Acid-catalyzed Hydrolysis of Alcohols and their β-*D*-Glucopyranosides. *J. Agric. Food Chem.* **2000**, *48*, 2033–2039.

14. Williams, P. J.; Strauss, C. R.; Wilson, B.; Massy-Westropp, R. A. Studies on the Hydrolysis of *Vitis vinifera* Monoterpene Precursor Compounds and Model Monoterpene β-*D*-Glucosides Rationalizing the Monoterpene Composition of Grapes. *J. Agric. Food Chem.* **1982**, *30*, 1219–1223.

15. Bentley, R. The Nose As a Stereochemist. Enantiomers and Odor. *Chem. Rev.* **2006**, *106*, 4099–4112.

16. Luan, F.; Mosandl, A.; Münch, A.; Wüst, M. Metabolism of geraniol in grape berry mesocarp of *Vitis vinifera* L. cv. Scheurebe: demonstration of stereoselective reduction, *E*/*Z*-isomerization, oxidation and glycosylation. *Phytochemistry* **2005**, *66*, 295–303.

17. Luan, F.; Hampel, D.; Mosandl, A.; Wüst, M. Enantioselective Analysis of Free and Glycosidically Bound Monoterpene Polyols in *Vitis vinifera* L. Cvs. Morio Muscat and Muscat Ottonel: Evidence for an Oxidative Monoterpene Metabolism in Grapes. *J. Agric. Food Chem.* **2004**, *52*, 2036–2041.

18. Luan, F.; Mosandl, A.; Gubesch, M.; Wüst, M. Enantioselective analysis of monoterpenes in different grape varieties during berry ripening using stir bar sorptive extraction- and solid phase extraction-enantioselective-multidimensional gas chromatography-mass spectrometry. *J. Chromatogr., A* **2006**, *1112*, 369–374.

Chapter 6

Biotechnological Production of C$_8$ Aroma Compounds by Submerged Cultures of Shiitake (*Lentinula edodes*)

Alexander H. Heuger, Marco A. Fraatz, and Holger Zorn[*]

**Institute of Food Chemistry and Food Biotechnology,
Justus Liebig University Giessen, Heinrich-Buff-Ring 17,
35392 Giessen, Germany
[*]E-mail: holger.zorn@uni-giessen.de.**

The submerged cultivation of basidiomycetous fungi offers biotechnological access to natural aroma compounds and flavor blends. Flavor mixtures with the aroma quality "mushroom" may be obtained from mycelia of *Lentinula edodes*. The culture medium was stepwise optimized for improving the growth of the basidiomycete and for induction of enzymes involved in the formation of C$_8$ volatiles. The post-harvest generation of aroma compounds was significantly increased by supplementation of the transformation buffer with linoleic acid. Under optimized process conditions, yields of up to 6,200 µg oct-1-en-3-ol per g mycelium (dry mass) were obtained. The character impact compound oct-1-en-3-ol showed a high enantiomeric excess in favor of the (*R*)-(-)-form (% ee > 90).

Introduction

Fungi of the phylum basidiomycota are valued foods all over the world because of their unique flavor and their high nutritional value. The most frequently cultivated and traded species include the oyster mushroom (*Pleurotus ostreatus*), the king trumpet (*P. eryngii*), the white button mushroom (*Agaricus bisporus*), the straw mushroom (*Volvariella volvacea*) and the shiitake (*Lentinula edodes*).

Common to the aroma profiles of these mushrooms is the occurrence of so called carbon-eight volatiles with (R)-(-)-oct-1-en-3-ol being the character impact compound of mushroom flavor (*1*). The formation of oct-1-en-3-ol proceeds via an enzymatic dioxygenation of linoleic acid to give a 10-hydroperoxide which is then cleaved stereospecifically by a hydroperoxide lyase (*2*, *3*).

Besides the natural growth on wood and other lignocellulosic materials and the traditional cultivation on solid substrates for production of fruiting bodies, basidiomycetes may be grown in liquid culture media in shake flasks or fermenters. This so-called submerged cultivation enables a faster and better reproducible growth behavior. Additionally, it allows for the use of defined nutrients and thus for studying the effects of specific supplements on the biotransformation of individual substances. The submerged cultivation of fungi is thus suitable for the biotechnological production of natural flavorings. Well studied applications include, amongst others, the oxyfunctionalization of terpenes (e.g., oxidation of valencene to nootkatone) as well as the biotransformation of sidestreams from the food industry to flavor blends with floral or fruity scent (*4*, *5*). In this study, *L. edodes* was used for the production of a flavoring mixture with the aroma quality "mushroom", which is sought after by the food industry for savory sauces or soups.

Materials and Methods

Materials

Chemicals were purchased from Acros Organics (Geel, Belgium), Alfa Aesar (Karlsruhe, Germany), Applichem (Darmstadt, Germany), Carl Roth (Karlsruhe, Germany), Fisher Scientific (Loughborough, UK), and Sigma-Aldrich (Steinheim, Germany), and were of analytical quality or highest purity available. Soy bean flour ("Hensel Soja fettarm") was from W. Schoenenberger (Magstadt, Germany).

Culture Media

The respective medium (100 mL) was filled into 250 mL Erlenmeyer flasks, and the flasks were capped with cellulose plugs and sterilized at 121 °C for 20 min.

Preculture medium (L^{-1}): 30.0 g malt extract, 3.0 g soy peptone, pH adjusted to 5.6.

Main culture media (L^{-1}): *Cf.* Table 1 for composition of the media. The pH of the media III-XI was adjusted to 5.0 prior to sterilization.

Minerals solution (L^{-1}): 2.48 g $MgSO_4$ x 7 H_2O, 0.10 g $FeSO_4$ x 7 H_2O, 0.023 g $MnSO_4$ x H_2O, 0.06 g $ZnSO_4$ x 7 H_2O, 0.08 g $CaCl_2$ x 2 H_2O, 0.03 g $CuSO_4$ x 5 H_2O.

87

Table 1. Compositions of Main Culture Media (L⁻¹)

ingredient	I	II	III	IV	V	VI	VII	VIII	IX	X	XI
						medium					
malt extract	20.0 g	20.0 g									
soy oil		2.5 g	2.5 g		2.5 g	2.5 g	2.5 g	2.5 g	2.5 g	2.5 g	2.5 g
$(NH_4)_2HPO_4$			0.2 g	0.2 g	0.2 g	0.2 g	0.2 g	0.2 g	0.2 g	0.2 g	0.2 g
soy flour			10.0 g	10.0 g	10.0 g	10.0 g	5.0 g				
KH_2PO_4			0.068 g	0.068 g	0.068 g	0.068 g	0.068 g	0.068 g	0.068 g	0.068 g	0.068 g
corn steep liquor			8.0 mL	8.0 mL	8.0 mL	8.0 mL	8.0 mL	8.0 mL		8.0 mL	8.0 mL
Tween 80				4.32 g	4.32 g					4.32 g	
glucose x H_2O											5.0 g
minerals solution			100 mL	100 mL	100 mL	100 mL	100 mL	100 mL	100 mL	100 mL	100 mL
citrate buffer (10 mM, pH 5.0)			900 mL	900 mL	900 mL						

Cultivation, Harvest, and Determination of Growth

The strain of *L. edodes* was obtained from the Centraalbureau voor Schimmelcultures (CBS, Utrecht, The Netherlands) and was kept on malt extract soy peptone-agar plates.

Submerged cultivation was conducted in two stages. The precultures were grown in 250 mL Erlenmeyer flasks containing 100 mL of medium. The media were inoculated using approx. 1 cm^2 pieces of agar overgrown with mycelium, and the agar plugs were dispersed by an Ultraturrax (IKA Werke, Staufen, Germany; 10,000 rpm, 30 s). The fungus was grown at 24 °C and 150 rpm (shaking diameter 25 mm) in the dark. The main cultures were grown in 250 mL Erlenmeyer flasks containing 100 mL medium. The media were inoculated with 10 mL homogenized preculture (Ultraturrax: 10,000 rpm, 30 s) per flask.

At the end of the cultivation period, the mycelia were harvested by filtrating the culture broth through a cotton cloth and washing the mycelia with distilled water to remove residual media components. The amount of wet mycelium was determined and the mycelium was stored on ice. Dry matter content was determined by lyophilization for at least 2 days in duplicate or triplicate and used for calculation of biomass production and of oct-1-en-3-ol yields.

Analysis of Flavor Formation

The wet mycelium (5.00 g) was weighed into a snap cap glass vial, and 15 mL of potassium phosphate buffer (50 mM, pH 6.5) or an emulsion of linoleic acid in this buffer were added. The linoleic acid emulsion was prepared by dispersing the appropriate amount of linoleic acid with an equal amount of Tween 20 in half of the desired final volume of water. The solution was neutralized with 1 M NaOH and half of the desired final volume of 100 mM potassium phosphate buffer (pH 6.5) was added. The final emulsion contained linoleic acid at the desired molarity in 50 mM potassium phosphate buffer with a pH of 6.5. Cell disruption was achieved by treatment with an Ultraturrax (10,000 rpm, 2 min). For incubation, the vial was capped and shaken at 24 °C and 150 rpm for the time given. For the quantification of volatiles, 10 mL of the homogenate were pipetted into a glass vial and 50 µL of a solution of the internal standard nonan-1-ol (0.964 or 0.865 mg mL^{-1} in methanol) was added. Cold n-pentane (2 mL) was added and, after capping, the mixture was shaken vigorously. Phase separation was achieved by centrifugation (Allegra X-15R, Beckman Coulter, Krefeld, Germany; 3,000 x *g*, 5 min, 4 °C), and the organic phase was recovered. After drying over anhydrous sodium sulfate, the sample was subjected to gas chromatographic analysis.

Gas Chromatography

GC-MS: Gas chromatography coupled to mass spectrometry was performed on a 7890A gas chromatograph equipped with an HP-INNOWax or a VF-WAXms column (30 m x 0.25 mm i.d., 0.25 µm film thickness) coupled to a 5975C MSD

(all Agilent Technologies, Waldbronn, Germany). The system was operated with He as carrier gas (1.2 mL min^{-1}, constant flow) in the splitless or in the split mode applying a split ratio of 10:1. The inlet temperature was 250 °C and the oven was programmed from 40 °C (3 min), 5 °C min^{-1} to 240 °C (12 min). The transfer line was held at 250 °C and the ion source and the quadrupole were heated to 230 and 150 °C, respectively. Electron impact ionization was used with 70 eV energy and mass spectra were recorded in the full scan mode (*m/z* 33-300).

Enantio-GC-FID: Chiral analysis of oct-1-en-3-ol was performed using a HP 5890 Series II gas chromatograph (Hewlett Packard [now: Agilent Technologies]), equipped with a Hydrodex *β*-TBDAc column (Macherey-Nagel, Düren, Germany; 25 m x 0.25 mm i.d.) operated in split mode (split ratio 71:1). The inlet temperature was set to 250 °C and nitrogen was used as carrier gas (12 psi head pressure, constant pressure). The oven temperature program was 80 °C, 2 °C min^{-1} to 120 °C, then 15 °C min^{-1} to 250 °C (5 min) and detection was achieved by a flame ionization detector (250 °C, 30 mL min^{-1} H$_2$, 400 mL min^{-1} pressurized air, 30 mL min^{-1} N$_2$ as make-up gas).

Kováts retention indices (RI) (*6*) were calculated using the retention times of n-alkanes from C$_8$ - C$_{20}$. The compounds were identified by comparison of their RI and mass spectra with those of authentic standards as well as with literature data and the NIST database, respectively. The concentration of oct-1-en-3-ol was calculated from the peak areas of the analyte and the internal standard using response factors of 1.198 (splitless injection) and 1.240 (split ratio 10:1). Enantiomers were assigned by using standards of racemic oct-1-en-3-ol and (*R*)-(-)-oct-1-en-3-ol with the elution order (*S*)-(+) eluting before (*R*)-(-). The enantiomeric excess (% ee) was calculated using the peak areas of the enantiomers:

% ee [*R*-(-)-oct-1-en-3-ol] = (area$_{R-(-)}$ - area$_{S-(+)}$) / (area$_{R-(-)}$ + area$_{S-(+)}$) * 100.

Results

Cultivation

The basidiomycete *L. edodes* was grown submerged in a 2-step process. The precultures provided homogeneously grown mycelia for the inoculation of the main cultures. The main culture medium was optimized to elicit enzyme activities for the formation of C$_8$ volatiles and simplified to reduce the costs. The suitability of the media was evaluated by the yields of the character impact compound oct-1-en-3-ol (initially without addition of linoleic acid) on the one hand, and the biomass production on the other hand (Table 2).

Table 2. Growth of *L. edodes* in Different Media and Production of Oct-1-en-3-ol (Biomass Results Given Are Mean Values of Multiple Samples, Oct-1-en-3-ol Concentrations Are Means of at Least Duplicate Analyses; Concentration Ranges Are Given in Parentheses for Multiple Replications)

medium	I	II	III	IV	V	VI	VII	VIII	**VIII**	IX	X	XI
culture period [d]	10	10	10	10	10	10	10	10	**8**	8	8	8
dry biomass mass (DM), [g L^{-1}]	1.1	2.9	5.9 (4.9-6.8)	4.3	6.8	4.9	4.2	3.7	**3.1 (2.4-4.0)**	1.8	4.3 (4.1-4.8)	3.5 (2.5-4.5)
oct-1-en-3-ol [µg g^{-1} DM]	305	416	515 (365-644)	90	279	470	882	546	**938 (650-1,531)**	976	400 (296-500)	772 (590-953)

The supplementation of the culture medium with plant oils may enhance the activity of enzymes involved in the formation of lipid-derived aroma compounds such as lipoxygenases and hydroperoxide lyases (*7*). Belinky *et al.* (*8*) described a complex medium for the cultivation of the basidiomycete *Pleurotus pulmonarius* containing soy oil and flour as carbon sources. This medium (III) as well as a malt extract medium (I) were selected as starting points for the optimization of the main culture medium.

The cultivation of *L. edodes* in medium I for 10 d resulted in poor biomass production and moderate yields of oct-1-en-3-ol. The addition of soy oil (medium II) promoted both, growth and aroma formation. Nevertheless, the formation of oct-1-en-3-ol was lower compared to mycelia grown in the medium developed by Belinky *et al.* (III; (*8*)). Likewise, the formation of biomass was significantly higher in medium III. However, these values apparently overestimate the growth of the fungus since the mycelial pellets contained insoluble particles originating from the medium. The soy flour does not dissolve well in the medium, and solid particles were overgrown by the mycelia. This effect was also observed with the media IV - VI, and less pronounced with medium VII which contained half of the amount of soy flour. The addition of an emulsifying agent should help to overcome the limited solubility of soy oil in the aqueous medium thus improving its availability as a carbon source for the fungus. While the fungus' growth rate in medium V was slightly higher than in medium III, the yields of oct-1-en-3-ol were low. In medium IV the soy oil was substituted by Tween 80. In this medium the production of oct-1-en-3-ol decreased drastically. Considering the essential role of soy oil for flavor production, the medium was stepwise simplified. Omitting the citrate buffer (VI) altered neither the production of biomass nor flavor formation significantly. In the next steps the amount of soy flour was first reduced to half (VII), and then soy flour was fully omitted (VIII). As expected, the apparent biomass production was lower compared to media containing more soy flour. However, the yields of oct-1-en-3-ol remained virtually unchanged. Shortening the culture period to 8 d resulted in comparable growth of *L. edodes* and allowed for a significantly increased formation of oct-1-en-3-ol. Further attempts to optimize the composition of the culture medium (media IX – XI) failed. Therefore, medium VIII was chosen for further investigations.

Optimization of Oct-1-en-3-ol Production

The fungal mycelia were subjected to cell disruption to initiate aroma formation. The flavor compounds were extracted from the homogenates and analyzed by means of gas chromatography. Oct-1-en-3-ol was found to be the main volatile metabolite, and further C_8 compounds like octan-1-ol and oct-2-en-1-ol were identified (Figure 1).
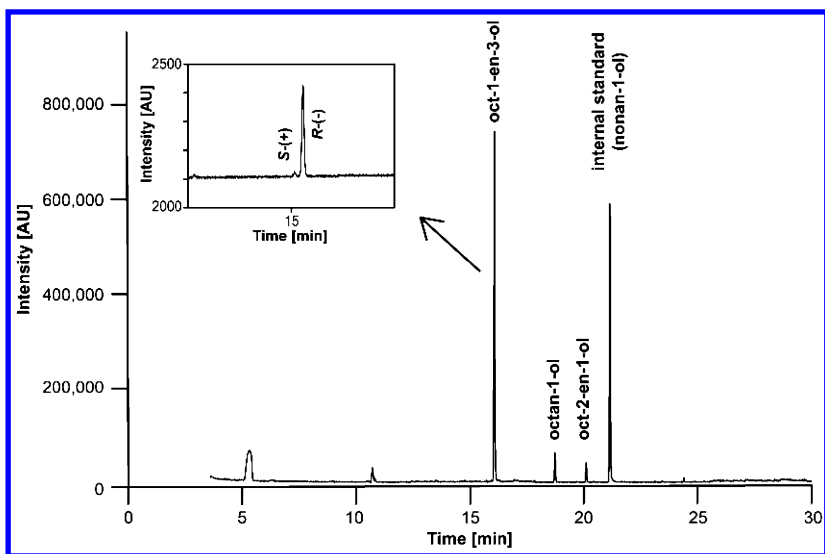
Figure 1. Exemplary Gas Chromatogram of an Extract of L. edodes (without addition of linoleic acid); insert: separation of oct-1-en-3-ol enantiomers.

Cell disruption by Ultraturrax treatment proved to be as suitable as grinding the mycelium in a glass bead mill (data not shown). Therefore, further experiments were performed using an Ultraturrax homogenizer. As linoleic acid represents the direct biogenetic precursor of oct-1-en-3-ol, linoleic acid was added to the fungal homogenate in various concentrations. With addition of 2 mM linoleic acid to the buffer, yields of approx. 4,500 µg g^{-1} (dry mass (DM); Figure 2) were observed. Moreover, the influence of the incubation time after cell disruption and addition of linoleic acid was analyzed. For samples with addition of 4 mM linoleic acid, increasing the incubation time to 15 min led to a 30% enhanced formation of oct-1-en-3-ol. The highest concentrations of 6,200 µg g^{-1} oct-1-en-3-ol were observed using an incubation period of 30 min. The enantiomeric composition of oct-1-en-3-ol was determined by chiral gas chromatography. In samples without addition of linoleic acid, the concentration of the (S)-(+)-enantiomer was below the limit of quantification, and the ee was estimated to be > 90% (Table 3). In samples with addition of linoleic acid the ee was around 92% in favor of the (R)-(-)-form.
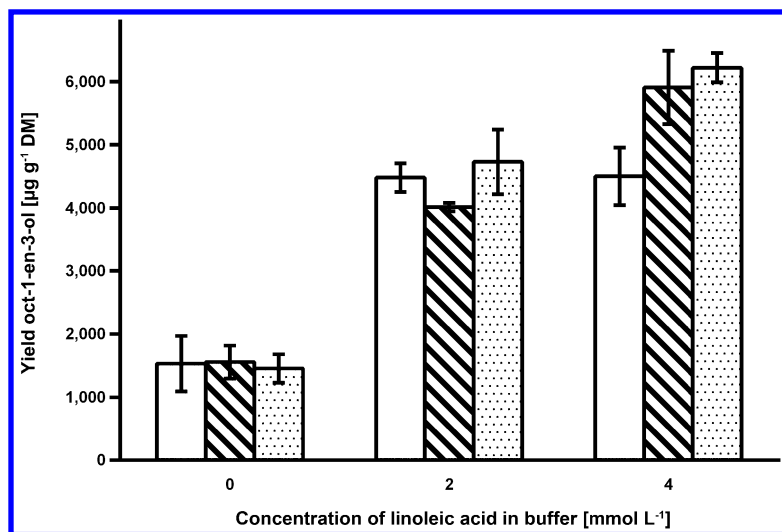
Figure 2. Formation of Oct-1-en-3-ol by L. edodes as a Function of Added Linoleic acid and Incubation Time. Plain: 0 min, striped: 15 min, dotted: 30 min.

Table 3. Enantiomeric Composition of Oct-1-en-3-ol Formed by Mycelia of
***L. edodes* and Comparison to Literature Data**

sample	*% ee (R)-(-)-oct-1-en-3-ol*
mycelium without addition of linoleic acid	> 90[1]
mycelium with addition of linoleic acid (2 mM)	92.1 - 92.4
mycelium with addition of linoleic acid (4 mM)	92.0 - 92.6
fruiting bodies (Zawirska-Wojtasiak, (*9*))	91.0

[1] (*S*)-(+)-oct-1-en-3-ol < LOQ.

Discussion

Starting from the medium described by Belinky *et al.* (*8*), the main culture medium for the submerged cultivation of *L. edodes* was optimized stepwise. For comparison, two malt extract-based media were chosen, and the influence of several medium ingredients on the growth rate and the flavor formation was investigated. The concentration of oct-1-en-3-ol was selected as a marker

for optimization of the flavor formation as it represents the character impact compound of mushroom flavor. In media containing soy flour, undissolved particles impeded a reliable quantification of the fungal biomass. Therefore, the lower dry masses observed for the cultures grown in the media VIII - XI do not necessarily reflect lower growth rates. The optimum flavor formation was obtained with mycelia grown in medium VIII and addition of linoleic acid to the transformation buffer. A significant increase of the formation of C_8 flavor compounds by supplementation of the buffer with linoleic acid is in good agreement with literature data. Without addition of linoleic acid, the concentrations of oct-1-en-3-ol amounted to approx. 1,500 µg g^{-1} DM (Figure 2). Upon addition of linoleic acid, a drastic increase in the concentrations of oct-1-en-3-ol was observed. When the transformation buffer was supplemented with 4 mM linoleic acid, a further significant increase of oct-1-en-3-ol yields was achieved by extending the incubation time to 15 or even 30 min. Referring to the transformation batch, the oct-1-en-3-ol yields ranged from approx. 8 – 35 mg L^{-1} depending on the respective experimental setup. Based on these findings, linoleic acid represents a limiting factor for the production of oct-1-en-3-ol although it is the main fatty acid in the mycelium of *L. edodes* (*10*).

By omitting the citrate buffer and the soy bean flour as ingredients, the total costs of the medium could be reduced without lowering the yields of oct-1-en-3-ol.

Out of the two enantiomers of oct-1-en-3-ol, only the (*R*)-(-)-form exhibits the typical mushroom flavor. The scent of the (*S*)-(+)-enantiomer has been described as "herbaceous"and "moldy grassy" (*11*). Thus, the enantiomeric composition of oct-1-en-3-ol is of utmost importance. The ee was > 90% (without addition of linoleic acid) and > 92% (with addition of linoleic acid) in favor of the desired (*R*)-(-)-enantiomer (Table 3). These results are in good accordance with literature data reported for fruiting bodies of *L. edodes* and other mushrooms (*9*).

Several microorganisms have been proposed for use in production of oct-1-en-3-ol including ascomycetous fungi (*Penicillium camemberti* (*7*), *Neurospora* species (*12*), *Morchella esculenta* (*13*)) as well as basidiomycetes (*P. pulmonarius* (*8*), *A. bisporus* (*14*, *15*)). The yields are sometimes difficult to compare as different bases are referenced (DM, protein, volume culture broth) but none of the processes seems to have gained economic importance. Compared to the data reported by Belinky et al. (*8*), an approximate 1.5 fold increase of the yields was achieved in this study. To the best of our knowledge, the yields of up to 6,200 µg oct-1-en-3-ol g^{-1} mycelium (DM) obtained in this study are the highest amounts reported so far for basidiomycetes grown in submerged culture.

Conclusions

Flavor extracts with the aroma quality "mushroom" may be produced by submerged cultivation of *L. edodes*. The yields of the impact flavor compound oct-1-en-3-ol were significantly increased by optimization of the culture medium and supplementation of the transformation buffer with linoleic acid. A high enantiomeric excess in favor of the desired (*R*)-(-)-oct-1-en-3-ol was observed.

Acknowledgments

References

1. Fraatz, M. A.; Zorn, H. Fungal flavours. In *The Mycota X: Industrial Applications*, 2nd ed.; Hofrichter, M., Ed.; The Mycota; Springer-Verlag: Berlin, Heidelberg, Germany, 2010; pp 249−268.

2. Wurzenberger, M.; Grosch, W. The enzymic oxidative breakdown of linoleic acid in mushrooms (*Psalliota bispora*). *Z. Lebensm.-Unters. Forsch.* **1982**, *175*, 186–190.

3. Wurzenberger, M.; Grosch, W. The formation of 1-octen-3-ol from the 10-hydroperoxide isomer of linoleic acid by a hydroperoxide lyase in mushrooms (*Psalliota bispora*). *Biochim. Biophys. Acta* **1984**, *794*, 25–30.

4. Fraatz, M. A.; Riemer, S. J. L.; Stöber, R.; Kaspera, R.; Nimtz, M.; Berger, R. G.; Zorn, H. A novel oxygenase from *Pleurotus sapidus* transforms valencene to nootkatone. *J. Mol. Catal. B: Enzym.* **2009**, *61*, 202–207.

5. Bosse, A. K.; Fraatz, M. A.; Zorn, H. Formation of complex natural flavours by biotransformation of apple pomace with basidiomycetes. *Food Chem.* **2013**, *141*, 2952–2959.

6. Kováts, E. Gas-chromatographische Charakterisierung organischer Verbindungen. *Helv. Chim. Acta* **1958**, *41*, 1915–1932.

7. Husson, F.; Krumov, K. N.; Cases, E.; Cayot, P.; Bisakowski, B.; Kermasha, S.; Belin, J. Influence of medium composition and structure on the biosynthesis of the natural flavour 1-octen-3-ol by *Penicillium camemberti*. *Process Biochem.* **2005**, *40*, 1395–1400.

8. Belinky, P. A.; Masaphy, S.; Levanon, D.; Hadar, Y.; Dosoretz, C. G. Effect of medium composition on 1-octen-3-ol formation in submerged cultures of *Pleurotus pulmonarius*. *Appl. Microbiol. Biotechnol.* **1994**, *40*, 629–633.

9. Zawirska-Wojtasiak, R. Optical purity of (R)-(−)-1-octen-3-ol in the aroma of various species of edible mushrooms. *Food Chem.* **2004**, *86*, 113–118.

10. Stahl, P. D.; Klug, M. J. Characterization and differentiation of filamentous fungi based on fatty acid composition. *Appl. Environ. Microbiol.* **1996**, *62*, 4136–4146.

11. Mosandl, A.; Heusinger, G.; Gessner, M. Analytical and Sensory Differentiation of 1-Octen-3-ol enantiomers. *J. Agric. Food Chem.* **1986**, *34*, 119–122.

12. de Carvalho, D. S.; Dionísio, A. P.; dos Santos, R.; Boguzs, S., Jr; Godoy, H. T.; Pastore, G. M. Production of 1-octen-3-ol by *Neurospora* species isolated from beiju in different culture medium. *Procedia Food Sci.* **2011**, *1*, 1694–1699.

13. Schindler, F.; Seipenbusch, R. Fungal flavour by fermentation. *Food Biotechnol.* **1990**, *4*, 77–85.
14. Husson, F.; Bompas, D.; Kermasha, S.; Belin, J. M. Biogeneration of 1-octen-3-ol by lipoxygenase and hydroperoxide lyase activities of *Agaricus bisporus*. *Process Biochem.* **2001**, *37*, 177–182.
15. Morawicki, R. O.; Beelman, R. B. Study of the biosynthesis of 1-octen-3-ol using a crude homogenate of *Agaricus bisporus* in a bioreactor. *J. Food Sci.* **2008**, *73*, C135–C139.

Chapter 7

(3*R*,4*R*)-3-Methyl-4-decanolide, a Novel Lactone Contributing to Fresh Wasabi (*Wasabia japonica*) Aroma

Akira Nakanishi,* Norio Miyazawa, Kenji Haraguchi, Hiroyuki Watanabe, Yoshiko Kurobayashi, Tsuyoshi Komai, and Akira Fujita

R&D Center, T. Hasegawa Co., Ltd., 29-7, Kariyado, Nakahara-ku Kawasaki-shi, Kanagawa, 211-0022, Japan
*E-mail: akira_nakanishi@t-hasegawa.co.jp.

Freshly grated wasabi aroma was investigated by aroma extract dilution analysis. At the highest flavor dilution factors of 1024 and 256, ten odorants were detected as odor-active compounds: allyl isothiocyanate, (*Z*)-1,5-octadien-3-one, 4-pentenyl isothiocyanate, 5-hexenyl isothiocyanate, 3-methyl-2-butene-1-thiol, 2-isopropyl-3-methoxypyrazine, 3-methyl-2,4-nonanedione, *cis*-3-methyl-4-decanolide, 6-(methylthio) hexyl isothiocyanate, and vanillin. To determine the absolute configuration of *cis*-3-methyl-4-decanolide in wasabi, the stereoisomers of 3-methyl-4-decanolide were synthesized from optically active *γ*-decalactone. Finally, the absolute configuration of *cis*-3-methyl-4-decanolide in wasabi was determined as (3*R*,4*R*)-3-methyl-4-decanolide by chiral GC-MS. Sensory analysis revealed that the (3*R*,4*R*)-3-methyl-4-decanolide constitutes an essential part of fresh wasabi aroma.

Introduction

Wasabi (*Wasabia japonica* Matsum.), otherwise known as Japanese horseradish, is a traditional Japanese spice of the *Brassicaceae* family. The length of wasabi root ranges from 10 to 30 cm, and its diameter is about 2 to 3 cm. The

underground root of wasabi is grated into a green, sticky and pungent paste and eaten as a condiment with sushi, raw fish (sashimi) and buckwheat noodles (soba). Anciently, the Japanese used wasabi as a medicinal herb. Later, it was used as a condiment and penetrated Japanese culture with the spread of sushi, raw fish, and buckwheat noodles. When Japanese cuisine, especially sushi, became popular in other countries, wasabi became well known and liked in many other parts of the world. Wasabi has recently come to be cultivated in England, the USA, Canada, China, and other countries. Some countries use it in popular dishes of their own, such as in sauces of French cuisine and mashed potatoes. With the increasing popularity of wasabi in other countries in recent years, the demand for wasabi has surged.

When wasabi is grated, the strong pungent aroma evolves. Isothiocyanates, chiefly allyl isothiocyanate, contribute to the pungent aroma and account for more than 90% of the wasabi aroma. These isothiocyanates are generated by a reaction between glucosinolate which abounds in the outer layer of the wasabi and myrosinase which is localized in the vascular cambium (*1–5*). However, the fresh wasabi aroma is clearly too complicated to be represented by the isothiocyanates alone. Several research groups have investigated odor-active compounds other than the isothiocyanates. Gas chromatography-olfactometry (GC-O) studies by Ohkawa *et al.* identified 3-methyl-2,4-nonanedione as a novel potent odorant contributing to wasabi aroma (*6*). They also detected vanillin as an odor-active component for the first time. In investigations by aroma extract dilution analysis (AEDA) Imazeki recently identified furfuryl mercaptan, 1-octen-3-one, *trans*-4,5-epoxy-(*E*)-2-decenal, methional, furaneol, 2-isopropyl-3-methoxypyrazine and 2-isobutyl-3-methoxypyrazine as odor-active components. They also found (3*S*,4*R*)-3-methyl-4-decanolide to be an important component for reconstructing wasabi aroma, even though it had a relatively low flavor dilution (FD) factor (*7*). Yet duplication of the freshly grated wasabi aroma using the known odor-active compounds alone is still difficult because the fresh wasabi aroma emitted just after grating is a complicated composite of a pungent odor combined with characteristic sweet, fruity, green and creamy odor. In this study, the aroma of freshly grated wasabi was investigated in further detail by AEDA for the purpose of finding novel odorants that contribute to fresh wasabi aroma. With regard to the novel odorant which was chiral, its absolute configuration was determined by chiral gas chromatography-mass spectrometry (GC-MS) and its importance in wasabi aroma was confirmed by sensory analysis.

Materials and Methods

Wasabi

Wasabi (Mazuma) was kindly provided by the Izu Agricultural Research Center of the Shizuoka Prefectural Research Institute of Agriculture and Forestry (Shizuoka, Japan).

Preparation of the Wasabi Aroma Concentrate

Wasabi root was cut at a point about 1 cm from the stem. After peeling, the root was grated with a traditional Japanese grater (samekawaoroshi) and 15 g of grated paste from three roots was extracted with CH_2Cl_2 (75 mL). The extract was filtered and distilled by solvent-assisted flavour evaporation (*8*). The distillate was concentrated at atmospheric pressure to obtain the aroma concentrate.

Fractionation of the Wasabi Aroma Concentrate by Silica Gel Chromatography

The wasabi aroma concentrate (125 mg) was pipetted into the top of a glass column filled with silica gel (10 g) slurry in *n*-pentane. The concentrate was fractionated by chromatography using *n*-pentane (Fr.1), followed by *n*-pentane/Et$_2$O (20/1, v/v, Fr.2), *n*-pentane/Et$_2$O (5/1, v/v, Fr.3) and *n*-pentane/Et$_2$O (1/1~0/1, v/v, Fr.4), to yield four fractions. In each fraction the solvent was removed at atmospheric pressure (Fr.1: 14.8 mg, Fr.2: 5.4 mg, Fr.3: 0.1 mg, Fr.4: 0.1 mg).

Aroma Extract Dilution Analysis (AEDA)

The FD factors of the odor-active compounds were determined by an AEDA approach (*9*). The wasabi aroma concentrate was diluted stepwise with CH_2Cl_2 to obtain dilutions at 1:4, 1:16, 1:64, 1:256 and 1:1024 ratios, and each dilution was analyzed by GC-O equipped with a TC-WAX capillary column (0.25 mm i.d. × 60 m, film thickness 0.25 μm; GL Sciences Co.). AEDA was performed by two experienced assessors.

Chemicals

A racemate of 3-methyl-4-decanolide was synthesized from *n*-heptanol and methyl crotonate by a method reported in literature (*10*). All stereoisomers of 3-methyl-4-decanolide were synthesized from optically active *γ*-decalactone. (*R*)-*γ*-Decalactone (>99.0% ee) was prepared from castor oil using lipase and yeast (*11–13*). (*S*)-*γ*-Decalactone (91.8% ee) was prepared from (*R*)-*γ*-decalactone via the Mitsunobu reaction of (*R*)-*N*-benzyl-4-hydroxydecanamide (*14*, *15*).

Gas Chromatography-Mass Spectrometry (GC-MS)

The GC-MS analyses were performed with an Agilent 6890 GC combined with a 5973 mass selective detector and a flame ionization detector (FID; 250 °C) equipped with a TC-WAX capillary column (0.25 mm i.d. × 60 m, film thickness 0.25 μm; GL Sciences Co.) or a heptakis-(2,3-di-*O*-acetyl-6-*O*-tert-butyldimethylsilyl)-*b*-cyclodextrin capillary column (0.25 mm i.d. × 60 m, film thickness 0.25 μm; prepared). Each sample was injected in 1 μL volumes in split mode (50:1) at a constant temperature of 250 °C. The linear retention indices (RIs) of the compounds were calculated from the retention times of *n*-alkanes.

Gas Chromatography-Mass Spectrometry-Olfactometry (GC-MS-O)

The GC-MS-O analyses were performed with an Agilent 6890 GC combined with a 5973 mass selective detector and a sniffing port equipped with a TC-WAX capillary column (0.25 mm i.d. × 60 m, film thickness 0.25 μm; GL Sciences Co.). Each sample was injected in 1 μL volumes in split mode (50:1) at a constant temperature of 250 °C.

Multidimensional-Gas Chromatography-Mass Spectrometry (MD-GC-MS)

The MD-GC-MS analyses were performed by a selectable ^{1}D/^{2}D GC-MS system with an Agilent 7890A GC equipped with a low thermal mass (LTM) system. The GC was combined with an FID (250 °C), a 5975 mass selective detector and a sniffing port equipped with a Gerstel multicolumn switching system, a DB-WAX capillary column (first column, 0.25 mm i.d. × 30 m, film thickness 0.25 μm, LTM; Agilent Technologies, Inc.) and a DB-1 capillary column (second column, 0.25 mm i.d. × 30 m, film thickness 0.25 μm; Agilent Technologies, Inc.). Each sample was injected in 1 μL volumes in splitless mode at a constant temperature of 250 °C.

Sensory Analyses

Each sample (0.5 ml) was put into a closed sensory vial (total volume = 30 ml) and coded by a random three-digit number. Each panelist was presented with a set of test samples with instructions to sniff each sample and rate the intensity according to six attributes (pungent, sulfurous, metallic, earthy, green and creamy) which were agreed in preliminary sessions using a seven-point linear scale from 1 (none) to 7 (very strong). The results were averaged for each attribute and plotted on a spider web diagram. The evaluation was conducted in a quiet room kept at 28 °C. The panel consisted of ten panelists, all of whom were employees of the Technical Research Center of T. Hasegawa Co., Ltd., Kawasaki, Japan. They were trained to recognize and quantify aromas with about 100 odorous chemicals and raw materials.

Wasabi aroma concentrate and two wasabi aroma reconstitutes were evaluated. The aroma reconstitutes were prepared based on quantitative data determined with an internal standard: Aroma reconstitute A was composed of 8 odor-active compounds [allyl isothiocyanate (256 mg/mL), (Z)-1,5-octadien-3-one (0.828 μg/mL), 4-pentenyl isothiocyanate (18.2 mg/mL), 5-hexenyl isothiocyanate (8.54 mg/mL), 2-isopropyl-3-methoxypyrazine (0.173 μg/mL), 3-methyl-2,4-nonanedione (67.8 ng/mL), 6-(methylthio)hexyl isothiocyanate (5.56 mg/mL), vanillin (13.9 μg/mL)]. Aroma reconstitute B additionally contained (3R,4R)-3-methyl-4-decanolide (1.52 μg/mL).

The differences among the average scores of the evaluated samples were compared by Tukey's multiple comparison tests. On the Tukey's multiple comparison tests, the standard error measurement and least significant differences for each attributes were calculated ($P < 0.05$) and compared with the subtracted values between the evaluated samples (*16–21*).

Results and Discussion

Identification of the Odorants

In GC-MS analysis of wasabi aroma concentrate, one hundred compounds were identified or tentatively identified. The main components of the wasabi aroma concentrate were isothiocyanates (96.86%), among which allyl isothiocyanate (73.82%) was predominant. The AEDA result for the wasabi aroma concentrate revealed ten odor-active compounds at FD factors of 1024 and 256 (Table 1). The following five compounds (Nos. 1, 3, 4, 9 and 10) were identified by matching the mass spectra (MS), RIs and odor qualities: allyl isothiocyanate (garlic-like, pungent), 4-pentenyl isothiocyanate (pungent), 5-hexenyl isothiocyanate (green, pungent), 6-(methylthio)hexyl isothiocyanate (green, oily), vanillin (vanilla-like). No clear MS data were obtained for the other five compounds, as four of them (Nos. 2, 5, 6 and 7) were present at trace levels and the fifth (No. 8) overlapped with the other compounds. To reveal these unknown compounds, further concentration was attempted. Allyl isothiocyanate was removed successfully by silica gel chromatography, and the further concentration allowed us to collect additional MS data for compounds Nos. 2, 6 and 7 and to identify them by matching the MS, RIs and odor qualities, as follows: (Z)-1,5-octadien-3-one, 2-isopropyl-3-methoxypyrazine, 3-methyl-2,4-nonanedione. Compound No. 5 was identified tentatively as 3-methyl-2-butene-1-thiol (hop-like, sulfurous) by matching the RI and odor qualities, though no clear MS data was available even after further concentration. Clear MS data was obtained for compound No. 8 using MD-GC-MS, which allowed us to identify it as *cis*-3-methyl-4-decanolide (celery-like). Among these odor-active compounds, (Z)-1,5-octadien-3-one and *cis*-3-methyl-4-decanolide were identified for the first time in wasabi.

Determination of the Absolute Configuration of *cis*- and *trans*-3-Methyl-4-decanolide in Wasabi

With regards to the identification of *trans*-3-methyl-4-decanolide, earlier reports have identified it in clary sage (*22*), orange juice, mandarin peel (*23*) and wasabi. The absolute configuration of *trans*-3-methyl-4-decanolide in wasabi has already been determined as (3*S*,4*R*)-3-methyl-4-decanolide. In our study, it was detected at an FD factor of 1 and found to be more abundant (0.008%) than the *cis*-isomer (trace) in the wasabi aroma concentrate. On the other hand, *cis*-3-methyl-4-decanolide has only been identified in orchid (*24*, *25*) and no reports regarding its identification in foods or the determination of its absolute configuration in nature were available. In order to address this question, absolute configurations of both *cis*- and *trans*-3-methyl-4-decanolide in wasabi were determined by means of chiral GC-MS.

All stereoisomers of 3-methyl-4-decanolide were synthesized from optically active γ-decalactones Figures 1 and 2). (*R*)-γ-Decalactone was converted to (3*S*,4*R*)-**1** by the introduction and subsequent oxidative elimination of phenylselenyl group, followed by stereoselective methylation. (3*R*,4*R*)-3-Methyl-4-decanolide was synthesized from (3*S*,4*R*)-**1** via the same olefin-forming method and subsequent nickel borate hydrogenation.

Table 1. Odor-Active Compounds (FD 1024, 256) in Freshly Grated Wasabi

No.	Odorant	Odor quality[a]	RI[a]	FD factor
1	allyl isothiocyanate	garlic-like, pungent	1383	1024
2	(Z)-1,5-octadien-3-one	metallic	1392	1024
3	4-pentenyl isothiocyanate	pungent	1564	1024
4	5-hexenyl isothiocyanate	green, pungent	1685	1024
5	3-methyl-2-butene-1-thiol	hop-like, sulfurous	1127	256
6	2-isopropyl-3-methoxypyrazine	earthy, nutty	1448	256
7	3-methyl-2,4-nonanedione	earthy	1741	256
8	cis-3-methyl-4-decanolide	celery-like	2221	256
9	6-(methylthio)hexyl isothiocyanate	green, oily	2406	256
10	vanillin	vanilla-like	2605	256

[a] Odor quality perceived at the sniffing port.   [b] TC-WAX.

(3R,4S)-3-Methyl-4-decanolide was obtained from (S)-**4** in the same manner as the synthesis of (3S,4R)-**1**. (3S,4S)-3-Methyl-4-decanolide could be synthesized in the same manner as (3R,4R)-**1** with (3R,4S)-**1** as starting material. However, (3R,4S)-**1** was obtained only in a small amount. Therefore, (3S,4S)-**1** was prepared by making use of by-product (S)-**7** which was available in relatively large amount. Bisphenylselenyl compound (S)-**7** was led to (4S)-**5** in the same manner as the synthesis of (3R,4S)-**1**, and the second oxidative elimination of the phenylselenyl group and hydrogenation provided (3S,4S)-**1**.
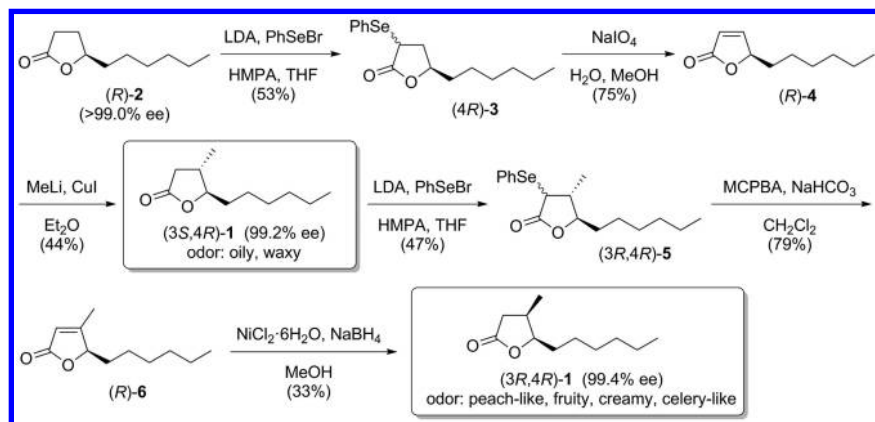
Figure 1. Synthesis of (3S,4R)- and (3R,4R)-3-Methyl-4-decanolide.
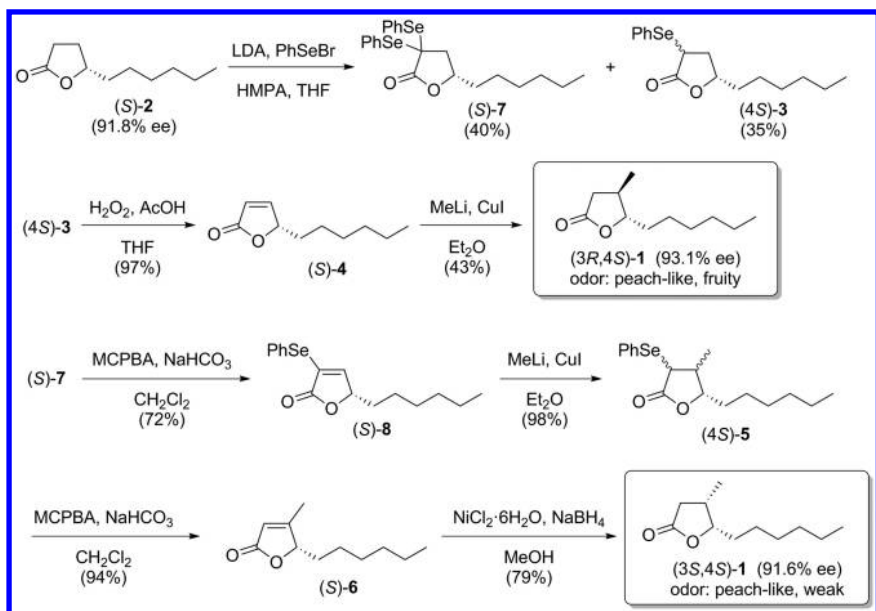
Figure 2. Synthesis of (3S,4S)- and (3R,4S)-3-Methyl-4-decanolide.
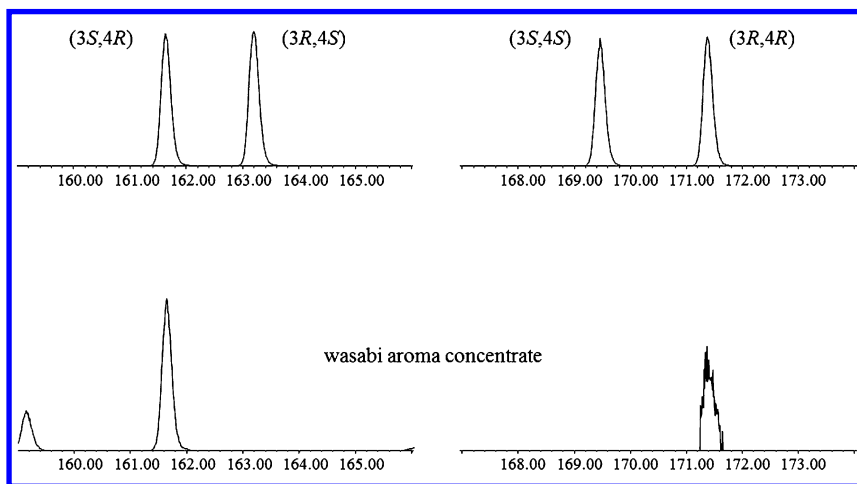
Figure 3. Comparison of Racemates of 3-Methyl-4-decanolide and Wasabi Aroma Concentrate.

The four synthesized stereoisomers and the wasabi aroma concentrate were subjected to GC-MS-SIM (*m/z* 99) using a heptakis-(2,3-di-*O*-acetyl-6-*O*-*tert*-butyldimethylsilyl)-*β*-cyclodextrin column (Figure 3). Finally, by matching the retention time and odor qualities, the absolute configurations of *cis*-3-methyl-4-decanolide and *trans*-3-methyl-4-decanolide in wasabi were determined as (3*R*,4*R*)-3-methyl-4-decanolide and (3*S*,4*R*)-3-methyl-4-decanolide, respectively. These analyses revealed for the first time the presence of (3*R*,4*R*)-3-methyl-4-decanolide in nature.

Effect of (3*R*,4*R*)-3-Methyl-decanolide on Wasabi Aroma

Sensory analysis was carried out employing a trained panel of ten people to assess the effect of (3*R*,4*R*)-3-methyl-4-decanolide (Figure 4). The scores for creamy and pungent odor of aroma reconstitute B were improved from those of aroma reconstitute A with a closer approximation to those of the wasabi aroma concentrate. This result indicates that (3*R*,4*R*)-3-methyl-4-decanolide constitutes an essential part of the aroma of freshly grated wasabi.
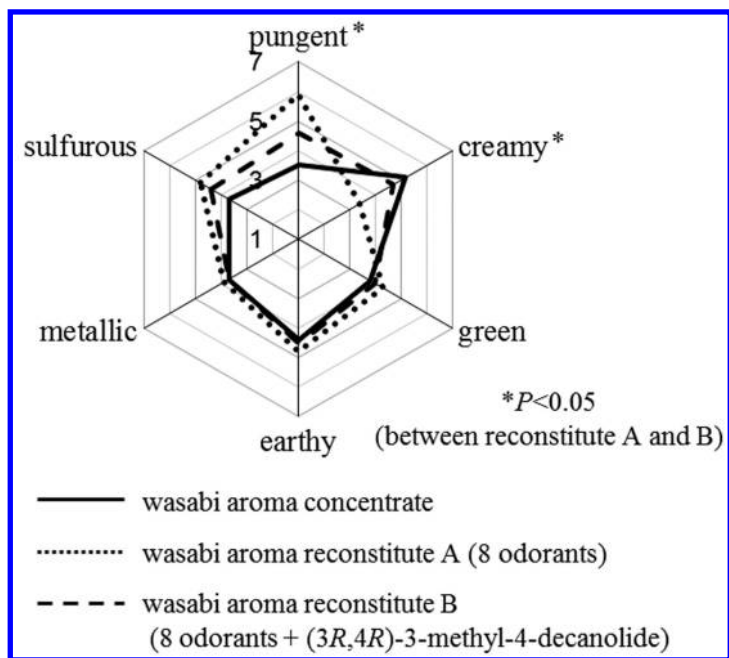
Figure 4. Spider Chart of Sensory Analysis of Wasabi Aroma Concentrate and Wasabi Reconstitutes.

Conclusion

Ten odor-active compounds were detected from freshly grated wasabi by AEDA technique at FD factors of 1024 and 254: 3-methyl-2-butene-1-thiol, allyl isothiocyanate, (*Z*)-1,5-octadien-3-one, 2-isopropyl-3-methoxypyrazine, 4-pentenyl isothiocyanate, 5-hexenyl isothiocyanate, 3-methyl-2,4-nonanedione, *cis*-3-methyl-4-decanolide, 6-(methylthio)hexyl isothiocyanate, and vanillin. (*Z*)-1,5-Octadien-3-one and *cis*-3-methyl-4-decanolide were identified in wasabi for the first time. The absolute configuration of *cis*-3-methyl-4-decanolide was determined as (3*R*,4*R*) by comparing the chiral GC-MS chromatogram of wasabi aroma concentrate obtained on chiral stationary phase with those of the synthetic stereoisomers. To our knowledge, this is the first time (3*R*,4*R*)-3-methyl-4-decanolide has been found in nature. The wasabi aroma reconstitute became more closer in "creamy" and "pungent" odor profile to the authentic wasabi aroma concentrate by adding (3*R*,4*R*)-3-methyl-4-decanolide. This result indicates that the (3*R*,4*R*)-3-methyl-4-decanolide constitutes an essential part of the aroma of freshly grated wasabi.

Acknowledgments

References

1. Ina, K. The volatile components of wasabi and Japanese mustard. *The Koryo* **1982**, *136*, 45–52.
2. Etoh, H.; Nishimura, A.; Takasawa, R.; Yagi, A.; Saito, K.; Sakata, K.; Kishima, I.; Ina, K. *ω*-Methylsulfinylalkyl isothiocyanates in wasabi, *Wasabia japonica* Matsum. *Agric. Biol. Chem.* **1990**, *54*, 1587–1589.
3. Ina, K.; Ina, H.; Ueda, M.; Yagi, A.; Kishima, I. *ω*-Methylthioalkyl isothiocyanates in wasabi. *Agric. Biol. Chem.* **1989**, *53*, 537–538.
4. Sultana, T.; Savage, G. P.; McNeil, D. L.; Porter, N. G.; Clark, B. Comparison of flavour compounds in wasabi and horseradish. *J. Food Agric. Environ.* **2003**, *1*, 117–121.
5. Masuda, H.; Harada, Y.; Tanaka, K.; Nakajima, M.; Tanabe, H. Characteristic odorants of wasabi (*Wasabia japonica matum*), Japanese horseradish, in comparison with those of horseradish (*Armoracia rusticana*). In *Biotechnology for Improved Foods and Flavours*; Takeoka, G. R., Teranishi, R., Williams, P. J., Kobayashi, A., Eds.; ACS Symposium Series 637; American Chemical Society: Washington, DC, 2009; pp 67−78.
6. Ohkawa, H.; Ikeda, S. Flavoring agent of wasabi. *Foods Food Ingredients J. Jpn.* **2008**, *213*, 768–771.
7. Imazeki, Y. The fresh green odor of wasabi. *The Koryo* **2012**, *254*, 37–42.
8. Engel, W.; Bahr, W.; Schieberle, P. Solvent assisted flavour evaporation – a new and versatile technique for the careful and direct isolation of aroma

compounds from complex food matrices. *Eur. Food Res. Technol.* **1999**, *209*, 237–241.

9. Schieberle, P. New developments in methods for analysis of volatile flavor compounds and their precursors. In *Characterization of Food: Emerging Methods*; Gaonkar, A. G., Ed.; Elsevier: Amsterdam, The Netherlands, ; pp 403−431.

10. Nikishin, G. I.; Spektor, S. S.; Glukhovtsev, V. G. Free-radical addition of alcohols and glycols to *α,β*-unsaturated acids and their esters. *Izv. Akad. Nauk SSSR, Ser. Khim.* **1971**, 389–393.

11. Okui, S.; Uchiyama, M.; Mizugaki, M. Metabolism of hydroxy fatty acids II. Intermediates of the oxidative breakdown of ricinoleic acid by genus *Candida*. *J. Biochem.* **1963**, *54*, 536–540.

12. Blin-Perrin, C.; Molle, D.; Dufosse, L.; Le-Quere, J.-L.; Viel, C.; Mauvais, G.; Feron, G. Metabolism of ricinoleic acid into γ-decalactone: β-oxidation and long chain acyl intermediates of ricinoleic acid in the genus *Sporidiobolus* sp. *FEMS Microbiol. Lett.* **2000**, *188*, 69–74.

13. Waché, Y.; Aguedo, M.; Niicaud, J.-M.; Belin, J.-M. Catabolism of hydroxyacids and biotechnological production of lactones by *Yarrowia lipolytica*. *Appl. Microbiol. Biotechnol.* **2003**, *61*, 393–404.

14. Shimotori, Y.; Miyakoshi, T. Synthesis of (*S*)-γ-lactones with a combination of lipase-catalyzed resolution and Mitsunobu reaction. *Synth. Commun.* **2009**, *39*, 1570–1582.

15. Shimotori, Y.; Miyakoshi, T. Combination of Novozym 435-catalyzed hydrolysis and Mitsunobu reaction for production of (*R*)-γ-lactones. *Synth. Commun.* **2010**, *40*, 1607–1613.

16. Aishima, T. Laboratory Methods for Sensory Analysis of Food: part 1. *J. Jpn. Soc. Food Sci. Technol.* **2001**, *48*, 311–320.

17. Aishima, T. Laboratory Methods for Sensory Analysis of Food: part 2. *J. Jpn. Soc. Food Sci. Technol.* **2001**, *48*, 378–392.

18. Aishima, T. Laboratory Methods for Sensory Analysis of Food: part 3. *J. Jpn. Soc. Food Sci. Technol.* **2001**, *48*, 453–466.

19. Aishima, T. Laboratory Methods for Sensory Analysis of Food: part 4. *J. Jpn. Soc. Food Sci. Technol.* **2001**, *48*, 539–548.

20. Aishima, T. Laboratory Methods for Sensory Analysis of Food: part 5. *J. Jpn. Soc. Food Sci. Technol.* **2001**, *48*, 637–642.

21. Aishima, T. Laboratory Methods for Sensory Analysis of Food: part 6. *J. Jpn. Soc. Food Sci. Technol.* **2001**, *48*, 697–703.

22. Maurer, B.; Hauser, A. In IXth International Congress of Essential Oils, March 13-17, 1983, Singapore; Book 3, pp 69−76.

23. Naef, R.; Velluz, A. Identification of *trans*-3-methyl-4-decanolide in blood orange juice and mandarin peel. *J. Essent. Oil Res.* **2005**, *17*, 681–682.

24. Kaiser, R. *The Scent of Orchids*; Elsevier: Basel, 1993; pp 128, 191−192.

25. Masuzawa, Y.; Tamogami, S.; Kitahara, T. Synthesis of both enantiomers of *cis*-methyl-4-decanolide, a key component for the scent of African orchids. *Nat. Prod. Lett.* **1999**, *13*, 239–246.

Chapter 8

Quantitation of *cis*- and *trans*-3,5-Diethyl-1,2,4-trithiolanes in Cooked *Allium* Varieties Using a Stable Isotope Dilution Assay

Mario Flaig and Michael Granvogl*

Technical University of Munich, Chair for Food Chemistry, Lise-Meitner-Straße 34, 85354 Freising, Germany
*E-mail: michael.granvogl@tum.de.

A quantitation method for 3,5-diethyl-1,2,4-trithiolane stereoisomers was newly developed on the basis of a stable isotope dilution assay using enantioselective, two-dimensional gas chromatography-mass spectrometry and synthesized [$^2H_4$]-3,5-diethyl-1,2,4-trithiolanes as internal standards. Application of the method to different *Allium* varieties revealed significantly different concentrations of the analytes. Determination of odor qualities and odor thresholds in air of all isomers by means of gas chromatography-olfactometry showed cooked onion-like/fruity and blackcurrant-like/fruity odor impressions for the *trans*-enantiomers as well as lower odor thresholds of 0.027 and 0.056 *n*g/L, respectively, compared to the *cis*-isomer eliciting a meat broth-like, cooked onion-like aroma at a five- to ten-fold higher threshold.

Introduction

Onions, shallots, and other *Allium* varieties are important and widespread culinary ingredients as vegetables and spices in numerous processed foods and dishes all over the world. It is well accepted, that mainly sulfur compounds contribute to the characteristic flavor of raw and processed edible *Alliums* (*1*, *2*), e.g., chiral heterocyclic alkyl-substituted sulfur compounds, such as *cis*- and *trans*-3,5-diethyl-1,2,4-trithiolane. They have been identified as important aroma-active compounds in cooked onions (*Allium cepa* L.) (*2*, *3*) and also in other *Allium* varieties (*4–6*). As stereochemistry is a

well-known aspect influencing sensory properties of aroma compounds (*7–10*), the aims of the present study were (i) to develop a suitable method for the simultaneous separation of *cis*-3,5-diethyl-1,2,4-trithiolane and both enantiomers of *trans*-3,5-diethyl-1,2,4-trithiolane applying chiral gas chromatography (GC), (ii) to determine odor qualities and odor thresholds in air of all three stereoisomers, and (iii) to develop a quantitation method for *cis*- and the enantiomers of *trans*-3,5-diethyl-1,2,4-trithiolane in cooked red, white and spring onions, shallots, and chives on the basis of a stable isotope dilution assay (SIDA) using GC/GC-MS.

Materials and Methods

Food Materials

Red onions (Italy/Spain), white onions (Germany/Spain), spring onions (Italy), shallots (France), and chives (Germany) were bought in local groceries (January-March 2014). Samples were worked-up at the day of purchase. Chives were freshly cut prior to analysis.

Chemicals

Ammonium sulfide (20%, aqueous solution) and sulfur were purchased from VWR (Darmstadt, Germany); propionaldehyde, sea sand, silica gel 60 (0.063-0.20 mm), and sodium sulfate from Merck (Darmstadt); (*E*)-2-decenal from TCI Europe (Eschborn, Germany); diethyl ether, *n*-pentane (both distilled prior to use) and tetrahydrothiophene from Sigma-Aldrich (Steinheim, Germany). [^{2}H$_2$]-Propionaldehyde was obtained from C/D/N Isotopes (Québec, Canada). Liquid nitrogen was from Linde (Munich, Germany).

Syntheses

Reference compounds and stable isotopically labeled standards were synthesized according to (*2*, *11*, *12*).

cis-/trans-3,5-Diethyl-1,2,4-trithiolanes (cis-/trans-3,5-DETTs)

Propionaldehyde (1.452 g; 25 mmol) was dissolved in an aqueous ammonium sulfide solution (20%; 85.2 g; 250 mmol) and elementary sulfur (2.40 g; 75 mmol) was added. The mixture was stirred for 2 h at room temperature and extracted with diethyl ether (3 x 70 mL) and *n*-pentane (1 x 70 mL). The organic phases were combined, dried over anhydrous sodium sulfate, and concentrated to a final volume of 1 mL by means of rotary evaporation (30 °C, 650 mbar). For purification, the solution was applied onto a silica gel column (water-cooled, 10 °C; 30 cm x 1.7 cm i.d.; sealed with defatted cotton and sea sand), packed with a slurry of silica gel 60 (9 g; 0.063-0.20 mm) in *n*-pentane. The target compounds were eluted

with *n*-pentane (80 mL) and finally concentrated to 1 mL applying again rotary evaporation.

[²H₄]-cis-/[²H₄]-trans-3,5-Diethyl-1,2,4-trithiolanes

[²H₂]-Propionaldehyde (0.108 g; 1.8 mmol) was dissolved in an aqueous ammonium sulfide solution (20%; 6.133 g, 18 mmol) and elementary sulfur (0.173 g; 5.4 mmol) was added. The mixture was stirred for 2 h at room temperature and extracted with diethyl ether (4 x 10 mL) and *n*-pentane (1 x 10 mL). Purification was performed as described above for the unlabeled compounds.

Determination of the Concentrations of the Synthesized Compounds

Since the synthesis of the labeled compounds was performed on a microscale basis, the target compounds could not be purified, for example, by distillation. Hence, the determination of their yields by weight was not possible. Therefore, the concentrations of the solutions of the labeled as well as the unlabeled 3,5-DETTs were determined via GC-FID according to the following procedure: First, a compound with a similar molecular structure and identical effective carbon number (C_{eff}) (*13, 14*) was chosen as internal standard, in this case tetrahydrothiophene (THT) having the same C_{eff} of 3 as 3,5-DETT (*15*). Then, a defined volume taken from the stock solution of THT was mixed with an aliquot of either the unlabeled or the labeled synthesis solution. The concentrations of the unlabeled and labeled compounds were finally calculated on the basis of the obtained FID peak areas.

Sample Preparation

Whole bulbs of red and white onions (each 150 g), spring onions (100 g), shallots (100 g), and chives barely cut from the bottom (60 g) were carefully cleaned and outer, dried leaf layers were gently removed without crushing the leaf tissue. The sample was cooked for 20 min (spring onions, shallots, and chives) or 25 min (red and white onions), respectively, in a pressure cooker (2 L, *Fissler*, Idar-Oberstein, Germany) as whole intact bulbs (except chives) with an equal amount of tap water (1/1, w/w). Immediately after the samples were cooled down to room temperature, appropriate amounts (determined in a preliminary experiment) of stable isotopically labeled internal standards were added for quantitation and the sample was homogenized for 2 min using an Ultra-Turrax (*Jahnke & Kunkel*, IKA-Labortechnik, Staufen, Germany). After stirring for 30 min, the samples were subjected to high vacuum distillation using the SAFE technique (*16*) to separate the volatiles from the non-volatiles. The aqueous distillate was extracted with diethyl ether (4 x 100 mL) and *n*-pentane (1 x 100 mL). The combined organic phases were dried over anhydrous sodium sulfate, concentrated to 300 μL using a Vigreux-column (50 cm x 1 cm; 45 °C) and, finally, subjected to two-dimensional gas chromatography-mass spectrometry (TD-HRGC-MS) as described below.

Instrumental Conditions

Method Development for Enantiomer Separation

A stock solution containing *cis*-3,5-diethyl-1,2,4-trithiolane and both enantiomers of *trans*-3,5-diethyl-1,2,4-trithiolane was used to evaluate the effects of different parameters of HRGC measurements on the separation of the stereoisomers. Carrier gas pressure and oven heating rate were stepwise varied to develop a method providing sufficient separation for quantitation.

In a first series of experiments, the carrier gas pressure (helium, 145 kPa) was kept constant, and different heating rates were applied: 1, 1.5, 2, 3, 4, or 6 °C/min. Next, the heating rate (2 °C/min) was kept constant and different carrier gas pressures were used: 60, 80, 100, 120, 140, and 160 kPa.

High-Resolution Gas Chromatography-Flame Ionization Detection (HRGC-FID) and High-Resolution Gas Chromatography-Olfactometry (HRGC-O)

HRGC was performed by means of a gas chromatograph type Trace GC 2000 (Thermo Scientific, Dreieich, Germany) running in constant pressure mode using the chiral BGB-175 column (30 m x 0.25 mm i.d., 0.25 μm film thickness; BGB Analytik GmbH, Rheinfelden, Germany). Aliquots of the samples (2 µL) were injected by the cold on-column technique at 40 °C. The initial temperature was held for 2 min and then raised at 2 °C/min to 150 °C and at 15 °C/min to 230 °C, which was held for 5 min.

For olfactometry, the effluent was split at the end of the capillary column and transferred in equal amounts to a sniffing port (230 °C) and an FID (250 °C). Retention indices were determined from the retention times of *n*-alkanes (C_6-C_{26}) by linear interpolation (*17*).

High-Resolution Gas Chromatography-Mass Spectrometry (HRGC-MS)

For synthesis verification and compound identification, mass spectra were generated by means of a gas chromatograph, type 5890 series II (Hewlett-Packard, Waldbronn, Germany) coupled to a sector field mass spectrometer, type MAT 95 S (Finnigan, Bremen, Germany) running in electron impact mode (EI; 70 eV ionization energy) or chemical ionization mode (CI; 115 eV ionization energy; reagent gas *iso*-butane), respectively. GC column and oven program were the same as mentioned above.

Quantitation Experiments Using a Stable Isotope Dilution Assay

Quantitation of *cis*- and *trans*-3,5-diethyl-1,2,4-trithiolanes was carried out by means of TD-HRGC-MS applying a stable isotope dilution assay. Aliquots of the sample extracts (2 µL) were injected at 40 °C by the cold on-column

technique using the achiral DB-FFAP column (30 m x 0.32 mm i.d., 0.25 μm film thickness; J&W Scientific, Cologne, Germany) in the first dimension (Trace GC 2000). The initial oven temperature was held for 2 min and then raised at 6 °C/min to 230 °C, which was held for 5 min. At the elution time of the target compounds, the effluent was quantitatively transferred by means of a moving column stream switching system (Thermo Finnigan, Egelsbach, Germany) onto a chiral GC-column (BGB-175) in the second dimension (gas chromatograph type CP 3800; Varian, Darmstadt). The oven temperature was held for 2 min at 40 °C and then raised at 2 °C/min to 150 °C and at 15 °C/min to 230 °C, which was held for 5 min. The effluent was monitored by means of an ion trap MS (Saturn 2000, Varian) running in CI mode (70 eV ionization energy) with methanol as the reactand gas.

Response factors of each compound were determined by analyzing defined mixtures of analyte and labeled standard in different mass ratios (5+1, 3+1, 1+1, 1+3, 1+5) by TD-HRGC-MS (Table 1).

Table 1. Selected Mass Fragments of Analytes and Stable Isotopically Labeled Standards as Well as Response Factors Used for Quantitation by Means of a Stable Isotope Dilution Assay

no.	analyte	m/z	internal standard	m/z	$R_f{}^a$
1	cis-3,5-diethyl-1,2,4-trithiolane	181	[^{2}H$_4$]-1	185	1.00
2a	trans-3,5-diethyl-1,2,4-trithiolane	181	[^{2}H$_4$]-2a	185	0.85
2b	trans-3,5-diethyl-1,2,4-trithiolane	181	[^{2}H$_4$]-2b	185	0.87

[a] Response factor.

Determination of Odor Qualities and Odor Thresholds in Air

Determination of odor qualities and odor tresholds in air of cis-3,5-diethyl-1,2,4-trithiolane and the enantiomers of trans-3,5-diethyl-1,2,4-trithiolane was carried out according to Ullrich and Grosch (18). Known amounts of the internal standard (E)-2-decenal, cis- and both enantiomers of trans-3,5-diethyl-1,2,4-trithiolane were dissolved in diethyl ether. The mixture was stepwise diluted with diethyl ether (1+1, v+v) and each dilution was subjected to HRGC-O as described above. Based on sniffing of the dilution series in order of descending concentrations, a flavor dilution (FD) factor, i.e. the highest dilution at which the substance was still smelled, was determined for the internal standard and each analyte. Odor thresholds in air were calculated from FD factors and the odor threshold in air of the internal standard using the following equation:

$$G_X = \frac{FD_S \times c_X}{FD_X \times c_S} \times G_S$$

G_x	=	odor threshold in air of X (ng/L)
FD_S	=	FD factor of (*E*)-2-decenal
FD_X	=	FD factor of X
c_X	=	concentration of X
c_S	=	concentration of (*E*)-2-decenal
G_S	=	odor threshold in air of the internal standard (*E*)-2-decenal (2.7 ng/L) (*19*)

Results and Discussion

Syntheses of the Analytes and the Stable Isotopically Labeled Internal Standards

To evaluate the impact of both different molar educt ratios and the presence of elementary sulfur on the yields of the target compounds, several synthetic approaches with alternating molar ratios of 1/1/0, 1/3/0, 1/10/0, and 1/10/3 (propionaldehyde/aqueous ammonium sulfide solution (20%)/elementary sulfur) were evaluated. Finally, a molar ratio of 1/10/3 resulted in the highest yields of *cis*-3,5-diethyl-1,2,4-trithiolane (28%) and of the enantiomers of *trans*-3,5-diethyl-1,2,4-trithiolane (each 19%) according to the proposed pathway illustrated in Figure 1. Mass spectrometry experiments in EI (Figures 2A and B) and CI (data not shown) mode proved the successful incorporation of the labeling into the internal standard [²H₄]-3,5-diethyl-1,2,4-trithiolane, whereat the mass spectra were the same for all stereoisomers (data not shown).
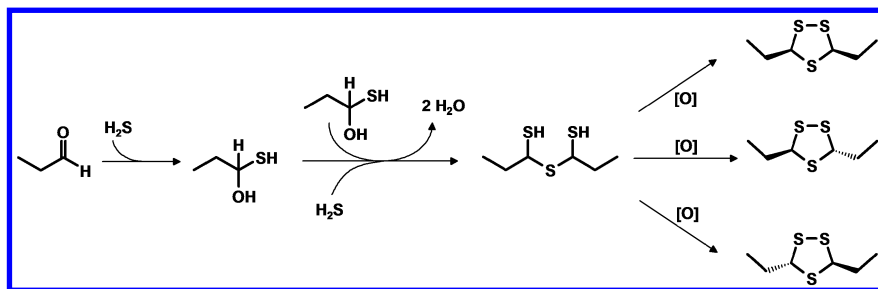
Figure 1. Proposed reaction pathway to 3,5-diethyl-1,2,4-trithiolanes according to (12).
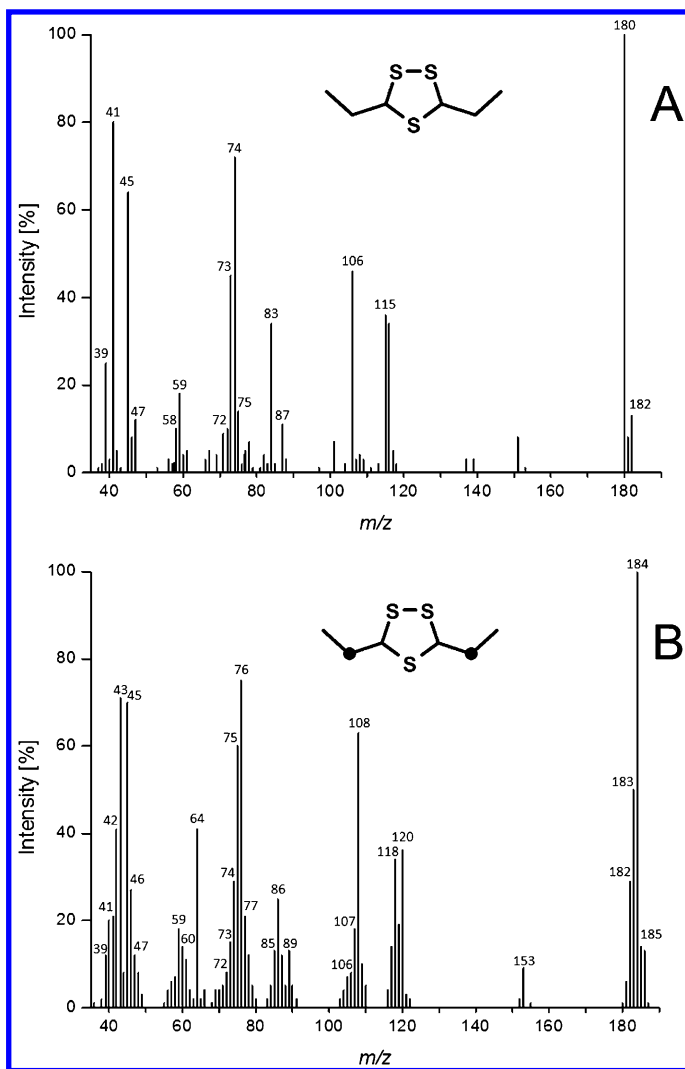
Figure 2. Mass spectra (EI mode) of 3,5-diethyl-1,2,4-trithiolane (A) and [$^2H_4$]-3,5-diethyl-1,2,4-trithiolane (B). • Position of [^2H]-labeling.

Method Development for Separation of Enantiomers Applying HRGC-FID

First, an optimized separation procedure for *cis*-3,5-diethyl-1,2,4-trithiolane and both enantiomers of *trans*-3,5-diethyl-1,2,4-trithiolane was developed on the basis of GC using a chiral column.
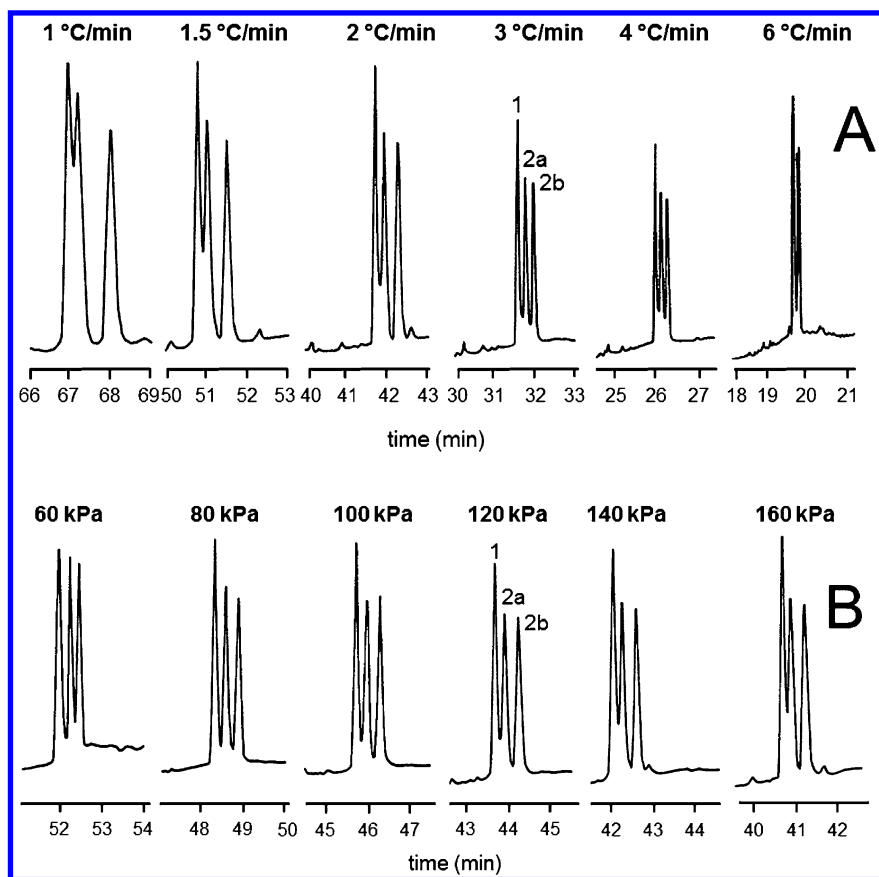
Figure 3. Dependency of the separation performance of cis- (1) and trans-3,5-diethyl-1,2,4-trithiolanes (2a, 2b) on heating rate (A) and carrier gas pressure (B).

Running in constant pressure mode, the carrier gas pressure and the heating rate showed the most significant impact on separation, and were, therefore, evaluated in more detail. One parameter was stepwise changed, while the remaining parameters were kept constant.

The heating rate showed the highest impact on separation of both *trans*-3,5-DETTs (**2a** and **2b**; Figure 3A). Enantiomer separation was improved by decreasing heating rates. But, simultaneously, co-elution of **2a** with *cis*-3,5-DETT (**1**) increased. Therefore, a heating rate of 2 °C/min showed sufficient enantiomer separation, in parallel with an acceptable separation of **1** and **2a**. The lower the carrier gas pressure, the better was the separation of **1** and **2a** (Figure 3B). Thus, for all following investigations, the carrier gas pressure was set to 100 kPa and the initial oven temperature of 40 °C was held for 2 min, then raised at 2 °C/min to 150 °C and finally at 15 °C/min to 230 °C, which was held for 5 min.

Identification Experiments and Determination of Odor Qualities and Odor Thresholds in Air

Identification of the 3,5-diethyl-1,2,4-trithiolanes in different *Allium* varieties was carried out by comparison of the chromatographic, sensorial (Table 2), and mass spectral data with the results obtained by the synthesized reference compounds and the data obtained by Granvogl (*2*). In more detail, identification was on the basis of TD-HRGC-MS, where each compound was singly transferred from the achiral DB-FFAP capillary column (first dimension) onto the chiral BGB-175 capillary column (second dimension), enabling an unequivocal assignment of the *cis-* and *trans-*isomers. After transferring only peak **1** from the achiral column onto the chiral column, again one single peak was obtained. In contrast, a transfer of only peak **2** onto the chiral column resulted in a separation of two peaks **2a** and **2b** (both *trans-*3,5-diethyl-1,2,4-trithiolane enantiomers) with identical mass spectra in EI and CI mode.

It is noteworthy, that during GC-O *cis-*(**1**) and one enantiomer of *trans-*3,5-DETT (**2a**) elicited a cooked onion-like odor attribute, beside a fruity odor note at higher concentrations for **2a**. In contrast, the other *trans-*3,5-DETT enantiomer (**2b**) only showed a blackcurrant-like, fruity aroma impression at all investigated concentrations (Table 2). The odor qualities of the stereoisomers were determined at low concentrations (fourfold above the respective odor thresholds in air) and high concentrations (at least 250-fold above the thresholds), respectively. In earlier reports, *cis-*3,5-diethyl-1,2,4-trithiolane was described with fruity, cooked onion-like, and blueberry-like odor qualities and *trans-*3,5-diethyl-1,2,4-trithiolane with onion-like, garlic-like, and sulfury odor impressions (*20*). With special emphasis on enantiomer separation, the results of the present study showed completely different results.

Table 2. Odor Qualities and Retention Indices of 3,5-Diethyl-1,2,4-trithiolane Stereoisomers

no.	aroma compound	odor quality	RI[a]	
			DB-FFAP	BGB-175
1	*cis-*3,5-diethyl-1,2,4-trithiolane	meat broth-like, cooked onion-like, sulfury	1752	1471
2a	*trans-*3,5-diethyl-1,2,4-trithiolane	cooked onion-like, fruity	1775	1473
2b	*trans-*3,5-diethyl-1,2,4-trithiolane	blackcurrant-like, fruity	1775	1480

[a] Retention index.

Determination of odor thresholds in air enabled a relative evaluation of odor potencies due to complete evaporation. Hence, matrix effects and undesirable impacts of contaminants or vapor pressure were eliminated due to chromatographic separation during GC analysis.

Beside significant differences in odor qualities, GC-O also showed variations in odor thresholds in air with 0.269 *n*g/L (**1**), 0.027 *n*g/L (**2a**), and 0.056 *n*g/L (**2b**), respectively. Differences in air odor thresholds depending on stereochemistry were also reported in previous studies, e.g., for the isomers of wine lactone (*8*) or of 3-mercapto-2-methylpentan-1-ol (*9*). According to the odor thresholds determined in this study, the 3,5-DETTs can be classified as odorants possessing a medium to strong potency, similar to allyl methyl sulfide (0.39 *n*g/L) (*21*), methional (0.08-0.16 *n*g/L) (*22*), and 2-furanmethanthiol (0.01-0.02 *n*g/L) (*22*).

Quantitation by TD-HRGC-MS.

In preliminary studies, the stereoisomers of 3,5-DETT were identified as potent odorants in cooked onions showing high FD factors during aroma extract dilution analysis and were quantitated by means of stable isotopically labeled internal standards (*2*). In this study, quantitations were carried out by means of an SIDA applying TD-HRGC-MS to different other *Allium* varieties. A typical chromatogram obtained for the quantitation of the 3,5-DETT stereoisomers is exemplarily shown for a sample of cooked spring onions (Figure 4).

The cooked samples showed clear differences in the concentrations of the stereoisomers in the analyzed *Allium* varieties (Table 3). Since whole, peeled bulbs of red, white, and spring onions as well as shallots were used for sample preparation, varying amounts of the analytes might be due to different origins and natural variations in the precursor concentrations in different *Allium* varieties (*23*). Further, as in case of red and white onions, the temperature permeation in the tissue system during cooking differs. At the beginning of the cooking process, the temperature inside the onion bulbs rises slowly. Hence, the enzyme alliinase (temperature optimum 34-40 °C) (*24*, *25*) enables conversions of non-aroma active flavor precursors into the aroma-active compounds until its thermal inactivation. The thinner tissue diameters of spring onions and chives might inactivate the enzyme quicker or even immediately. This hypothesis is in good agreement with the lower concentrations of trithiolanes analyzed in spring onions and chives as well as the ratios of cis- and *trans*-3,5-diethyl-1,2,4-trithiolanes in the present study. The concentrations of **1**, **2a**, and **2b** showed approximately statistical distribution (3:2:2 for **1**:**2a**:**2b**) including a nearly racemic ratio of the *trans*-3,5-diethyl-1,2,4-trithiolane enantiomers, also reflected in the low enantiomeric excess (Table 3).

This finding indicates a thermal or non-stereospecific, enzymatic formation pathway, at least for the final step.

Earlier reports on the concentrations of 3,5-DETT isomers showed 195 *µ*g/kg in freshly heated mixtures of sliced onions in sunflower oil and 148 *µ*g/kg in heated, stored mixtures thereof (*26*). The studies of Granvogl (*2*) revealed 151 *µ*g/kg (*cis*-3,5-DETT) and 101 *µ*g/kg (both *trans*-3,5-DETTs), respectively, for cooked onions.
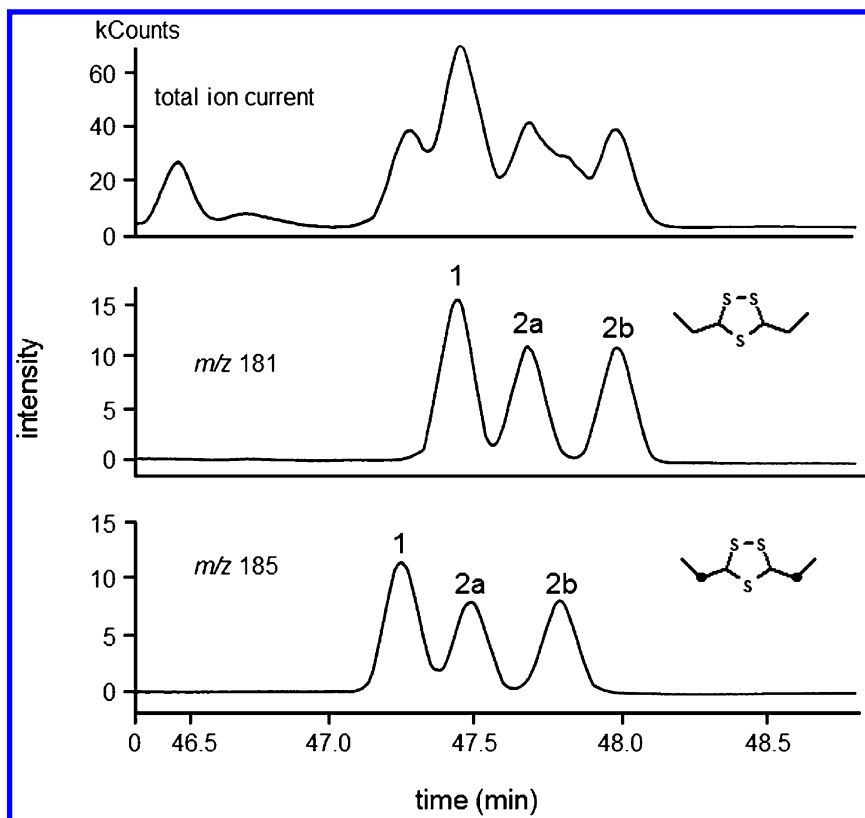
Figure 4. Extract of a GC/GC-MS chromatogram (CI mode) obtained during the quantitation of 3,5-diethyl-1,2,4-trithiolane isomers in a cooked spring onion sample. m/z 181: isomers of 3,5-DETT (analytes); m/z 185: isomers of [²H₄]-3,5-DETT (standards). • Position of [²H]-labeling

In summary, a quantitation of all 3,5-diethyl-1,2,4-trithiolane stereoisomers was successfully established by means of a newly developed method based on enantioselective, two-dimensional GC-MS using a stable isotope dilution assay. The obtained data revealed significant differences in the concentrations of the 3,5-DETT isomers in different *Allium* varieties, which might be both due to different precursor concentrations in the respective samples and different heat permeation during cooking, influencing enzyme activity.

Table 3. Concentrations of 3,5-Diethyl-1,2,4-trithiolane Stereoisomers in Various Cooked *Allium* Varieties

| sample | *conc.[a] (µg/kg)* | | | *enantiomeric excess (ee) of* **2b** *(%)* |
	cis-3,5-diethyl-1,2,4-trithiolane **1**	*trans-3,5-diethyl-1,2,4-trithiolane* **2a**	*trans-3,5-diethyl-1,2,4-trithiolane* **2b**	
red onion	58.7 (41.8-68.0)	41.4 (31.1-48.7)	44.4 (34.1-50.8)	3.5
white onion	49.6 (34.4-66.4)	35.2 (24.4-49.9)	37.3 (26.6-52.4)	2.9
spring onion	16.8 (10.9-27.3)	10.9 (7.0-17.9)	11.9 (7.6-19.2)	4.4
shallot	39.5 (29.0-52.3)	29.0 (20.9-38.7)	31.5 (23.1-42.2)	4.1
chives	3.1 (2.9-3.5)	2.0 (1.8-2.2)	2.2 (2.0-2.3)	4.8

[a] Data are mean values of triplicates; concentration ranges in parentheses.

References

1. Block, E. The organosulfur chemistry of the genus *Allium* and its importance to the organic chemistry of sulfur. *Angew. Chem., Int. Ed. Engl.* **1992**, *31*, 1135–1178.
2. Granvogl, M. A. Thermally induced changes of key aroma compounds in onions (*Allium cepa*) (in German). Ph.D. Thesis, Technical University of Munich, Munich, Germany; Deutsche Forschungsanstalt für Lebensmittelchemie: Garching, Germany, 2009.
3. Kameoka, H.; Demizu, Y. 3,5-Diethyl-1,2,4-trithiolane from *Allium cepa*. *Phytochemistry* **1979**, *18*, 1397–1398.
4. Hashimoto, S.; Miyazawa, M.; Kameoka, H. Volatile flavor components of chives (*Allium schoenoprasum* L.). *J. Food Sci.* **1983**, *48*, 1858–1859, 1873.
5. Kameoka, H.; Iida, H.; Hashimoto, S.; Miyazawa, M. Sulfides and furanones from steam volatile oils of *Allium fistulosum* and *Allium chinense*. *Phytochemistry* **1984**, *23*, 155–158.
6. Stephani, A.; Baltes, W. New aroma compounds of leek oil. *Z. Lebensm.-Unters. Forsch.* **1992**, *194*, 21–25.
7. Russell, G. F.; Hills, J. I. Odor differences between enantiomeric isomers. *Science* **1971**, *172*, 1043–1044.
8. Guth, H. Determination of the configuration of wine lactone. *Helv. Chim. Acta* **1996**, *79*, 1559–1571.

9. Lüntzel, C. S.; Widder, S.; Vössing, T.; Pickenhagen, W. Enantioselective syntheses and sensory properties of the 3-mercapto-2-methylpentanols. *J. Agric. Food Chem.* **2000**, *48*, 424–427.

10. Steinhaus, M.; Fritsch, H. T.; Schieberle, P. Quantitation of (*R*)- and (*S*)-linalool in beer using solid phase microextraction (SPME) in combination with a stable isotope dilution assay (SIDA). *J. Agric. Food Chem.* **2003**, *51*, 7100–7105.

11. Asinger, F.; Thiel, M. Simple synthesis and chemical behavior of new heterocyclic ring systems (in German). *Angew. Chem.* **1958**, *70*, 667–683.

12. Kuo, M.-C.; Ho, C.-T. Volatile Constituents of the Distilled Oils of Welsh Onions (*Allium fistulosum* L. variety Maichuon) and Scallions (*Allium fistulosum* L. variety Caespitosum). *J. Agric. Food Chem.* **1992**, *40*, 111–117.

13. Sternberg, J. C.; Gallaway, W. S.; Jones, D. T. L. Mechanism of response of flame ionization detectors. *Gas Chromatogr., Int. Symp. (U.S.)* **1961**, *3*, 231–267.

14. Scanlon, J. T.; Willis, D. E. Calculation of flame ionization detector relative response factors using the effective carbon number concept. *J. Chromatogr. Sci.* **1985**, *23*, 333–340.

15. Andreatch, A. J.; Feinland, R. Continuous Trace Hydrocarbon Analysis by Flame Ionization. *Anal. Chem.* **1960**, *32*, 1021–1024.

16. Engel, W.; Bahr, W.; Schieberle, P. Solvent assisted flavour evaporation - a new and versatile technique for the careful and direct isolation of aroma compounds from complex food matrices. *Eur. Food Res. Technol.* **1999**, *209*, 237–241.

17. Van den Dool, H.; Kratz, P. D. A generalization of the retention index system including linear temperature programmed gas-liquid partition chromatography. *J. Chromatogr.* **1963**, *11*, 463–471.

18. Ullrich, F.; Grosch, W. Identification of the most intense volatile flavour compounds formed during autoxidation of linoleic acid. *Z. Lebensm.-Unters. Forsch.* **1987**, *184*, 277–282.

19. Teranishi, R.; Buttery, R. G.; Guadagni, D. G. Odor quality and chemical structure in fruit and vegetable flavors. *Ann. N. Y. Acad. Sci.* **1974**, *237*, 209–216.

20. Krafft, C.; Brennecke, S.; Ott, F.; Backes, M.; Salzer, R.; Grunenberg, J.; Ley, J. P.; Krammer, G. E.; Weber, B. High-impact sulfur compounds: constitutional and configurational assignment of sulfur-containing heterocycles. *Chem. Biodiversity* **2008**, *5*, 1204–1212.

21. Eisgruber, K. Aroma compounds in fresh and heated garlic - correlation with the impairment of breath (in German). Ph.D. Thesis, Technical University of Munich, Munich, Germany; Deutsche Forschungsanstalt für Lebensmittelchemie: Freising, Germany, 2011.

22. Blank, I.; Sen, A.; Grosch, W. Potent odorants of the roasted powder and brew of Arabica coffee. *Z. Lebensm.-Unters. Forsch.* **1992**, *195*, 239–245.

23. Block, E. *Garlic and Other Alliums - The Lore and the Science*; Royal Society of Chemistry: Cambridge, United Kingdom, 2010.

24. Krest, I.; Glodek, J.; Keusgen, M. Cysteine Sulfoxides and Alliinase Activity of Some *Allium* Species. *J. Agric. Food Chem.* **2000**, *48*, 3753–3760.
25. Keusgen, M.; Schulz, H.; Glodek, J.; Krest, I.; Krüger, H.; Herchert, N.; Keller, J. Characterization of Some *Allium* Hybrids by Aroma Precursors, Aroma Profiles, and Alliinase Activity. *J. Agric. Food Chem.* **2002**, *50*, 2884–2890.
26. Ayverdi, Y. N. *Key aroma active compounds in raw onions*. Ph.D. thesis, Technical University of Munich, Munich, Germany; Deutsche Forschungsanstalt für Lebensmittelchemie: Garching, Germany, 2006.

Chapter 9

Characteristic Chiral Sulfur Compounds Aroma-Active in Cempedak (*Artocarpus integer* (Thunb.) Merr.) Fruits

Martin Steinhaus* and Johanna E. Grimm

Deutsche Forschungsanstalt für Lebensmittelchemie (German Research Center for Food Chemistry) Lise-Meitner-Straβe 34, 85354 Freising, Germany
*E-mail: martin.steinhaus@lrz.tum.de.

A comparative gas chromatography−olfactometry (GC-O) analysis of the volatiles isolated from tree-ripened fruits of cempedak (*Artocarpus integer* (Thunb.) Merr.) and jackfruit (*Artocarpus heterophyllus* Lam.) afforded 33 aroma-active compounds. Two of them were detected in the cempedak fruit sample, but not in the jackfruit sample and exhibited an odor corresponding to the characteristic sulfury, smear cheese-like note distinguishing cempedak fruit aroma from jackfruit aroma. These compounds were identified as 2-(methylthio)-butane and 2-(methylthio)pentane. Both compounds have rarely been reported from nature and were as yet unknown in any fruit. Enantio-GC analysis revealed an (*R*)/(*S*) ratio of 33/67 for 2-(methylthio)butane and 41/59 for 2-(methylthio)pentane in cempedak fruit. The odor qualities of the enantiomers were virtually identical, but slight differences were found in the odor threshold values.

Introduction

The cempedak tree (*Artocarpus integer* (Thunb.) Merr.) is an evergreen tropical tree in the mulberry family Moraceae. It is native to Southeast Asia and is nowadays particularly found in Indonesia, Malaysia, and New Guinea, but also some parts of Thailand, India, and Australia. Cempedak fruits are multiple fruits derived from the coalescence of the individual fruits of a whole inflorescence and

grow directly from the trunk of the tree. They are cylindrically shaped and reach a length of up to 40 cm. A leathery skin of yellow, green or brown color covers numerous seeds attached to the peduncle. Each seed is covered by a fleshy edible aril. The ripe arils are mainly eaten fresh. They are pale yellow to orange in color, soft, sweet, and fragrant.

Cempedak fruits in many respects resemble jackfruits, the fruits of *Artocarpus heterophyllus* Lam., a closely related, but more widely known species. Jackfruits are cultivated in the entire tropics today, but their natural origin is in Southern Asia. Compared to cempedak fruits, jackfruits are bigger in size and may reach a length of 1 m and a weight of 30 kg. The arils of major jackfruit varieties are less soft than cempedak arils and are often sold packaged and refrigerated as "seedless jackfruit flesh" in supermarkets, whereas cempedak is typically sold as fresh whole fruit.

The aroma properties of cempedak and jackfruit arils are similar, but differ in a specific characteristic: Both are dominated by sweet, fruity and malty notes, but cempedak arils exhibit an additional intensely sulfury, smear cheese-like aroma note, not perceived in jackfruit aroma. The molecular background of this specific note has yet been unclear.

In jackfruit, numerous volatile constituents have been identified so far. Major compounds include alcohols such as 1-propanol, 1-butanol, 2-methyl-1-propanol, 2-methyl-1-butanol, 3-methyl-1-butanol, and 2-phenylethanol, as well as esters such as methyl 3-methylbutanoate, ethyl 3-methylbutanoate, propyl 3-methylbutanoate, butyl acetate, 3-methylbutyl acetate, 2-methylpropyl 3-methylbutanoate, butyl 3-methylbutanoate, and 3-methylbutyl 3-methylbutanoate (*1–8*). Application of gas chromatography−olfactometry (GC-O) and aroma extract dilution analysis (AEDA) (*9*) to an extract obtained from jackfruit arils revealed ethyl butanoate, ethyl 3-methylbutanoate, butyl butanoate, and butyl 3-methylbutanoate as major aroma-active compounds (*10*).

In cempedak fruits, 3-methylbutanoic acid, 3-methyl-1-butanol, 3-hydroxy-2-butanone, 2-phenylethanol, 2-methyl-1-propanol, ethyl 3-methylbutanoate, 2,3-pentanedione, and methyl 3-methylbutanoate were identified as dominating volatiles (*3*). An early GC-O analysis suggested 3-methylbutyl 3-methylbutanoate and butyl 3-methylbutanoate as major odorants (*11*). More recently, potent odorants in two cempedak cultivars were systematically characterized using AEDA, quantitation assays, calculation of odor activity values (OAV), aroma reconstitution, and omission tests (*12*). AEDA resulted in high flavor dilution (FD) factors for 4-hydroxy-2,5-dimethyl-3(2*H*)-furanone (HDMF), ethyl 3-methylbutanoate, ethyl 2-methylbutanoate, 3-methylbutanal, 3-(methylthio)propanal, 2-acetyl-1-pyrroline, and 3-methylbutanoic acid. Sulfury odor characteristics were attributed to 2-(methylthio)acetaldehyde (meaty), 3-(methylthio)-1-butanol (meaty), 3-(methylthio)propanal (potato-like), 3-(methylthio)butanal (potato-like), and dimethyl trisulfide (catty). The aroma of cempedak, cultivar Tongtapan, was reported to be successfully reconstituted using 12 odorants in their natural concentrations, namely 3-methylbutanal, ethyl 3-methylbutanoate, methyl 3-methylbutanoate, octanal, HDMF, 3-(methylthio)propanal, 4-methoxy-2,5-dimethyl-3(2*H*)-furanone (MDMF), 3-methyl-1-butanol, 3-methylbutanoic acid, vanillin, benzaldehyde, and 2-phenylethanol.

However, when we repeated the reconstitution experiment detailed in (*12*), we observed that the aroma of the model was closely resembling the aroma of jackfruit, but lacking the typical sulfury, smear cheese-like aroma note characterizing cempedak fruits. Therefore, the aim of the present study was to reinvestigate the aroma-active compounds in cempedak in comparison to jackfruit by GC-O with special emphasis to compounds potentially contributing to this characteristic aroma difference.

Materials and Methods

Fruit Samples

Tree-ripened cempedak fruits and jackfruits organically grown in Thailand were handpicked by local farmers and sent to Germany by air freight within two days.

Chemicals

Reference samples of the following odorants were purchased from commercial vendors: **1**, **14** (Alfa Aesar, Karlsruhe, Germany); **2**, **3**, **5–7**, **10–13**, **17–21**, **22–25**, **27**, **28**, **30–33** (Sigma-Aldrich, Taufkirchen, Germany); **9** (Merck, Darmstadt, Germany). **15** was synthesized according to (*13*). **4**, 3-methyl-2-(methylthio)butane, (*R*)-**1**, and (*R*)-**4** were synthesized as detailed below.

(*S*)-2-Butanol, (*E*)-2-decenal, 3-methyl-2-butanol, *rac*-2-pentanol, (*S*)-2-pentanol, sodium methanethiolate, and tosyl chloride (4-methylbenzenesulfonyl chloride) were from Sigma-Aldrich. Dichloromethane, diethyl ether, and pentane (Merck) were freshly distilled before use.

Synthesis of 2-(Methylthio)alkanes

Starting from the corresponding 2-alcohols, **4**, 3-methyl-2-(methylthio)butane, (*R*)-**1**, and (*R*)-**4** were synthesized by tosylation and subsequent substitution of tosylate for methanethiolate.

Tosylation of the 2-alcohols was accomplished by reaction with tosyl chloride in pyridine as detailed in (*14*).

To the 2-alkyl tosylates (2-3 mmol) 2.5 equivalents of sodium methanethiolate in DMF (15 mL) were added and the mixture was heated (80 °C) for 2 h. After cooling to ambient temperature, brine (50 mL) was added. The mixture was extracted with diethyl ether (3 × 50 mL). The combined organic phases were washed with brine (5 × 50 mL). After drying over anhydrous sodium sulfate, the solvent was removed in vacuo and the residue was purified by flash chromatography (silica gel, pentane) to yield between 12% and 35% 2-(methylthio)alkane in ≥ 90% purity (GC).

GC-O, GC-MS, and Heart-Cut GC-GC-MS Analyses

Cempedak and jackfruit arils (100 g), respectively, were homogenized under addition of dichloromethane (300 mL) and anhydrous sodium sulfate (250 g) using a stainless steel blender. After further magnetic stirring (30 min), the mixture was filtered and the eluate was subjected to solvent-assisted flavor evaporation (SAFE) (*15*). The distillate was stepwise concentrated to 1 mL using a Vigreux column (50 cm × 1 cm) and a microdistillation device.

Aliquots (1 μL) of the concentrates were analyzed by GC-O, GC-MS, and heart-cut GC-GC-MS using the instruments, columns, and procedures detailed in (*16*). GC-O results of four trained panelists were combined.

Odor Threshold Values

An AEDA was applied to a mixture of racemic 2-(methylthio)butane, racemic 2-(methylthio)pentane, and (*E*)-2-decenal as internal standard using a chiral BGB-176 column (BGB Analytik, Rheinfelden, Germany). Odor thresholds in air were calculated from the FD factors obtained according to the approach detailed in (*17*) and a threshold of 2.7 ng/L for (*E*)-2-decenal (*18*). Results of three trained panelists were averaged.

Results and Discussion

Comparative GC-O Analysis

Arils obtained from a freshly opened cempedak fruit were homogenized together with dichloromethane as extraction solvent and anhydrous sodium sulfate as desiccant. After filtration, the volatile fraction was isolated by SAFE. The distillate was concentrated and subjected to GC-O analysis. In parallel, the same procedure was applied to jackfruit arils.

The comparative GC-O analysis of cempedak and jackfruit aril volatiles resulted in 33 aroma-active compounds in the retention index (RI) range of < 1000 to 2203 on an FFAP capillary (Table 1). Comparison of the RI data and odor qualities with in-house database entries allowed for the structural assignment of 26 compounds. Identifications were confirmed by parallel GC-O and GC-MS analyses of authentic reference compounds and the fruit volatile isolates using two GC columns of different polarity (FFAP and DB-5). The identities of seven compounds, however, remained unclear. Among these, compounds **1** and **4** (cf. Table 1) particularly attracted our attention, because their odor clearly represented the characteristic sulfury, smear cheese-like aroma note of cempedak fruits. Both were detected during GC-O of the cempedak fruit aroma isolate, but not in the jackfruit sample, indicating that they might play a major role for the aroma difference between both fruits.

Identification of Compounds 1 and 4

GC-MS analysis of the cempedak fruit volatile fraction resulted in the mass spectra displayed in Figure 1 for compounds **1** and **4**. The mass spectrum of **1** matched the MS database (*19*) entry of 2-(methylthio)butane. GC-O and GC-MS analysis of a purchased 2-(methylthio)butane reference using FFAP and DB-5 GC columns confirmed the structure assignment.

Database search for the mass spectrum of **4** was unsuccessful. However, comparison with the mass spectrum of **1** suggested that **4** was a homologue differing from **1** by an additional methylene group. Major peaks in the mass spectrum of **1** included m/z 104 corresponding to the molecular ion, m/z 89 indicating loss of a methyl group, the base peak m/z 75 indicating loss of an ethyl group, and m/z 56 indicating loss of methanethiol. Analogous interpretation of the mass spectrum of **4** suggested m/z 118 as molecular ion, m/z 103 as loss of methyl, m/z 89 as loss of ethyl, and m/z 70 as loss of methanethiol. The base peak m/z 75 would then correspond to the loss of propyl, suggesting that **4** was either 2-(methylthio)pentane or 3-methyl-2-(methylthio)butane.

Table 1. Aroma-Active Compounds in Cempedak Fruit and Jackfruit

No.	Compound[a]	Odor[b]	RI[c]	Odor Intensity[d]	
				Cempedak	Jackfruit
1	**unknown**	**cempedak**	**<1000**	++	−
2	methyl 3-methylbutanoate	fruity	1013	++	−
3	ethyl butanoate	fruity	1028	++	++
4	**unknown**	**cempedak**	**1041**	++	−
5	ethyl 2-methylbutanoate	fruity	1044	−	++
6	ethyl 3-methylbutanoate	fruity	1061	+++	+++
7	hexanal	grassy	1073	++	+
8	unknown	skunky	1103	++	+
9	1-butanol	malty	1140	++	++
10	methyl hexanoate	fruity	1180	++	+
11	2-/3-methyl-1-butanol	malty	1207	++	++
12	ethyl hexanoate	fruity	1225	++	−
13	octanal	citrusy	1279	++	+
14	1-octen-3-one	mushroom	1290	++	+
15	2-acetyl-1-pyrroline	popcorn	1332	+++	++

Continued on next page.

Table 1. (Continued). Aroma-Active Compounds in Cempedak Fruit and Jackfruit

No.	Compound[a]	Odor[b]	RI[c]	Odor Intensity[d]	
				Cempedak	Jackfruit
16	unknown	sulfury	1365	+++	+
17	acetic acid	vinegar	1454	+	++
18	3-(methylthio)propanal	potato	1457	+++	++
19	decanal	citrusy	1485	++	−
20	(E)-2-nonenal	fatty	1530	++	+
21	MDMF	caramel	1589	++	−
22	unknown	fruity	1610	++	+
23	butanoic acid	cheesy	1620	+	++
24	phenylacetaldehyde	flowery	1645	++	+
25	3-methylbutanoic acid	cheesy	1665	+++	++
26	unknown	meaty	1724	++	+++
27	hexanoic acid	cheesy	1844	++	++
28	2-methoxyphenol	smoky	1863	+	++
29	unknown	fruity	1887	++	+
30	2-phenylethanol	flowery	1916	++	++
31	HDMF	caramel	2047	+++	+++
32	ethyl cinnamate	fruity	2120	++	−
33	sotolon	seasoning	2203	++	++

[a] Compounds are listed in the order of increasing retention time observed during GC-O (FFAP column). [b] Odor quality as perceived at the sniffing port during GC-O. [c] Retention index (FFAP column). [d] Odor intensity as perceived at the sniffing port during GC-O: +++, intense; ++, moderate; +, weak; −, not detected.

As neither 2-(methylthio)pentane nor 3-methyl-2-(methylthio)butane was commercially available, both compounds were synthesized from the corresponding alcohols via tosylation followed by substitution of tosylate for methanethiolate as detailed in Figure 2. The structures of the reaction products were confirmed by NMR (data not shown) and they were then analyzed by GC-O and GC-MS in parallel to the cempedak fruit volatile isolate.
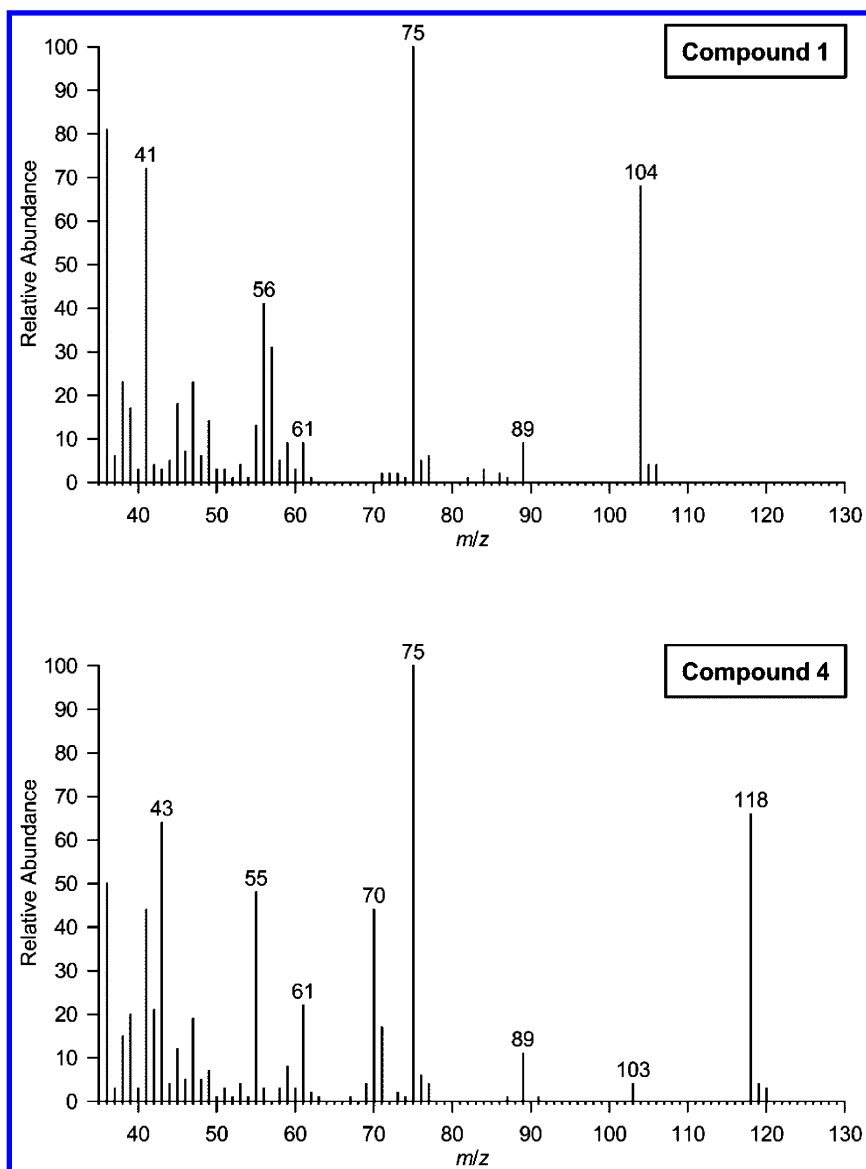
Figure 1. Mass Spectra Obtained for Compounds 1 and 4 by GC-MS(EI) of the Cempedak Fruit Volatile Isolate.

Results showed identical RIs for 2-(methylthio)pentane and **4** on the FFAP (1041) and DB-5 column (870), identical mass spectra, and identical odor properties. 3-Methyl-2-(methylthio)butane, on the other hand, although exhibiting the same cempedak-like odor, clearly differed in its RI data (FFAP: 1031; DB-5: 861) and the intensities of major fragments in the mass spectrum (data not shown). Thus, compound **4** was identified as 2-(methylthio)pentane.
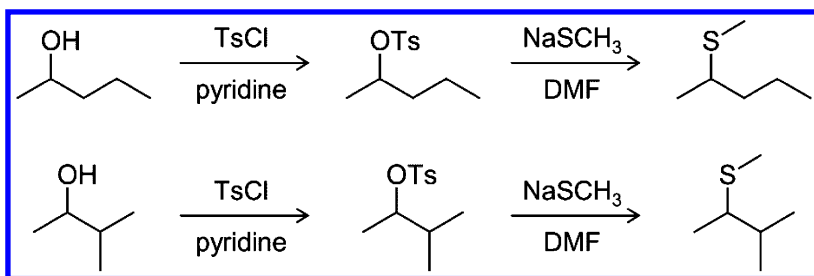
Figure 2. Synthetic Route to 2-(Methylthio)pentane and 3-Methyl-2-(methylthio)butane.

Neither 2-(methylthio)butane nor 2-(methylthio)pentane has been reported in cempedak fruit before. 2-(Methylthio)butane, however, has been found among the volatiles of asafoetida, a gum exuded from *Ferula assa-foetida* L. that is used as spice in South Asian cuisines (*20*), and 2-(methylthio)pentane has previously been found in fermented fish sauce (*21*).

Enantiomeric Distributions of the 2-(Methylthio)alkanes in Cempedak

2-(Methylthio)butane and 2-(methylthio)pentane are chiral compounds with one stereogenic center each and therefore exist as pairs of enantiomers. As enantiomers may fundamentally differ in their odor properties, we assessed the enantiomeric distribution of both compounds in cempedak and evaluated odor qualities and odor thresholds of the individual isomers.

Analytical enantiomer separation was achieved by heart-cut GC-GC-MS using a chiral cyclodextrin phase in the second dimension. The elution order was determined by analysis of enantiopure samples of (*R*)-2-(methylthio)butane and (*R*)-2-(methylthio)pentane, which were obtained from the corresponding enantiopure (*S*)-alcohols using the above mentioned tosylation/substitution approach (Figure 3).
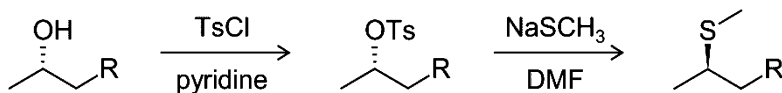
Figure 3. Synthetic Route to Enantiopure (R)-2-(Methylthio)butane (R = CH₃)
and (R)-2-(Methylthio)pentane (R = CH₂CH₃).

Results (Table 2) showed that all four compounds exhibited virtually the same sulfury, cempedak-like odor quality, but slightly differed in their odor threshold values. In 2-(methylthio)butane as well as in 2-(methylthio)pentane the less odor-active (*S*)-isomer predominated with 67% and 59%, respectively.

Table 2. (Methylthio)butane and 2-(Methylthio)pentane Enantiomers: Chromatographic/Sensory Properties and Distribution in Cempedak Fruits

Compound	RI[a]	Odor[b]	OTV[c] (ng/L)	Enantiomeric Ratio[d]
(*R*)-2-(methylthio)butane	718	sulfury, cempedak	1	33%
(*S*)-2-(methylthio)butane	725	sulfury, cempedak	2	67%
(*R*)-2-(methylthio)pentane	802	sulfury, cempedak	2	41%
(*S*)-2-(methylthio)pentane	804	sulfury, cempedak	5	59%

[a] Retention index on the chiral, 2,3-dimethyl-6-*tert*-butyldimethylsilyl-β-cyclodextrin-based BGB-176 column used for enantio-GC analysis. [b] Odor quality as perceived at the sniffing port during GC-O. [c] Odor threshold value in air. [d] Enantiomeric ratio determined in the cempedak fruit arils.

Conclusions

In summary, the results detailed above suggest that 2-(methylthio)butane and 2-(methylthio)pentane play a major role for the characteristic aroma of cempedak fruit and particularly account for the aroma difference to jackfruit. Nevertheless, further studies are needed to confirm this assumption. These will have to include exact quantitation of 2-(methylthio)butane, 2-(methylthio)pentane, and other potent odor-active compounds in cempedak fruit and jackfruit by application of stable isotope dilution assays, aroma reconstitution experiments, and omission tests.

References

1. Swords, G.; Bobbio, P. A.; Hunter, G. L. K. A research note: Volatile constituents of jack fruit (*Artocarpus heterophyllus*). *J. Food Sci.* **1978**, *43*, 639–640.
2. Rasmussen, P. Identification of Volatile Components of Jackfruit by Gas Chromatography/Mass Spectrometry with Two Different Columns. *Anal. Chem.* **1983**, *55*, 1331–1335.
3. Wong, K. C.; Lim, C. L.; Wong, L. L. Volatile flavour constituents of Chempedak (*Artocarpus polyphema* Pers.) fruit and jackfruit (*Artocarpus heterophyllus* Lam.) from Malaysia. *Flavour Fragrance J.* **1992**, *7*, 307–311.

4. Selvaraj, Y.; Shivashankara, K. S.; Roy, T. K. Characterization of aroma components of jackfruit (*Artocarpus heterophyllus* Lam.). *Indian Perfum.* **2002**, *46*, 335–339.

5. Maia, J. G. S.; Andrade, E. H. A.; Zoghbi, M. G. B. Aroma volatiles from two fruit varieties of jackfruit (*Artocarpus heterophyllus* Lam.). *Food Chem.* **2004**, *85*, 195–197.

6. Ong, B. T.; Nazimah, S. A. H.; Osman, A.; Quek, S. Y.; Voon, Y. Y.; Mat Hashim, D.; Chew, P. M.; Kong, Y. W. Chemical and flavour changes in jackfruit (*Artocarpus heterophyllus* Lam.) cultivar J3 during ripening. *Postharvest Biol. Technol.* **2006**, *40*, 279–286.

7. Ong, B. T; Nazimah, S. A. H.; Mirhosseini, H.; Osman, A.; Mat Hashim, D.; Rusul, G. Analysis of volatile compounds in five jackfruit (*Artocarpus heterophyllus* L.) cultivars using solid-phase microextraction (SPME) and gas chromatography-time-of-flight mass spectrometry (GC-TOFMS). *J. Food Compos. Anal.* **2008**, *21*, 416–422.

8. Peng, S.; Lin, L.; Ouyang, L.; Zhu, B.; Yuan, Y.; Jing, W.; Li, J. Comparative analysis of volatile compounds between jackfruit (*Artocarpus heterophyllus* L.) peel and its pulp. *Adv. Mater. Res. (Durnten-Zurich, Switz.)* **2013**, *781−784*, 1413–1418.

9. Schieberle, P.; Grosch, W. Evaluation of the flavour of wheat and rye bread crusts by aroma extract dilution analysis. *Z. Lebensm.-Unters. Forsch.* **1987**, *185*, 111−113.

10. Gomes Fraga, S. R. Investigação dos voláteis e precursores de voláteis glicosilados da Jaca (*Artocarpus heterophyllus* Lam.) e do Muruci (*Byrsonima crassifolia* Lam. Rich). Ph.D. Thesis, Universidade Federal do Rio de Janeiro, Brazil, 2005.

11. Wijaya, C. H.; Ngakan, T. A.; Utama, I.; Suryani, E.; Apriyantono, A. Exploration of an exotic tropical fruit flavour – optimisation of cempedak (*Artocarpus integer* (Thunb.) Merr.) flavour extraction. In *Flavour Science. Recent Developments*; Taylor, A. J., Mottram, D. S., Eds.; Royal Society of Chemistry: Cambridge, U.K., 1996; pp 86−89.

12. Buttara, M.; Intarapichet, K.-O.; Cadwallader, K. R. Characterization of potent odorants in Thai chempedak fruit (*Artocarpus integer* Merr.), an exotic fruit of Southeast Asia. *Food Res. Int.* **2014**, *66*, 388–395.

13. Buttery, R. G.; Ling, L. C.; Juliano, B. O.; Turnbaugh, J. G. Cooked Rice Aroma and 2-Acetyl-1-pyrroline. *J. Agric. Food Chem.* **1983**, *31*, 823–826.

14. Polster, J.; Schieberle, P. Structure−Odor Correlations in Homologous Series of Alkanethiols and Attempts to Predict Odor Thresholds by 3D-QSAR Studies. *J. Agric. Food Chem.* **2015**, *63*, 1419–1432.

15. Engel, W.; Bahr, W.; Schieberle, P. Solvent assisted flavour evaporation − a new and versatile technique for the careful and direct isolation of aroma compounds from complex food matrices. *Eur. Food Res. Technol.* **1999**, *209*, 237–241.

16. Steinhaus, M. Characterization of the Major Odor-Active Compounds in the Leaves of the Curry Tree *Bergera koenigii* L. by Aroma Extract Dilution Analysis. *J. Agric. Food Chem.* **2015**, *63*, 4060–4067.

17. Ullrich, F.; Grosch, W. Identification of the most intense volatile flavor compounds formed during autoxidation of linoleic acid. *Z. Lebensm.-Unters. Forsch.* **1987**, *184*, 277–282.

18. Teranishi, R.; Buttery, R. G.; Guadagni, D. G. Odor quality and chemical structure in fruit and vegetable flavors. *Ann. N.Y. Acad. Sci.* **1974**, *237*, 209–216.

19. U.S. Department of Commerce. *Mass Spectral Library NIST11*; National Institute of Standards and Technology: Gaithersburg, MD.

20. Takeoka, G. R. Volatile constituents of asafoetida. In *Aroma Active Compounds in Foods. Chemistry and Sensory Properties*; Takeoka, G. R., Güntert, M., Engel, K.-H., Eds.; ACS Symposium Series 794; American Chemical Society: Washington, DC, 2001; pp 33−44.

21. McIver, R. C.; Brooks, R. I.; Reineccius, G. A. Flavor of Fermented Fish Sauce. *J. Agric. Food Chem.* **1982**, *30*, 1017–1020.

Chapter 10

Influence of Structural Modification and Chirality on the Odor Potency and Odor Quality of Thiols

Sebastian Schoenauer, Johannes Polster, and Peter Schieberle*

Lehrstuhl für Lebensmittelchemie, Technische Universitaet Muenchen, Lise-Meitner-Straße 34, D-85354 Freising, Germany
***E-mail: Peter.Schieberle@lrz.tum.de.**

Due to their extremely low odor thresholds, thiols often show a major impact on the overall aroma of foods, even if present in trace amounts. However, odor qualities as well as odor thresholds of thiols are often influenced by carbon chain length and chirality. In order to get a deeper insight into structure-odor correlations, different series of chiral mercapto-containing key aroma compounds and their homologues were synthesized, such as 3-mercaptoalkyl acetates and 3-mercaptoalkan-1-ols. Enantiomers were separated and their odor qualities and odor thresholds were determined. Absolute configurations were elucidated using a chiral derivatizing agent and ^{1}H NMR anisotropy methods.

Introduction

In spite of their low concentrations in many foods, volatile thiols often rank among the key aroma compounds, due to their extremely low thresholds. So far, more than 100 different odor-active thiols have been identified in foods. These include a variety of low molecular weight alkanethiols and various alkenethiols. In addition, polyfunctional thiols, like mercaptoalkanones, mercaptoalkanols, and mercaptoalkylesters were also found in foods. In total, seven 3-mercaptoalkan-1-ols and 3-mercaptoalkyl acetates, respectively, could be identified in exotic fruits, wines, beers, hops, and other foods, and among them 3-mercaptohexan-1-ol and 3-mercaptohexyl acetate seem to be the most important compounds (*1–18*). The information is listed in Table 1.

Table 1. Occurrence of 3-Mercaptoalkan-1-ols and 3-Mercaptoalkyl Acetates in Foods (1st Report)

compound	food
3-mercaptobutan-1-ol	wine (*1*), hops (*2*), beer (*2*), durian (*3*),
3-mercaptobutyl acetate	coffee (*4*), hops (*2*), beer (*5*)
3-mercaptopentan-1-ol	wine (*1*), hops (*6*)
3-mercaptohexan-1-ol	passion fruit (*7*), wine (*8*), grapefruit (*9*), beer (*10*), pink guava (*11*), hops (*12*), peanut (*13*), coffee (*14*)
3-mercaptohexyl acetate	passion fruit (*7*), beer (*12*), hops (*2*), musk strawberry (*15*), gulupa (*16*), curuba (*17*), lulo (*18*)
3-mercaptoheptan-1-ol	wine (*1*)
3-mercaptooctyl acetate	hops (*2*)

Very few studies have been done on structure-odor relationships of thiols. For example, Meilgaard showed that tertiary thiols exhibit lower odor thresholds than primary and secondary analogues (*19*). Later it was observed that a replacement of a hydroxyl group by a thiol group led to a change to unpleasant odor qualities and that the odor activity of alkane-1-thiols decreased with increasing chain length (*20, 21*). Finally, Polster and Schieberle synthesized and investigated 11 homologous series of sulfur-containing compounds and showed that the odor thresholds are influenced by steric effects. In particular, a minimum in thresholds was observed for thiols with five to seven carbon atoms, while a longer chain length led to an exponential increase of the thresholds in all homologous series, as exemplarily shown in Figure 1 for alkane-1-thiols (*22*).
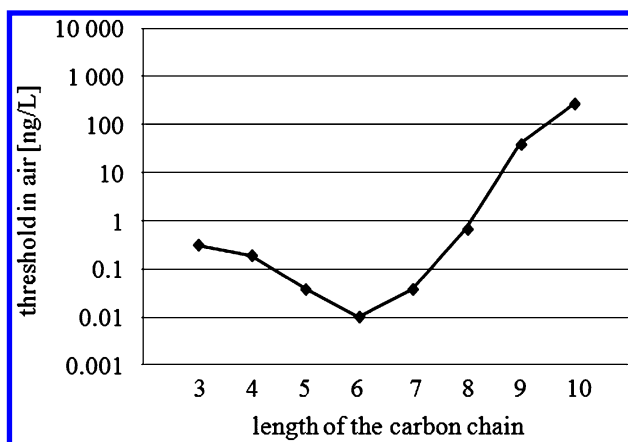
Figure 1. Thresholds of the homologous series of alkane-1-thiols. Adapted with permission from ref. (22). Copyright 2015 Polster and Schieberle.

To get a deeper insight into structure/odor relationships among thiols, homologous series of enantiopure 3-mercaptoalkan-1-ols and 3-mercaptoalkyl acetates were synthesized, the absolute configurations were assigned and odor qualities and thresholds were determined.

Material and Methods

Syntheses

3-Mercaptoalkan-1-ols

Step 1: Piperidine (40 mg; 0.5 mmol) and the respective alk-2-enal (20 mmol) were placed in a round-bottomed flask and thioacetic acid (2.28 g; 30 mmol) was added at 0 °C. The mixture was stirred for 24 h at room temperature and then diluted with diethyl ether (80 mL). The solution was washed twice with hydrochloric acid (2 N; 25 mL) and aqueous saturated sodium hydrogen carbonate solution (30 mL). After drying over sodium sulfate, the solvent was removed under reduced pressure.

Step 2: The thioacetate (15 mmol) was dissolved in diethyl ether (20 mL) and the solution was added dropwise to a solution of lithium aluminium hydride (1.14 g; 30 mmol) in dried diethyl ether (20 mL) at 0 °C. After stirring for 2 h at room temperature, diethyl ether (50 mL) and saturated ammonium chloride solution (20 mL) were carefully added at 0 °C. Then hydrochloric acid (2 N; 50 mL) was added dropwise and the organic layer was separated. The aqueous phase was washed twice with diethyl ether (100 mL) and the combined organic layers were washed with saturated sodium hydrogen carbonate solution (50 mL), dried over sodium sulfate and filtered. Solvent was removed under reduced pressure and the analyte was purified by means of column chromatography on silica gel with pentane/diethyl ether (90:10; by volume) as the eluent.

3-Mercaptoalkyl Acetates

Syntheses of 3-mercaptoalkyl acetates were performed as decribed above for the 3-mercaptoalkan-1-ols. In addition, a third synthesis step was performed after steps 1 and 2.

Step 3: Acetyl chloride (1.47 g; 18.75 mmol) in dichloromethane (10 mL) was added to a solution of the 3-mercaptoalkan-1-ols (7.5 mmol) in dichloromethane (10 mL) at 0 °C. After stirring for 2 h at room temperature, the solvent and the remaining acetyl chloride were removed under reduced pressure. The product was purified by means of column chromatography on silica gel with pentane/diethyl ether (95:5; by volume) as the eluent.

Conversion to the Diastereomeric Thioesters

4-(Dimethylamino)pyridine (1.83 g; 15 mmol) and the respective thiol (5 mmol) were dissolved in dichloromethane (30 mL). (*S*)-3,3,3-Trifluoro-2-methoxy-2-phenylpropanoyl chloride ("Mosher's acid chloride") (2.53 g; 10 mmol) was added to the mixture and it was stirred for 2 d at room temperature and then refluxed for 3 h. After diluting with diethyl ether (70 mL), the solution was washed with water (50 mL), aqueous sodium hydroxide solution (0.5 N; 50 mL) and finally with water (50 mL). The organic layer was dried over anhydrous sodium sulfate, the solvent was removed by rotary evaporation and the diastereomers were separated by means of column chromatography on silica gel using pentane/diethyl ether (98:2; by volume) as the eluent.

Enantiopure 3-Mercaptoalkan-1-ols and 3-Mercaptoalkyl Acetates

To obtain the single enantiomers of 3-mercaptoalkan-1-ols, the thioesters were reduced by means of the method described above in step 2 and syntheses of enantiopure 3-mercaptoalkyl acetates were performed by acetylation as described above in step 3.

Determination of Odor Qualities and Odor Thresholds in Air

Thresholds were determined by aroma extract dilution analysis of a mixture containing known amounts of the target odorant and (*E*)-2-decenal as the internal standard. Thresholds were calculated from the flavor dilution (FD) factors determined by using the method previously described (*23*) and a threshold of 2.7 ng/L for (*E*)-2-decenal (*24*). Odor qualities were assigned during GC-olfactometry at threshold level.

Results and Discussion

Odor Qualities and Odor Thresholds of the Racemic Thiols

In total, seven 3-mercaptoalkyl acetates and seven 3-mercaptoalkan-1-ols were synthesized. Whereas most of the 3-mercaptoalkyl acetates showed black currant-like scents, 3-mercaptoalkan-1-ols were mostly described as grapefruit-like; shorter-chain compounds like 3-mercaptobutyl acetate and 3-mercaptobutan-1-ol exhibited rather unpleasant odor qualities like burned and onion-like, respectively. However, compounds with nine or ten carbon atoms in the alkyl chain showed fatty, soapy, and mushroom-like odors (Table 2 and 3).

The lowest thresholds (0.053 and 0.058 ng/L in air) could be found for 3-mercaptoalkan-1-ols with six and seven carbon atoms. Table 3 shows that this tendency was also true for the 3-mercaptoalkyl acetates, in spite of the additional acetate group. While 3-mercaptohexyl acetate showed an odor threshold of 0.039 ng/L in air, the longest-chain compound 3-mercaptodecyl acetate exhibited a value which was higher by four powers of ten (260 ng/L).

Table 2. Odor Qualities and Thresholds of Racemic 3-Mercaptoalkan-1-ols

compound (racemate)	odor quality	odor threshold in air [ng/L]
3-mercaptobutan-1-ol	onion-like, leek-like	1.8
3-mercaptopentan-1-ol	grapefruit-like	0.23
3-mercaptohexan-1-ol	grapefruit-like	0.053
3-mercaptoheptan-1-ol	grapefruit-like	0.058
3-mercaptooctan-1-ol	grapefruit-like, burned	0.26
3-mercaptononan-1-ol	fatty, soapy	13
3-mercaptodecan-1-ol	fatty, soapy	140

Table 3. Odor Qualities and Thresholds of Racemic 3-Mercaptoalkyl Acetates

compound (racemate)	odor quality	odor threshold in air [ng/L]
3-mercaptobutyl acetate	roasty, burned	0.29
3-mercaptopentyl acetate	black currant-like	0.36
3-mercaptohexyl acetate	black currant-like	0.039
3-mercaptoheptyl acetate	black currant-like	0.56
3-mercaptooctyl acetate	black currant-like	2.1
3-mercaptononyl acetate	mushroom-like	4.8
3-mercaptodecyl acetate	fatty	260

Determination of the Absolute Configurations

To determine the odor qualities and thresholds of the enantiomers, those had to be isolated. For the separation and the determination of the absolute configurations a chiral derivatizing agent was used: (*S*)-3,3,3-trifluoro-2-methoxy-2-phenylpropanoyl chloride, the so-called "Mosher's acid chloride". By conversion of the enantiomeric mixture of 3-mercaptoalkyl acetates into a mixture of diastereomers it was possible to separate them by means of column chromatography. In the following, the procedure is shown using 3-mercaptohexyl acetate as example (Figure 2). A similar method was used by Heusinger and Mosandl (*25*) for the determination of the stereochemistry of related mercapto-containing compounds identified in yellow passion fruit.
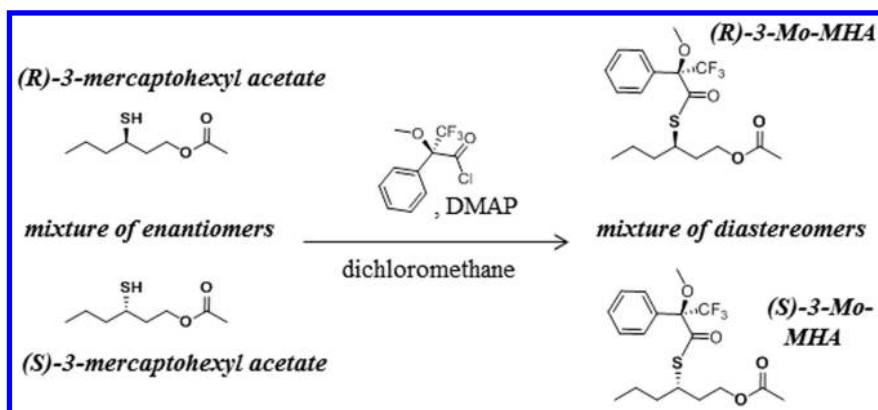
Figure 2. Synthetic route to the 3-(((S)-3,3,3-trifluoro-2-methoxy-2-phenylpropanoyl)thio)alkyl acetate diastereomers ((R)- and (S)-Mo-MHA).

After purification the two diastereomers (*R*)- and (*S*)-3-(((*S*)-3,3,3-trifluoro-2-methoxy-2-phenylpropanoyl)thio)hexyl acetate ((*R*)- and (*S*)-Mo-MHA) were available in purities higher than 95 % and, thus, suitable for NMR experiments and determination of the absolute configuration.

In contrast to enantiomers, diastereomers are usually distinguishable by NMR experiments. When comparing the two ^{1}H NMR spectra of (*R*)- and (*S*)-Mo-MHA, quite strong differences in the δ-values could be observed. In particular, the phenyl group of the chiral derivatizing agent caused a shielding and hence a shift to higher field of signals for protons loctated near the aromatic system. As shown in Figure 3, for (*S*)-Mo-MHA a propyl group is closer to the phenyl group (Ph), whereas for (*R*)-Mo-MHA an ethyl acetate group is nearer to the aromatic system. Because of the shielding the three signals for the propyl group of (*S*)-Mo-MHA (δ 0.71 ppm, 1.13 ppm, 1.26 ppm) showed lower values than those of (*R*)-Mo-MHA (δ 0.74 ppm, 1.21 ppm, 1.29 ppm). For the ethyl acetate a similar trend was observed. The signal of the acetate protons was shifted from δ 1.71 ppm for (*S*)-Mo-MHA to δ 1.67 ppm for (*R*)-Mo-MHA and the signals of the ethyl protons showed the same tendency. The (*R,S*)-diastereomer exhibited signals at δ 1.39 ppm, 1.66 ppm, 3.82 ppm and 3.95 ppm, whereas signals at δ 1.52 ppm, 1.71 ppm, 3.98 ppm and 4.13 ppm were observed for the (*S,S*)-diastereomer. So, a clear trend was noticed for the 3-mercaptohexyl acetate derivatives, which was also shown for the other 3-mercaptoalkyl acetates. Consequently, the absolute configurations of all compounds could be determined.
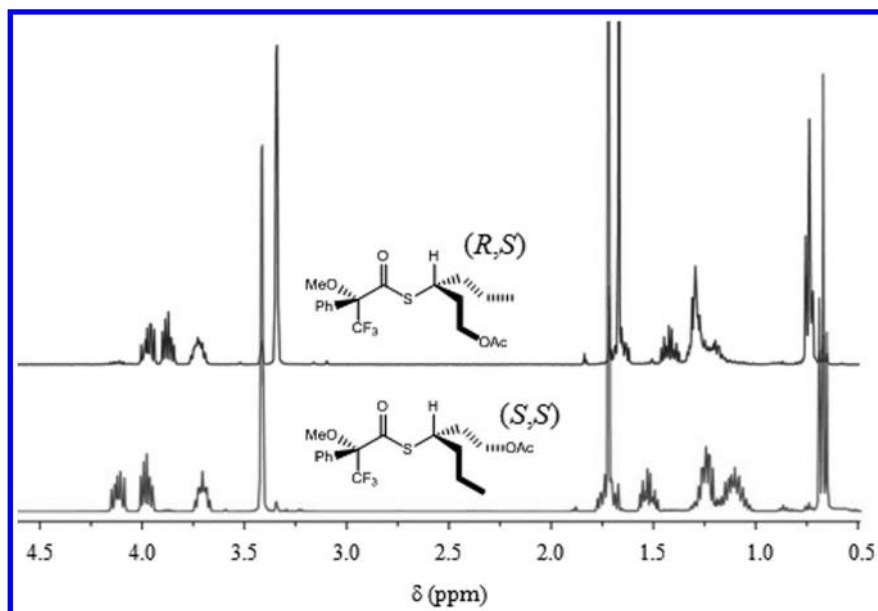
Figure 3. ¹H NMR spectra of (R)- and (S)-Mo-MHA.

After the assignment of the diastereomers, the compounds were reduced to the enantiopure 3-mercaptoalkan-1-ols and also acetylated to the 3-mercaptoalkyl acetates. Thus, the absolute configurations of the 3-mercaptoalkan-1-ols and the respective acetates could be determined.

Separation of the Enantiomers

The enantiomers of 3-mercaptoalkan-1-ols and 3-mercaptoalkyl acetates were separated by means of chiral stationary phases. For the separation of the 3-mercaptoalkan-1-ols a so-called BGB-174 (50 % 2,3-diacetyl-6-*tert*-butyldi-methylsilyl-*β*-cyclodextrin dissolved in 14 % cyanopropylphenyl- and 86 % methylpolysiloxane) (BGB Analytik Vertrieb, Anwil, Switzerland) was used and a heating rate of 1 °C/min up to 220 °C was applied. The chromatogram for the homologous series from 3-mercaptopentan-1-ol to 3-mercaptodean-1-ol is shown in Figure 4. For all compounds a baseline separation was achieved.

The 3-mercaptoalkyl acetates also could also be separated by using a chiral column; only for 3-mercaptononyl and 3-mercaptodecyl acetate a sufficient baseline separation could not be achieved. A so-called BGB-175 (50 % 2,3-diacetyl-6-*tert*-butyldimethylsilyl-*γ*-cyclodextrin dissolved in 14 % cyanopropylphenyl- and 86 % methylpolysiloxane) (BGB Analytik Vertrieb, Anwil, Switzerland) was used as column, and again the heating rate of the temperature program was 1 °C/min.
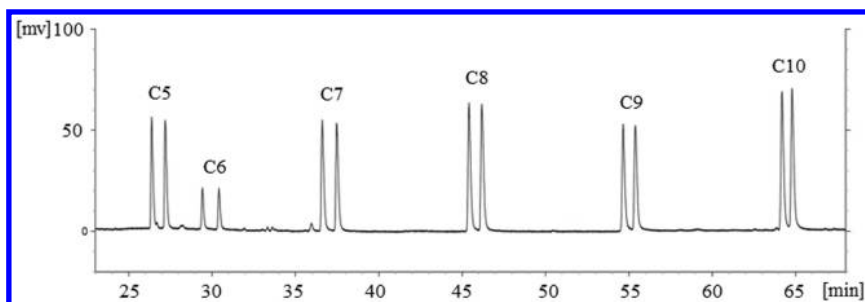
*Figure 4. Separation of (S)- and (R)-3-mercaptoalkan-1-ols using a
β-cyclodextrin phase (BGB-174).*

Odor Qualities and Odor Thresholds of the Enantiomers

Due to the fact that the enantiomers could be separated, their odor qualities and odor thresholds in air could be determined by GC-O. First of all, no differences in odor qualities were noticed for the enantiomers in comparison to the racemic mixtures; most of (*S*)- and (*R*)-3-mercaptoalkan-1-ols were described as grapefruit-like and (*S*)- and (*R*)-3-mercaptopentyl up to 3-mercaptooctyl acetate again showed black currant-like scents. The shorter- and longer-chain compounds once more exhibited rather unpleasant onion-like, burned, and fatty odors, respectively. Thus, chirality had no influence on the odor qualities of 3-mercaptoalkan-1-ols and 3-mercaptoalkyl acetates.

As shown in Figure 5, there was also nearly no influence on the odor thresholds of the 3-mercaptoalkan-1-ol enantiomers. No threshold value differed more than by the factor 5 from the odor threshold of its respective enantiomer. Taking into account the precision of the determination of thresholds in air, there are no differences in thresholds for (*S*)- and (*R*)-3-mercaptoalkan-1-ols.
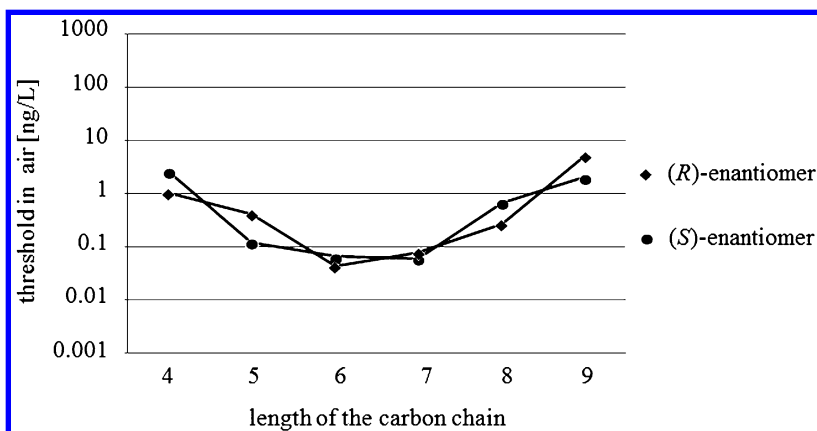
Figure 5. Thresholds of (S)- and (R)-3-mercaptoalkan-1-ols.

However, looking at the tendency of thresholds of 3-mercaptoalkyl acetates, the situation is different. While the thresholds of the (*R*)-enantiomers slightly increased from 0.28 to 5.0 ng/L, the (*S*)-enantiomers showed a significant minimum of thresholds for 3-mercaptohexyl acetate. While the shorter-chain (*S*)-enantiomers showed thresholds of 1.1 and 0.41 ng/L, 3-mercaptohexyl acetate exhibited a very low threshold value of 0.0063 ng/L in air. For the longer-chain thiols the thresholds increased quite strongly up to 9.7 and 5.0 ng/L, respectively (Figure 6).
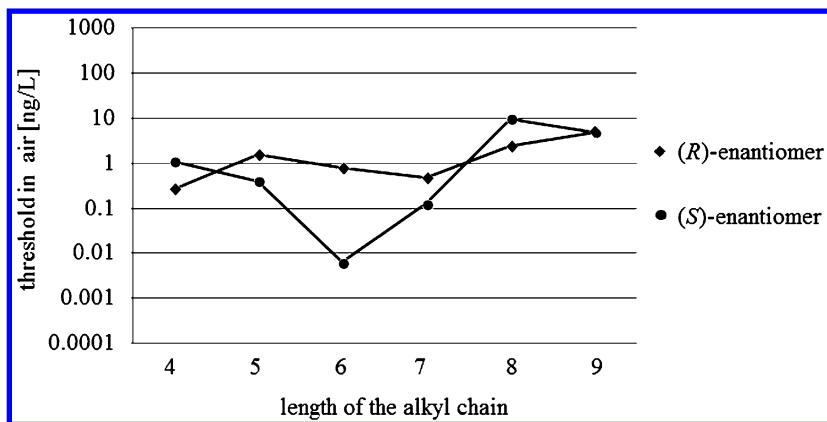
Figure 6. Thresholds of (S)- and (R)-3-mercaptoalkyl acetates.

Discussion

For the homologous series of 3-mercaptoalkan-1-ols a minimum of odor thresholds for compounds with five to seven carbon atoms was determined. This was also true for the respective acetates. Thus, the tendencies of thresholds in homologous series found recently by Polster and Schieberle (*22*) could again be observed for 3-mercaptoalkan-1-ols and 3-mercaptoalkyl acetates, which are representatives of polyfunctional thiols. Furthermore it is obvious that 3-mercaptohexan-1-ol and its respective acetate, which seem to be the most important compounds of the homologous series investigated (Table 1), showed the lowest threshold within the respective homologous series.

The results also showed that there was no influence of chirality on odor qualities and odor thresholds among the 3-mercaptoalkan-1-ols and 3-mercaptoalkyl acetates considered. Only (*S*)-3-mercaptohexyl acetate exhibited a considerably lower threshold than its enantiomer.

For the most part the odor qualities described in this work are in good agreement with those of Vermeulen et al. (*26*, *27*) who investigated odor qualities of racemic 3-mercaptoalkan-1-ols and 3-mercaptoalkyl acetates. The shorter-chain compounds were also described as onion-like and roasty, respectively. While most of the compounds showed grapefruit-like and black currant-like scents, respectively, Vermeulen et al. (*26*, *27*) used different descriptors, but all in all also fruity odor qualities were determined.

To verify that receptors have developed in close correlation to naturally occurring compounds, it would be interesting to investigate whether (*S*)-3-mercaptohexyl acetate is the generally dominating enantiomer in foods. Steinhaus et al. (*11*), for example, quantified both enantiomers in pink guavas and did not find a dominating enatiomer. They determined a ratio of 58/42 (*S*/*R*).

Conclusions

The results showed once again that volatile compounds bearing a mercapto group do not consequently show low odor thresholds or strong sulfury odors. These attributes clearly depended on the length of the carbon chain, and of course the presence of a second structural function. Together with previous results, these data support the assumption that human odorant receptors were tailor-made to detect aroma volatiles present in nature.

References

1. Sarrazin, E.; Shinkaruk, S.; Tominaga, T.; Bennetau, B.; Frérot, E.; Dubourdieu, D. Odorous Impact of Volatile Thiols on the Aroma of Young Botrytized Sweet Wines: Identification and Quantification of New Sulfanyl Alcohols. *J. Agric. Food Chem.* **2007**, *55*, 1437–1444.
2. Gros, J.; Nizet, S.; Collin, S. Occurrence of Odorant Polyfunctional Thiols in the Super Alpha Tomahawk Hop Cultivar. Comparison with the Thiol-Rich Nelson Sauvin Bitter Variety. *J. Agric. Food Chem.* **2011**, *59*, 8853–8865.
3. Li, J.-X.; Schieberle, P.; Steinhaus, M. Characterization of the Major Odor-Acitve Compounds in Thai Durian (*Durio zibethinus L. 'Monthong'*) by Aroma Extract Dilution Analysis and Headspace Gas Chromatography-Olfactometry. *J. Agric. Food. Chem.* **2012**, *60*, 11253–11262.
4. Kumazawa, K.; Masuda, H. Identification of Odor-Active 3-Mercapto-3-methylbutyl Acetate in Volatile Fraction of Roasted Coffee Brew Isolated by Steam Distillation under Reduced Pressure. *J. Agric. Food Chem.* **2003**, *51*, 3079–3082.
5. Gros, J.; Peeters, F.; Collin, S. Occurrence of odorant polyfunctional thiols in beers hopped with different cultivars. First evidence of an *S*-cysteine conjugate in hop (*Humulus lupulus L.*). *J. Agric. Food Chem.* **2012**, *60*, 7805–7816.

6. Takoi, K.; Degueil, M.; Shinkaruk, S.; Thibon, C.; Maeda, K.; Bennetau, B.; Dubourdieu, D.; Tominaga, T. Identification and Characteristics of New Volatile Thiols Derived from the Hop (*Humulus lupulus L.*) Cultivar Nelson Sauvin. *J. Agric. Food Chem.* **2009**, *57*, 2493–2502.

7. Engel, K. H.; Tressl, R. Identification of New Sulfur-Containing Volatiles in Yellow Passion Fruit (*Passiflora edulis f. flavicarpa*). *J. Agric. Food Chem.* **1991**, *39*, 2249–2252.

8. Tominaga, T.; Furrer, A.; Henry, R.; Dubourdieu, D. Identification of new volatile thiols in the aroma of *Vitis vinifera* L. var. Sauvignon blanc wines. *Flavour Fragrance J.* **1998**, *13*, 159–162.

9. Lin, J.; Rouseff, R.; Barros, S.; Naim, M. Aroma Composition Changes in Early Season Grapefruit Juice Produced from Thermal Concentration. *J. Agric. Food Chem.* **2002**, *50*, 813–819.

10. Vermeulen, C.; Lejeune, I.; Tran, T. T. H.; Collin, S. Occurrence of Polyfunctional Thiols in Fresh Lager Beers. *J. Agric. Food Chem.* **2006**, *54*, 5061–5068.

11. Steinhaus, M.; Sinuco, D.; Polster, J.; Osorio, C.; Schieberle, P. Characterization of the Aroma-Active Compounds in Pink Guava (*Psidium guajava L.*) by Application of the Aroma Extract Dilution Analysis. *J. Agric. Food Chem.* **2008**, *56*, 4120–4127.

12. Kishimoto, T.; Kobayashi, M.; Yako, N.; Iida, A.; Wanikawa, A. Comparison of 4-Mercapto-4-methylpentan-2-one Contents in Hop Cultivars from Different Growing Regions. *J. Agric. Food Chem.* **2008**, *56*, 1051–1057.

13. Kaneko, S.; Sakai, R.; Kumazawa, K.; Usuki, M.; Nishimura, O. Key aroma compounds in roasted in-shell peanuts. *Biosci., Biotechnol., Biochem.* **2013**, *77*, 1467–1473.

14. Vichi, S.; Jeri, Y.; Cortes-Francisco, N.; Palacios, O.; Caixach, J. Determination of volatile thiols in roasted coffee by derivatization and liquid chromatography-high resolution mass spectrometric analysis. *Food Res. Int.* **2014**, *64*, 610–617.

15. Pet'ka, J.; Leitner, E.; Parameswaran, B. Musk strawberries: The flavour of a formerly famous fruit reassessed. *Flavour Fragrance J.* **2012**, *27*, 273–279.

16. Conde-Martínez, N.; Jimenez, A.; Steinhaus, M.; Schieberle, P.; Sinuco, D.; Osorio, C. Key aroma volatile compounds of gulupa (*Passiflora edulis Sims fo edulis*) fruit. *Eur. Food Res. Technol.* **2013**, *236*, 1085–1091.

17. Conde-Martínez, N.; Sinuco, D.; Osorio, C. Chemical studies on curuba (*Passiflora mollissima (Kunth) L. H. Bailey*) fruit flavor. *Food Chem.* **2014**, *157*, 356–363.

18. Forero, D.; Orrego, C.; Peterson, D.; Osorio, C. Chemical and sensory comparison of fresh and dried lulo (*Solanum quitoense Lam.*) fruit aroma. *Food Chem.* **2015**, *169*, 85–91.

19. Meilgaard, M. C. Flavor chemistry of beer. II. Flavor and threshold of 239 aroma volatiles. *Tech. Q. – Master Brew. Assoc. Am.* **1975**, *12*, 151–168.

20. Wannagat, U.; Damrath, V.; Schliephake, A.; Harder, U. Sila-substituted perfumes and isosteric compounds of perfumes. XI. Comparison of carbinols and silanols with thiocarbinols and silanethiols. *Monatsh. Chem.* **1987**, *118*, 779–788.

21. Node, M.; Kumar, K.; Nishide, K.; Ohsugi, S.-i.; Miyamoto, T. Odorless substitutes for foul-smelling thiols: syntheses and applications. *Tetrahedron Lett.* **2001**, *42*, 9207–9210.
22. Polster, J.; Schieberle, P. Structure-Odor Correlations in Homologous Series of Alkanethiols and Attempts to Predict Odor Thresholds by 3D-QSAR Studies. *J. Agric. Food Chem.* **2015**, *63*, 1419–1432.
23. Ullrich, F.; Grosch, W. Identification of the most intense volatile flavour compounds formed during autoxidation of linoleic acid. *Z. Lebensm. Unters. Forsch.* **1987**, *184*, 277–282.
24. Teranishi, R.; Buttery, R. G.; Guadagni, D. G. Odor quality and chemical structure in fruit and vegetable flavors. *Ann. NY Acad. Sci.* **1974**, *237*, 209–216.
25. Heusinger, G.; Mosandl, A. Chiral, sulfur-containing aroma substances of the yellow passion fruit (*Passiflora edulis f. flavicarpa*). Preparation of enantiomers and absolute configuration. *Tetrahedron Lett.* **1984**, *25*, 507–510.
26. Vermeulen, C.; Collin, S. Combinatorial Synthesis and Sensorial Properties of 21 Mercapto Esters. *J. Agric. Food Chem.* **2003**, *51*, 3618–3622.
27. Vermeulen, C.; Guyot-Declerck, C.; Collin, S. Combinatorial Synthesis and Sensorial Properties of Mercapto Primary Alcohols and Analogues. *J. Agric. Food Chem.* **2003**, *51*, 3623–3628.

Structure Elucidation of Novel Norcysteine-Containing Dipeptides from the Chinese Vegetable *Toona sinensis*

J.-X. Li,[2] K. Eidman,[3] X.-W. Gan,[4] O. P. Haefliger,[4] P. J. Carroll,[5] and J. Pika[*,1]

[1]Firmenich Inc., P.O. Box 5880, Princeton, New Jersey 08546, United States
[2]L'Oréal (China) R&D Center, 1028 Yun Qiao Road, Pudong New Area, Shanghai 201206 China
[3]Ungerer and Co., 4 Bridgewater Lane, Lincoln Park, New Jersey 07035
[4]Firmenich Aromatic (China) Co. Ltd, No. 3901 Jin Du Road, Xinzhuang Industry Park, Minhang, Shanghai, 201108, China
[5]Department of Chemistry, University of Pennsylvania, Philadelphia, Pennsylvania 19104, United States
[*]E-mail: jxp@firmenich.com.

A study of metabolites of the Chinese vegetable *Toona sinensis* resulted in the isolation and structure elucidation of three new sulfur-containing mono- and dipeptides including *cis-* and *trans-(S,S)*-γ-glutamyl-(*S*-1-propenyl)thioglycine, which contain the unusual amino acid norcysteine.

Introduction

As part of an on-going program to study the botanical diversity of mainland China, and in particular plants which have traditionally been used for food or medicine and might provide interesting seasonings and flavors, we investigated the popular Northern Chinese vegetable, *Toona sinensis* ((A. Juss.) Roem, synonym *Cedrela sinensis*). *T. sinensis*, also known as Chinese mahogany or Xiang chun, is a rapidly growing deciduous tree belonging to the family Meliaceae (*1*). For a short period in the spring, the new growth of the tree can be harvested and is typically eaten as a vegetable. This much-loved flavor is unique but has some sulfur-like character, reminiscent of onion. In recent years *T. sinensis* sprouts have become available on the market year-long and these have a flavor which is very

similar to that of the tender shoots that appear on the trees in the spring. Few studies have addressed the sulfur-containing volatile and non-volatile metabolites of *Toona sinensis* (*2*).

Freshly chopped *T. sinensis* has a strong sulfur impact. Our investivation of many recipes for this vegetable led to the realization that most preparations involve a blanching step. Shoots or sprouts are typically blanched for a few minutes in boiling water and then cooled and finely chopped. The chopped *T. sinensis* is used to flavor egg, tofu, meat, fish and noodles with little or no further cooking. We reasoned that one purpose of blanching is to inactivate enzymes and thus to prevent the degradation of flavor precursors. A sample of blanched *T. sinensis* shoots was subjected to simultaneous distillation-extraction and the resulting extract was analyzed by GC-MS. The blanched shoots were found to contain a complex mixture of volatile sulfur-containing compounds including methyl, propyl and 1-propenyl sulfides, disulfides and trisulfides. Because of the importance of these types of molecules to the flavors of many, primarily savory foods, and because of their chemical instability, we were interested in understanding the sulfur-containing precursors of *T. sinensis*. We reasoned that the precursors were likely to be similar to those of *Allium cepa*, onions, however, *T. sinensis* did not appear to generate the lachrymatory factor, propanethiol S-oxide, upon disruption of the plant tissues (*3*).

Results and Discussion

In order to test our hypothesis that *Toona sinensis* contained nonvolatile sulfur-containing precursors, whole, fresh shoots were rapidly frozen using liquid nitrogen. The frozen shoots were ground and lyophilized to yield an odorless, dry powder. Upon addition of an aliquot of the powder (2 mg) to water (2 mL), a solution was generated that smelled fresh, green, chive, wild garlic, onion, leek and with slightly earthy forest notes. The solution was extracted using solid phase microextraction (SPME) with analysis by GC-MS. The major product in this extract was 1-propenethiol of undefined stereochemistry.

We developed extraction and analytical protocols using onions purchased in a Shanghai market. The whole onions were ground in 5% aqueous trifluoroacetic acid to denature all enzymes. After filtration, the crude extract was analyzed by LC-ion trap mass spectrometry in positive electrospray ionization mode. By screening mass spectrometric patterns for those that possessed ^{34}S-containing ions in positive ion mode, we were able to extract traces corresponding to the molecular ions of the known major non-volatile sulfur-containing metabolites, isoalliin (*trans-S*-1-propenyl-L-cysteine sulfoxide), propyl cysteine sulfoxide and methyl cysteine sulfoxide in addition to the analogous sulfides; *trans-S*-1-propenyl-L-cysteine sulfide, propyl cysteine sulfide and methyl cysteine sulfide.

The LC-MS method was applied to samples of *T. sinensis* shoots and sprouts prepared in the same manner as the onions (inactive enzyme sample) and to samples ground in water, centrifuged and filtered (active enzyme sample). By careful examination of the mass spectra of the inactive enzyme sample, we were

In Importance of Chirality to Flavor Compounds; Engel, et al.;
ACS Symposium Series; American Chemical Society: Washington, DC, 2015.

able to identify the sulfur-containing metabolites from characteristic molecular ions and their isotope clusters, which indicated that each molecule contained a single sulfur atom. Major sulfur-containing metabolites of molecular weight 161 g/mol (*m/z 162*, 100% relative abundance, *m/z 164*, 4.9% relative abundance), 276 g/mol (*m/z 277*, 100% relative abundance, *m/z 279*, 6.5% relative abundance) and 290 g/mol (*m/z 291*, 100% relative abundance, *m/z 293*, 5.6% relative abundance) were observed. In each instance the HPLC peak was broadened or split, suggesting related pairs of isomers. By comparison, the active enzyme sample contained major sulfur-containing metabolites of molecular weight 161 g/mol and 290 g/mol, which eluted at the same retention times as the inactive enzyme sample. The pair of HPLC peaks of molecular weight 276 g/mol were no longer observed in the active enzyme sample, indicating that these metabolites were likely to be most important for the strong sulfur character of chopped, raw *T. sinensis* shoots and sprouts. An aliquot of the crude *T. sinensis* deactivated enzyme sample (1.4 mL) was mixed at room temperature with hydrogen peroxide (0.1 mL of a 30% aqueous solution) for 1.5 h, conditions which have been shown to result in oxidation of sulfides but not sulfoxides (*4*). By LC-MS, all of the major sulfur-containing metabolites observed in the crude *T. sinensis* deactivated enzyme sample were oxidized by the hydrogen peroxide solution, indicating that the metabolites were sulfides.
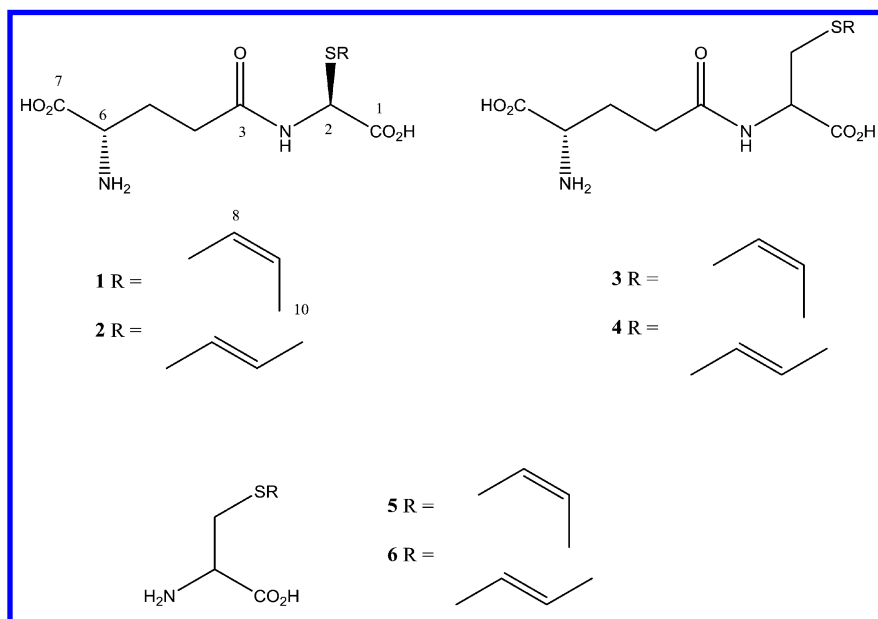
Figure 1. Structures of Major Sulfur-Containing Metabolites of Toona sinensis.

We focused our effort on elucidation of the structures of sulfur-containing metabolites **1** and **2**, which were degraded by the enzymes in *T. sinensis* (Figure 1). The mass spectra of metabolites **1** and **2** both displayed mass spectra with *m/z* 277 in positive electrospray ionization mode and *m/z* 275 in negative electrospray

ionization mode, consistent with a molecular weight of 276 g/mol. In positive ionization MS/MS mode, the *m/z* 277 molecular ion fragmented to produce an ion at *m/z* 130, consistent with the presence, in **1**, of a glutamate moiety (*5*).

A sample of *T. sinensis* shoots (300 g) was extracted by grinding in an aqueous 5% trifluoroacetic acid solution. The resulting crude extract was purified by ion exchange chromatography (Dowex 50 WX8, H⁺) eluted with an aqueous ammonium hydroxide gradient of increasing concentration. Eight fractions were collected and concentrated by lyophilization. The fractions were desalted by reverse phase (C_{18}) solid phase extraction and further processed by preparative HPLC (HSF-5 column) to yield pure samples of metabolites **1**, **3** and **5**. By high resolution mass spectrometry, the molecular formula of **1** was consistent with the molecular formula $C_{10}H_{16}N_2O_5S$. From this molecular formula we determined that **1** possessed four degrees of unsaturation.

Table 1. ¹H and ¹³C NMR Data for 1 and 2 (500 and 125 MHz, respectively)

Position	*1 in DMSO-d_6* δ_C, multiplicity	δ_H, (J)	*2 in DMSO-d_6* δ_C, multiplicity	δ_H, (J)
1	169.2, s		170.9, s	
2	55.7, d	5.34, (d, 9 Hz)	55.6, d	5.27 (br d)
3	171.1, s		170.9, s	
4	31.7, t	2.34, (t, 8 Hz)	31.5, t	2.33 (br tr)
5	27.2, t	1.89 (m), 1.97 (m)	27.0, t	1.88 (m), 1.96 (m)
6	53.0, d	3.45 (br t)	52.8, d	3.41 (m)
7	170.5, s		170.9, s	
8	122.9, d	6.25 (d, 9 Hz)	121.1, d	6.14 (d, 15 Hz)
9	123.3, d	5.62 (m)	128.8, d	5.69 (m)
10	14.4, q	1.58 (d, 7 Hz)	18.3, q	1.69 (d, 7 Hz)
N-H		8.74 (d, 9 Hz)		

The structure of **1** was determined from its mass spectrometric as well as ¹H and ¹³C NMR data which are summarized in Table 1. The ¹³C NMR spectrum contained three closely spaced carbonyl resonances and a pair of singlets at δ 122.9 and 123.3 ppm, consistent with the presence of a double bond, which accounted for all four unsaturations. As can be seen in Figure 2, a proton NMR spectrum of metabolite **1** in DMSO-d_6 contained doublets corresponding to one proton each at

δ 5.34 and 8.74 ppm with coupling constants of 8.5 Hz. Upon addition of a drop of D_2O, the resonance at 8.74 ppm disappeared and the resonance at 5.34 ppm collapsed to a singlet, consistent with the assignment of a methine, H-2, adjacent to an exchangeable proton. The proton NMR also contained a doublet at δ 6.25 ppm with a coupling constant of 9 Hz, consistent with the presence of a *cis*-double bond.
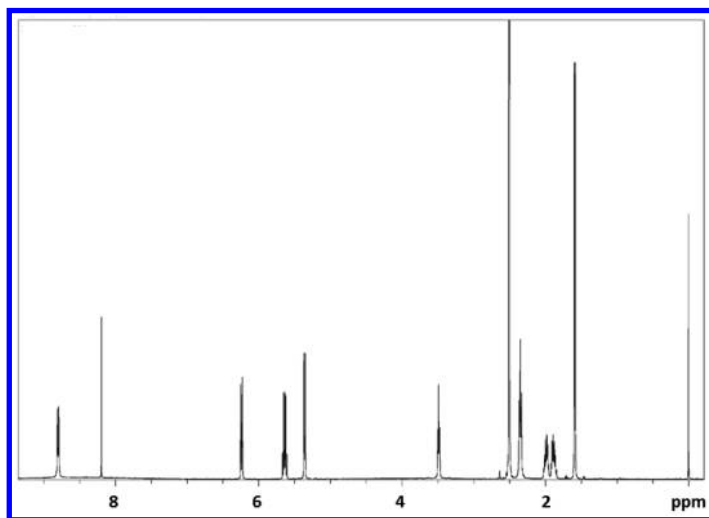
Figure 2. 500 MHz Proton NMR of Metabolite 1 in DMSO-d₆.

The proton COSY of metabolite **1** shown in Figure 3 contained two spin systems, one consisting of a triplet corresponding to one proton at δ 3.90 ppm coupled to a multiplet (2H) at 2.18 ppm which was in turn coupled to a triplet at 2.54 (2H). This spin system was consistent with the presence of a glutamate moiety in **1**. A second spin system consisted of a doublet (1H) at δ 6.08 ppm that was coupled to a multiplet at 5.97 ppm (1H) which was in turn coupled to a doublet of doublets (3H) at 1.70 ppm was assigned to a 1-propenyl moiety. Accounting for glutamate and propenyl moieties, the molecular formula contained an unassigned sulfur, a carboxyl group and a methine (C-2), which corresponded to a second amino acid group but lacked the methylene associated with a cysteine moiety. We suspected that **1** contained an amino acid not previously identified in a natural compound.
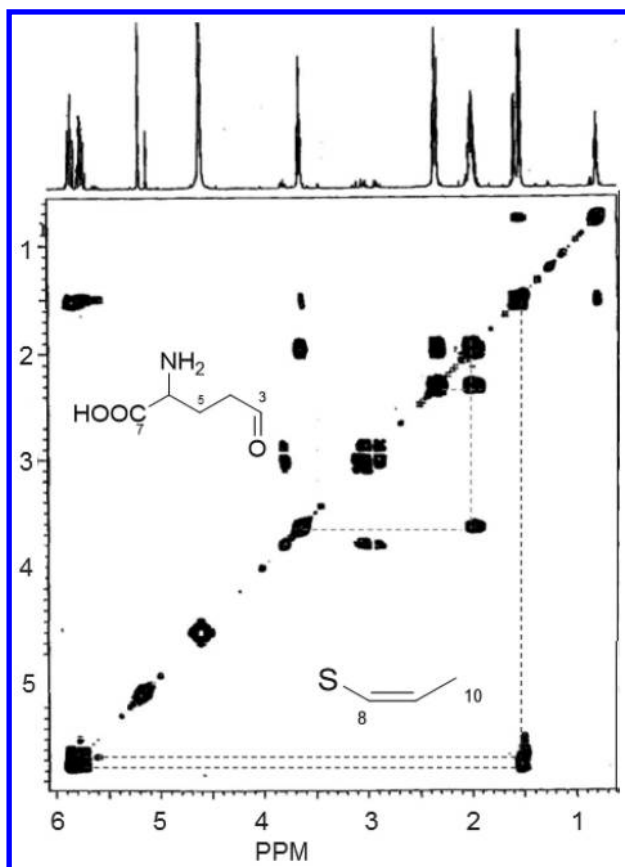
*Figure 3. 500 MHz ^1H-^1H COSY Spectrum of **1** in D$_2$O.*

The ^{13}C NMR spectrum of **1** was assigned from an HSQC spectrum. In the HMBC spectrum recorded in DMSO-d$_6$ with a drop of D$_2$O shown in Figure 4, we observed correlations from protons at δ 3.38 (H-6), 1.88 (H-5) and 2.0 (H 5') to a carbon resonance at 169.1 ppm (C-7). Additional resonances from the methylene resonances at δ 1.88 (H-5) and 2.0 (H-5') and 2.32 (H-4) to a carbon resonance at 171.1 ppm (C-3) were consistent with the presence of a glutamate moiety in **1**. Correlations were observed from the methine resonance at δ 5.29 (H-2) to carbon resonances at 122.9 (C-8), 169.1 (C-1) and 171.1 (C-3) which led us to conclude the **1** contained a norcysteine, or α-thioglycine group and the structure of the compound was determined to be γ-glutamyl-(*cis-S*-1-propenyl)thioglycine.

Although only 21 proteinogenic amino acids are commonly found in eukaryotes, over 500 non-proteinogenic amino acids with diverse functions have been reported in nature (*6*). Norcysteine-containing molecules have been prepared synthetically, however, this is the first example of this amino acid being observed in a natural source. Kingsbury *et al* (*7*) showed that synthetic norcysteine-containing compounds were cleaved by peptidases to yield unstable

norcysteine intermediates such as **7** which are rapidly hydrolyzed to ammonia, pyruvic acid and an alkyl thiol, as shown in Figure 5. Synthetic compounds containing this amino acid have been used to transport precursors of antimicrobial compounds across the membranes of pathogenic bacteria and as probes for quantitation of peptidase activity (*8*).
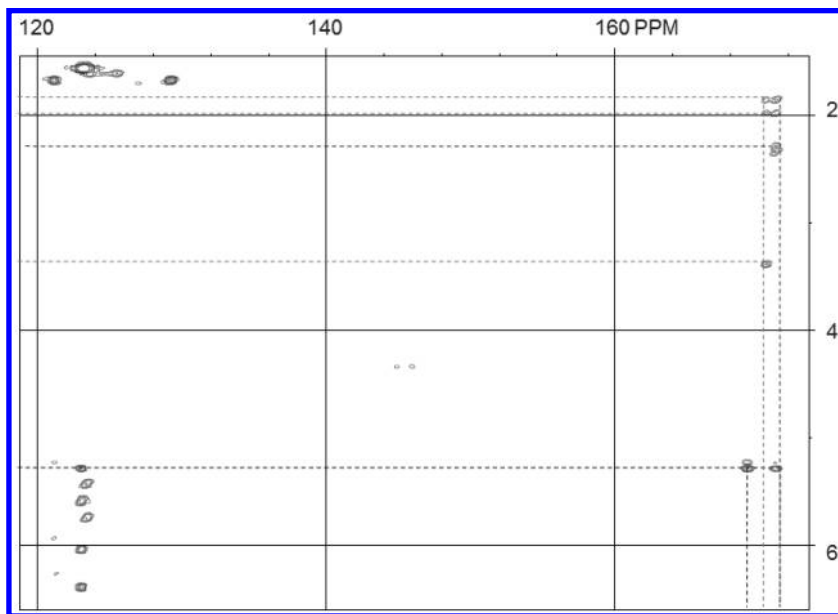
*Figure 4. HMBC Spectrum of **1** in DMSO-d₆ with a drop of D₂O.*
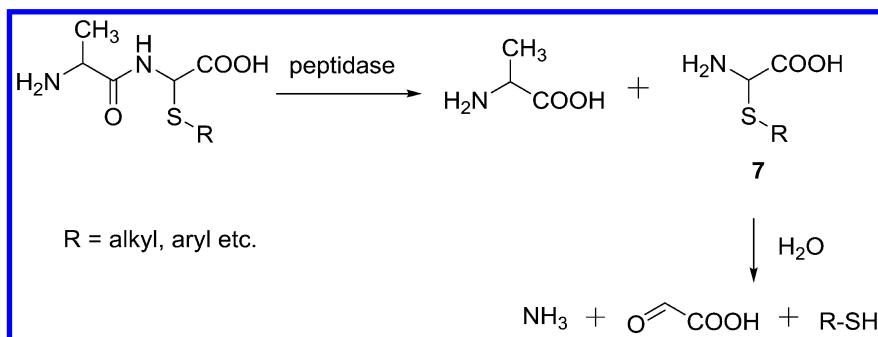
Figure 5. Generic Scheme for Thiol Release from Norcysteine-Containing Peptides.

We undertook the synthesis of **1** to confirm its novel structure. As shown in Figure 6, N-Boc-protected glutamine was reacted with ethyl glyoxalate in acetone. The resulting intermediate, N-Boc-glutamyl-2-hydroxyglycine ethyl ester was successfully reacted with propanethiol under acidic conditions to yield γ-glutamyl-2-propylthioglycine ethyl ester which was deprotected under basic conditions to give glutamyl-propyl-thioglycine, **8**. Efforts to prepare the 1 propenyl analogue by reaction with 1-propenyl thiol or by isomerization of the 2-propenyl thiol-containing analogue were unsuccessful. However, reduction of **1** isolated from *T. sinensis* resulted in a sample of **8** that was identical with the synthetic material by NMR and LC-MS.
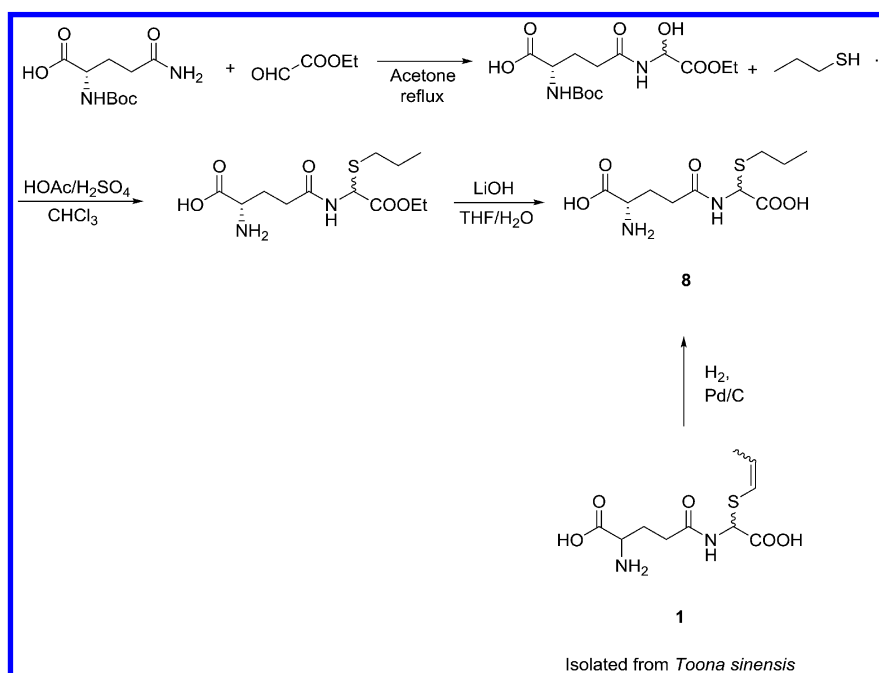
Figure 6. Preparation of Synthetic and Semisynthetic Glutamyl-S-propylthioglycine.

We were also interested in determination of the absolute configuration of norcysteine-containing metabolite **1**. Our initial efforts to crystallize **1** were unsuccessful so we decided to approach the problem using vibrational circular dichroism (VCD). In order to eliminate water solvation and to simplify

conformational calculations, we prepared derivate **9** by protecting the amine functionality of **1** with a Boc group and methylating the acid groups with diazomethane (Figure 7). As shown in Figure 8, the observed vibrational circular dichroism and IR spectra, measured by BioTools (Jupiter, FL, USA) Inc, were a good match with the calculated Boltzmann population weighted VCD and IR spectra of the *(S,S)* configuration of **9**. Furthermore, using BioTools proprietary algorithms to compare the observed with the calculated spectra, the confidence level for assignment of the configuration of **9** as *(S,S)* was calculated to be 100% while the confidence level for the *(R,S)* configuration was determined to be 13%.

Derivative **9** was found to be a crystalline solid and X-ray quality crystals were grown from a solution of tetrahydrofuran and hexane. By X-ray crystallography, the configuration of **9** was confirmed to be *(S,S)* allowing us to conclude that **1** also occurred in the *(S,S)* configuration. Figure 9 shows the 3 dimensional structure of **9** as determined by X-ray crystallography.
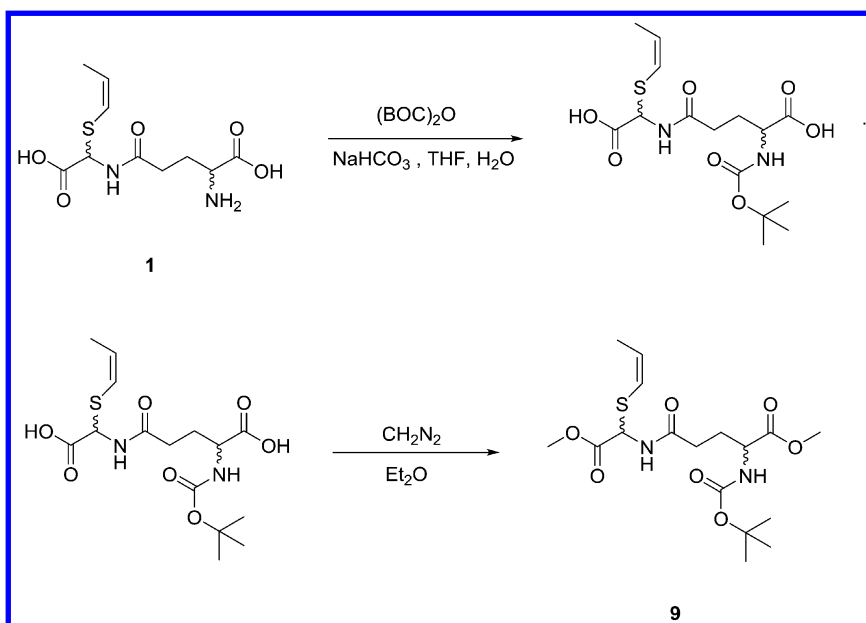
*Figure 7. Preparation of Derivative **9** by Protection of **1**.*
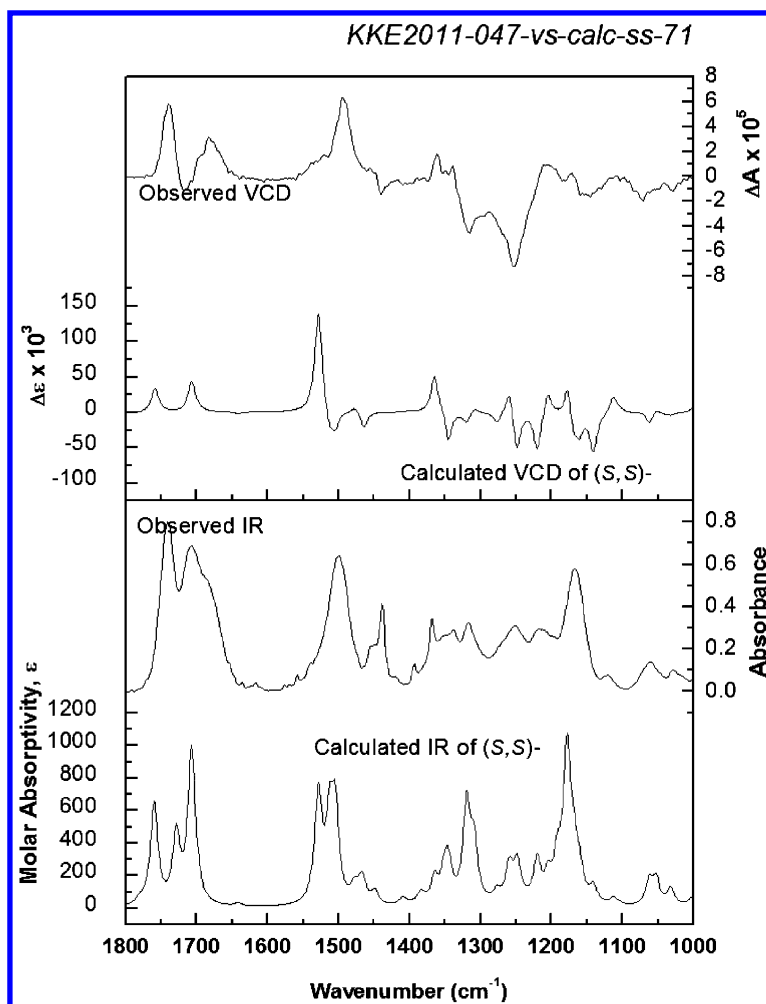
*Figure 8. Observed versus Calculated Boltzman Population Weighted IR and VCD Spectra of the (S,S) Configuration of Derivative **9**.*

A second metabolite, **2**, that eluted very closely to **1** in the liquid chromatogram and was present in extracts of *T. sinensis* at concentrations that were approximately 25% of the concentrations of **1** had similar proton and ^{13}C NMR spectra as **1**. A significant difference was the coupling constant of H-9 which, at 15 Hz, allowed the identification of **2** as γ-glutamyl-(*trans*-1-propenyl)thioglycine, also a novel chemical. Since the optical rotation of **2** ($[\alpha]^{22}_D$ +233.5° (*c* 0.17, H$_2$O)) was very similar to that of **1** ($[\alpha]^{22}_D$ +258.6° (*c* 0.21, H$_2$O)), we assigned the same *(S,S)* configuration to metabolite **2**.
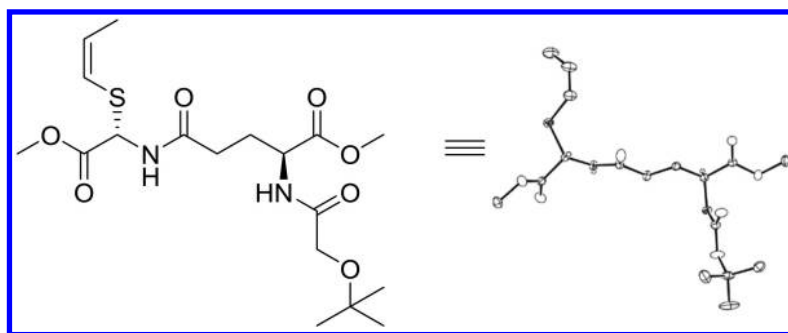
*Figure 9. 3-Dimensional Structure of **9** Determined by X-Ray Crystallography.*

Further investigation allowed us to identify known metabolite **4** in addition to the novel *cis* analogue **3** (*9*). Previously reported c*is* and *trans*-1-propenylcysteine **5** and **6** were identified in aqueous extracts of *T. sinensis*. Metabolites **3** to **6** were stable in *T. sinensis* extracts containing active enzymes (*10*).

Table 2. Concentrations of Norcysteine-Containing Metabolites in *Toona sinensis* Shoots

Sample	Water Content %	UV 250 nm [*1*+*2*]g/kg dry weight	MS/MS 277→203 [*1*+*2*]g/kg dry weight	MS/MS 277→130 [*1*+*2*]g/kg dry weight
T. sinensis **shoots batch 1**	85	11.9	11.4	11.0
T. sinensis **shoots batch 2**	88	8.72	7.48	7.73

The concentrations of norcysteine-containing metabolites **1** and **2** were quantified in *T. sinensis* shoots by LC-UV-MS/MS and the results are listed in Table 2. As can be seen, two batches of *T. sinensis* shoots with inactivated enzymes were found to contain approximately 1% norcysteine-containing metabolites **1** and **2** on a weight per dry plant weight basis. Based on this work we hypothesized that the relatively high concentrations of these metabolites in whole *T. sinensis* plant tissues may serve as herbivore deterrents, with release of *cis*- and *trans*-1-propenylthiol upon disruption of the uncooked leaves. Conversely, blanching of *T. sinensis* shoots and sprouts denatures proteases allowing the ingestion of this nutritious plant with the release of only relatively low levels of thiols which lead to the greatly appreciated, characteristic and subtle flavor.

References

1. Dong, C.; Nie, F. Research and exploitation of *Toona sinensis*. *Shengwuxue* **2002**, *19*, 35–37.
2. Mu, R. M.; Wang, X. R.; Liu, S. X.; Yuan, X. L.; Wang, S. B.; Fan, Z. Q. Rapid determination of volatile compounds in *Toona sinensis* (A. Juss.) Roem. by MAE-HS-SPME followed by GC-MS. *Chromatographia* **2007**, *65*, 463–467.
3. Block, E. The organosulfur chemistry of the genus *Allium*: implications for the organic chemistry of sulfur. *Angew. Chem., Int. Ed. Engl.* **1992**, *31*, 1135–1178.
4. Kaczorowska, K.; Kolarska, Z.; Mitka, K.; Kowalski, P. Oxidation of sulfides to sulfoxides. Part. 2: Oxidation by hydrogen peroxide. *Tetrahedron* **2005**, *61* (35), 8315–8327.
5. Li, J.-X.; Eidman, K.; Gan, X.-W.; Haefliger, O. P.; Carroll, P. J.; Pika, J. Identification of *(S,S)*-γ-glutamyl-(*cis-S*-1-propenyl)thioglycine, a Naturally Ocurring Norcysteine Derivative, from the Chinese Vegetable *Toona sinensis*. *J. Agric. Food Chem.* **2013**, *61*, 7470–7476.
6. Wagner, I.; Musso, H. New naturally occurring amino acids. *Angew. Chem., Int. Ed. Engl.* **1983**, *22*, 816–828.
7. Kingsbury, W. D.; Boehm, J. C.; Perry, D.; Gilvary, C. Portage of various compounds into bacteria by attachment to glycine residues in peptides. *Proc. Natl. Acad. Sci. U.S.A.* **1984**, *81*, 4573–4576.
8. McCarthy, P. J.; Nisbet, L. J.; Boehm, J. C.; Kingsbury, W. D. Multiplicity of peptide permeases in Candida albicans: evidence from novel chromophoric peptides. *J. Bacteriol.* **1985**, *162*, 1024–1029.
9. Mütsch-Eckner, M.; Meier, B.; Wright, A. D.; Sticher, O. γ-Glutamyl peptides from *Allium sativum* bulbs. *Phytochemistry* **1992**, *31*, 2389–2391.
10. Carson, J. F.; Wong, F. F. Synthesis of *cis-S*-(prop-1-enyl)-*L*-cysteine. *Chem. Ind.* **1963**, 1764–1765.

Chapter 12

Chirality Matters – Enantioselective Orthologous Odorant Receptors for Related Terpenoid Structures

Christiane Geithe and Dietmar Krautwurst*

Deutsche Forschungsanstalt fuer Lebensmittelchemie, Leibniz Institut, Lise-Meitner Strasse 34, 85354 Freising, Germany
*E-mail: Dietmar.Krautwurst@lrz.tum.de.

Humans can discriminate between a variety of enantiomeric odorants with different odor qualities, such as the spearmint-like *(R)*-(-)-carvone and the caraway-like *(S)*-(+)-carvone. Moreover, a specific anosmia for *(R)*-carvone, but not for *(S)*-carvone, was observed in 8% of the population. Recently, the odorant receptor OR1A1 has been identified to selectively respond to *(R)*-carvone over *(S)*-carvone. We screened 391 human odorant receptors (OR) versus (-)-menthone and (+)-menthone, and identified OR1A1 as best receptor for both menthone enantiomers. OR1A1 also responded to both, *(S)*-(-)-limonene and *(R)*-(+)-limonene. We compared potency and efficacy of the carvone, menthone, and limonene enantiomers on OR1A1 and on its orthologous receptor in chimpanzee. Both receptors differ in just three single nucleotide polymorphism(SNP)-affected amino acid positions, which in sum render the chimp receptor non-selective for the carvone enantiomers, and with a generally attenuated efficacy for terpenoids. Three other SNP-based single amino acid changes lead to either gain-of-function or loss-of-function OR1A1 phenotypes. Our data suggest OR1A1 haplotypes being involved in an enantioselective perception of terpenoids.

Introduction

Certain volatile enantiomeric odorants have different organoleptic properties (e.g., odor qualities and intensities) (*1*). A common pair of enantiomers with different odor qualities is carvone, where the (-)-enantiomer smells like spearmint and the (+)-enantiomer like caraway (*2–4*). However, for some enantiomeric odor pairs, e.g., camphor or fenchone, no differences in odor quality is observable (*5*). Humans can distinguish between some enantiomeric odorants (*6, 7*). The ability to discriminate between enantiomeric odorants is not a general phenomenon in primates, but probably limited to certain substances (*8, 9*). Several studies across different species including human subjects showed the ability to discriminate always between the enantiomeric odor pairs of limonene and carvone, but for example not between the pairs of fenchone, champhor, rose-oxide or 2-butanol (*9–14*).

The sense of smell enables humans and other species to detect and discriminate between thousands of volatile compounds. With a wealth of ca. 400 odorant receptors (OR) encoded in the human genome (*15, 16*), an activation of receptor activity patterns appears to be an early basic principle in olfaction (*17*). The ability to discriminate between enantiomeric odorants suggests enantiomer-specific OR (*18, 19*). Recently, we identified 9 human receptors responding specifically to either of the carvone enantiomers, and OR1A1 being the only receptor responding to both carvone enantiomers, albeit with a selectivity for *(R)*-(-)-carvone over *(S)*-(+)-carvone (*18*).

Here, we used a fast cAMP-dependent luminescence-based test cell system, which enabled us to investigate odorant/OR interactions on a molecular level. We established a enantioselective receptor activity pattern for menthone, and investigated the structurally related enantiomeric terpenoid odorants *(R)*-(-)-carvone (spearmint-like) (*2–4*), *(S)*-(+)-carvone (caraway-like) (*2–4*), *(S)*-(-)-limonene (turpentine-like) (*20*), *(R)*-(+)-limonene (orange-like) (*20*), (-)-menthone (mint-like, strong cooling) and (+)-menthone (mint-like, less cooling) (Table 1) on the human odorant receptor OR1A1 and its orthologous receptor in chimpanzee, PTOR1A1. Further, we investigated the impact of certain frequent single nucleotide polymorphism (SNP) in OR1A1 on the discrimination of these enantiomeric terpenoid odorants.
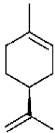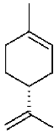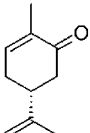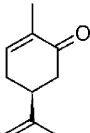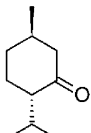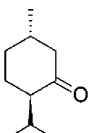
Materials and Methods

Molecular Cloning of Human OR1A1

The protein-coding region (NCBI reference sequence: NM_014565.2) of human OR1A1 was amplified from human genomic DNA with gene-specific primers (Table 2) by polymerase chain reaction (PCR). Human genomic DNA was purified from cell culture cells using the blood and tissue kit (Qiagen, Hilden, Germany). The PCR reaction (final volume: 50 µL) was performed in a C-1000 thermocycler (Bio-Rad, München, Germany) with 150 ng of genomic DNA, 0.5 µL phusion hot start DNA-polymerase (Thermo Scientific, Waltham, U.S.A.), 2.5 mM dNTPs (Promega, Madison, U.S.A.), 1.5 µL DMSO (Promega, Madison,

U.S.A.) and 0.5 µM of each primer using the following protocol: denaturation (98°C, 3 min), 10 cycles containing denaturation (98°C, 30 s), annealing (start 66°C, 30 s, with -1°C increment each cycle), extension (72°C, 2 min), 30 cycles containing denaturation (98°C, 30 s), annealing (58°C, 30 s), extension (72°C, 2 min) and final elongation (72°C, 10 min). The control PCR reaction was without genomic DNA. The PCR product was purified (gel extraction kit, Qiagen, Hilden, Germany), digested Mfe1/Not1 and ligated (T4 DNA ligase, Promega, Madison, U.S.A.) into pI2-dk(39AS rho-tag) (*21*, *22*) which provides the first 39 amino acids of the bovine rhodopsin as an N-terminal tag for the full-length OR. Mfe1 was from New England BioLabs, Ipswich, U.S.A. and Not1 was from Promega, Madison, U.S.A.. The plasmid-DNA was transformed by heat shock in competent *E. coli* (XL1-blue, Agilent Technologies, Santa Clara, U.S.A.) and purified with pure yield plasmid midiprep kit (Promega, Madison, U.S.A.). Plasmid-DNA concentration was determined with Nanodrop 2000 (Thermo Fisher Scientific, Waltham, U.S.A.).

Table 1. Chemical Properties of Investigated Enantiomeric Terpenes

	(S)-(-)-limonene	(R)-(+)-limonene	(R)-(-)-carvone	(S)-(+)-carvone	(-)-menthone	(+)-menthone
Chemical structure						
Common name	L-limonene	D-limonene	L-carvone	D-carvone	L-menthone	D-menthone
Chemical description	Monocyclic terpene-hydrocarbon	Monocyclic terpene-hydrocarbon	Monocyclic terpene-ketone	Monocyclic terpene-ketone	Monocyclic terpene-ketone	Monocyclic terpene-ketone
IUPAC name	(4*S*)-4-Isopropenyl-1-methylcyclohexene	(4*R*)-4-Isopropenyl-1-methylcyclohexene	(5*R*)-5-Isopropenyl-2-methyl-2-cyclohexen-1-one	(5*S*)-5-Isopropenyl-2-methyl-2-cyclohexen-1-one	(2*S*,5*R*)-2-Isopropyl-5-methylcyclohexanone	(2*R*,5*S*)-2-Isopropyl-5-methylcyclohexanone
Chemical formula	$C_{10}H_{16}$	$C_{10}H_{16}$	$C_{10}H_{14}O$	$C_{10}H_{14}O$	$C_{10}H_{18}O$	$C_{10}H_{18}O$
Molecular weight	136.23	136.23	150.22	150.22	154.25	154.25
Odor quality	Turpentine	Orange	Spearmint	Caraway	Mint, strong cooling	Mint, less cooling

PCR-Based Site-Directed Mutagenesis

The protein-coding DNA region of the OR1A1 chimpanzee ortholog PTOR1A1 (NCBI reference sequence: NM_001009115.1) and the different OR1A1-variants were generated from OR1A1 by PCR-based site-directed

mutagenesis in two steps. Gene-specific primers carrying the nucleotides of interest (mutation-primer) as well as the OR1A1 gene-specific (344) forward primer and a vector-internal (dk-232a) reverse primer were used (Table 2). The forward and reverse mutation-primers were designed to overlap. One PCR reaction was performed with the forward gene-specific OR1A1 primer 344 and the respective reverse mutation-primer, and another PCR with the respective forward mutation-primer and the reverse vector-internal primer using the protocol as described above. The two purified PCR products were used as template for the second PCR. Here, the two templates were first annealed using the following protocol: denaturation (98°C, 3 min), 10 cycles containing denaturation (98°C, 30 s), annealing (start 58°C, 30 s) and extension (72°C, 2 min). Then, the forward gene-specific OR1A1 primer 344 and the vector-internal reverse primer dk-232a were added, and the PCR was performed as described above. All following steps containing digest, ligation, transformation and plasmid purification were performed as described above.

RNA Isolation, cDNA Synthesis, and Reverse Transcriptase Polymerase Chain Reaction (RT-PCR) for Adenylyl Cyclase III (ACIII)

Isolation of total RNA from HEK-293 cells was done with RNeasy mini kit (Qiagen, Hilden, Germany) according to manufacturer´s instructions. The following cDNA synthesis was performed with iScript cDNA synthesis kit (Bio-Rad Laboratories, Hercules, U.S.A.) according to manufacturer´s instructions. Therefore, a negative (-RT, without reverse transcriptase) and positive (+RT, with reverse transcriptase) cDNA synthesis was performed. PCR reactions for adenylyl cyclase and the reference gene glyceraldehyde 3-phosphate dehydrogenase (GAPDH) were performed with GoTaq PCR Master Mix (1/2 reaction volume, Promega, Mannheim, Germany) using gene-specific primers (Table 2). The expected size for ACIII was 316 base pairs (bp) and for GAPDH 308 bp.

Sequencing

The coding region amplicons of OR1A1 and mutated receptors were verified by Sanger sequencing (Eurofins Genomics, Ebersberg, Germany) using the two vector internal primers dk-231 and dk-232a (Table 2). All mutated ORs were named with the respective amino acid position (e.g., OR1A1-$R_{54}H$). The agarose gel-purified RT-PCR amplicon of ACIII was sequenced with cg-306 (Table 2).

Cell Culture

HEK-293 cells (a human embryonic kidney cell line) (*23*) were cultivated at 37°C, 5% CO_2 and 100% humidity in 4.5 g/L D-glucose containing DMEM with 10% fetal calf serum, 2 mM L-glutamine, 100 units/ml penicillin and 100 µg/ml streptomycin. Cell culture medium and supplementals were obtained from Biochrom, Germany.

Table 2. Oligonucleotides for Molecular Cloning, Site-Directed Mutagenesis Sequencing and RT-PCR

Gene	Oligo-nucleo-tide	TM (°C)		Sequence 5′→3′	Template
Molecular cloning of OR1A1					
OR1A1	344	66	fw	CGAT*CAATTG***ATG**AGGGAAAATAACCAGTCCTCTACACTGGAATTCATCC	human genomic DNA
	cg-196	61	rv	CTGC*GCGGCCGC***TTA**CGAGGAGATTCTCTTGTTGAAGAGTTTCC	
Site-directed mutagenesis of OR1A1 to generate PTOR1A1					
OR1A1- $R_{54}H$	cg-230	59	fw	CTCTGATGTTCACCTTCACAACCCC	OR1A1 plasmid-DNA (Ref.Seq.)
	cg-231	59	rv	CATGGGGTTGTGAAGGTGAACATCAG	
OR1A1- $T_{257}M$	cg-232	59	fw	CAGTCATGGGCATGTATTTCCGCC	OR1A1 plasmid-DNA (Ref.Seq.)
	cg-233	59	rv	CGGAAATACATGCCCATGACTGTACC	
OR1A1- $M_{295}V$	cg-234	62	fw	CGGGACGTGAAGGCTGCCCTG	OR1A1 plasmid-DNA (Ref.Seq.)
	cg-235	60	rv	GGGCAGCCTTCACGTCCCGATTTC	
OR1A1- $R_{54}H/$ $T_{257}M$	cg-232	59	fw	CAGTCATGGGCATGTATTTCCGCC	OR1A1-$R_{54}H$ plasmid-DNA
	cg-233	59	rv	CGGAAATACATGCCCATGACTGTACC	
OR1A1- $R_{54}H/$ $M_{295}V$	cg-234	62	fw	CGGGACGTGAAGGCTGCCCTG	OR1A1-$R_{54}H$ plasmid-DNA
	cg-235	60	rv	GGGCAGCCTTCACGTCCCGATTTC	

Table 2. (Continued). Oligonucleotides for Molecular Cloning, Site-Directed Mutagenesis Sequencing and RT-PCR

Gene	Oligo-nucleotide	TM (°C)		Sequence 5′→3′	Template
OR1A1- $T_{257}M$/ $M_{295}V$	cg-234	62	fw	CGGGACGTGAAGGCTGCCCTG	OR1A1-$T_{257}M$ plasmid-DNA
	cg-235	60	rv	GGGCAGCCTTCACGTCCCGATTTC	
OR1A1- $R_{54}H$/ $T_{257}M$/$M_{295}V$ (PTOR1A1)	cg-234	62	fw	CGGGACGTGAAGGCTGCCCTG	OR1A1-$R_{54}H$/$T_{257}M$ plasmid-DNA
	cg-235	60	rv	GGGCAGCCTTCACGTCCCGATTTC	
pI2-dk(39AS rho-tag) internal oligonucleotides					
	dk-231	57	fw	GCAGAGCTGGTTTAGTGAACCG	
	dk-232a	59	rv	GCAAGTAAAACCTCTACAAATGTGGTATGG	
RT-PCR					
AC III	cg-306	59	fw	GCTGTGGGCATCATGTCCTACTAC	
	cg-307	59	rv	GCTTCACAAGCTCCTGGGCACTG	
GAPDH	dk-918a	60	fw	CATGGGTGTGAACCATGAGAAGTATGAC	
	dk-919	64	rv	CACGGAAGGCCATGCCAGTGAGCTTC	

TM = melting temperature, fw = forward, rv = reverse. Restriction sites (MfeI, Not1) are underlined italic letters, and Start and Stop codons are bold.

Transfection

One day before transfection, HEK-293 cells were transferred with a density of 12000 cells per well in white 96-well plates (Nunc, Roskilde, Denmark). The transfection was done by the cationic lipid-lipofection method (lipofectamine 2000, Life Technologies, Carlsbad, U.S.A.), using 100 ng of the respective OR plasmid-DNA, 50 ng olfactory G protein Gαolf (*22*, *24*), 50 ng RTP1S (*25*), 50 ng Gγ13 (*26*) and 50 ng genetically modified luciferase pGloSensor-22F-cAMP (*27*) (Promega, Madison, U.S.A.) each. A transfection of the vector plasmid pI2-dk(39AS rho-tag) (*21*, *22*) lacking the coding-information for an OR was performed as a control. The cells were taken into experiment 42 h post transfection.

Luminescence Assay

Transfected HEK-293 cells were transferred into physiological salt buffer (pH 7.5) containing 140 mM NaCl, 10 mM HEPES, 5 mM KCl, 1 mM CaCl$_2$, 10 mM glucose and 2% beetle luciferin sodium salt (Promega, Madison, U.S.A.). The cells were incubated with luciferin-supplemented buffer at room temperature for 1h in the dark. This was necessary for the uptake of luciferin into the cells, which is required as a substrate for the luminescence reaction. After this incubation, a basal luminescence signal readout (three consecutive data points) before odorant application was recorded with GloMax Multi+® Detection System (Promega, Madison, U.S.A.). For each well, luminescence was recorded in 63 s intervals. Thereafter, the corresponding terpenoid enantiomeric odorants which were serially diluted in physiological salt buffer, were pipetted to the cells. The carvone stock solutions were prepared in dimethyl-sulfoxide (DMSO) and diluted 1:1000 in physiological salt buffer, resulting in a final concentration of 0.1% DMSO on the cells. The limonene and menthone stock solutions were prepared in ethanol and diluted 1:1000 in physiological salt buffer resulting in a final concentration of 0.2% ethanol on the cells. All substances had a purity of at least 98-99 % and were obtained from Fluka. After adding the odorants to the cells, a second readout (three consecutive data points) was recorded after reaching maximum receptor stimulation (4 min after odorant addition). This luminescence assay allows real-time determinations of changes in the intracellular cAMP, which in our hands reached a maximum within 4 min after receptor stimulation. The cells were stimulated only once with the corresponding odorant. We performed no wash-out experiments. Application of different odorants or odorant concentrations required separate wells/transfections.

Data Analysis of Luminescence Measurements

The raw luminescence data obtained from the GloMax Multi+® detection system were converted to an Excel document using Instinct Software (Promega, U.S.A.). Three data points before and after odorant addition were averaged, and the respective baseline was subtracted from each signal. Each screening experiment was repeated three times and subsequently multiplied. The data were

always normalized to the maximum responding receptor. All OR signals which exceeded the 3-sigma threshold (mean ± 3 standard deviations over all signals), were monitored as responding receptors.

Concentration-response relations were obtained by normalizing the baseline-corrected data to maximum. The respective data from vector-transfected cells (mock control) were subtracted. EC_{50} values (half maximal effective concentration) were derived from fitting the function $f(x) = 1/(1+(EC_{50}/x)^h)$ to the data by nonlinear regression, where h = hill coefficient.

Results

Establishment of a Dynamic cAMP Luminescence Online Assay for the Investigation of Odorant/Receptor Interactions

To investigate specific interactions of odorant receptors (OR) with their respective odorants outside the human nose, an expression of OR in heterologous test cell systems (mostly HEK-293 cells) has been the most commonly used method in the recent years. Therefore, we established a cAMP-induced chemiluminescence HEK-293 cell-based, dynamic online assay, employing a genetically modified cAMP-sensitive luciferase. Odorant-induced cAMP signals thus can be recorded directly after application of the odorant. Our assay does not require a cAMP-induced transcription of a luciferase gene, and thus differs from the luminescence-based static endpoint assay described by Zhuang and Matsunami (*28*).

The heterologous expression of the respective OR together with the signal transduction components Gαolf, Gγ13, and RTP1S in HEK-293 enables the imitation of the signaling pathway in olfactory neurons up to the second-messenger cAMP. For the detection of cAMP, we used a genetically modified luciferase with a specific cAMP binding site (*27*). The interaction of an odorant with its respective OR leads to an activation of the α-subunit of the heterotrimeric G protein, which ultimately activates cAMP-synthesis by an adenylyl cyclase. Subsequently, the cAMP binds to the luciferase and a luminescence signal can be recorded (Figure 1a). Since ACIII is necessary for cAMP signaling in olfactory neurons (*29*), and HEK-293 cells have been reported to endogenously express ACIII (*30*), we examined whether ACIII is expressed in our test cells (Figure 1b). Figure 1c show cAMP luminescence kinetics of OR1A1-transfected HEK-293 cells upon *(R)*-(-)-carvone (1000 μM and 300 μM) stimulation. The human OR1A1 was previously shown to respond to the spearmint-like *(R)*-(-)-carvone, when heterologously expressed in the HEK-293 derived Hana3A cell line (*31*). Hence, we used this OR for the validation of our cell system. First, we recorded a basal luminescence before odorant application. This includes three consecutive data points, which were recorded in 63 s intervals. Thereafter, the odorant *(R)*-(-)-carvone (1000 μM or 300 μM) was added to the transfected cells and 12 consecutive data points were recorded. The kinetics show that a concentration-dependent maximum luminescence signal arose within 4 minutes. We therefore always recorded three consecutive data points after 4 min of odorant application. The specificity of cAMP luminescence in our test cell system was

confirmed by the OR1A1- *vs.* mock-transfection and the application of either 1000 µM and 300 µM *(R)*-(-)-carvone or buffer, and the activation of endogenous GPCR (e.g., β2-adrenergic receptors) with 30 µM isoproterenol (selective β-adrenergic agonist with an $EC_{50} \sim 0.2$ µM, (*32, 33*)) in cAMP-luciferase transfected cells. Figure 1d shows OR1A1-specific cAMP responses to *(R)*-(-)-carvone, but not to the buffer. The application of isoproterenol induced cAMP luminescence in cAMP-luciferase-transfected HEK-293 cells, whereas buffer did not.
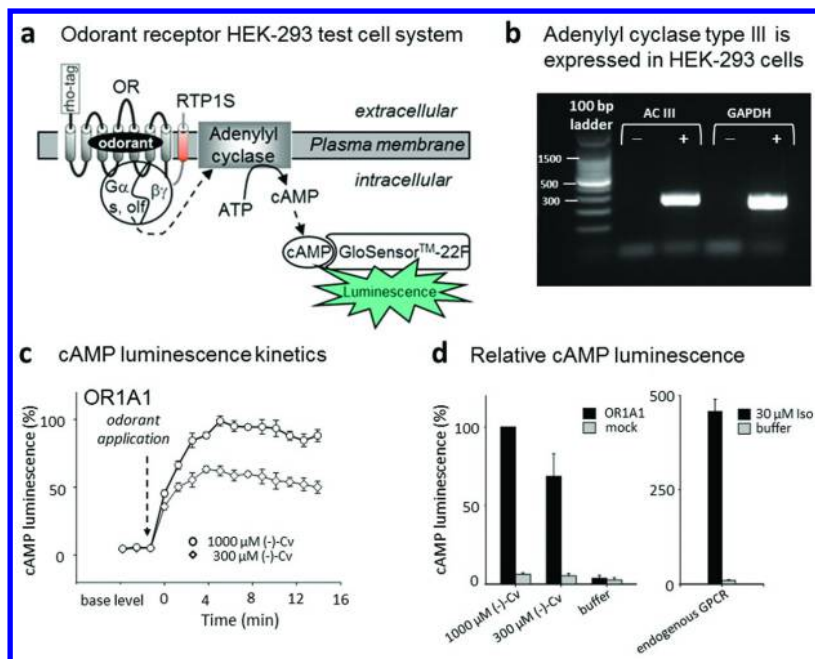
Figure 1. Dynamic cAMP Luminescence Online Assay for the Investigation of Odorant/Receptor Interactions. a) Odorant receptor HEK-293 test cell system. An odorant/receptor-interaction leads to an activation of the α-subunit of heterotrimeric G protein, which ultimately activates cAMP synthesis by an adenylyl cyclase. Subsequently, the cAMP binds to a genetically modified luciferase (27), and the luminescence signal is detected by the GloMax Multi+™ detection system (Promega, Madison, U.S.A.). The N-terminal extension (rho-tag) and RTP1S are important and synergistic for OR membrane expression in heterologous test cells (21, 25). b) RT-PCR for adenylyl cyclase III (ACIII). Shown are −RT (without reverse transcriptase) and +RT (including reverse transcriptase), for ACIII and the reference gene GAPDH. Expected size for ACIII was 316 base pairs (bp) and for GAPDH 308 bp. c) Representative (R)-(-)-carvone- induced cAMP luminescence kinetic in OR1A1-transfected HEK-293 cells d) relative cAMP luminescence values for (R)-(-)-carvone in OR1A1-transfected and mock-transfected HEK-293 cells, as well as for isoproterenol on endogenous GPCRs in luciferase-transfected HEK-293 cells. Each data set was normalized to (R)-(-)-carvone (1000 µM) maximum luminescence value. Shown are mean ± standard deviation of 6 wells. Consecutive data points were recorded in 63 s intervals. (-)-Cv = (R)-(-)-carvone, Iso = isoproterenol.

Odorant Receptor Activity Pattern for Enantiomeric Odorants

Screening experiments with 1000 µM (-)-menthone and (+)-menthone against 391 putative functional human ORs in our HEK-293 cAMP luminescence assay (Figure 1) revealed enantiomer-specific odorant receptor activity patterns (Figure 2). For both menthones, OR1A1 was the major candidate OR. Besides OR1A1, we identified four other ORs for (-)-menthone, and only one for (+)-menthone. Previous screening experiments with the structurally related terpenoids *(R)*-(-)-carvone and *(S)*-(+)-carvone against the same set of 391 OR showed also enantiomer-specific odorant receptor activity patterns (*18*). In both cases, OR1A1 emerged as the only receptor responding to both carvone and menthone enantiomers.
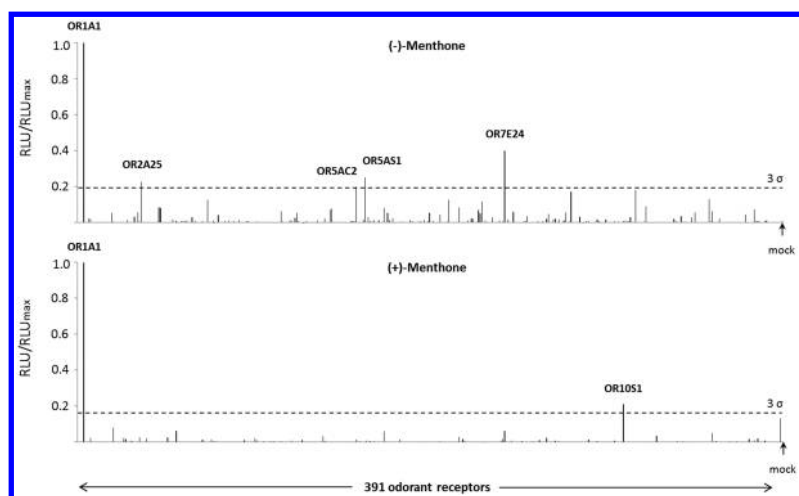
Figure 2. In-vitro Odorant Receptor (OR) Activity Pattern for Menthone. Screening of 391 odorant receptors with 1000 µM (-)-menthone and (+)-menthone. Data were normalized to the maximum responding OR. ORs which reached the 3σ-threshold are given with their names. Dashed lines indicate a 3σ-threshold. RLU=relative luminescence units.

The Enantiomeric Odorants (*R*)-(-)-Carvone and (*S*)-(+)-Carvone Activate Human OR1A1 and Chimpanzee PTOR1A1 in a Concentration-Dependent Manner

We investigated the human odorant receptor OR1A1 which was reported to respond to the spearmint-like *(R)*-(-)-carvone (*18*, *31*) and the caraway-like *(S)*-(+)-carvone (*15*, *18*, *31*, *34*). Our results show OR1A1 as an enantioselective receptor for *(R)*-(-)-carvone over *(S)*-(+)-carvone (Figure 3b).
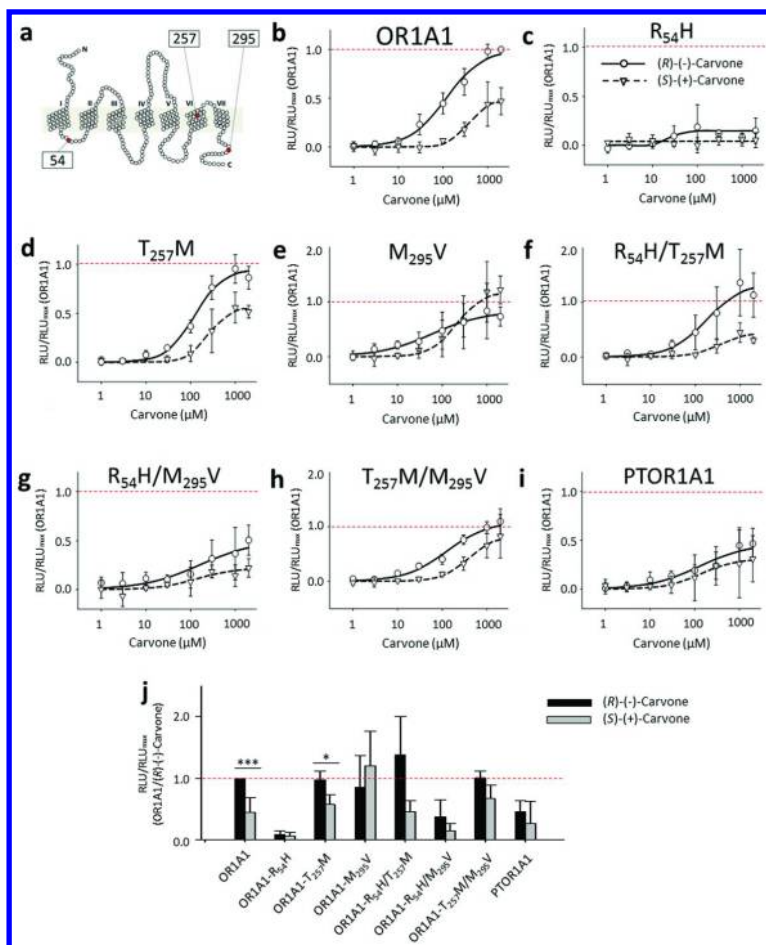
Figure 3. (R)-(-)-Carvone and (S)-(+)-Carvone. a) Schematic snake diagram with localization of mutated amino acid positions within OR1A1 and PTOR1A1. Concentration-response relations of (R)-(-)-carvone and (S)-(+)-carvone for b) OR1A1 (human), c) OR1A1-$R_{54}H$, d) OR1A1-$T_{257}M$, e) OR1A1-$M_{295}V$, f) OR1A1-$R_{54}H/T_{257}M$, g) OR1A1-$R_{54}H/M_{295}V$, h) OR1A1-$T_{257}M/M_{295}V$ and i) PTOR1A1 (chimpanzee). PTOR1A1 refers to OR1A1-$R_{54}H/T_{257}M/M_{295}V$. j) Effect of 1000 μM (R)-(-)-carvone and (S)-(+)-carvone on OR1A1 (human), OR1A1 variants and PTOR1A1 (chimpanzee). Shown are mean ± SD of n = 3-5. Mock control was subtracted. Data were normalized to human OR1A1 maximum amplitude. The dashed lines indicate the normalization level. RLU = relative luminescence units. Significant differences between (R)-(-)-carvone and (S)-(+)-carvone effects were calculated by 2-sided t-test. ***p<0.001, *p<0.05.

Interestingly, the orthologous OR1A1 receptor in chimpanzee, PTOR1A1, which is to 99% identical, showed no enantioselectivity for the carvones. This 1% of mismatch refers to exactly three amino acids. Therefore, we generated PTOR1A1 by PCR-based site-directed mutagenesis from the human OR1A1. The different amino acids are located at the positions 54 in the intracellular loop 1, position 257 in the transmembrane helix 6 and position 295 in the C-terminus of the receptor (Figure 3a). We elucidated the impact of those three amino acids which differed between OR1A1 and PTOR1A1 on a carvone function. In the first step, we changed only one single amino acid from OR1A1 to the respective amino acid of PTOR1A1. The exchange of the histidine (H) to arginine (R) on position 54 ($R_{54}H$) resulted in a complete loss-of-function for carvone (Figure 3c), whereas a methionine (M) instead of threonine (T) at position 257 ($T_{257}M$) did not alter carvone function (Figure 3d, Figure 3j, Table 3). A valine (V) instead of methionine on 295 ($M_{295}V$), however, slightly changed the enantioselectivity of OR1A1 for *(S)-(+)-carvone* over *(R)-(-)-carvone*, based on efficacies (Figure 3e). The EC_{50} for *(R)-(-)-carvone* differed significantly from that of *(S)-(+)-carvone* (Table 3). Further, all combinations of possible double mutations were investigated (Figure 3f-h). The triple OR1A1 mutant (OR1A1-$R_{54}H/T_{257}M/M_{295}V$) represents PTOR1A1. The chimpanzee receptor showed a loss-of-function for both carvone enantiomers, as compared to the human receptor (Figure 3i, Figure 3j). Further, there was no significant selectivity of one enantiomer over the other (Table 3).

In-silico analysis (*35–37*) showed high frequencies of three different OR1A1 haplotypes, defined by either of the three SNPs, $R_{128}H$, $V_{233}M$, and $P_{285}S$. OR1A1-$R_{128}H$ occurs with an allel frequency of 6.1%, OR1A1-$V_{233}M$ with 9.9% and OR1A1-$P_{285}S$ with 34.2% in the human population (*35–37*). The SNP $R_{128}H$ is located in the the intracellular loop 2, $V_{233}M$ in the intracellular loop 3, and $P_{285}S$ in transmembrane helix 7 of OR1A1 (Figure 4a). Each SNP had a different impact on an *in-vitro* OR1A1 function. In contrast to wild-type OR1A1, the OR1A1-$R_{128}H$ showed higher EC_{50} values for *(R)-(-)-carvone* and *(S)-(+)-carvone*, with similar efficacies (Table 3, Figure 4b, Figure 4e). In contrast, OR1A1-$V_{233}M$ responded with increased efficacies (Figure 4c, Figure 4e), but unaffected EC_{50} values (Table 3). Comparison of EC_{50} values showed that both haplotypes, as well as the wild-type receptor, were able to significantly discriminate between *(R)-(-)-carvone* and *(S)-(+)-carvone* (Table 3). Changing the highly conserved proline to serine ($P_{285}S$) resulted in a complete loss-of-function for both carvone enantiomers (Figure 4d, Figure 4e).

The Carvone-Related Enantiomeric Odorants (-)-Menthone and (+)-Menthone Activate Human OR1A1 and Chimpanzee PTOR1A1 in a Concentration-Dependent Manner

The enantiomeric odorants (-)- and (+)-menthone, which both display a minty odor, with either a strong or less cooling effect such as menthol (*20*), are carvone-related ketones. Screening of 391 odorant receptors with 1000 µM (-)-menthone and (+)-menthone revealed OR1A1 as major OR candidate for both enantiomers (Figure 2).
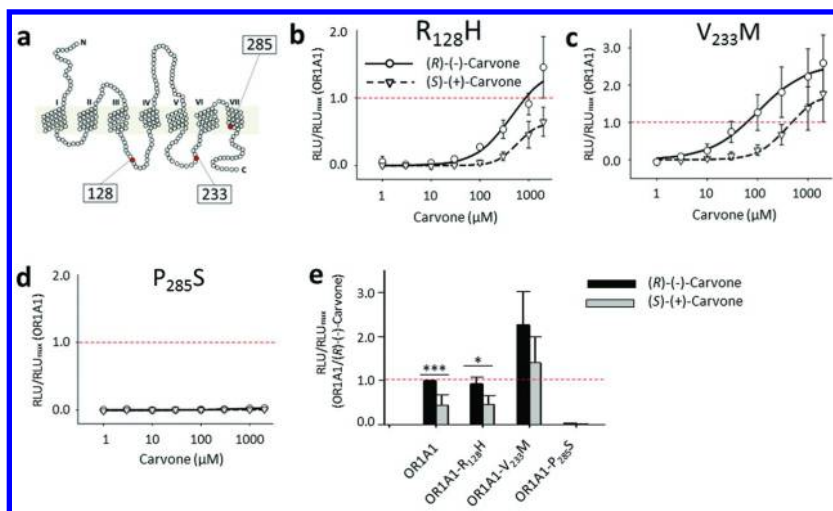
Figure 4. Impact of Single Nucleotide Polymorphism (SNP) in Human OR1A1 on the Detection of (R)-(-)-Carvone and (S)-(+)-Carvone. a) Schematic snake diagram with localization of SNP positions within OR1A1. Concentration-response relations of (R)-(-)-carvone and (S)-(+)-carvone for b) OR1A1-$R_{128}H$, c) OR1A1-$V_{233}M$, and d) OR1A1-$P_{285}S$. e) Effect of 1000 μM (R)-(-)-carvone and (S)-(+)-carvone on OR1A1 SNP-variants. Shown are mean ± SD of n = 3-5. Mock control was subtracted. Data were normalized to human OR1A1 maximum amplitude. The dashed lines indicate the normalization level. RLU = relative luminescence units. Significant differences between (R)-(-)-carvone and (S)-(+)-carvone effects were calculated by 2-sided t-test. ***p<0.001, *p<0.05.

Concentration-response relations revealed OR1A1 as an enantioselective receptor for (+)-menthone over (-)-menthone (Figure 5a, Figure 5c, Table 3). Its ortholog, PTOR1A1, responded less to both enantiomers, but with the ability to significantly distinguish between the (-)- and (+)-enantiomer (Figure 5a, Figure 5b, Table 3). The two SNPs $R_{128}H$ and $V_{233}M$ had no influence on receptor performance, and the ability of the receptor to distinguish between both enantiomers was retained (Figure 5c). The highly frequent SNP $P_{285}S$ resulted in a OR1A1 loss-of-function.
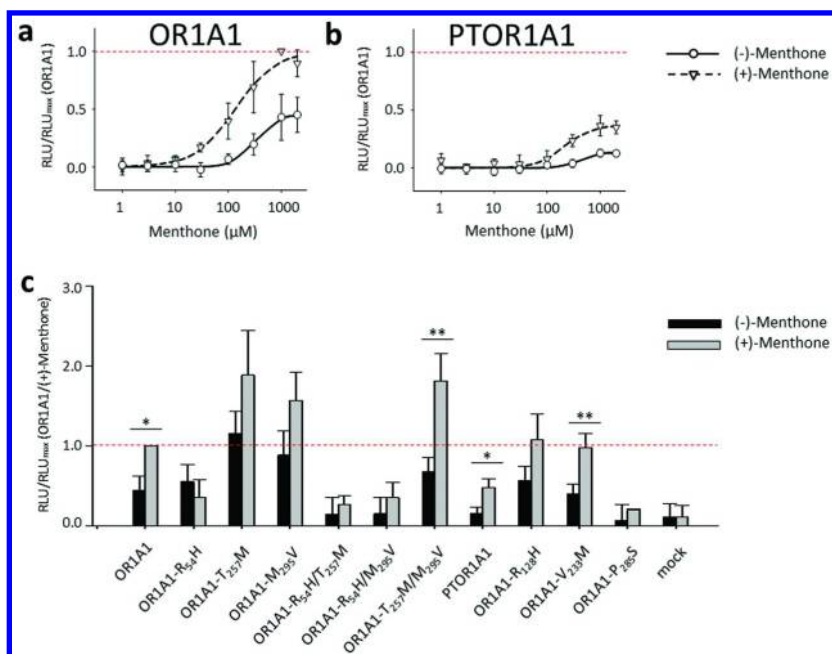
Figure 5. (-)-Menthone and (+)-Menthone. Concentration-response relations of (-)-menthone and (+)-menthone for a) OR1A1 (human) and b) PTOR1A1 (chimpanzee). Shown are mean ± SD of n = 3. Mock control was subtracted. Data were normalized to human OR1A1 maximum amplitude. The dashed line indicates the normalization level. c) Effect of 1000 μM (-)-menthone and (+)-menthone on OR1A1 (human), OR1A1 variants and PTOR1A1 (chimpanzee). Shown are mean ± SD of n = 3. Data were normalized to human OR1A1 vs. (+)-menthone. RLU = relative luminescence units. Significant differences between (-)-menthone and (+)-menthone effects were calculated by 2-sided t-test. **p<0.01, *p<0.05.

The Carvone-Related Enantiomeric Odorants *(S)*-(-)-Limonene and *(R)*-(+)-Limonene Activate Human OR1A1 and Chimpanzee PTOR1A1 in a Concentration-Dependent Manner

Limonene is a carvone-related hydrocarbon, which lacks the ketone function at the ring. Due to the ability of OR1A1 as an enantioselective receptor for carvone and menthone, we assumed the same for limonene, since limonene is also an enantiomeric odorant with different odor qualities.
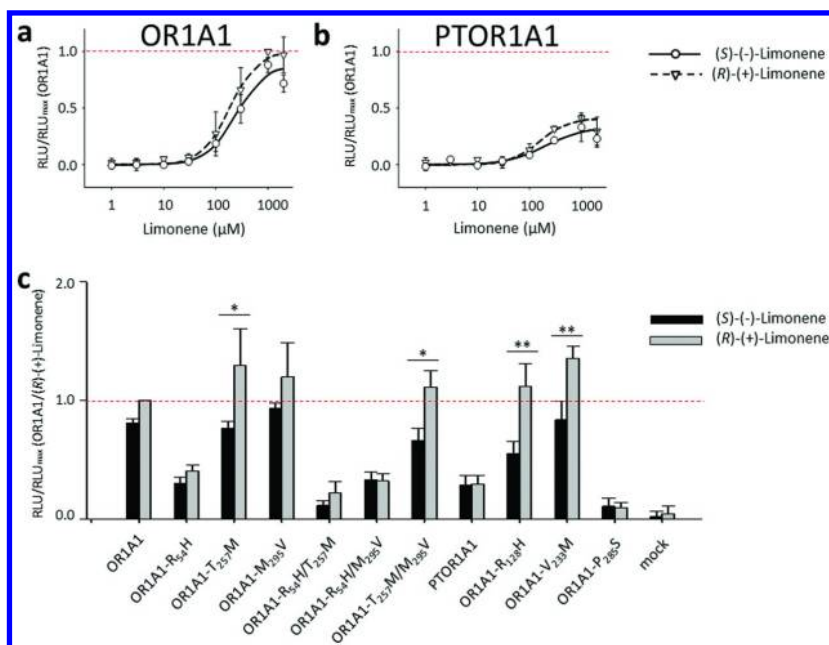
Figure 6. (S)-(-)-Limonene and (R)-(+)-Limonene. Concentration-response relations of (S)-(-)-limonene and (R)-(+)-limonene for a) OR1A1 (human) and b) PTOR1A1 (chimpanzee). Shown are mean ± SD of n = 3. Mock control was subtracted. Data were normalized to human OR1A1 maximum amplitude. The dashed line indicates the normalization level. c) Effect of 1000 μM (S)-(-)-limonene and (R)-(+)-limonene on OR1A1 (human), OR1A1 variants and PTOR1A1 (chimpanzee). Shown are mean ± SD of n = 3. Data were normalized to human OR1A1 vs. (R)-(+)-limonene. RLU = relative luminescence units. Significant differences between (S)-(-)-limonene and (R)-(+)-limonene effects were calculated by 2-sided t-test. **p<0.01, *p<0.05.

Our results show that both limonene enantiomers activated OR1A1 with the same efficacies (Figure 6a, Figure 6c), without significant differences in EC_{50} values between the *(S)*-(-)-limonene and *(R)*-(+)-limonene (Table 3). The ability to discriminate between the (-)- and (+)-enantiomer was introduced by the mutation $T_{257}M$ as well as by the double mutation $T_{257}M/M_{295}V$ (Figure 6c). Interestingly, the naturally occurring SNPs $R_{128}H$ and $V_{233}M$ introduced enantioselectivity.   OR1A1-$P_{285}S$ consistently showed a loss-of-function for all enantiomers tested.   The chimpanzee PTOR1A1 responded with decreased efficacies to the *(S)*-(-)-limonene and *(R)*-(+)-limonene, as the human OR1A1 (Figure 6a, Figure 6c).   Here, the efficacies and EC_{50} values showed also no significant differences between both enantiomers (Table 3).

Table 3. EC$_{50}$ Values for Investigated OR1A1 Variants

OR1A1 variants	(R)-(-)-Carvone EC$_{50}$ (µM)	(S)-(+)-Carvone EC$_{50}$ (µM)
OR1A1***	116.69 ± 18.79	352.28 ± 32.89
OR1A1-R$_{54}$H	n.d.	n.d.
OR1A1-T$_{257}$M*	123.48 ± 13.41	224.25 ± 31.53
OR1A1-M$_{295}$V**	59.55 ± 12.33	207.97 ± 26.39
OR1A1-R$_{54}$H/T$_{257}$M*	179.04 ± 33.01	346.72 ± 111.08
OR1A1-R$_{54}$H/M$_{295}$V	161.31 ± 52.53	138.90 ± 64.60
OR1A1-T$_{257}$M/M$_{295}$V***	125.47 ± 17.80	372.98 ± 34.28
PTOR1A1	128.00 ± 37.24	136.46 ± 23.85
OR1A1-R$_{128}$H*	440.32 ± 79.07	582.56 ± 45.34
OR1A1-V$_{233}$M***	102.68 ± 10.99	391.04 ± 36.39
OR1A1-P$_{285}$S	n.d.	n.d.
	(-)-Menthone EC$_{50}$ (µM)	(+)-Menthone EC$_{50}$ (µM)
OR1A1***	320.00 ± 28.22	135.61 ± 16.20
PTOR1A1*	384.14 ± 94.79	208.12 ± 37.65
	(S)-(-)-Limonene EC$_{50}$ (µM)	(R)-(+)-Limonene EC$_{50}$ (µM)
OR1A1	242.70 ± 37.42	185.06 ± 13.09
PTOR1A1	202.15 ± 63.10	156.78 ± 40.57

Significant differences between the EC$_{50}$ values of the respective (-)-enantiomer and the (+)-enantiomer for each OR1A1 variant were calculated by 2-sided t-test. ***$p<0.001$, **$p<0.01$, *$p<0.05$. n.d.= not detectable.

Discussion

Chirality of enantiomers with identical physicochemical properties matters at the level of their natural biological targets, the receptors, which may be enantioselective. Here we demonstrate the human OR1A1 as a receptor cognate for several monoterpenes, being selective for (R)-(-)-carvone over (S)-(+)-carvone, and for (+)-menthone over (-)-menthone, but without selectivity for any limonene enantiomer, suggesting the ketone function as a requirement for the enantioselective recognition of carvone and menthone enantiomers by the human OR1A1.

Interestingly, only an enantioselective recognition of (+)-menthone over (-)-menthone is conserved in both chimpanzee and human OR1A1, but the chimp receptor lacks any enantioselectivity for carvone and limonene, and had a generally lower efficacy in responding to these terpenes. We pinpointed these

functional discrepancies to the differences between the amino acid sequences of human and chimp OR1A1 at positions 54, 257 and 295. Consistently, the single mutation of position 54 from arginine (human) to histidine (chimp) had the most deleterious effects on enantioselectivity, at least for the menthone enantiomers, as well as on the efficacy in general. Notably, amino acid position 54 in human OR1A1 may be affected by underlying coding SNPs resulting in the single-SNP haplotypes $R_{54}H$ or $R_{54}C$, albeit with no reported minor allele frequencies, at least not $\geq 1\%$ (*35–37*).

Single SNP-based amino acid changes may have a significant impact on an OR's responsiveness for certain odorants (*38–41*). In our hands, the single-SNP haplotypes had differential effects on the enantioselectivity of OR1A1 for the enantiomers tested. The SNP-based mutation $R_{128}H$ worsened the potency of both carvone enantiomers, without effect on their efficacy, but both SNP-based mutations $R_{128}H$ and $V_{233}M$ introduced enantioselectivity of OR1A1 for the limonene enantiomers. The SNP-based mutation $V_{233}M$ resulted in a gain-of-function phenotype with respect to the carvone enantiomer efficacies, but without effect on the menthones. In contrast, the SNP-based mutation $P_{285}S$ consistently caused a loss-of-function in OR1A1 for all terpenoids tested. The Proline 7.50 at position 285 in OR1A1 is conserved in 97% of all human OR (C. Geithe, unpublished observation), and is highly conserved over all GPCR (*42*), suggesting an evolutionary conserved structural requirement for GPCR function. However, none of the SNP-related amino acid positions investigated in this study has been suggested to be directly involved in an interaction with odorants in OR in general (*43*), or in OR1A1 in particular (*44*), suggesting rather sterical effects on the OR1A1 conformation. Alternatively, some mutations in the intracellular domains of OR1A1 may affect interactions with other intracellular proteins, e.g., G proteins or chaperones.

In summary, we have identified human OR1A1 as an enantioselective receptor for terpenoid odorants. Our results demonstrate that single-SNP haplotypes display differential enantioselectivity, potency and efficacy towards carvone, menthone, and limonene enantiomers.

However, the ability to discriminate between enantiomeric odorants may not depend on a single OR. Laska and colleagues have shown that human subjects or squirrel monkeys were able to significantly discriminate the optical isomers of carvone and limonene, whereas they failed to distinguish between the (+)- and (-)-forms of menthol (*9, 14*). This is not entirely congruent to the functional properties of OR1A1, and may suggest additional OR to be involved in creating enantioselective receptor activity patterns as a basis for the discrimination of optical isomers of terpenoid odorants. Indeed, we have presented such receptor activity patterns, in the present study for the menthone enantiomers, and in a previous study for the carvone enantiomers (*18*). Screening an entire OR library, ideally including the most frequent haplotypes, in a test cell system such as in our study, will reveal enantiomer-specific receptor activity patterns in future experiments.

Beyond their hedonic value as character impact odorants in a variety of foods (*45–47*), terpenoids have been attributed biofunctionality for humans (*48–51*). Given the ever increasing evidence of OR expression in cells and tissues outside of

the olfactory epithelium (*52–54*), odorants thus have to be considered bioactives in the widest sense. Knowing the cognate OR/odorant pairs will therefore not only lead to an understanding of odorant coding at the receptor level, but will also reveal bioactive potencies of odorants and their enantiomers.

References

1. Brenna, E.; Fuganti, C.; Serra, S. Enantioselective perception of chiral odorants. *Tetrahedron: Asymmetry* **2003**, *14*, 1–42.
2. Leitereg, T. J.; Guadagni, D. G.; Harris, J.; Mon, T. R.; Teranish, R Chemical and Sensory Data Supporting Difference between Odors of Enantiomeric Carvones. *J. Agric. Food Chem.* **1971**, *19*, 785–787.
3. Leitereg, T. J.; Guadagni, D. G.; Harris, J.; Mon, T. R.; Teranishi, R. Evidence for the difference between the odours of the optical isomers (+)- and (-)-carvone. *Nature* **1971**, *230*, 455–456.
4. Pelosi, P.; Viti, R. Specific Anosmia to L-Carvone - Minty Primary Odor. *Chem. Senses Flavour* **1978**, *3*, 331–337.
5. Theimer, E. T.; Yoshida, T.; Klaiber, E. M. Olfaction and Molecular Shape. Chirality as a Requisite for Odor. *J. Agric. Food Chem.* **1977**, *25*, 1168–77.
6. Laska, M. Olfactory discrimination ability of human subjects for enantiomers with an isopropenyl group at the chiral center. *Chem. Senses* **2004**, *29*, 143–52.
7. Laska, M.; Teubner, P. Olfactory discrimination ability for homologous series of aliphatic alcohols and aldehydes. *Chem. Senses* **1999**, *24*, 263–70.
8. Joshi, D.; Volkl, M.; Shepherd, G. M.; Laska, M. Olfactory sensitivity for enantiomers and their racemic mixtures--a comparative study in CD-1 mice and spider monkeys. *Chem. Senses* **2006**, *31*, 655–64.
9. Laska, M.; Liesen, A.; Teubner, P. Enantioselectivity of odor perception in squirrel monkeys and humans. *Am. J. Physiol.* **1999**, *277*, R1098–103.
10. Heth, G.; Nevo, E.; Ikan, R.; Weinstein, V.; Ravid, U.; Duncan, H. Differential olfactory perception of enantiomeric compounds by blind subterranean mole rats (Spalax ehrenbergi). *Experientia* **1992**, *48*, 897–902.
11. Laska, M.; Galizia, C. G. Enantioselectivity of odor perception in honeybees (Apis mellifera carnica). *Behav. Neurosci.* **2001**, *115*, 632–9.
12. Laska, M.; Genzel, D.; Wieser, A. The number of functional olfactory receptor genes and the relative size of olfactory brain structures are poor predictors of olfactory discrimination performance with enantiomers. *Chem. Senses* **2005**, *30*, 171–5.
13. Laska, M.; Shepherd, G. M. Olfactory discrimination ability of CD-1 mice for a large array of enantiomers. *Neuroscience* **2007**, *144*, 295–301.
14. Laska, M.; Teubner, P. Olfactory discrimination ability of human subjects for ten pairs of enantiomers. *Chem. Senses* **1999**, *24*, 161–70.
15. Mainland, J. D.; Keller, A.; Li, Y. R.; Zhou, T.; Trimmer, C.; Snyder, L. L.; Moberly, A. H.; Adipietro, K. A.; Liu, W. L.; Zhuang, H.; Zhan, S.; Lee, S. S.; Lin, A.; Matsunami, H. The missense of smell: functional variability in the human odorant receptor repertoire. *Nat. Neurosci.* **2014**, *17*, 114–20.

16. Olender, T.; Waszak, S. M.; Viavant, M.; Khen, M.; Ben-Asher, E.; Reyes, A.; Nativ, N.; Wysocki, C. J.; Ge, D.; Lancet, D. Personal receptor repertoires: olfaction as a model. *BMC Genomics* **2012**, *13*, 414.

17. Buck, L.; Axel, R. A novel multigene family may encode odorant receptors: a molecular basis for odor recognition. *Cell* **1991**, *65*, 175–87.

18. Geithe, C.; Krautwurst, D. Chirality matters and SNPs make the difference - genetic variations on enantiomer-specific odorant receptors for carvone. In *Flavour Science: Proceedings of the XIV Weurman Flavour Research Symposium*; Taylor, A. J., Mottram, D. S., Eds.; Context Products Ltd.: Leicestershire, U.K., 2015; pp 297−302.

19. Takai, Y.; Touhara, K. Enantioselective recognition of menthol by mouse odorant receptors. *Biosci. Biotechnol. Biochem.* **2015**, 1–7.

20. Ohloff, G. *Scent and Fragrances. The Fascination of Odors and their Chemical Perspectives*; Springer: Berlin, 1994.

21. Krautwurst, D.; Yau, K.; Reed, R. Identification of ligands for olfactory receptors by functional expression of a receptor library. *Cell* **1998**, *95*, 917–926.

22. Shirokova, E.; Schmiedeberg, K.; Bedner, P.; Niessen, H.; Willecke, K.; Raguse, J. D.; Meyerhof, W.; Krautwurst, D. Identification of specific ligands for orphan olfactory receptors. G protein-dependent agonism and antagonism of odorants. *J. Biol. Chem.* **2005**, *280*, 11807–15.

23. Graham, F. L.; Smiley, J.; Russell, W. C.; Nairn, R. Characteristics of a human cell line transformed by DNA from human adenovirus type 5. *J. Gen. Virol.* **1977**, *36*, 59–74.

24. Jones, D. T.; Reed, R. R. Golf: an olfactory neuron specific-G protein involved in odorant signal transduction. *Science* **1989**, *244*, 790–5.

25. Saito, H.; Kubota, M.; Roberts, R. W.; Chi, Q.; Matsunami, H. RTP Family Members Induce Functional Expression of Mammalian Odorant Receptors. *Cell* **2004**, *119*, 679–91.

26. Li, F.; Ponissery-Saidu, S.; Yee, K. K.; Wang, H.; Chen, M. L.; Iguchi, N.; Zhang, G.; Jiang, P.; Reisert, J.; Huang, L. Heterotrimeric G protein subunit Ggamma13 is critical to olfaction. *J. Neurosci.* **2013**, *33*, 7975–84.

27. Binkowski, B.; Fan, F.; Wood, K. Engineered luciferases for molecular sensing in living cells. *Curr. Opin. Biotechnol.* **2009**, *20*, 14–8.

28. Zhuang, H.; Matsunami, H. Evaluating cell-surface expression and measuring activation of mammalian odorant receptors in heterologous cells. *Nat. Protoc.* **2008**, *3*, 1402–13.

29. Bakalyar, H. A.; Reed, R. R. Identification of a specialized adenylyl cyclase that may mediate odorant detection. *Science* **1990**, *250*, 1403–6.

30. Xia, Z.; Choi, E. J.; Wang, F.; Storm, D. R. The type III calcium/calmodulin-sensitive adenylyl cyclase is not specific to olfactory sensory neurons. *Neurosci. Lett.* **1992**, *144*, 169–73.

31. Saito, H.; Chi, Q.; Zhuang, H.; Matsunami, H.; Mainland, J. D. Odor coding by a Mammalian receptor repertoire. *Sci. Signaling* **2009**, *2*, ra9.

32. MacGregor, D. A.; Prielipp, R. C.; Butterworth, I. V. J. F.; James, R. L.; Royster, R. L. RElative efficacy and potency of β-adrenoceptor agonists for generating camp in human lymphocytes. *Chest* **1996**, *109*, 194–200.

33. Schimanski, S.; Scofield, M. A.; Wangemann, P. Functional beta2-adrenergic receptors are present in nonstrial tissues of the lateral wall in the gerbil cochlea. *Sci. Signaling* **2001**, *6*, 124–31.

34. Adipietro, K. A.; Mainland, J. D.; Matsunami, H. Functional evolution of Mammalian odorant receptors. *PLoS* **2012**, *8*, e1002821.

35. Abecasis, G. R.; Altshuler, D.; Auton, A.; Brooks, L. D.; Durbin, R. M.; Gibbs, R. A.; Hurles, M. E.; McVean, G. A. A map of human genome variation from population-scale sequencing. *Nature* **2010**, *467*, 1061–73.

36. Abecasis, G. R.; Auton, A.; Brooks, L. D.; DePristo, M. A.; Durbin, R. M.; Handsaker, R. E.; Kang, H. M.; Marth, G. T.; McVean, G. A. An integrated map of genetic variation from 1,092 human genomes. *Nature* **2012**, *491*, 56–65.

37. NCBI. *National Center for Biotechnology Information, Gene Search Tool*; 2014 2 May 2014; Verfügbar auf: http://www.ncbi.nlm.nih.gov/gene/.

38. Jaeger, S. R.; McRae, J. F.; Bava, C. M.; Beresford, M. K.; Hunter, D.; Jia, Y.; Chheang, S. L.; Jin, D.; Peng, M.; Gamble, J. C.; Atkinson, K. R.; Axten, L. G.; Paisley, A. G.; Tooman, L.; Pineau, B.; Rouse, S. A.; Newcomb, R. D. A mendelian trait for olfactory sensitivity affects odor experience and food selection. *Curr. Biol.* **2013**, *23*, 1601–5.

39. Keller, A.; Zhuang, H.; Chi, Q.; Vosshall, L. B.; Matsunami, H. Genetic variation in a human odorant receptor alters odour perception. *Nature* **2007**, *449*, 468–72.

40. McRae, J. F.; Jaeger, S. R.; Bava, C. M.; Beresford, M. K.; Hunter, D.; Jia, Y.; Chheang, S. L.; Jin, D.; Peng, M.; Gamble, J. C.; Atkinson, K. R.; Axten, L. G.; Paisley, A. G.; Williams, L.; Tooman, L.; Pineau, B.; Rouse, S. A.; Newcomb, R. D. Identification of regions associated with variation in sensitivity to food-related odors in the human genome. *Curr. Biol* **.2013**, *23*, 1596–600.

41. McRae, J. F.; Mainland, J. D.; Jaeger, S. R.; Adipietro, K. A.; Matsunami, H.; Newcomb, R. D. Genetic Variation in the Odorant Receptor OR2J3 Is Associated with the Ability to Detect the "Grassy" Smelling Odor, cis-3-hexen-1-ol. *Chem. Senses* **2012**.

42. Ballesteros, J. A.; Weinstein, H. Integrated methods for the construction of three-dimensional models and computational probing of structure-function relations in G protein-coupled receptors. *Methods Neurosci.* **1995**, *25*, 366–428.

43. Man, O.; Gilad, Y.; Lancet, D. Prediction of the odorant binding site of olfactory receptor proteins by human-mouse comparisons. *Protein Sci.* **2004**, *13*, 240–54.

44. Schmiedeberg, K.; Shirokova, E.; Weber, H.-P.; Schilling, B.; Meyerhof, W.; Krautwurst, D. Structural determinants of odorant recognition by the human olfactory receptors OR1A1 and OR1A2. *J. Struct. Biol.* **2007**, *159*, 400–412.

45. Dunkel, A.; Steinhaus, M.; Kotthoff, M.; Nowak, B.; Krautwurst, D.; Schieberle, P.; Hofmann, T. Nature's chemical signatures in human olfaction: a foodborne perspective for future biotechnology. *Angew. Chem., Int. Ed.* **2014**, *53*, 7124–43.

46. Grosch, W. Specificity of the human nose in perceiving food odorants. In *Frontiers of Flavour Science*; Schieberle, K.-H. E. P., Ed.; Deutsche Forschungsanstalt für Lebensmittelchemie: München, 2000.

47. Krautwurst, D.; Kotthoff, M. A hit map-based statistical method to predict best ligands for orphan olfactory receptors: natural key odorants versus "lock picks". *Methods Mol. Biol.* **2013**, *1003*, 85–97.

48. Kezic, S. Bioactivity and analysis of chiral compounds. *Arh. Hig. Rada Toksikol.* **2000**, *51*, 335–341.

49. McKay, D. L.; Blumberg, J. B. A review of the bioactivity and potential health benefits of peppermint tea (Mentha piperita L.). *Phytother. Res* **2006**, *20*, 619–33.

50. Riachi, L. G.; De Maria, C. A. Peppermint antioxidants revisited. *Food Chem.* **2015**, *176*, 72–81.

51. Wagner, K. H.; Elmadfa, I. Biological relevance of terpenoids. Overview focusing on mono-, di- and tetraterpenes. *Ann. Nutr. Metab.* **2003**, *47*, 95–106.

52. Feldmesser, E.; Olender, T.; Khen, M.; Yanai, I.; Ophir, R.; Lancet, D. Widespread ectopic expression of olfactory receptor genes. *BMC Genomics* **2006**, *7*, 121.

53. Foster, S. R.; Roura, E.; Thomas, W. G. Extrasensory perception: odorant and taste receptors beyond the nose and mouth. *Pharmacol. Ther.* **2014**, *142*, 41–61.

54. Malki, A.; Fiedler, J.; Fricke, K.; Ballweg, I.; Pfaffl, M. W.; Krautwurst, D. Class I odorant receptors, TAS1R and TAS2R taste receptors, are markers for subpopulations of circulating leukocytes. *J. Leukocyte Biol.* **2015**, *97*, 533–45.

Chapter 13

Ligand Recognition of Taste Receptors

Wolfgang Meyerhof,* **Alessandro Marchiori, Kristina Lossow,**
Masataka Narukawa,[1] **and Maik Behrens**

Department Molecular Genetics,
German Institute of Human Nutrition Potsdam-Rehbruecke,
Arthur-Scheunert-Allee 114-116, 14558 Nuthetal, Germany
[1]Present Address: Graduate School of Agricultural and Life Science,
The University of Tokyo, 1-1-1 Yayoi, Bunkyo-ku, 113-8657 Tokyo, Japan
*E-mail: meyerhof@dife.de.

We tested the prediction that enantiomeric pairs of compounds of which one partner elicits sweetness and the other partner bitterness should not be recognized by structurally unrelated taste receptors with independent evolutionary origins. They rather have been proposed to be recognized by structurally related pairs of receptors. To this end we focused on the D- and L-forms of tryptophan and phenylalanine. We used *in vitro* assays to examine receptor responsiveness to the test substances and genetically engineered mice to test implications of taste quality coding. Our data are inconsistent with the prediction. They indicate that D- and L-forms of tryptophan and phenylalanine are recognized by the unrelated sweet and bitter taste receptors, respectively.

Introduction

The five basic tastes are represented in the mouth by functionally segregated populations of receptor cells each characterized by the presence of a special type of receptor molecules (*1*). This organization explains the high discriminatory power of the taste system across taste qualities and the low discriminatory power within a quality. The five different cell populations are wired to the brain in such a way that excitation in one of them causes the perception of the corresponding taste quality (*2*, *3*).

Bitter compounds are recognized by receptor molecules of the taste 2 receptor (TAS2R) family (*4*, *5*). These G protein-coupled receptors (GPCRs) which are devoid of pronounced sequence homology to other GPCR classes are expressed by oral taste receptor cells dedicated to bitter (*6*, *7*). Humans possess ~25 TAS2Rs that differ in the breadth of their agonist profiles (*5*). Whereas some TAS2Rs are quite narrowly tuned to detect one or few compounds, others are very broadly tuned being sensitive to numerous bitter tasting substances. The majority of TAS2Rs display an average breadth of tuning. The combined tuning properties form the basis for our ability to detect the countless bitter compounds with a limited number of receptors.

Sweet and umami compounds are sensed by members of the taste 1 receptor (TAS1R) family. This family is comprised of three members that belong to the class C GPCRs (*8–10*). TAS1Rs and TAS2Rs are unrelated and have a different phylogenetic origin. Unlike most members of this receptor class which form homodimers, TAS1Rs heterodimerize to assemble functional receptors (*11–13*). In humans, the dimer TAS1R1-TAS1R3 functions as a receptor for umami that is activated by the amino acid glutamate and strongly enhanced by the simultaneous presence of ribonucleotides, while in mouse the receptor is less selective and recognizes other L-amino acids (*12*, *13*). The dimer TAS1R2-TAS1R3 forms the canonical sweet receptor that could be activated by all tested sweet tasting compounds (*10*). There is limited evidence for T1R3 homodimers which respond selectively to high concentrations of sucrose and glucose (*14*). Thus, the mode of detection of sweet/umami compounds differs fundamentally from that of bitter molecules.

It is amazing to note that slight structural changes in a molecule can switch its taste between sweet and bitter (Figure 1) (*15*). For example, the neohesperidin and naringin dihydrochalcones are sweet, whereas neohesperidin and naringin are bitter. Similarly, replacing the carbonyl oxygen in the high intensity sweetener saccharin by sulfur renders the compound bitter. The most impressive example, however, are aromatic L- and D-amino acids. Whereas the L-forms of tryptophan, tyrosine, and phenylalanine are bitter their D-forms taste sweet. Thus, only the inversion of a single chirality center converted the taste of these compounds from bitter to sweet.

It has been questioned if such "sweet-bitter pairs" of substances are detected by structurally unrelated taste receptors that evolved independently during evolution (*15*, *16*). In this regard a particularly strong claim has been made for the case of enantiomeric pairs and other chiral isomers. Instead, the interesting proposal has been put forward that such "sweet-bitter compound pairs" are recognized by structurally related pairs of receptors, i.e., the sweet receptor binds the "sweet partner" and the umami receptor the "bitter partner". Bitter taste coding for the "bitter partner" is then predicted to proceed via receptor cells that host both, bitter and umami taste receptors, or by crosstalk that exists between different types of receptor cells (*15*, *16*).

In the present report we examined this hypothesis by surveying the current literature, recording the responses to "sweet-bitter compound pairs" of recombinant sweet, umami, and bitter taste receptors by functional expression in

heterologous systems, and by analyzing bitter and umami receptor cells in wild type and genetically modified strains of mice.
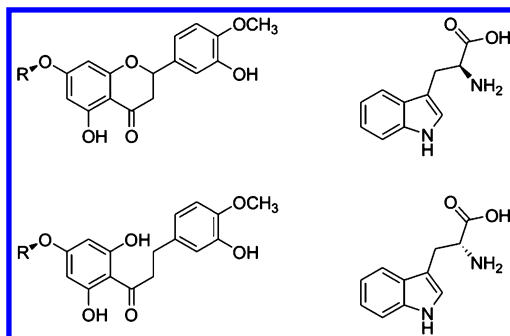
Figure 1. Structures of pairs of similar compounds that taste either sweet or bitter. Left, neohesperidin (top) and neohesperidin dihydrochalcone (bottom). R, rhamnose. Right, L-tryptophan (top) and D-tryptophan (bottom).

Materials and Methods

Calcium Imaging

cDNA coding for the different TAS2Rs were cloned into pcDNA5/FRT or pEAK10 vector. The plasmid presented an amino terminal export tag corresponding to the first 45 amino acids of rat somatostatin receptor 3 and a carboxy-terminal herpes simplex virus glycoprotein D tag. The vector was transiently transfected with Lipofectamine2000 (Invitrogen) in HEK 293T cells stably expressing the chimeric G protein subunit Gα16gust44. Twenty four hours after transfection, cells were loaded with Ca^{2+}-sensitive Fluo4-AM dye, washed 3 times in 130 mM NaCl, 5.00 mM KCl, 10.0 mM Na-Hepes, 2.00 mM $CaCl_2$, 10.0 mM glucose, pH 7.4 and changes in intracellular Ca^{2+}-concentration following application of agonists were recorded, at least 3 times independently, using a fluorometric imaging plate reader FLIPR[TETRA] (Molecular Devices). Agonists were dissolved into 130 mM NaCl, 5.00 mM KCl, 10.0 mM Na-Hepes, 2.00 mM $CaCl_2$, 10.0 mM glucose, pH 7.4.

Transgenic Animals

The generation of a double transgenic strain of mice carrying knockin alleles for the umami receptor specific subunit Tas1r1 and for the bitter receptor Tas2r131 has been described in detail (*17*). In these animals the taste receptor genes have been knocked out by replacing them with the coding region for fluorescence proteins. They were generated by crossing mice that express the green fluorescent protein in all cells that would normally express the Tas2r131 bitter receptor with mice expressing the red fluorescent protein mCherry in all cells that normally

would express the Tas1r1 umami receptor subunit. Palatal tissue was dissected, fixed, and mounted on microscopic slides. Finally, images from palatal epithelium were obtained by means of a laser scanning microscope (Leica). The effect of the loss of the Tas1r1 umami receptor subunit on taste-stimulated gustatory nerve activity has also been described previously (*18*).

Results and Discussion

Responsiveness of Sweet and Umami Receptors to Sweet and Bitter Amino Acids

In order to test the hypothesis that "sweet-bitter pairs" of structurally similar compounds including enantiomeric pairs bind to structurally related pairs of receptors to elicit their taste perception we focused on the D- and L-forms of phenylalanine and tryptophan and examined the potential of these substances to activate sweet and umami receptors. A number of previous reports describe the functional responses of sweet and umami receptors to various L- and D- amino acids in special receptor assays (*12*, *13*, *19*, *20*). The data show that D-Trp and D-Phe are potent agonists for the mouse and human Tas1r2-Tas1r3 sweet receptor. L-Phe and L-Trp, do, however, not activate the sweet receptor from both species. These observations are in line with the taste profiles of the respective amino acids, i.e., the D-forms but not the L-forms taste sweet. In marked contrast, the Tas1r1-Tas1r3 umami receptor from mouse is insensitive to D-Trp and D-Phe which is in agreement with their lack of umami taste. L-Trp and L-Phe, unlike various other proteinogenic L-amino acids, do not activate the mouse umami receptor. Only in the presence of the well-known umami taste enhancer IMP is L-Phe but not L-Trp capable of stimulating mTas1R1-Tas1r3 to some extent. Ribonucleotide enhancement is the hallmark of the umami taste (*21*, *22*) and indicates that the interaction of L-Phe with mTas1r1-Tas1r3 underlies umami but not bitter taste. The human TAS1R1-TAS1R3 is quite selective for glutamate; L-Trp and L-Phe are unable to activate the human umami receptor. Taken together, the data demonstrate that the "sweet partners" of the "sweet-bitter pairs" of enantiomers, D-Trp and D-Phe, stimulate the Tas1r2-Tas1r3 sweet receptor to evoke sweetness. On the other hand the "bitter partners", L-Trp and L-Phe, fail to activate the structurally related partner receptor, Tas1r1-Tas1r3. Accordingly, the umami receptor which is structurally related to the sweet receptor cannot be involved in the bitterness of L-Trp and L-Phe. This conclusion is further supported by the IMP-dependent activation of Tas1r1-Tas1r3 by L-Phe, which strongly suggests that this action of L-Phe evokes umami taste but not bitterness.

Umami and Bitter Receptor Expressing Cells Form Different Populations

Next, we investigated if umami and bitter receptors occur in the same taste receptor cells. To this end, we used a strain of mice engineered to express the red fluorescence protein, mCherry, in all cells that would normally express the specific Tas1r1 subunit of the umami receptor and the green fluorescence protein in all cells that would normally express the bitter receptor Tas2r131 (*17*). Since

several or many bitter receptors are coexpressed in one taste receptor cell (*6*, *7*, *23*), Tas2r131 cells form a large fraction of the population of bitter-sensing cells (*17*). We observed a complete segregation of the red fluorescent umami-sensing cells and the green fluorescent bitter-sensing cells. This segregation covers the topographical distribution of taste cells in the mouth as well as within taste buds. Whereas in the vallate and foliate taste buds numerous green fluorescent cells were seen, red fluorescent cells were extremely rare. In marked contrast, the fungiform papillae were rich in red and poor in green fluorescent cells (data not shown). Unlike lingual taste buds, palatal taste buds contained similar numbers of both red and green fluorescent cells (Figure 2). However, the populations of red and green fluorescent cells were strictly segregated in different populations; we never observed a cell that appeared in yellow color, i.e., that expressed both fluorescent markers indicative of simultaneous umami and bitter receptor expression. Even though we cannot formally exclude the possibility that bitter cells that are not labeled by our experimental approach could coexpress bitter and umami receptors, the present and published data strongly argue against this possibility.
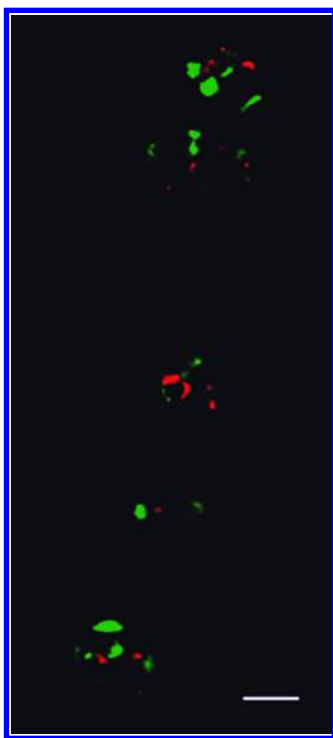
Figure 2. Complete segregation of oral Tas2r131 receptor expressing bitter cells and Tas1r1 expressing umami cells. Tas2r131 cells are visualized by green fluorescence protein fluorescence whereas Tas1r1 is visualized by mCherry fluorescence. The image shows a confocal micrograph of a section of the palatal epithelium containing five taste buds of a double transgenic mouse with modified Tas1r1 and Tas2r131 alleles. Scale bar, 25 μm.

Coexpression of Tas1rs and Tas2rs has not been observed by in situ hybridization (*6*). Moreover, knockout animals for phospholipase C-beta 2, a crucial signaling protein for sweet, umami and bitter taste, have lost their ability to recognize corresponding taste substances (*3*). When these animals were rescued for phospholipase C-beta 2 expression under the control of bitter receptor gene promoters specifically bitter perception of a number of compounds was restored whereas sweet and umami taste remained abolished (*2*). Finally, the knockout of the Tas1r1 subunit attenuated specifically nerve and behavioral responses in mice to umami compounds (Figure 3), whereas bitter responses remained unaffected (*14*, *24*). Thus, the available evidence strongly suggests that umami receptors are not expressed in bitter-dedicated cells and therefore cannot mediate the bitterness of L-Phe and L-Trp or that of other compounds.
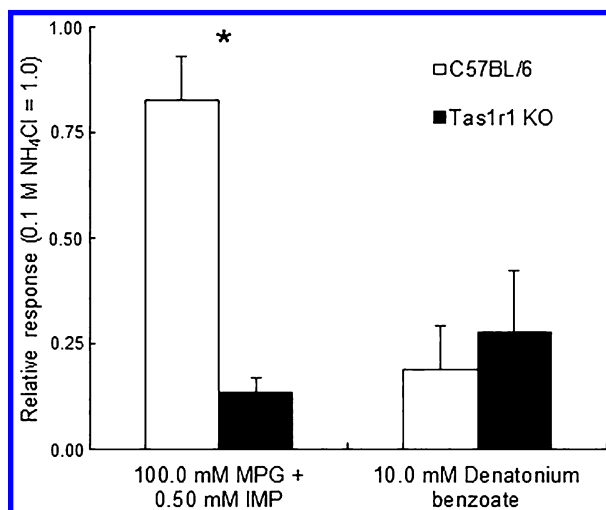
*Figure 3. Tas1r1 knockout mice have largely diminished gustatory nerve response to umami stimuli whereas responses to bitter compounds remained normal. Responses to a mixture of monopotassium glutamate (MPG) and IMP or to the prototypical bitter compound denatonium benzoate were recorded from the chorda tympani of control and knockout mice and normalized to those of ammonium chloride. Values are mean ± SEM. N= 4-6 animals; *p<0.0001.*

Umami Cells Do Not Signal to Presynaptic Cells in Order To Elicit Bitterness

Another proposed coding strategy for eliciting bitterness of L-Trp and L-Phe through umami cell activation holds that some umami receptor expressing cells are wired to so-called presynaptic cells in the taste bud which then convey the signal to the brain in a way that results in bitterness perception. The presynaptic cell is the only cell type that forms conventional chemical synapses with the

afferent nerves (*25*). When these cells were functionally analyzed *ex vivo* in isolation they respond only to sour stimulation (*26*). However, in the intact taste bud presynaptic cells are also sensitive to the transmitter substance ATP released from sweet, bitter, and umami receptor cells. Thus, presynaptic cells can be directly activated through acids and indirectly through activation of receptor cells (*27*). Whereas the consequences of the latter remain unresolved, those of the former are very clear. Genetic ablation of the presynaptic cells specifically abolished sour taste, leaving the other basic tastes, bitter and umami included, intact. Therefore, the available experimental evidence does not support the possibility that bitterness of L-Trp and L-Phe are evoked by a Tas1r1-Tas1r3 expressing bitter-dedicated cell type that interacts with special presynaptic cells.

Tas2r Bitter Receptors for L-Trp and L-Phe

The above evidence is inconsistent with the hypothesis that the bitter partner of the enantiomeric pairs of Trp and Phe, i.e., L-Trp and L-Phe, are recognized by the Tas1r1-Tas1r3 umami receptor and evoke bitterness through umami receptor expressing bitter-dedicated cells or through signaling of some umami receptor expressing cells to specialized presynaptic cells. It is therefore likely that L-Trp and L-Phe have cognate Tas2r bitter taste receptors. We therefore screened the 25 human TAS2Rs with the L- and D-forms of Trp and Phe using a heterologous expression system (*28*). We found that 3 out of the 25 TAS2Rs were sensitive to the amino acids (*28*). Interestingly, D-Trp elicited large responses in cells expressing TAS2R4 and much smaller responses in TAS2R39 expressing cells. Thus, these two receptors appear to mediate the known slight off-taste of D-Trp (*29*, *30*). The D-form of Phe failed to activate any of the TAS2Rs. Moreover, we identified TAS2R4 as responder to L-Trp and TAS2R1 as being sensitive to L-Phe indicating that bitter L-amino acids have a single cognate TAS2R responsible for L-amino acid detection. Each of the two L-amino acids has its own special bitter receptor which appears to mediate the bitterness of the L- forms of Trp and Phe. It is interesting to note that whereas TAS2R1 and TAS2R39 are selective for only one of the two enantiomeric forms of Phe and Trp, TAS2R4 does not discriminate between D- and L-Trp showing similar dose-response functions for both enantiomers, even though D-Trp elicits stronger responses (*28*). Stereoselectivity of bitter taste receptors has been observed previously in case of TAS2R16 which is sensitive to beta- but not alpha-glucopyranosides (*31*). These findings have been virtually confirmed by another study (*20*). Because we have not identified TAS2Rs for other bitter tasting amino acids such as L-Ile, L-Val or L-Leu, we can, of course, not formally rule out the possibility that other receptors expressed by bitter taste cells recognize these substances. Whereas metabotropic glutamate receptors are unlikely to serve this role because they only respond to glutamate and analogs, the calcium sensing receptor CaSR could be a potential candidate. This receptor responds to various L-amino acids some of which taste bitter (L-Phe and L-Trp). However, as this receptor does not respond to L-Ile, L-Val, and L-Leu and it is unknown if CaSR is expressed by bitter-dedicated cells its potential role in amino acid bitterness remains speculative.

Conclusions

Taken together and contrary to the expectations, our data demonstrate that enantiomeric pairs of compounds are recognized by structurally unrelated receptor types that independently evolved during evolution. Whereas the D-forms of Trp and Phe act on Tas1r2-Tas1r3 receptors to evoke sweetness, the bitter tasting "partners" L-Trp and L-Phe activate TAS2R bitter taste receptors. Given their common and ubiquitous presence in biological systems, it may be not too surprising that different receptor systems have evolved independently to recognize L-amino acids. It may also be of importance to briefly look at carbohydrates. Both, L- and D-glucose taste sweet and are devoid of bitterness. However, only beta-methylglucopyranoside and other beta-glucopyranosides with various aglycon moieties taste bitter by activating the bitter receptor TAS2R16 whereas the alpha-counterparts do not (*31*).

Acknowledgments

References

1. Yarmolinsky, D. A.; Zuker, C. S.; Ryba, N. J. Common sense about taste: from mammals to insects. *Cell* **2009**, *139*, 234–244.
2. Mueller, K. L.; Hoon, M. A.; Erlenbach, I.; Chandrshekar, J.; Zuker, C. S.; Ryba, N. J. P. The receptors and coding logic for bitter taste. *Nature* **2005**, *434*, 225–229.
3. Zhang, Y.; Hoon, M. A.; Chandrashekar, J.; Mueller, K. L.; Cook, B.; Wu, D.; Zuker, C. S.; Ryba, N. J. Coding of sweet, bitter, and umami tastes. Different receptor cells sharing similar signaling pathways. *Cell* **2003**, *112*, 293–301.
4. Chandrashekar, J.; Mueller, K. L.; Hoon, M. A.; Adler, E.; Feng, L.; Guo, W.; Zuker, C. S.; Ryba, N. J. T2Rs function as bitter taste receptors. *Cell* **2000**, *100*, 703–711.
5. Meyerhof, W.; Batram, C.; Kuhn, C.; Brockhoff, A.; Chudoba, E.; Bufe, B.; Appendino, G.; Behrens, M. The molecular receptive ranges of human TAS2R bitter taste receptors. *Chem. Senses* **2010**, *35*, 157–170.
6. Adler, E.; Hoon, M. A.; Mueller, K. L.; Chandrashekar, J.; Ryba, N. J.; Zuker, C. S. A novel family of mammalian taste receptors. *Cell* **2000**, *100*, 693–702.
7. Matsunami, H.; Montmayeur, J. P.; Buck, L. B. A family of candidate taste receptors in human and mouse. *Nature* **2000**, *404*, 601–604.
8. Chandrashekar, J.; Hoon, M. A.; Ryba, N. J.; Zuker, C. S. The receptors and cells for mammalian taste. *Nature* **2006**, *444*, 288–294.
9. Li, X. T1R receptors mediate mammalian sweet and umami taste. *Am. J. Clin. Nutr.* **2009**, *90*, 733S–737S.

10. Behrens, M.; Meyerhof, W.; Hellfritsch, C.; Hofmann, T. Sweet and umami taste: natural products, their chemosensory targets, and beyond. *Angew. Chem., Int. Ed.* **2011**, *50*, 2220–2242.

11. Nelson, G.; Hoon, M. A.; Chandrashekar, J.; Zhang, Y.; Ryba, N. J.; Zuker, C. S. Mammalian sweet taste receptors. *Cell* **2001**, *106*, 381–390.

12. Nelson, G.; Chandrashekar, J.; Hoon, M. A.; Feng, L.; Zhao, G.; Ryba, N. J.; Zuker, C. S. An amino-acid taste receptor. *Nature* **2002**, *416*, 199–202.

13. Li, X.; Staszewski, L.; Xu, H.; Durick, K.; Zoller, M.; Adler, E. Human receptors for sweet and umami taste. *Proc. Natl. Acad. Sci. U.S.A.* **2002**, *99*, 4692–4696.

14. Zhao, G. Q.; Zhang, Y.; Hoon, M. A.; Chandrashekar, J.; Erlenbach, I.; Ryba, N. J.; Zuker, C. S. The receptors for Mammalian sweet and umami taste. *Cell* **2003**, *115*, 255–266.

15. Temussi, P. A. Sweet, bitter and umami receptors: a complex relationship. *Trends Biochem. Sci.* **2009**, *34*, 296–302.

16. Temussi, P. A. New insights into the characteristics of sweet and bitter taste receptors. *Int. Rev. Cell Mol. Biol.* **2011**, *291*, 191–226.

17. Voigt, A.; Hubner, S.; Lossow, K.; Hermans-Borgmeyer, I.; Boehm, U.; Meyerhof, W. Genetic Labeling of Tas1r1 and Tas2r131 Taste Receptor Cells in Mice. *Chem. Senses* **2012**, *37*, 897–911.

18. Kusuhara, Y.; Yoshida, R.; Ohkuri, T.; Yasumatsu, K.; Voigt, A.; Hubner, S.; Maeda, K.; Boehm, U.; Meyerhof, W.; Ninomiya, Y. Taste responses in mice lacking taste receptor subunit T1R1. *J. Physiol.* **2013**, *591*, 1967–1985.

19. Winnig, M.; Bufe, B.; Kratochwil, N. A.; Slack, J. P.; Meyerhof, W. The binding site for neohesperidin dihydrochalcone at the human sweet taste receptor. *BMC Struct. Biol.* **2007**, *7*, 66.

20. Bassoli, A.; Borgonovo, G.; Caremoli, F.; Mancuso, G. The taste of D- and L-amino acids: In vitro binding assays with cloned human bitter (TAS2Rs) and sweet (TAS1R2/TAS1R3) receptors. *Food Chem.* **2014**, *150*, 27–33.

21. Lindemann, B.; Ogiwara, Y.; Ninomiya, Y. The discovery of umami. *Chem. Senses* **2002**, *27*, 843–844.

22. Zhang, F.; Klebansky, B.; Fine, R. M.; Xu, H.; Pronin, A.; Liu, H.; Tachdjian, C.; Li, X. Molecular mechanism for the umami taste synergism. *Proc. Natl. Acad. Sci. U.S.A.* **2008**, *105*, 20930–20934.

23. Behrens, M.; Foerster, S.; Staehler, F.; Raguse, J. D.; Meyerhof, W. Gustatory expression pattern of the human TAS2R bitter receptor gene family reveals a heterogenous population of bitter responsive taste receptor cells. *J. Neurosci.* **2007**, *27*, 12630–12640.

24. Kusuhara, Y.; Yoshida, R.; Ohkuri, T.; Yasumatsu, K.; Voigt, A.; Hubner, S.; Maeda, K.; Boehm, U.; Meyerhof, W.; Ninomiya, Y. Taste responses in mice lacking taste receptor subunit T1R1. *J. Physiol.* **2013**, *591*, 1967–1985.

25. Roper, S. D. Taste buds as peripheral chemosensory processors. *Semin. Cell Dev. Biol.* **2013**, *24*, 71–79.

26. Huang, Y. A.; Maruyama, Y.; Stimac, R.; Roper, S. D. Presynaptic (Type III) cells in mouse taste buds sense sour (acid) taste. *J. Physiol.* **2008**, *586*, 2903–2912.

27. Tomchik, S. M.; Berg, S.; Kim, J. W.; Chaudhari, N.; Roper, S. D. Breadth of tuning and taste coding in mammalian taste buds. *J. Neurosci.* **2007**, *27*, 10840–10848.

28. Kohl, S.; Behrens, M.; Dunkel, A.; Hofmann, T.; Meyerhof, W. Amino acids and peptides activate at least five members of the human bitter taste receptor family. *J. Agric. Food Chem.* **2013**, *61*, 53–60.

29. Schiffman, S. S.; Sennewald, K.; Gagnon, J. Comparison of taste qualities and thresholds of D- and L-amino acids. *Physiol. Behav.* **1981**, *27*, 51–59.

30. Kawai, M.; Sekine-Hayakawa, Y.; Okiyama, A.; Ninomiya, Y. Gustatory sensation of (L)- and (D)-amino acids in humans. *Amino Acids* **2012**, *43*, 2349–2358.

31. Bufe, B.; Hofmann, T.; Krautwurst, D.; Raguse, J. D.; Meyerhof, W. The human TAS2R16 receptor mediates bitter taste in response to beta-glucopyranosides. *Nat. Genet.* **2002**, *32*, 397–401.

Subject Index